BILE ACIDS AND NUCLEAR RECEPTORS: THEIR ROLES IN NUTRITION AND CANCER

APPROVED BY SUPERVISORY COMMITTEE

David J. Mangelsdorf, Ph.D. _____

Steven A. Kliewer, Ph.D. _____

Hongtao Yu, Ph.D. _____

David W. Russell, Ph.D. _____

Luis Parada, Ph.D. _____

To my wife, Shanna.

For her constant love and support.

BILE ACIDS AND NUCLEAR RECEPTORS: THEIR ROLES IN NUTRITION AND CANCER

by

DANIEL R. SCHMIDT

DISSERTATION

Presented to the Faculty of the Graduate School of Biomedical Sciences

The University of Texas Southwestern Medical Center at Dallas

In Partial Fulfillment of the Requirements

For the Degree of

DOCTOR OF PHILOSOPHY

The University of Texas Southwestern Medical Center at Dallas

Dallas, Texas

June, 2010

BILE ACIDS AND NUCLEAR RECEPTORS: THEIR ROLES IN NUTRITION AND CANCER

Daniel R. Schmidt, Ph.D.

The University of Texas Southwestern Medical Center at Dallas, 2010

Supervising Professor: David J. Mangelsdorf, Ph.D.

The bile acid receptor, also known as farnesoid X receptor (FXR), is essential for feedback regulation of bile acid synthesis. Bile acids are required for the proper absorption of dietary lipids, including fat-soluble vitamins; however, some bacterial metabolites of bile acids have been shown to promote intestinal tumorigenesis in rodent models. Since high fat diet is considered a major risk factor for colorectal cancer (CRC), and is associated with increased bile acid concentrations in the colon, it has been proposed that bile acids contribute to the

pathogenesis of CRC. This study was undertaken to investigate the mechanism of tumor promotion by bile acids and determine whether FXR is involved in this process. The effects of bile acids and FXR on intestinal tumorigenesis were studied in mouse models of CRC and in colon cancer cell lines. In addition, the effects of FXR on bile acid-induced intestinal proliferation were investigated. To gain insight into the function of FXR in the large intestine, transcriptional profiling experiments were performed in mouse colon treated with natural and synthetic FXR agonists. Finally, a variety of mouse models were used to understand how fat-soluble vitamins affect bile acid synthesis at a molecular level. These studies found that FXR plays a role in protecting against colorectal cancer. *Akr1b7* was identified as a novel FXR target gene and was shown to detoxify bacterial bile acid metabolites, suggesting that FXR may play a role in protecting intestinal mucosa by inducing bile acid detoxification. The proliferative effects of bile acids *in vivo* were found to be independent of FXR, and instead involved activation of PI3K/AKT signaling. Finally, vitamins A and D were found to activate nuclear receptors in the intestine and repress bile acid synthesis. These results underscore the role of nuclear receptors and their ligands in maintaining intestinal homeostasis and in protecting against the tumor-promoting effects of bile acids.

TABLE OF CONTENTS

ACKNOWLEDGEMENTS

I am grateful to my mentor Dr. David Mangelsdorf and co-mentor Dr. Steven Kliewer for entrusting me with the FXR/colon cancer project and for providing me with the tools necessary to explore a variety of hypotheses pertaining to this and other projects. I also thank them for allowing me to "follow the data" into new and unexpected directions and for their guidance in how to think, explore, and collaborate as a scientist. In addition, I have been privileged to be supervised in my graduate studies by Dr. David Russell, Dr. Hongtao Yu, and Dr. Luis Parada, all of whom have been great role models and phenomenal mentors. Moreover, I wish to thank Dr. Antonio Moschetta, who, as a senior postdoctoral fellow during my first year in the lab played an integral role in my scientific training. I also benefitted from several helpful discussions about my projects with other UT Southwestern faculty, including Dr. Joyce Repa, Dr. Mike White, Dr. Richard Auchus, and Dr. Melanie Cobb.

The work presented in this dissertation would not have been possible without the help and advice of many past and current members of the Mangelsdorf/Kliewer laboratory, who provided a highly collaborative and congenial environment. In particular, I wish to thank Dr. Carolyn Cummins for assistance in developing the LC/MS methods for bile acid analysis; Angie Bookout for training me in quantitative PCR methods; Eva Borowicz for primer

validation; Dr. Yuan Zhang, Hannah Perkins, and Kevin Vale for assistance with animal experiments and breeding; and Aurora del Rosario and Gail Wright for administrative support. Specific contributions of other members of the lab, the UT Southwestern community, and outside collaborators, including Dr. Sam Holmstrom, Samuel Schmidt, Serkan Kir, Xiaoyong Xi, Dr. Klementina FonTacer, Angie Bookout, Genvieve Armstrong, Laura Brulé, Dr. John Minna, Dr. David Russell, Dr. Ruth Yu, Dr. Jeffrey Gordon, David O'Donnell, Dr. Douglas Covey, Dr. Bryson Katona, Dr. Mark Pruzanski, and Dr. Luciano Adorini are described in detail in the relevant chapters and sections. I also received an enormous amount of guidance and assistance with histologic analysis from Dr. James Richardson, John Shelton, and Jesse Morris in the Molecular Pathology core facility at UT Southwestern.

I thank the current and former administrators and administrative assistants of the Cell Regulation Graduate Program, Dr. Paul Sternweis and Carla Childers, and the Medical Scientist Training Program, Dr. Mike Brown, Dr. Rod Ulane, Dr. Dennis McKearin, Dr. Andrew Zinn, Robin Downing and Stephanie Robertson, for helping me navigate and survive the many years of graduate and medical training.

I also wish to thank my parents, Wolfgang and Daniela Schmidt, my brother Samuel, and my sisters Angela, Marianne, Sara, Elizabeth, and Joanna,

who have all been very supportive and understanding of my choice to pursue a lengthy education so far away from home.

Most importantly, I thank my wife, Shanna, to whom I have dedicated this thesis because she has been my partner through the good times and the bad, and has always been very encouraging of my decision to pursue a career as a physician-scientist.

PRIOR PUBLICATIONS

Schmidt DR, Holmstrom SR, Fon Tacer K, Bookout AL, Kliewer SA, Mangelsdorf DJ. Regulation of bile acid synthesis by fat-soluble vitamins A and D. *Journal of Biological Chemistry* **2010** May 7;285(19):14486-94. PubMed PMID: 20233723; PubMed Central PMCID: PMC2863217.

Modica S, Murzilli S, Salvatore L, Schmidt DR, Moschetta A. Nuclear bile acid receptor FXR protects against intestinal tumorigenesis. *Cancer Research* **2008** Dec 1;68(23):9589-94. PubMed PMID: 19047134.

Schmidt DR, Mangelsdorf DJ. Nuclear receptors of the enteric tract: guarding the frontier. *Nutrition Reviews* **2008** Oct;66(10 Suppl 2):S88-97. Review. PubMed PMID: 18844851; PubMed Central PMCID: PMC2741173.

Lee YK, Schmidt DR, Cummins CL, Choi M, Peng L, Zhang Y, Goodwin B, Hammer RE, Mangelsdorf DJ, Kliewer SA. Liver receptor homolog-1 regulates bile acid homeostasis but is not essential for feedback regulation of bile acid synthesis. *Molecular Endocrinology* **2008** Jun;22(6):1345-56. PubMed PMID: 18323469; PubMed Central PMCID: PMC2409274.

Katona BW, Cummins CL, Ferguson AD, Li T, Schmidt DR, Mangelsdorf DJ, Covey DF. Synthesis, characterization, and receptor interaction profiles of enantiomeric bile acids. *Journal of Medicinal Chemistry* **2007** Nov 29;50(24):6048-58. PubMed PMID: 17963371.

Moore DD, Kato S, Xie W, Mangelsdorf DJ, Schmidt DR, Xiao R, Kliewer SA. International Union of Pharmacology. LXII. The NR1H and NR1I receptors: constitutive androstane receptor, pregnene X receptor, farnesoid X receptor alpha, farnesoid X receptor beta, liver X receptor alpha, liver X receptor beta, and vitamin D receptor. *Pharmacological Reviews* **2006** Dec;58(4):742-59. Review. PubMed PMID: 17132852.

LIST OF FIGURES AND TABLES

LIST OF ABBREVIATIONS

1,2-DMH	1,2-dimethylhyrazine
ABC	ATP-binding cassette
ACTH	adrenocorticotropic hormone
AKR	aldo-keto reductase
AKT	also known as Protein Kinase B (PKB)
ALT	alanine aminotransferase
AOM	azoxymethane
APC	adenomatosis polyposis coli
ASBT	apical sodium-dependent bile acid transporter
AST	aspartate aminotransferase
βgal	β galactosidase
BrdUrd	bromodeoxyuridine
BSA	bovine serum albumin
BSEP	bile salt export pump
CA	cholic acid
CAR (NR1I3)	constitutive androstane receptor
CDC25	cell division cycle 25
CDCA	chenodeoxycholic acid
CDK	cyclin-dependent kinase
CMC	critical micellar concentration
CRAD2	*cis*-retinol/androgen dehydrogenase 2
CRC	colorectal cancer
CYP	cytochrome P450
ChIP	chromatin immunoprecipitation
DBD	DNA binding domain

DCA	deoxycholic acid
DMSO	dimethyl sulfoxide
DR3	direct repeat 3
EGF	epidermal growth factor
EGFR	epidermal growth factor receptor
ERK	extracellular signal-regulated kinase
FABP	fatty acid binding protein
FGF	fibroblast growth factor
FGFR	fibroblast growth factor receptor
FXR (NR1H4)	farnesoid X receptor
FXRE	FXR response element
GST	glutathione S-transferase
HDCA	hyodeoxycholic acid
HNF4 (NR2A)	hepatocyte nuclear factor 4
HSD	hydroxysteroid dehydrogenase
IBABP	ileal bile acid binding protein
IBAT	ileal bile acid transporter
IR1	inverse repeat 1
JNK	c-Jun N-terminal kinase
K-RAS	Kirsten rat sarcoma viral oncogene
LBD	ligand binding domain
LC/MS	liquid chromatography/mass spectrometry
LCA	lithocholic acid
LRH-1 (NR5A2)	liver receptor homolog-1
LXR (NR1H)	liver X receptor
MAPK	mitogen activated protein kinase
MCA	muricholic acids
MEK	MAP kinse-ERK kinase

MRP	multidrug resistance-associated protein
MYC	myelocytomatosis oncogene
NTCP	Na/taurocholate cotransporting polypeptide
OST	organic solute transporter
PARP	poly ADP-ribose polymerase
PBS	phosphate buffered saline
PCNA	proliferating cell nuclear antigen
PI3K	phosphoinositide 3-kinase
PKC	protein kinase C
PPAR (NR1C)	peroxisome proliferator activated receptor
PXR (NR1I2)	pregnane X receptor
QPCR	quantitative RT-PCR
RAR (NR1B)	retinoic acid receptor
RLU	relative luciferase units
ROR (NR1F)	RAR-related orphan receptor
RT-PCR	reverse transcription-polymerase chain reaction
RXR (NR2B)	retinoid X receptor
SHP (NR0B2)	small heterodimer partner
SLC	solute carrier
SMAD3	mothers against DPP homolog 3
SPF	specific pathogen free
STAR	steroidogenic acute regulatory protein
SULT	sulfotransferase
TGF	transforming growth factor
TGR5 (GPBAR1)	G protein-coupled bile acid receptor 1
TR (NR1A)	thyroid receptor
tCA	tauro-cholic acid
tCDCA	tauro-chenodeoxycholic acid

tDCA	tauro-deoxycholic acid
tLCA	tauro-lithocholic acid
tUDCA	tauro-ursodeoxycholic acid
tMCA	tauro-muricholic acids
tHDCA	tauro-hyodeoxycholic acid
UDCA	ursodeoxycholic acid
VDR (NR1I1)	vitamin D receptor
VDRE	VDR response element
VP-16	viral protein 16

CHAPTER 1
Background and Objective

1.1 Introduction

Gastrointestinal tissues express a distinct group of nuclear receptors that function as regulators of bile acid and xenobiotic metabolism. This group of functionally and evolutionarily related proteins include the bile acid receptor (FXR), the vitamin D receptor (VDR), and the xenobiotic receptors, pregnane X receptor (PXR) and constitutive androstane receptor (CAR). By acting as sensors of absorbed lipids, these transcription factors allow intestinal cells to activate appropriate gene expression programs in response to nutrients, toxic dietary components, and microbial metabolites.

I begin this introductory chapter with pertinent background on nuclear receptor biology and the basis for the classification of an enteric nuclear receptor network. Subsequently, I review the major function of bile acids and why some bile acids are considered etiologic agents in colorectal cancer (CRC). Finally, I describe current understanding of how FXR and related nuclear receptors function in bile acid metabolism, and conclude with the primary objective of my dissertation and an outline of the studies described in subsequent chapters.

1.2 The Nuclear Receptor Superfamily

The nuclear receptor superfamily comprises 48 ligand-activated transcription factors that have been grouped on the basis shared structural features (Mangelsdorf, 1995). A DNA binding domain (DBD) in most nuclear receptors allows binding to conserved elements in the regulatory regions of specific groups

of genes, while the adjacent ligand binding domain (LBD) functions to activate or inactivate transcription when bound by a small diffusible molecule referred to as its ligand. This unique property has rendered nuclear receptors particularly useful as intracellular sensors for endocrine hormones and dietary lipids. Nuclear receptors typically bind DNA either as homodimers or heterodimers, although some may also bind as monomers. The retinoid X receptors (RXRs) are obligate heterodimeric partners, meaning that all nuclear receptor heterodimers must include one of the RXRs.

The nuclear receptor superfamily can be subdivided into four groups based on the type of ligand bound and the DNA binding mechanism (Chawla, 2001). The first of these are the endocrine receptors that bind DNA as homodimers. These include the estrogen, androgen, progesterone, glucocorticoid, and mineralocorticoid receptors, which all bind with nanomolar affinity to systemically-circulating steroid hormones synthesized by endocrine tissues. The transcriptional programs activated by these receptors provide negative feedback to the endocrine system to turn off ligand synthesis. The second group of receptors form heterodimers with RXR and are activated by a wide range of dietary lipids including fatty acids (activate peroxisome proliferator-activated receptors, PPARs), bile acids (activate FXR), xenobiotics (activate PXR and CAR), and a variety of cholesterol metabolites referred to as oxysterols (activate liver X receptors, LXRs). Such ligands exist at relatively high concentrations, particularly within enterohepatic tissues and portal circulation, where they bind their cognate receptors with micromolar affinity. In contrast to the endocrine receptors, the metabolic receptors activate gene expression programs that turn on catabolic pathways for dietary lipids. The third group comprises receptors for vitamins A and D (retinoic acid receptors, RARs and VDR respectively), and the thyroid hormone receptors (TRs). These also function as RXR heterodimers, yet

their ligands are synthesized in the body from precursors that are derived from the diet; or in the case of vitamin D, sunlight. Like other endocrine receptors, this group binds ligands with high affinity. It is now known that VDR also binds bile acids and thus satisfies the criteria of both the second and third groups (Makishima, 2002; Nehring, 2007). The final group includes receptors with no known ligands, which are referred to as orphan nuclear receptors.

An additional layer of complexity is afforded by receptors that function as RXR heterodimers. RXR itself is activated by the endogenous vitamin A derivative, 9-cis retinoic acid. In theory, therefore, heterodimers can be activated by two ligands, that of RXR and that of its partner. In reality, RXR heterodimers exhibit three modes of activation: permissive, conditional, and non-permissive (Shulman, 2004). Permissive heterodimers can be activated by either receptor's ligand, and are exemplified by the dietary lipid-sensing receptors (e.g., LXRs). In contrast, conditional heterodimers can only be activated by RXR agonist when the partner ligand is also present (e.g., RARs). Non-permissive heterodimers are endocrine receptors in which the RXR agonist has no effect on the activity of the heterodimer (e.g., TRs). RXR/VDR heterodimers can function as both non-permissive and permissive types, since the VDR can bind both an endocrine hormone and a bile acid.

1.3 The Enteric Nuclear Receptor Clade

Sequenced-based clustering of the nuclear receptor superfamily has provided valuable information regarding the evolutionary relatedness of receptors and has led to a better understanding of the function of individual receptors. One way to provide more information regarding this large family of transcription factors is to use anatomical-based expression profiling to cluster the nuclear receptor superfamily on the basis of shared expression patterns. The discovery of

bile acids as the endogenous ligands for FXR is a prime example of how expression analysis was used to characterize receptor function. The tell-tale expression pattern of FXR in tissues involved in bile acid synthesis and circulation was part of the rationale to pursue the bile acid receptor hypothesis (Makishima, 2002). The advantages of understanding the global expression pattern of all nuclear receptors are that 1) new targets or functions can be identified on the basis of common expression, 2) predictions can be made regarding coordinated transcriptional programs within a given tissue involving multiple receptors with known functions, 3) physiologic processes regulated by distinct receptors can be linked, 4) information can be gathered regarding the coordination of physiological processes involving multiple organs and levels of regulation, and finally 5) predictions can be made regarding the systems that regulate the expression of nuclear receptor themselves.

A recent study used quantitative real-time PCR to determine the relative expression level of the entire nuclear receptor superfamily in 39 distinct tissues (Bookout, 2006). A systems-biology approach was taken to cluster the nuclear receptors based on the similarity of these expression profiles (Figure 1.1). Broadly, the superfamily divides into two major divisions; one whose members regulate reproduction, development and growth; the other whose members regulate nutrient uptake, metabolism, and excretion. FXR falls into a clade of nuclear receptors that function largely in both bile acid and xenobiotic metabolism (Bookout, 2006; Moore, 2006). The members of this group are expressed in the gastrointestinal tract and like FXR, most are involved in nutrient uptake and/or the elimination of drugs and toxic dietary components (Kliewer, 2002; Handschin, 2003). Within this group FXR, VDR, PXR and CAR function as RXR heterodimers and are activated by dietary lipids. Although the other members of this group, LRH-1, HNF4α, HNF4γ, SHP, and RORγ are not ligand

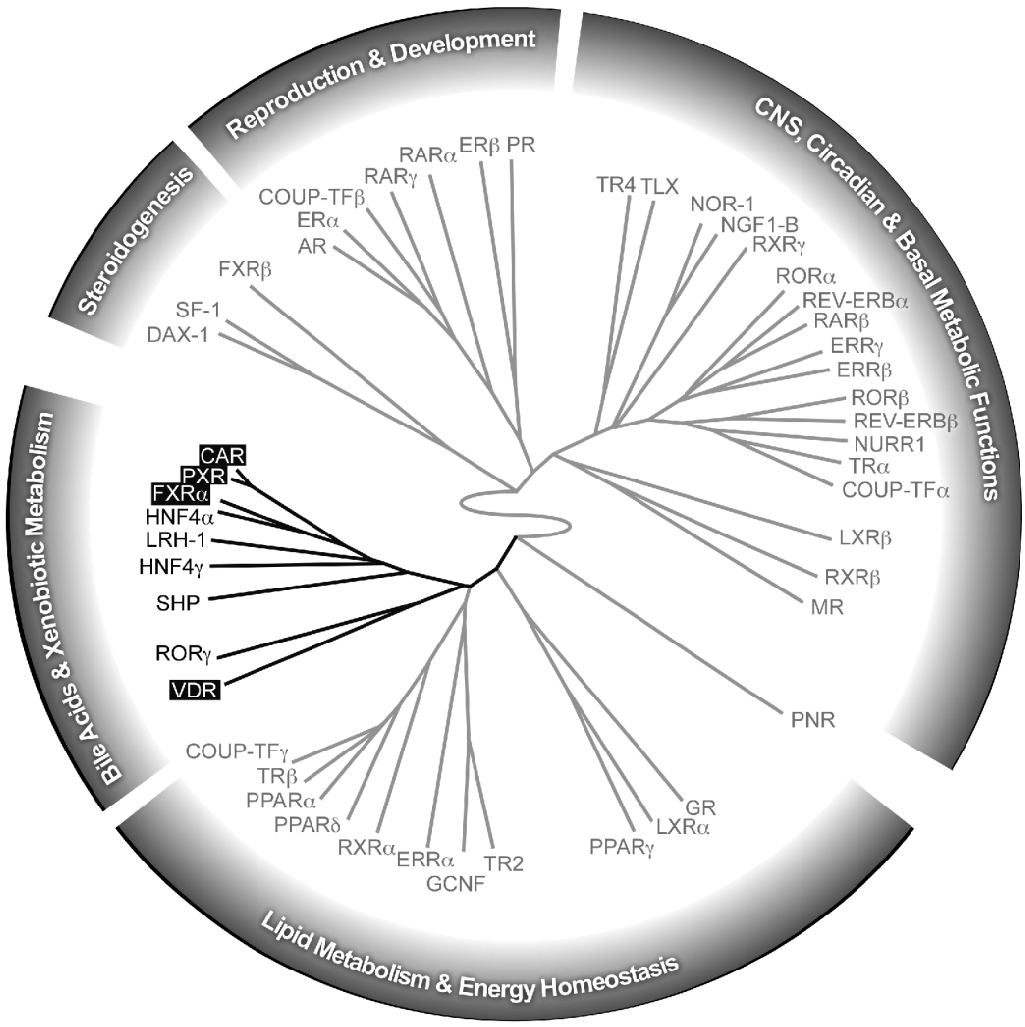

Figure 1.1 Dendrogram of enteric nuclear receptors.
The dendrogram was created using hierarchical, unsupervised clustering of the 49 mouse nuclear receptor tissue expression profiles. Branch length denotes relatedness in organism-wide tissue expression profiles. The enteric nuclear receptor clade is shown in black. All members of this group are expressed in the intestine. Receptors in black boxes denote ligand-activated RXR heterodimers discussed in the text. Note that in mice there are two FXR genes (FXRα and FXRβ). FXRβ is a pseudogene in humans and in mice its ligand and function are unknown. For simiplicity, the text refers to FXRα as FXR. Figure adapted from Bookout et al. (2006).

activated, some of them are known to mediate or moderate the activity of the ligand-activated receptors in this group.

1.4 Bile Acids and Colorectal Cancer

Bile acids are amphipathic sterols synthesized from cholesterol in the liver and secreted into the intestine where they play an essential role in emulsifying dietary lipids. In the terminal small intestine most bile acids are reabsorbed and returned to the liver through a process called enterohepatic circulation (Hofmann, 2009). Approximately five percent of bile acids escape reabsorption and enter the large intestine where they are efficiently metabolized by colonic flora (Ridlon, 2006). The bacterial bile acid metabolites, termed secondary bile acids, are more hydrophobic than primary bile acids produced by the liver. The major secondary bile acids in humans are deoxycholic acid (DCA) and lithocholic acid (LCA). In cultured cells it has been shown that these hydrophobic bile acids cause direct damage to cell membranes and induce the generation of reactive oxygen species resulting in DNA damage, apoptosis, and necrosis (reviewed in Bernstein, 2009; Perez, 2009). Furthermore, secondary bile acids have been shown to promote intestinal and hepatic tumorigenesis in animal models, and their concentrations are reportedly higher in patients with colorectal cancer (Reddy, 1977b; Reddy, 1979; Kim, 2007b; Yang, 2007). These studies have led to the idea that chronic exposure to elevated concentrations of secondary bile acids may contribute to the pathogenesis of cancer in gastrointestinal and hepatic tissues (Nagengast, 1995; Bernstein, 2005). In particular, a strong link has been made between increased colonic levels of bile acids and CRC. The high incidence of CRC in western nations is thought to be the result of a high-fat diet and the associated increase in secondary bile acids (Reddy, 1981; Lipkin, 1999). Fortunately, cells of the intestine, liver, and kidney are equipped with enzymes that detoxify bile acids

through the addition of functional groups that decrease their hydrophobicity and speed their elimination from the body. In many cases expression of these enzymes is controlled by members of the enteric nuclear receptor clade (see below).

1.5 Bile Acid Synthesis and Transport is Regulated by FXR

FXR activity determines the total level of bile acids in the body and it regulates the movement of bile acids between organ systems (Eloranta, 2008). These functions of FXR are the result of its ability to transcriptionally regulate key enzymes involved in bile acid synthesis and hepatic and intestinal transporters involved in enterohepatic circulation.

The enzymatic conversion of cholesterol to bile acids is regulated by feedback repression, and FXR plays a central role in this process (Chiang, 2002; Russell, 2003). In the terminal small intestine, bile acids activate FXR and induce the expression of the fibroblast growth factor 15/19 (FGF15/19), an endocrine hormone that signals to the liver to repress expression of the rate limiting enzyme in bile acid synthesis CYP7A1 (Inagaki, 2005). In liver, FXR induces the expression of a transcriptional repressor, small heterodimer partner (SHP), which cooperates with FGF15/19 to suppress bile acid synthesis. Loss of FXR in mice results in de-repression of bile acid synthesis genes and expansion of the bile acid pool (Sinal, 2000).

Major bile acid transporters in the liver include the bile salt export pump (BSEP) and the sodium taurocholate cotransporter (NTCP), both of which are regulated at the transcriptional level by FXR (Kullak-Ublick, 2000a; Kullak-Ublick, 2000b). The intracellular concentration of bile acids in hepatocytes is estimated to be in the low micromolar range, while in hepatic bile their concentration is as high as 40 millimolar (Hofmann, 1999b). The active transport

of bile acids into bile is carried out by BSEP and is positively regulated by FXR (Ananthanarayanan, 2001). At the sinusoidal membrane, NTCP and other transporters function in the reclamation of bile acids returning from the intestine via the portal circulation. NTCP is negatively regulated by FXR, and in the setting of cholestasis, this regulation serves to protect the hepatocyte from exposure to toxic levels of bile acids (Denson, 2001; Kullak-Ublick, 2004). Thus, FXR coordinates the synthesis of bile acids with their export from hepatocytes. Loss of FXR results in hepatocellular carcinoma in older mice, presumably as a result of the toxic effects of high bile acid levels in the liver (Yang, 2007).

Although passive absorption of bile acids occurs in all segments of the small and large intestine (Schiff, 1972), in the distal small intestine the reabsorption of bile acids is a highly efficient process that is regulated by in part by FXR (Hofmann, 2009; Kullak-Ublick, 2004). Active transport of bile acids across the brush border membrane is mediated by the ileal bile acid transporter (IBAT), also known as the apical sodium-dependent bile acid transporter (ASBT). This process does not appear to be regulated by FXR. At the basolateral membrane, bile acid efflux into the portal circulation occurs via the heterodimeric organic solute transporter (OST) alpha/beta, both subunits of which are upregulated by FXR (Dawson, 2005; Landrier, 2006). Finally, FXR upregulates fatty acid binding protein 6 (FABP6) also known as the ileal bile acid binding protein (IBABP), which binds to bile acids in the cytosol and may facilitate intracellular bile acid transport (Gong, 1994; Grober 1999).

1.6 Nuclear Receptors Regulate Bile Acid Detoxification

In addition to regulating synthesis and transport, nuclear receptors also control the biological activity of bile acids by regulating their rate of catabolism. Several xenobiotic/drug metabolizing pathways involving phase I and II enzymes

have been shown to contribute to the detoxification of secondary bile acids. While first-pass metabolism by the liver has been regarded as the major pathway for xenobiotic catabolism, it is now recognized that the intestine expresses many of the same enzymes that breakdown xenobiotic compounds as the liver, and thereby contributes to the catabolism of xenobiotics (Berggren, 2007; Kutuzova, 2007). The two most abundantly expressed phase I (oxidation) enzymes in the intestine are CYP3A4 and CYP2B6 (the mouse orthologs are CYP3A11 and CYP2B10 respectively). The genes encoding both enzymes are induced by PXR and CAR (Sueyoshi, 1999; Maglich, 2002; Tirona, 2003; Gnerre, 2004; Ma, 2007), while *CYP3A4* is also induced by VDR and possibly FXR (Schmiedlin-Ren,1997; Makishima, 2002; Matsubara, 2008; Thummel, 2001). CYP3A enzymes have been shown to detoxify cholestatic bile acids such as LCA (Araya, 1999; Xie, 2001). Phase II (conjugating) enzymes regulated by nuclear receptors in the intestine include sulfotrasferases (SULTs) and glutathione S-transferases (GSTs). The bile acid sulfotransferase, SULT2A1, is regulated in liver by PXR and CAR and promotes excretion of bile acids such as LCA (Sonoda, 2002; Wagner 2005). SULT2A1 has also been shown to be up-regulated by VDR and FXR in hepatic and intestinal cell lines (Echchgadda, 2004; Song, 2001). A number of GSTs are up-regulated by PXR and CAR ligands in the intestine (Maglich, 2002). In general, this class of enzymes, which catalyze the conjugation of glutathione to various chemical substrates including xenobiotics and carcinogens, are thought to reduce oxidative stress and protect from cancer (Grubben, 2001). Their role in bile acid metabolism is not known.

While FXR is considered the major bile acid sensor, some bile acids also activate VDR and PXR (Staudiger, 2001; Xie, 2001; Goodwin, 2003; McCarthy, 2005). Thus, not only do FXR, VDR, CAR, and PXR regulate many of the same

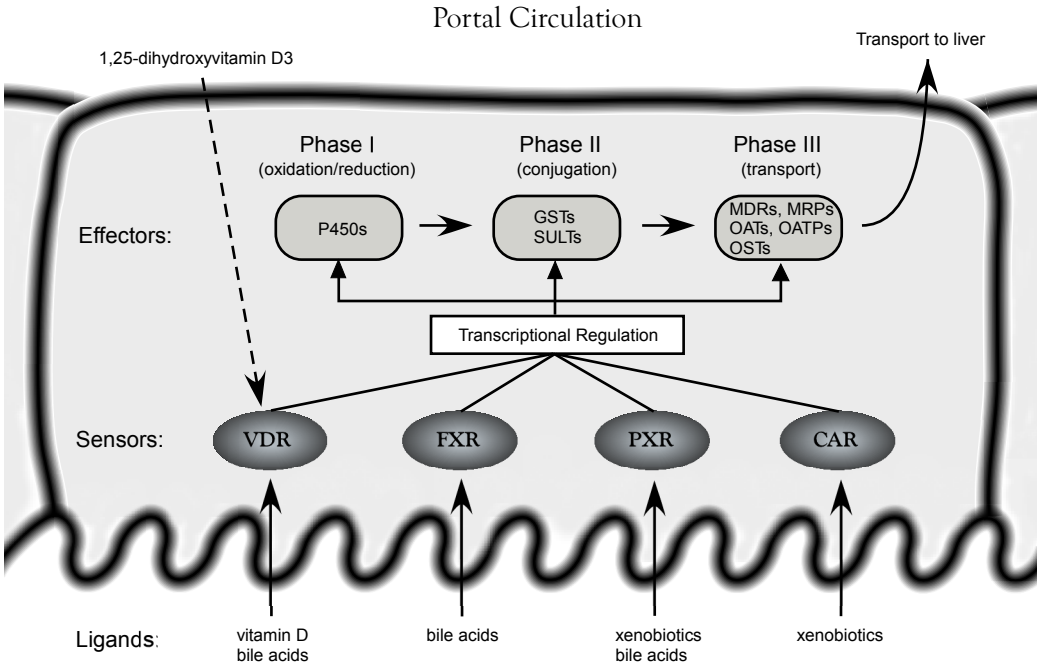

Figure 1.2 Regulation of the intestinal detoxification system by the enteric nuclear receptor clade.
As a group, the vitamin D receptor (VDR), the bile acid receptor (FXR), and the xenobiotic receptors (PXR and CAR) function as sensors in the gut to protect the body from excess exposure to toxic dietary lipids. All three phases of xenobiotic and bile acid metabolism, including oxidation/reduction, conjugation, and transport, are regulated at the transcriptional level by this group of receptors within the intestine. The robustness of the intestinal detoxification system is a consequence of the ligand binding characteristics of these receptors. While each receptor binds a unique set of ligands with high affinity, most also bind common ligands with lower affinity (e.g., bile acids). The result is a system adapted to a wide range of insults that is able to limit damage should one of its members become compromised. The redundancy in ligand binding reflects the important evolutionary conservation of this subgroup of receptors.

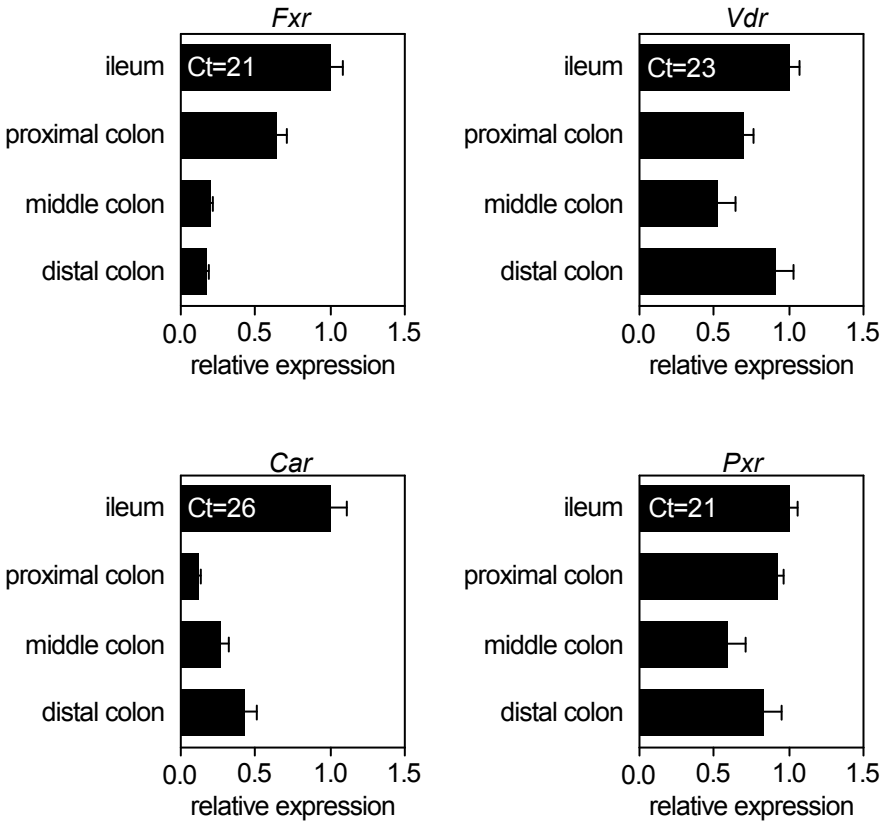

Figure 1.3 Profile of enteric nuclear receptor expression in mouse intestine.
Relative mRNA expression of the indicated nuclear receptors in 3-5 centimeter segments of the small and large intestine. The ileum segment was immediately proximal to the ileocecal valve. The colon (from anal verge to attachment to cecum) was divided into three equal length segments. mRNA was measured by quantitative RT PCR. The average cycle time (Ct) in the ileum is shown. The level of mRNA expression was normalized to c*yclophilin* and graphed relative to ileum. Data represent the mean ± SEM of 5-6 animals per group. See Chapter 2 for description of methods.

detoxifying enzymes, there is also overlap in the ligands that activate them (Figure 1.2; Schmidt, 2008).

Interestingly, although FXR, VDR, CAR, and PXR are expressed in the colon (Figure 1.3), little is known about their function in this organ. Since ligands for these receptors are present in the colon it is reasonable to assume that they contribute to colon physiology. Consistent with their role in bile acid and xenobiotic metabolism in the liver and small intestine, these receptors may constitute a functional detoxification system for bile acids in the colon.

1.7 Statement of Purpose

The fact that nuclear receptor expression and activity is often altered in cancer has prompted an interest in defining the role of nuclear receptors in cancer progression. In addition, the amenability of nuclear receptors to pharmacological modulation makes them prime candidates for molecularly targeted therapies. Since FXR is a major regulator of bile acid metabolism, and elevated levels of secondary bile acids have been shown to promote CRC, I have sought to assess the role of FXR in the pathogenesis of CRC and understand mechanisms responsible for tumor promotion by bile acids. Since little is known about the function of FXR in the colon, my studies have also been designed to indentify novel functions of FXR and related nuclear receptors in colon physiology and bile acid homeostasis.

To assess whether FXR plays a role in the pathogenesis of colorectal cancer, I examined effects of biallelic loss of *Fxr* (*Fxr*–/–) on tumor incidence in chemical (dimethylhydrazine and azoxymethane) and genetic (SMAD3 and K-RAS) mouse models of colon cancer. Results from chemical-induced tumor studies showed that loss of FXR in mice increased susceptibility to colon cancer. Loss of function studies involving *Fxr*–/– and *Smad3*–/– double knockout mice

were discontinued since these animals did not breed. Studies in the oncogenic K-RAS model are ongoing. In addition a gain of function study was performed that involved the treatment of *Smad3*–/– mice with bile acids and synthetic FXR agonists. This study was designed to investigate the potential of FXR agonists as chemopreventive agents in a model of CRC. One of these compounds reduced bile acid levels in the colon and decreased the incidence of CRC. Data from these studies are presented in Chapter 2.

To investigate novel functions of FXR in the colon, a transcriptional profiling study was performed. *Akr1b7* was identified as an FXR target gene in the intestine and was shown to detoxify bile acids. These data are presented in Chapter 3.

To address the mechanism underlying tumor promotion by bile acids, I investigated the effect of bile acids on proliferation in cultured cells (Chapter 4) and mouse intestine (Chapter 5). These studies revealed that the phosphoinositide 3-kinase signaling pathway plays a role in bile acid-induced proliferation *in vivo*. Implications for the contribution of dietary factors to intestinal proliferation are discussed.

Finally, Chapter 6 describes the unexpected finding that fat-soluble vitamins A and D regulate bile acid biosynthesis. The mechanism underlying these effects is presented and the implication for colon cancer prevention is discussed.

CHAPTER 2

Bile Acids and FXR in Mouse Models of Colorectal Cancer

2.1 Introduction

The experiments described in this chapter test the hypothesis that loss of FXR or pharmacological activation of FXR affects the incidence and rate of tumorigenesis in mouse colon. Results from these studies were subsequently used to design additional experiments to investigate a mechanism for the contribution of FXR and bile acids to the pathogenesis of colorectal cancer. These studies are described in subsequent chapters.

To test whether loss of FXR affects tumorigenesis, I treated wild-type and *Fxr*-null (*Fxr*–/–) mice with chemical carcinogens commonly used to induce tumors in the colon of mice. In addition, *Fxr*–/– mice were bred into a number of genetic colon cancer models including *Smad3*–/–, *K-ras*$^{LSL\text{-}G12D}$, and *Apc*$^{Min/+}$. Studies in *Apc*$^{Min/+}$ mice were conducted in collaboration with Dr. Antonio Moschetta at the Mario Negri Institute in Italy and are not included in this chapter.

While the *Apc*$^{Min/+}$ mouse is the most commonly used model of intestinal tumorigenesis it may not represent the best model for colon cancer. One of the problems with this model is a lack of tumors in the colon. Greater than 95% of tumors occur in the small intestine and the vast majority of these are benign polyps. In contrast, *Smad3*–/– mice develop tumors exclusively in the proximal colon and rectum and many are malignant neoplasms that rapidly metastasize (Zhu, 1998). Thus, the location and behavior of tumors in *Smad3*–/– mice is similar to what is seen in human CRC. The development of CRC is a multi-step

process that begins with "at-risk mucosa" and proceeds through a hyper-proliferative stage to early adenoma, adenoma, and lastly frank carcinoma (Kinzler, 1996). The progression through these stages is driven by the accumulation of genetic mutations. Activation of oncogenic K-RAS in intestinal mucosa has been shown to result in a premalignant model of intestinal hyperplasia (Tuveson, 2004). The following two paragraphs contain pertinent background on the SMAD3 and K-RAS colon cancer models used in these studies.

TGFβ signaling regulates the expression of genes encoding extracellular matrix proteins and genes involved in cell cycle regulation (Massague, 1998). SMAD proteins transduce signals from TGFβ receptors to the nucleus. They associate with DNA site-specific proteins and activate or repress target genes. For example, in mammalian epithelial cells, SMADs 2, 3 and 4 mediate both cell cycle arrest and growth inhibition by up-regulation of p21 and p15 (CDK inhibitors) and down-regulation of MYC and CDC25 respectively. SMAD3 is expressed in the adult colon in mice, as is the TGFβ receptor and ligand (Zhu, 1998). *Smad3* heterozygous animals (*Smad3*+/–) have no observable phenotype. *Smad3*–/– mice have 20-30% reduced body weight and a shortened life span. 100% of inbred (129/Sv) *Smad3*–/– mice spontaneously develop colorectal adenocarcinomas between 18-24 weeks of age (Zhu, 1998). In hybrid (129/Sv; C57BL/6) mice, 30% develop colon tumors. The tumors occur in the proximal colon and rectum and often metastasize to mesenteric lymph nodes. In has been reported that *Smad3*–/– mice housed in a specific pathogen free (SPF) facility and followed for up to 9 months did not develop colon cancer (Maggio-Price, 2006). Upon infecting the mice with different species of *Helicobacter*, 50-60% developed colon cancer. Animals were reported to have widespread mucosal inflammation prior to development of tumors. Thus, the inflammatory response

to micro-organisms may contribute to the pathogenesis of colon cancer in this model.

K-RAS is a membrane-localized small GTPase which functions to transduce extracellular growth signals from receptor tyrosine kinases to downstream protein kinases (Karnoub, 2008). Mutations in *K-RAS* are detected in up to 50% of sporadic colorectal cancer (Calvert, 2002). One form of oncogenic K-RAS has been shown to cause gastrointestinal tumors in transgenic mice (Janssen, 2002). In the *K-ras*$^{LSL\text{-}G12D}$ mouse one of the *K-ras* genes has been replaced with the oncogenic *K-ras*^{G12D} gene preceded by a lox-stop-lox cassette. This allows expression of oncogenic *K-ras*^{G12D} from the endogenous locus only in Cre expressing cells. Colon-specific expression of *K-ras*^{G12D} resulted in 100% incidence of hyperplasia at one month of age; however, mice as old as one year did not develop colon cancer (Tuveson, 2004; Haigis 2008). When crossed with mice lacking APC, high-grade adenomas are formed (Haigis, 2008).

In addition to testing loss of FXR on tumor formation, I sought to determine whether gain of function affected tumorigenesis. To this end, I initially planned to generate a transgenic mouse expressing chimeric VP16-FXR in the colon. Since VP16 is a strong transcriptional activator this would allow me to evaluate the effects of constitutively active FXR on tumorigenesis. Questions regarding the relevance of VP16-coactivated FXR and the lack of a good colon-specific promoter caused me to abandon this approach. Instead, I obtained two synthetic bile acids that are potent agonists of FXR developed by Intercept Pharma to treat metabolic disorders. These compounds were administered for three months to *Smad3*–/– mice with the goal of determining whether pharmacological activation of FXR could affect tumor incidence in the *Smad3*–/– model. This study has been the first to examine whether FXR agonists have potential as chemopreventive agents for colorectal cancer.

2.2 Methods

2.2.1 Animals and Animal Husbandry

K-ras$^{LSL-G12D}$ (C57BL/6;129S background) mice generated in the Jacks Laboratory at MIT, Boston, MA and Tg(Fabp1-Cre) (FVB/N background) mice generated in the Gordon Laboratory at Washington University, St. Louis, MO were obtained from the Mouse Models for Human Cancer Consortium (MMHCC). *Smad3*+/– mice (129S and mixed C57BL/6;129S background) were obtained from the Parada Laboratory, UT Southwestern, Dallas, TX. Tg(Villin-Cre) (C57BL/6 background) mice were purchased from Jackson Laboratories (Stock #004586). *Fxr*–/– (pure 129S and pure C57BL/6 backgrounds) were available in the Mangelsdorf/Kliewer Laboratory. All animals were housed in the same specific-pathogen-free facility. Animals were maintained under a temperature controlled environment and 12 hour light/dark cycles with ad libitum access to water and irradiated rodent chow (TD.2916, Harlan-Teklad). Mice were euthanized by isofluorane or carbon dioxide inhalation and exsanguinated via the descending vena cava prior to tissue collection. All animal experiments were approved by the Institutional Animal Care and Research Advisory Committee at the University of Texas Southwestern Medical Center.

2.2.2 Animal Treatment and Diet

1,2-dimethylhydrazine (1,2-DMH, Sigma) dissolved in 0.9% saline, 1 mM EDTA, 10 mM sodium citrate, pH 6.5, was sterile filtered and administered by weekly intraperitoneal injection for 10 weeks at a dose of 20 mg/kg. The cumulative dose of 1,2-DMH was 200 mg/kg. Azoxymethane (AOM, Sigma) was dissolved in sterile saline and administered by weekly intraperitoneal injection for 5 weeks at a dose of 10 mg/kg. The cumulative dose of AOM was 50 mg/kg. For the AOM/FXR study a sixth injection was administered one month after the fifth

injection; therefore the cumulative AOM dose for this study was 60 mg/kg. Diets containing bile acids were prepared by Harlan-Teklad using TD.2016 base chow and either 2% (w/w) cholic acid, 2% (w/w) chenodeoxycholic acid, 2% (w/w) deoxycholic acid or 2% (w/w) lithocholic acid (all from Steraloids). Diets containing INT compounds were prepared by Harlan-Teklad using TD.2016 base chow and either 0.005% (w/w) INT-747 or 0.015% (w/w) INT-767 (both from Intercept). All diets were in pellet form, irradiated, and provided ad libitum. 30 mg/kg GW4064 in DMSO was administered by intraperitoneal injection four hours before sacrifice.

2.2.3 Measurement of Liver Enzymes and Plasma Bilirubin

Blood was collected in heparinized tubes and immediately centrifuged at 4°C, 500 g for 30 minutes. Plasma was stored for maximum 24 hours at 4°C. AST , ALT, and total bilirubin levels were measured using a VITROS® 250 chemistry analyzer (Johnson & Johnson).

2.2.4 Histology

Tissues were formalin-fixed for 48 hours at 4°C. 5 μm paraffin-embedded sections were cut and stained with hematoxylin and eosin. Sections were interpreted by a trained pathologist.

2.2.5 Fecal Bile Acid Analysis

Fecal pellets collected over 72 hours from individually-housed animals, were dried and pulverized. Bile acids were extracted from one gram of dried feces and measured by colorimetric assay for 3α-hydroxysteroid dehydrogenase (Sigma) activity at 340 nM (Turley, 1978).

2.2.6 Bile Acid Extraction and Analysis by LC/MS

To measure bile acid pool size, animals were weighed and euthanized by isofluorane inhalation. Liver, gallbladder, intestines, and attached mesentery were removed en bloc and homogenized in ethanol. Homogenates were heating to boiling, cooled, and then filtered. This step was repeated twice. Filtrates were combined and adjusted to a constant volume. For collection of hepatic bile, mice were anesthetized with avertin and placed on a 37°C slide warmer. The common bile duct was exposed through a 2-3 cm abdominal incision and cannulated (PE-10 tubing, BD Biosciences). The cannula was advanced to the common hepatic duct and bile was collected for 30 minutes. Hepatic and gallbladder bile was diluted in ethanol prior to analysis. Bile acids were resolved by reverse-phase liquid chromatography (C8 pre-column, C18 analytical column) and quantified by mass spectrometry with electrospray ionization in negative ion mode. The following unconjugated and taurine-conjugated bile acids were used as calibration standards: cholic acid (5β-cholanic acid-3α,7α,12α-triol); α-muricholic acid (5β-cholanic acid-3α,6β,7α-triol); β-muricholic acid (5β-cholanic acid-3α,6β,7β-triol); ω-muricholic acid (5β-cholanic acid-3α,6α,7β-triol); hyocholic acid (5β-cholanic acid-3α,6α,7α-triol); chenodeoxycholic acid (5β-cholanic acid-3α,7α-diol); deoxycholic acid (5β-cholanic acid-3α,12α-diol); hyodeoxycholic acid (5β-cholanic acid-3α,6α-diol); ursodeoxycholic acid (5β-cholanic acid-3α,7β-diol); murocholic acid (5β-cholanic acid-3α,6β-diol); lithocholic acid (5β-cholanic acid-3α-ol); taurocholic acid [5β-cholanic acid-3α,7α,12α-triol-N-(2-sulphoethyl)-amide]; tauro-α-muricholic acid [5β-cholanic acid-3α,6β,7α-triol-N-(2-sulphoethyl)-amide]; tauro-β-muricholic acid [5β-cholanic acid-3α,6β,7β-triol-N-(2-sulphoethyl)-amide]; tauro-ω-muricholic acid [5β-cholanic acid-3α,6α,7β-triol-N-(2-sulphoethyl)-amide]; taurohyocholic acid [5β-cholanic acid-3α,6α,7α-triol-N-(2-sulphoethyl)-amide]; taurochenodeoxycholic acid [5β-cholanic acid-3α,7α-diol-N-(2-sulphoethyl)-amide]; taurodeoxycholic acid [5β-cholanic acid-3α,12α-

diol-N-(2-sulphoethyl)-amide]; tauroursodeoxycholic acid [5β-cholanic acid-3α,7β-diol-N-(2-sulphoethyl)-amide]; taurohyodeoxycholic acid [5β-cholanic acid-3α,6α-diol-N-(2-sulphoethyl)-amide]; taurolithocholic acid [5β-cholanic acid-3α-ol-N-(2-sulphoethyl)-amide];]; and taurolithocholic acid 3-sulfate [5β-cholanic acid-3α-ol-N-(2-sulphoethyl)-amide 3-sulfate]. Deuterium-labeled chenodeoxycholic acid (5β-cholanic acid-3α,7α-diol-2,2,4,4-d4) was used as a recovery control. Dehydrocholic acid (5β-cholanic acid-3,7,12-trioxo) was used as sample loading control.

2.2.7 *In situ* Hybridization.

Formaldehyde-perfused, paraffin-embedded sections of intestine were incubated with ^{35}S labeled sense and antisense probes against the FXR ligand binding domain (nucleotides 910-1367; GenBank Accession Number NM_009108.1). Slides were exposed at 4°C for 14 days.

2.2.8 RNA Extraction and Quantitative RT-PCR

Following euthanasia, tissues were collected and frozen immediately in liquid nitrogen. Intestinal segments were flushed with PBS prior to freezing. Total RNA was extracted using RNA STAT-60 (IsoTex Diagnostics). Four micrograms of RNA from each sample were DNAse treated and reverse transcribed using random hexamers. The resulting complementary DNA (cDNA) was analyzed by quantitative RT-PCR using a protocol previously described in detail (Bookout, 2003). Briefly, quantitative PCR reactions containing 25 ng of cDNA, 150 nmol of each primer, and SYBR® GreenER TM PCR Master Mix (Invitrogen) were carried out in triplicate in 384-well format using an ABI PRISM® 7900HT instrument (Applied Biosystems). Relative mRNA levels were calculated using the comparative CT method normalized to *cyclophilin* or *U36b4*. The primer sequences used for gene expression analyses are listed in Appendix A.

They were designed using Primer Express® software (Applied Biosystems) and validated as previously described (Bookout, 2003).

2.2.9 DNA Dot Blot

This method is described in Chapter 5.

2.2.10 Western Blot

This method is described in Chapter 5. Antibodies from Santa Cruz were used to detect K-RAS (clone F234, sc-30), PCNA (sc-56), and actin (sc-8432).

2.2.11 Statistical Analysis

Data are presented as mean ± SEM and were analyzed by two-tailed, unpaired Student's t-test. Tumor incidence was analyzed by Chi squared test. For both tests P values less than 0.05 were considered significant.

2.3 Results

2.3.1 Bile Acid Metabolism is Dysregulated in *Fxr*–/– Mice

Fxr–/– mice are viable and have no overt anatomic or developmental phenotypes. Major metabolic phenotypes include increased concentrations of cholesterol, triglyceride, and bile acids in serum and liver (Sinal, 2000). The underlying cause of disrupted bile acid homeostasis is decreased feedback repression of bile acid synthesis resulting in elevated expression of the rate-limiting enzyme in bile acid synthesis, CYP7A1 (Sinal, 2000). Tissue-specific disruption of FXR demonstrated that its activity in both liver and intestine is required to maintain bile acid homeostasis (Kim 2007a).

Initially it was reported that the bile acid pool size (quantity of bile acids in the body) and fecal bile acid excretion was decreased, a phenotype which was

attributed to decreased expression of the hepatic bile salt export pump (BSEP) (Sinal, 2000). A subsequent study by a different group reported that despite decreased BSEP expression, *Fxr*–/– mice had an enlarged bile acid pool size and increased excretion of fecal bile acids (Kok, 2003). Our laboratory has confirmed these results (Dr. Amy Liverman, dissertation 2004). To extend these studies, I used liquid chromatography coupled with mass spectrometry to analyze and quantitate bile acids in hepatic bile, gallbladder bile, and total enterohepatic tissue extracts of wild-type and *Fxr*–/– mice. In line with previous studies, bile acid pool size was significantly increased in *Fxr*–/– mice (Figure 2.1A). In addition, bile acid concentration in hepatic bile was increased more than 2-fold. This data suggests that despite lower levels of BSEP in *Fxr*–/– mice, bile acid secretion is increased. Since bile acid synthesis in *Fxr*–/– mice is increased, it is possible that other canalicular bile acid transporters such as MRP2 (St-Pierre, 2001) are involved in secreting excess bile acids. Notably, the total concentration of bile acid in the gallbladder was not significantly changed, indicating that the major function of this organ (to concentrate and store bile acids) is not compromised by the loss of FXR (Figure 2.1A). Analysis of gallbladder bile acids revealed that tauro-cholic acid (tCA) was increased relative to tauro-muricholates (tMCA) (Figure 2.1B). Since muricholates are more hydrophilic than cholic acid, this means that the bile acid pool in *Fxr*–/– mice is more hydrophobic than in wild-type mice. Hydrophobic bile acids such as DCA are associated with increased cholestasis and hepatotoxicity, while hydrophilic bile acids such as UDCA alleviate cholestasis and hepatoxicity (Heuman, 1991). The relative amount of tauro-deoxycholic acid (tDCA, a hydrophobic bile acid) was increased while tauro-ursodeoxycholic acid (tUDCA, a hydrophilic bile acid) was decreased. These changes in bile acid composition may contribute to the etiology of maladaptive phenotypes in *Fxr*–/– mice.

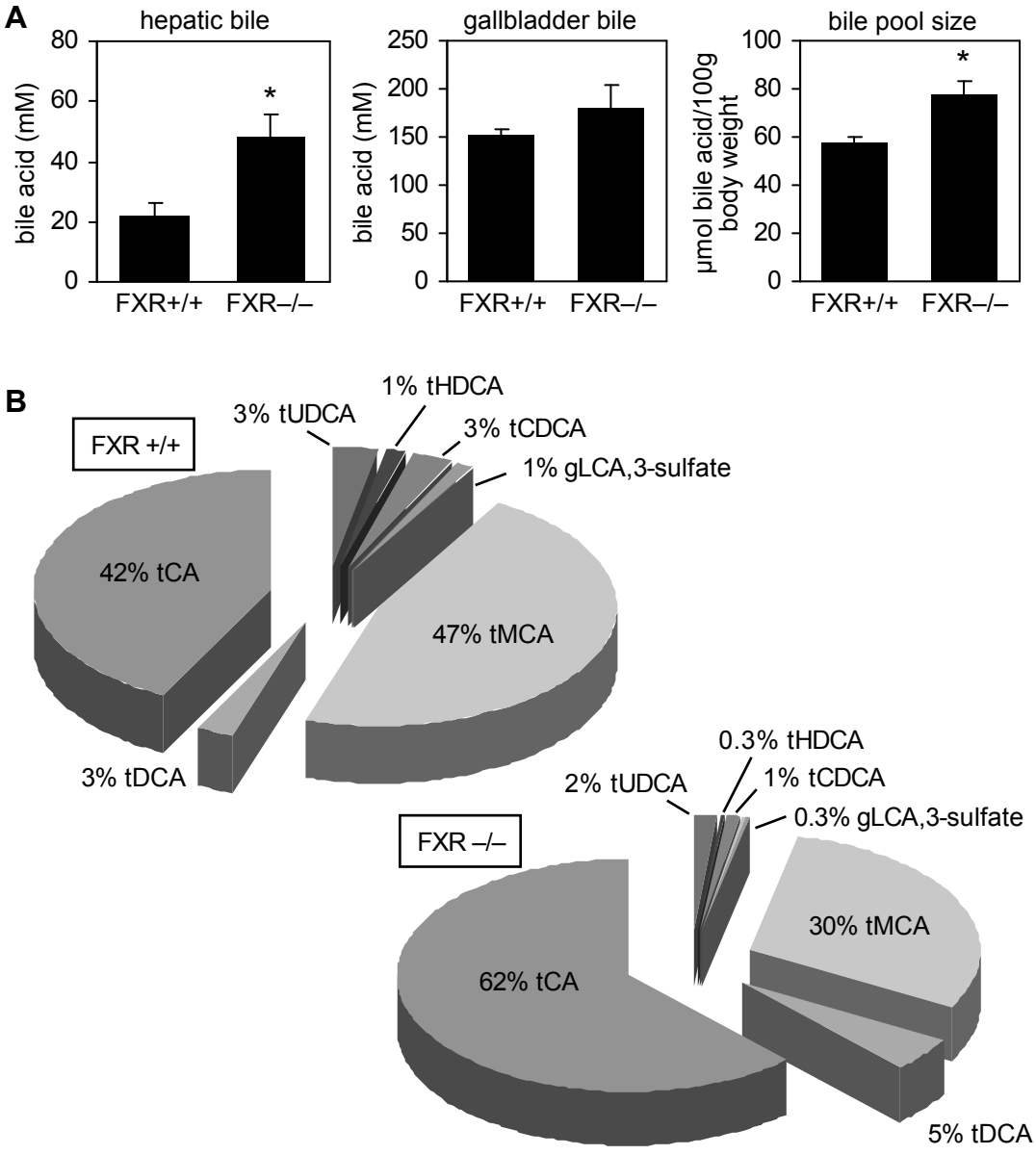

Figure 2.1 Bile acid levels are increased in *Fxr–/–* mice.
(A) Hepatic bile was collected from live, anesthetized animals via a cannula placed in the hepatic bile duct. Bile acids for pool size analysis were extracted from gallbladder, liver, intestine, and portal blood. Bile acids were quantitated by LC/MS. Results shown are the total concentration of bile acids in hepatic and gallbladder bile and the bile acid pool size in 3 month-old male mice of the indicated genotype. **(B)** Composition of gallbladder bile acids in mice of the indicated genotype. Data represent the mean ± SEM of 5 animals per group. * $p < 0.05$ compared to wild-type.

2.3.2 FXR Regulates Gene Transcription in Colon

In mice, tissues with the highest level of *Fxr* expression include the liver, ileum (terminal small intestine), and kidney. High expression has also been reported in the proximal small intestine and colon and lower expression in the adrenal (Lu, 2001; Bookout 2006). The expression of *Fxr* in various segments of the colon was determined by quantitative reverse transcriptase PCR (QPCR). Expression in the proximal colon was 25% lower than in the ileum and decreased by another 50% in the distal colon and rectum (Figure 2.2). In small intestine, *Fxr* expression is highest in the intestinal epithelium (Dr. Takeshi Inagaki, unpublished observation). To determine the location of *Fxr* expression in the colon, *in situ* hybridization was performed using a 458 nucleotide probe complementary (antisense) to the ligand binding domain of FXR. The antisense probe was validated using tissues from *Fxr*–/– mice and a sense probe was used as a negative control. Consistent with previous findings, *Fxr* expression was highest in the villous epithelium of the ileum (Figure 2.3A). In the proximal colon *Fxr* was expressed in the mucosa, and was absent in the submucosa and muscularis layers (Figure 2.3C). Expression in the distal colon was too low to be detected by standard *in situ* analysis (Figure 2.3A). Structurally, the colonic mucosa consists of crypts and surface epithelium. Proliferation-competent stem cells and proliferating progenitor cells reside at the base of the crypts (Sancho 2004). As cells travel from the base of the crypt to the epithelial surface they become terminally differentiated and lose the ability to divide. Eventually surface epithelial cells are shed into the colonic lumen and are replaced by newly differentiated cells from the crypts. In the proximal colon *Fxr* expression was only detected in the upper 1/3 of the crypts. Thus, *Fxr* appears to be expressed in the terminally differentiated epithelial cells of the colon. It has recently been

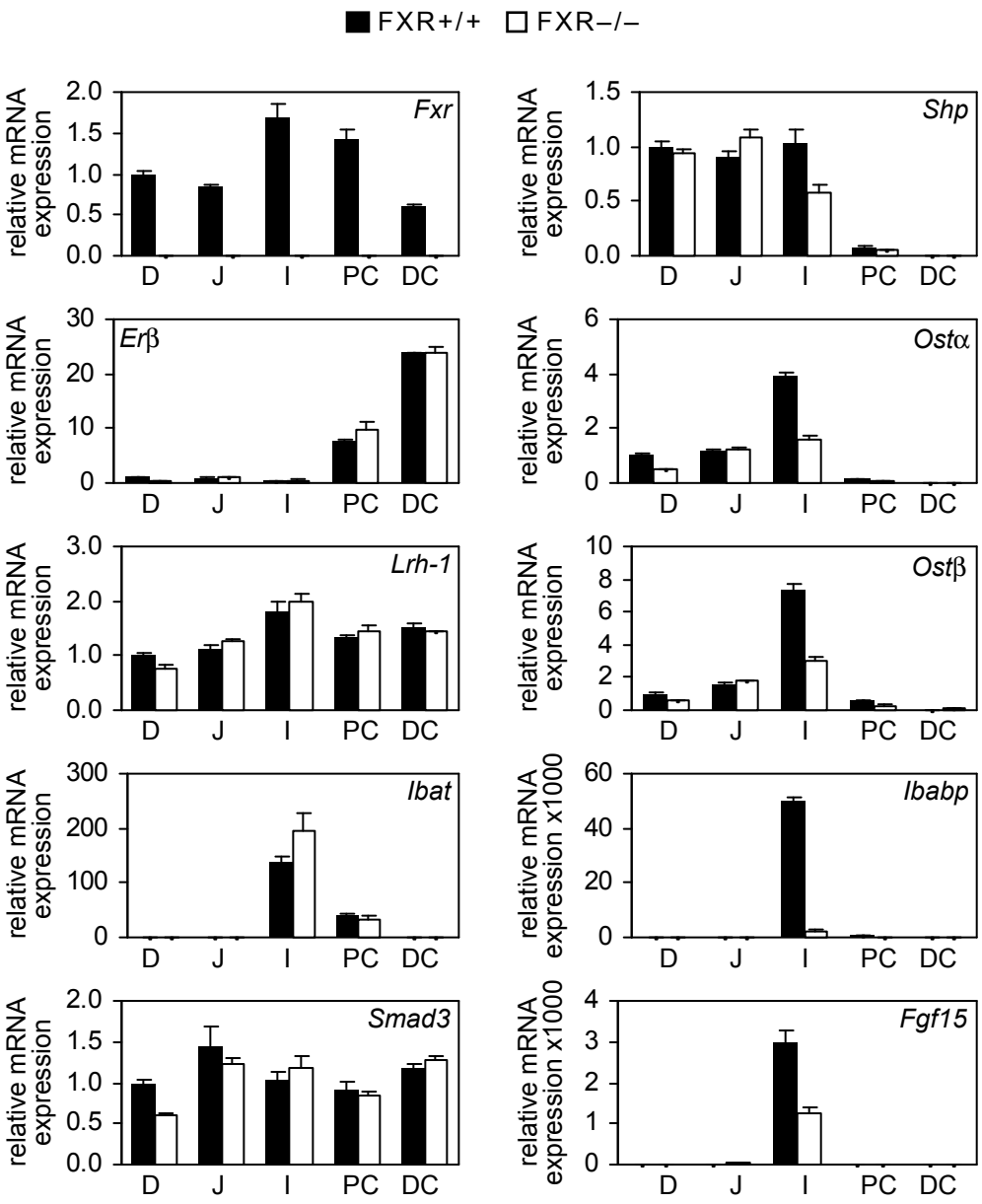

Figure 2.2 Gene expression profile in *Fxr*+/+ and *Fxr*–/– mouse intestine.
mRNA expression of the indicated genes in contiguous segements of the small and large intestine in *Fxr*+/+ and *Fxr*–/– mice was measured by QPCR. The level of mRNA expression was normalized to *cyclophilin* and graphed relative to wild-type duodenum. Data represent the mean ± SD of 3 measurements. D: duodenum, J: jejunum, I: ileum, PC: proximal colon, DC: distal colon.

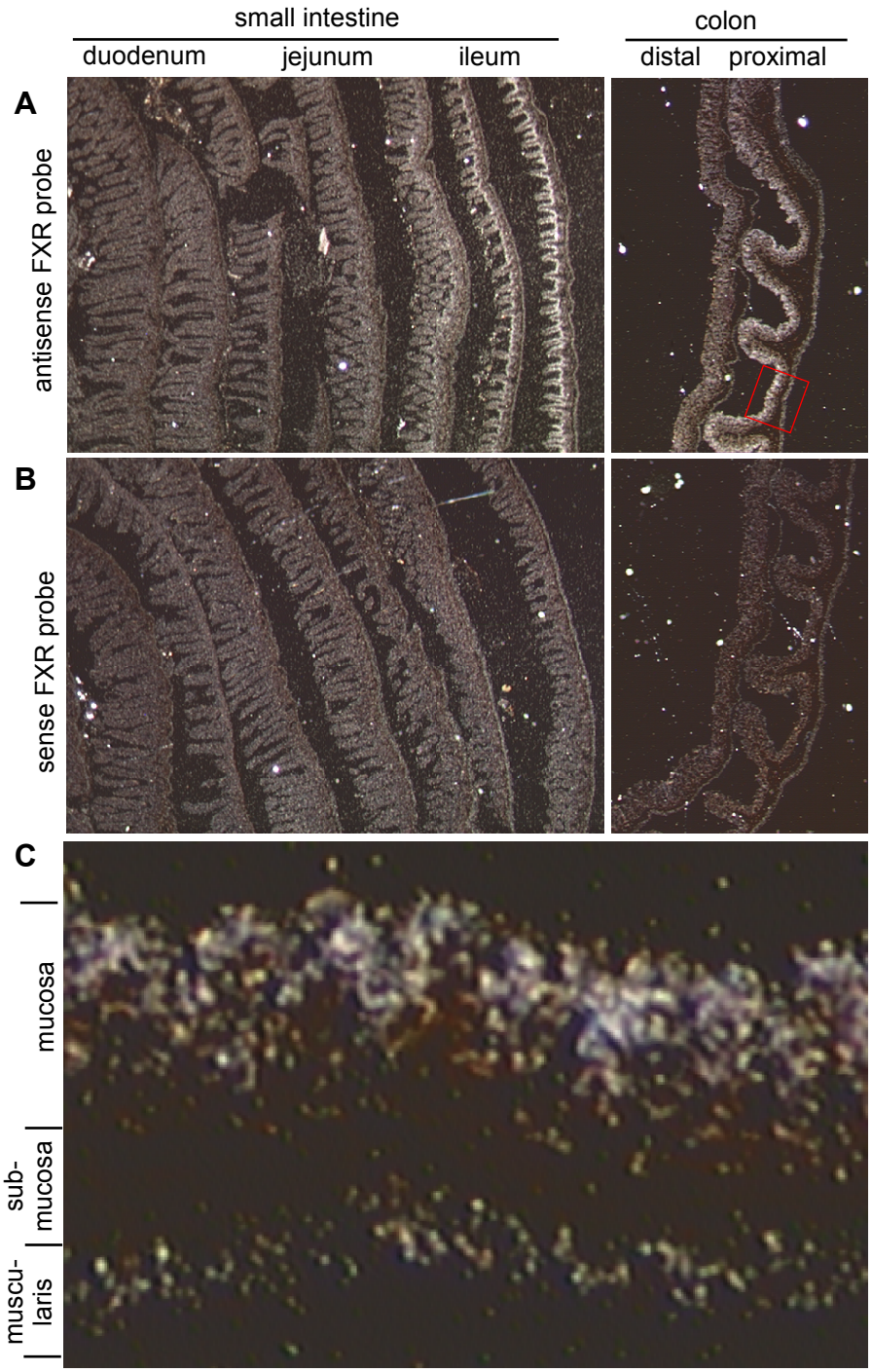

Figure 2.3 ***In situ*** **expression analysis of FXR.**
Darkfield image of silver-labeled probe. **(A and B)** Swiss-roll with mucosal surface oriented to the left. **(C)** High magnification of proximal colon region shown in (A). See text for details.

shown that FXR protein is also present only in the surface epithelium of mouse colon (Modica, 2008).

In liver and in small intestine FXR transcriptionally regulates expression of small heterodimer partner (*Shp*). The level of *Shp* induction following treatment with GW4064 (a potent and selective FXR agonist) was determined for various segments of the mouse colon. In cecum, the most proximal segment of the colon, *Shp* induction was comparable to that in ileum; however, while *Shp* was increased in more distal segments of the colon the level of induction was not significant. *Shp* expression in the mouse colon is exceedingly low (Figure 2.2 and average cycle time values shown in Figure 2.4A) and may account for the lack of *Shp* induction by FXR. It is possible that additional transcription factors required for *Shp* expression are not present in the colon. Other genes regulated by FXR in the ileum include ileal bile acid binding protein (*Ibabp*) and organic solute transporter β (*Ostβ*). Expression of both genes was dramatically increased by GW4064, demonstrating that FXR plays a functional role in gene regulation in the colon (Figure 2.4B; Table 2.1 and 2.2). The fold-induction of *Ibabp* and *Ostβ* in colon was much greater than in ileum (Table 2.1 and 2.2). A likely explanation for this finding is that endogenous ligands for FXR (bile acids) are normally present at comparatively low concentrations in the colon resulting in low basal expression of FXR target genes. Addition of exogenous ligand increases FXR target genes to levels normally seen the small intestine. This idea is supported by a comparison of cycle time (Ct) values in control and GW4064 intestines (Table 2.1 and 2.2). These data indicate that FXR is a target for pharmacological activation in the colon.

2.3.3 FXR Expression is Decreased in Colon Tumors

To determine whether loss of FXR affects susceptibility to colorectal cancer, I treated *Fxr*+/+ and *Fxr*–/– mice with the genotoxic agent 1,2-

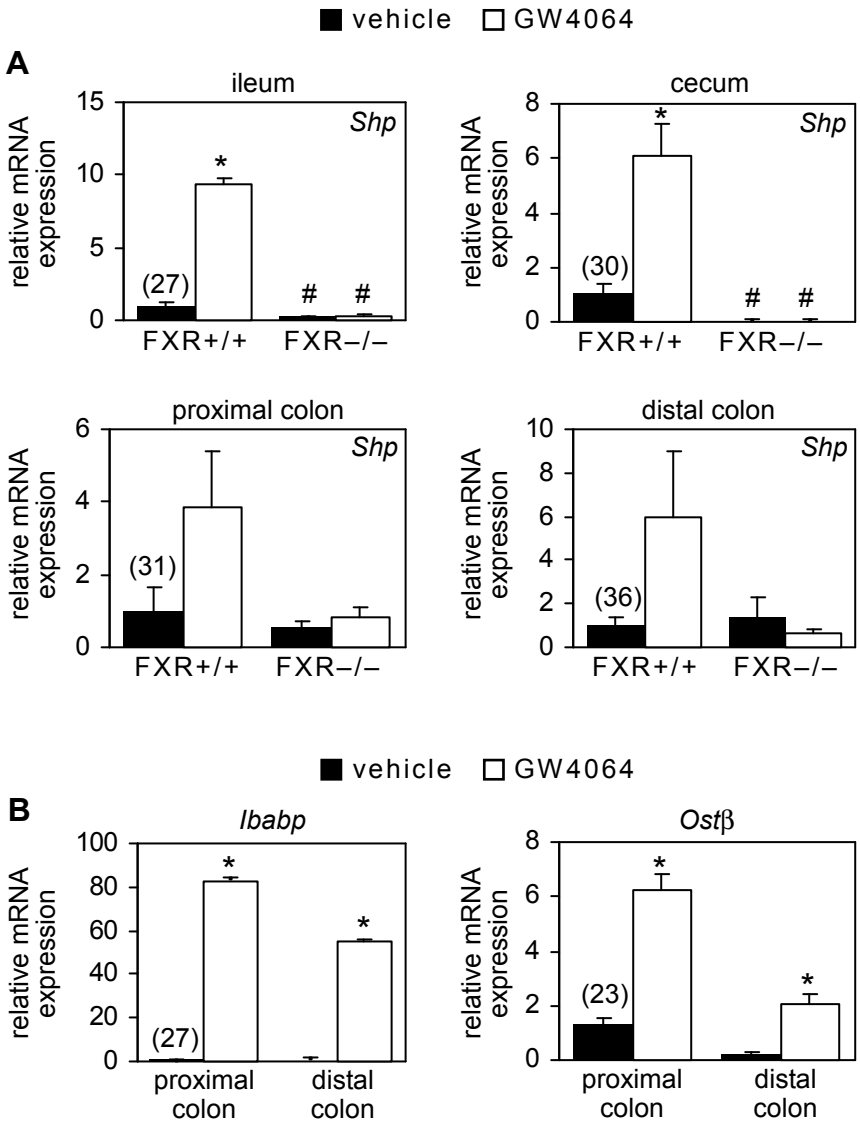

Figure 2.4 GW4064 induces FXR target genes in the colon.
Mice of the indicated genotype were treated for 4 hours by intraperitoneal injection of 30 mg/kg GW4064. **(A)** *Shp* expression in ileum and colon was determined by QPCR, normalized to *cyclophilin*, and graphed relative to wild-type, vehicle-treated control. **(B)** *Ibabp* and *Ost*β expression in colon was determined by QPCR, normalized to *cyclophilin*, and graphed relative to vehicle-treated proximal colon. Data represent the mean ± SEM of 5 animals per group. * $p < 0.05$ compared to vehicle of the same genotype (A) or same tissue (B). # $p < 0.05$ compared to wild-type of the same treatment group. Numbers in parentheses represent the average cycle time.

Table 2.1
Induction of *Ibabp* by GW4064 in ileum and colon.

tissue	treatment[1]	*Ct* value[2]	induction[3]
ileum	vehicle	16	
	GW4064	14	4x
cecum	vehicle	32	
	GW4064	18	20,000x
proximal colon	vehicle	28	
	GW4064	16	4,000x
distal colon	vehicle	32	
	GW4064	22	1,000x

[1] 30 mg/kg GW4064 was administered by intraperitoneal injection for 4 hours.
[2] Determined by QPCR. Average of 5 animals.
[3] Fold-increase in mRNA levels of GW4064 over vehicle.

Table 2.2
Induction of *Ost*β by GW4064 in ileum and colon.

tissue	treatment[1]	*Ct* value[2]	induction[3]
ileum	vehicle	21	
	GW4064	22	2x
cecum	vehicle	26	
	GW4064	22	10x
proximal colon	vehicle	24	
	GW4064	22	5x
distal colon	vehicle	28	
	GW4064	27	3x

[1] 30 mg/kg GW4064 was administered by intraperitoneal injection for 4 hours.
[2] Determined by QPCR. Average of 5 animals.
[3] Fold-increase in mRNA levels of GW4064 over vehicle.

dimethylhydrazine (1,2-DMH) according to a treatment regimen known to induce tumor formation in colon. 1,2-DMH is metabolized *in vivo* to azoxymethane (AOM), which is a DNA methylating agent that specifically causes tumors in the mid-distal colon of rodents (Campbell, 1975; Jackson, 2003). Strain differences in susceptibility to carcinogen-induced tumors in mice have been reported (Papanikolaou, 1998). SWR/J mice are highly susceptible while AKR/J and C57BL/6 mice are resistant. No data were available for 129 mice. Generally 129 mice are considered more susceptible to tumors than C57BL/6; therefore, 129S mice were used in these studies. Various studies have shown that cholic acid (CA), chenodeoxycholic acid (CDCA), deoxycholic acid (DCA), and lithocholic acid (LCA) increase DNA damage and tumor incidence in carcinogen-treated mice and rats (Reddy, 1977a; Cohen 1981; Earnest 1994; Flynn 2007). To evaluate whether the tumor-promoting effect of bile acids were dependent upon FXR, half of the mice in each group were fed a diet supplemented with DCA (0.2% w/w). DCA was chosen for this study because it is the most abundant bile acid in human feces and, unlike LCA, it does not cause liver damage at equivalent doses. After two-three weeks on this diet it became apparent that *Fxr*–/– mice did not tolerate the DCA treatment regimen, becoming moribund and hypothermic. At this point all mice were put back on standard diets and the *Fxr*–/– mice regained body weight (Figure 2.5A). After this, mice in the DCA group were given DCA diet and regular diet on alternating weeks. This regimen was tolerated by *Fxr*–/– mice, although their body weight remained below that of mice in the other groups (Figure 2.5A). To determine how the diet affected bile acid levels in the colon, total bile acid concentration was measure in feces collected during the week animals were fed DCA diet (Figure 2.5B). As expected, total fecal bile acids were greater in *Fxr*–/– mice relative to wild-type mice fed a standard diet (Figure 2.5B). DCA feeding dramatically increased fecal bile acids to similar total levels in both wild-type and *Fxr*–/– mice (Figure 2.5B). Moribund mice

were sacrificed as necessary and tissues were collected for gene expression analysis. Eighty-five percent of the mice remained asymptomatic at nine months, at which time the experiment was terminated. Serum bilirubin levels indicated that *Fxr*–/– mice fed DCA diet were cholestatic (Figure 2.5C). All animals in this group had visible signs of chronic liver damage (fibrosis and carcinoma) as well as acute toxicity (necrosis) (Figure 2.5D). Analysis of gallbladder bile acids showed enrichment of hydrophobic bile acids, tCA and tDCA, and decreased hydrophilic bile acids, tMCA and tHDCA, in animals treated with DCA diet (Figure 2.6). Interestingly, in *Fxr*–/– mice fed DCA diet, 85% of all bile acids were tCA, indicating that a significant portion of DCA was converted to CA in these animals (Figure 2.6). Gene expression analysis in the ileum demonstrated that DCA feeding induced FXR target genes (Figure 2.7). No significant change was seen in key cell cycle regulators (Figure 2.7). All animals were sacrificed at the same time of day, but had access to food ad libitum. Since proliferation in the intestine and expression of cyclins are affected by feeding, these data must be interpreted with caution.

Gross inspection of the large intestine revealed that only 20-40% of the mice in each of the four groups developed colorectal tumors (Table 2.3). Due to the low incidence of tumors, there was no significant difference in tumor burden between any of the groups. All of the tumors were low to high-grade adenomas and many were adjacent to mucosa-associated lymphoid tissue or had inflammatory cell infiltrates (Figure 2.8). Tumors in wild-type mice were typically polypoid adenomas, while *Fxr*–/– mice had mostly sessile adenomas (Table 2.4). The reason for this difference in gross tumor appearance is not known.

To determine whether tumors from wild-type and *Fxr*–/– mice were qualitatively different at the molecular level, I evaluated the expression of cell

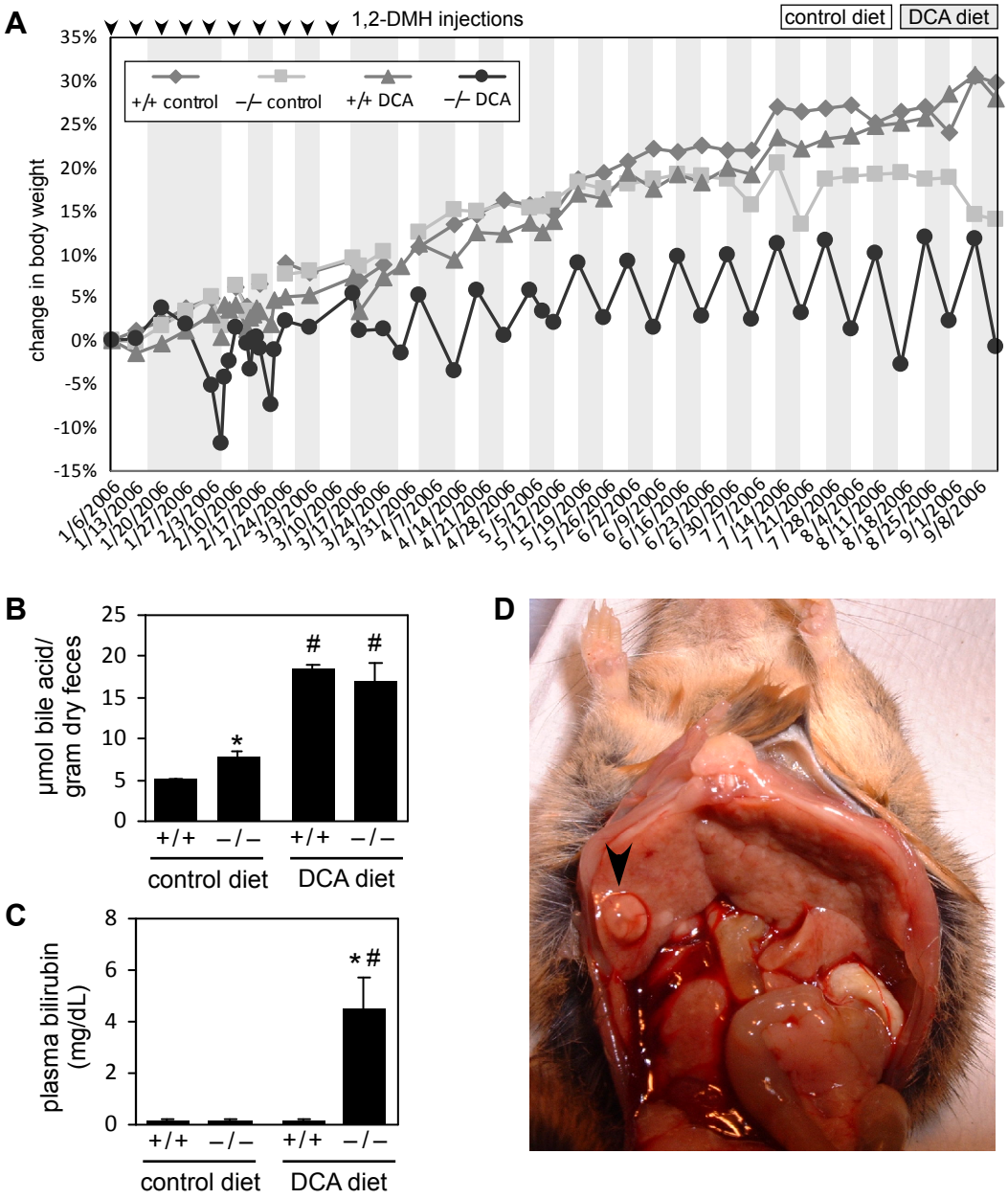

Figure 2.5 DCA toxicity in 1,2-DMH carcinogen study.
(A) 20 *Fxr+/+* and 20 *Fxr–/–* mice received 1,2-DMH (20 mg/kg) by intraperitoneal injection on the indicated dates. Half of the mice of each genotype received 0.2% (w/w) DCA diet as shown. Graph shows average change in body weight relative to the start of the study. (B) Total bile acids were measured in feces collected during DCA feeding. (C) Total bilirubin levels in plasma were measured at the end of the study. (D) Cirrhotic liver of a DCA treated *Fxr–/–* mouse. Arrow indicates a large hepatocellular carcinoma. * $p < 0.05$ compared to wild-type of the same treatment group. # $p < 0.05$ compared to control diet of the same genotype.

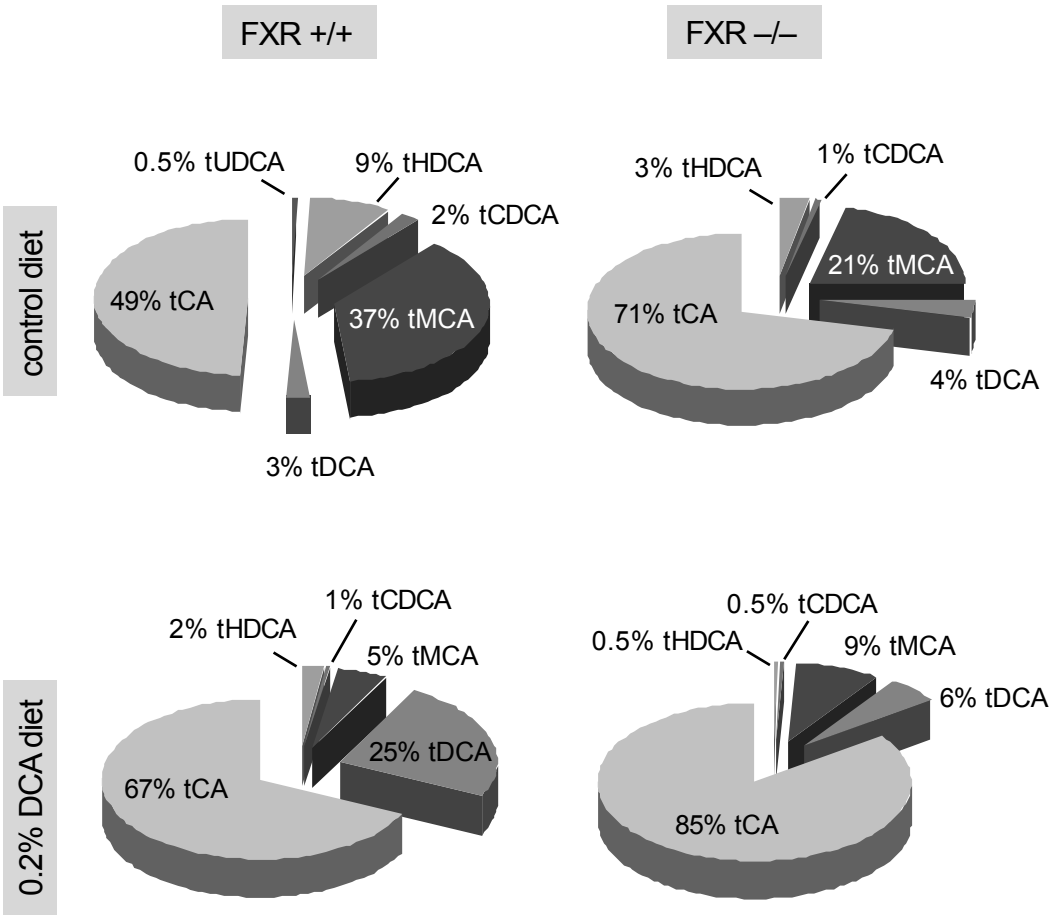

Figure 2.6 DCA treatment increases hydrophobic bile acids.
Gallbladder bile acids from animals described in Figure 5 were quantitated by LC/MS.

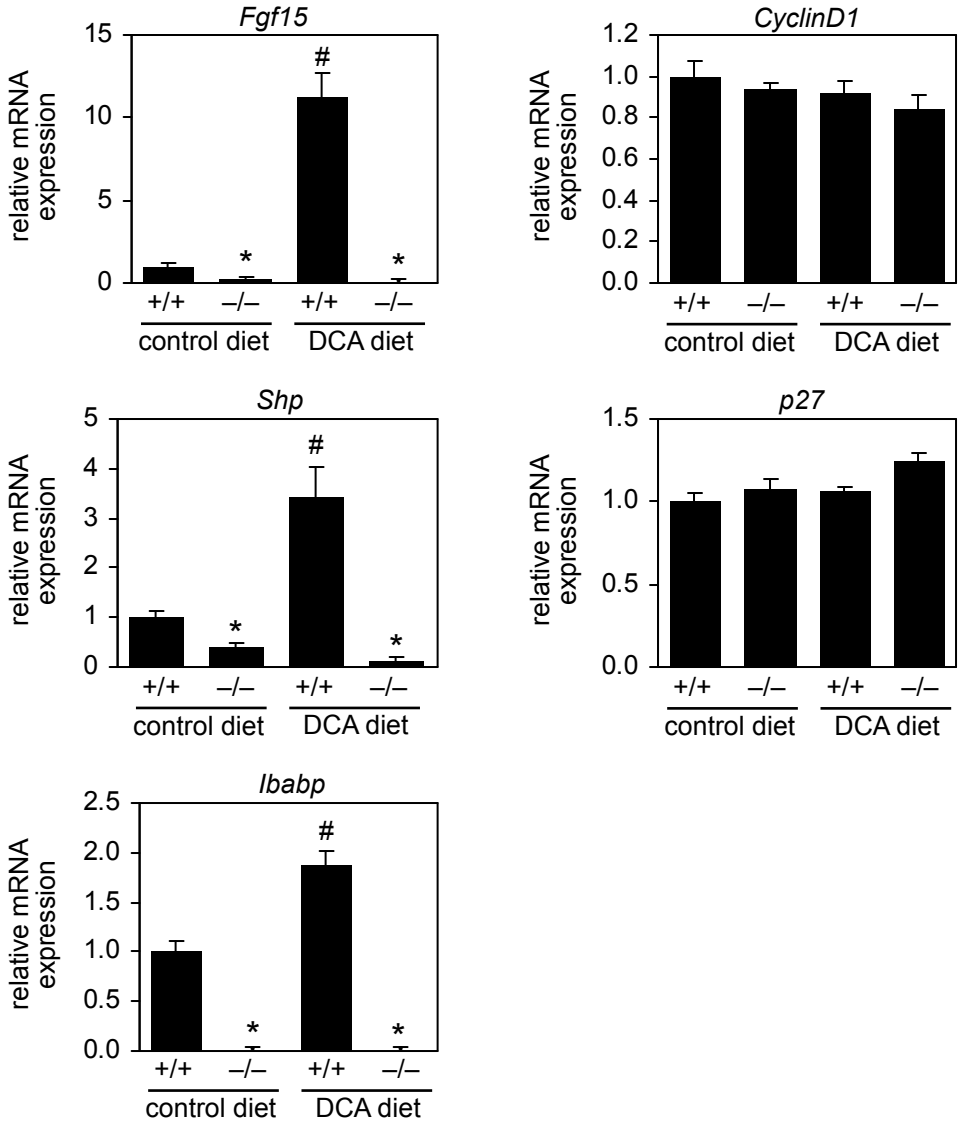

Figure 2.7 DCA induces known FXR target genes but not cell cycle regulators. RNA was extracted from the ileum of animals described in Figure 5. mRNA expression was determined by QPCR, normalized to *cyclophilin*, and graphed relative to wild-type fed control diet. Data represent the mean ± SEM of 10 animals per group. * $p < 0.05$ compared to wild-type of the same treatment group. # $p < 0.05$ compared to control diet of the same genotype.

Table 2.3
1,2-DMH study: tumor incidence.

genotype	diet	tumor incidence[1]	tumor multiplicity[2]
Fxr+/+	control	3/10	1.3
Fxr–/–	control	4/10	1.5
Fxr+/+	DCA	2/10	1.5
Fxr–/–	DCA	2/10	1.5

[1] number of animals with tumor/number in group
[2] tumor number/number of animals with tumor

Table 2.4
1,2-DMH study: tumor volume, location, and appearance.

genotype	diet	tumor volume (mm^3)	distance from anus (cm)	tumor type
Fxr+/+	control	45	3.7	polypoid adenoma
		36	3.5	polypoid adenoma
		225	1.4	polypoid adenoma
		80	4.0	polypoid adenoma
Fxr–/–	control	96	5.0	polypoid adenoma
		168	2.5	sessile adenoma
		8	1.0	sessile adenoma
		27	3.0	sessile adenoma
		36	5.0	sessile adenoma
		2	2.0	early adenoma
Fxr+/+	DCA	125	2.8	polypoid adenoma
		8	3.1	polypoid adenoma
		72	2.5	polypoid adenoma
Fxr–/–	DCA	12	2.5	polypoid adenoma
		8	4.5	sessile adenoma
		8	5.5	sessile adenoma

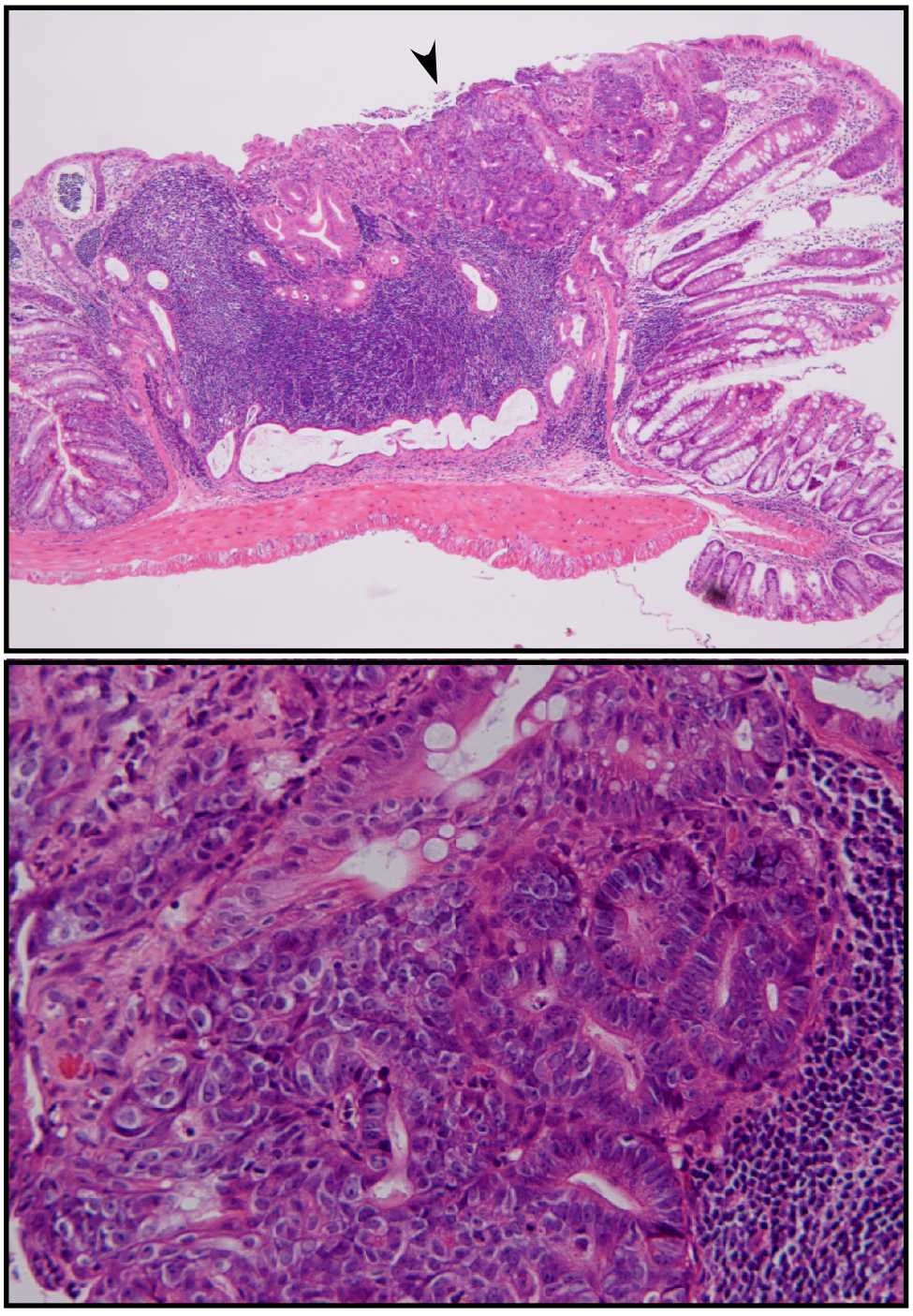

Figure 2.8 Histology of colorectal adenomas induced by 1,2-DMH.
Upper image shows H&E stained transverse section of mouse colon containing tumor. Region of adenoma indicated by arrowhead is shown in high magnification in the lower image.

cycle regulators and nuclear receptors in tumors and normal colon tissue adjacent to the tumor. Expression of *c-Myc* and *CyclinD1* were increased and *p27* was decreased in tumors relative to normal colon (Figure 2.9). No differences in expression were observed between wild-type and *Fxr*–/– mice fed control diet. The most surprising result from this analysis was that expression of FXR and other nuclear receptors was greatly reduced in tumors. These changes are likely the result of cellular dedifferentiation and major changes at the chromatin level favoring expression of genes promoting cell cycle progression rather than genes engaged in the normal metabolic processes of differentiated cells. Importantly, these data indicate that FXR is unlikely to be a pharmacologic target in tumor cells.

2.3.4 DCA Increases Tumor Incidence in Carcinogen Treated Mice

Surprisingly, the groups treated with DCA did not show increased number of tumors (Table 2.3). It is possible that the alternating DCA treatment regimen used in this study was not sufficient to promote the genotoxic effects of 1,2-DMH. Previous studies in rats with chemically-induced tumors have repeatedly shown promotion of tumorigenesis by DCA (Narisawa, 1974; Reddy, 1977a; Cohen, 1981). To confirm previous published findings and develop a more effective model of chemically-induced colon cancer in mice, a large cohort of wild-type mice was treated with the potent carcinogen AOM. The advantage of using this carcinogen is that it does not require activation in the liver and therefore is less subject to confounding effects caused by metabolic changes in the liver. DCA diet was begun one month prior to administration of the carcinogen and was continued without interruption for seven months until termination of the experiment. Tumor incidence was significantly increased in animals fed DCA diet (Table 2.5). Although animals in the DCA group were nearly twice as likely to develop colorectal tumors, the number of tumors per tumor-bearing animal

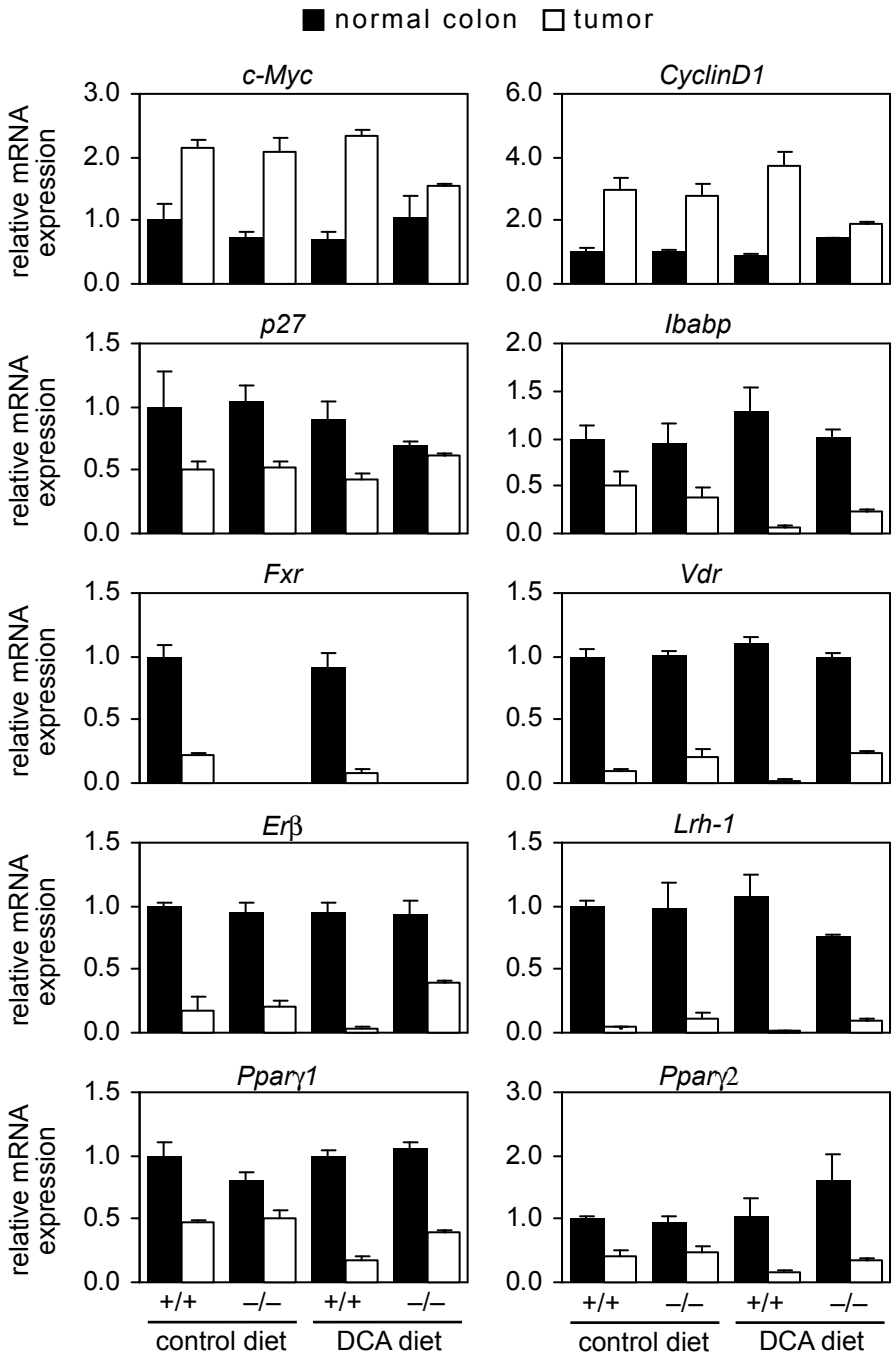

Figure 2.9 Nuclear receptor expression is decreased in tumors.
RNA was extracted from colon tumors and normal adjacent colon of animals described in Figure 5. mRNA expression was determined by QPCR, normalized to *U36b4*, and graphed relative to normal tissue of wild-type animals fed control diet. Data represent the mean ± SEM of 2-4 samples per group.

Table 2.5
AOM/DCA study: tumor incidence and statistical significance.

parameter	control	DCA[1]
number of animals in study	97	37
number of animals with tumor	43	31
tumor incidence	44%	84%
P (χ^2 test)[§]		<.0001
risk ratio[§]		1.9
tumor multiplicity[2]	1.5	1.7

[§] DCA relative to control group.
[1] 0.2% DCA (w/w) in diet administered ad libitum.
[2] tumor number/number of animals with tumor.
DCA diet was begun at 3 months of age. AOM injections were begun at 4 months of age. The cumulative dose of AOM was 50 mg/kg. See methods for details. Tumor incidence was determined at 10 months of age.

(tumor multiplicity) was not significantly increased (Table 2.5). Previous studies in rats showed increase tumor incidence and tumor multiplicity (Cohen, 1981). It is possible that species-specific responses to carcinogen or DCA may account for these differences.

2.3.5 *Fxr*–/– Mice Have Increased Incidence of Colorectal Cancer

Based on results obtained in the DCA/AOM study, wild-type and *Fxr*–/– mice were treated with a dose of AOM estimated to induce tumors in 50-60% of wild-type animals. Due to the toxic effects of DCA previously observed in *Fxr*–/– mice, all animals were maintained on normal diet for the duration of the study. Moribund mice were sacrificed as necessary and tissues were collected for gene expression analysis. At one year of age, the incidence of colorectal tumors was 71% in *Fxr*+/+ mice versus 94% in *Fxr*–/– mice (Table 2.6). Only four *Fxr*–/– animals remained tumor-free at one year of age. Tumor multiplicity was not different and there was no significant difference in tumor size or location between genotypes (Table 2.6 and 2.7). Concurrent studies from another laboratory have shown increases in both tumor number and size in AOM-treated C57BL/6 *Fxr*–/– mice (Maran, 2009). The reason for these differences is not known, but may be related to differences in genetic background. Interestingly, although *Fxr*–/– mice rarely develop spontaneous liver tumors at this age, all *Fxr*–/– animals in the current study had fibrotic liver disease and multiple hepatocarcinomas. In contrast, the liver of wild-type animals treated with AOM appeared normal. Although AOM is a genotoxic agent, it normally induces tumors only in the colon. These data suggest that loss of FXR increases susceptibility to hepatic and intestinal cancer.

Table 2.6
AOM/FXR study: tumor incidence and statistical significance.

Parameter	*Fxr*+/+	*Fxr*–/–
number of animals in study	58	64
number of animals with tumor	44	60
tumor incidence	76%	94%
P (χ^2 test)[§]		0.0054
risk ratio[§]		1.23
total number of tumors	122	172
tumor multiplicity[1]	2.8	2.9

[§] *Fxr*–/– relative to *Fxr*+/+ group.
[1] tumor number/number of animals with tumor.
AOM injections were begun at 3 months of age. The cumulative dose of AOM was 60 mg/kg. See methods for details. Tumor incidence was determined at 9 months of age.

Table 2.7
AOM/FXR study: tumor location and volume.

location	genotype	# of tumors	tumor volume (mm^3)
middle colon	*Fxr*+/+	20	69±21
	Fxr–/–	32	79±16
distal colon	*Fxr*+/+	88	58±8
	Fxr–/–	115	55±7
rectum	*Fxr*+/+	14	17±9
	Fxr–/–	25	34±10

2.3.6 Analysis of the Oncogenic K-RAS Mouse Model

While genetic models of cancer are more costly and often require time consuming breeding strategies, they have the advantage of being more predictable than the chemical-induced models and they provide additional information about the role of specific signaling pathways in oncogenesis. Decreased expression of FXR in colon adenomas (Figure 2.9) suggested that it was most likely to affect tumor outcomes during the early stages of tumor development. Conditional expression of oncogenic K-RAS (K-RASG12D) in mouse colon is reported to cause hyperproliferation and hypertrophy (Tuveson, 2004). Animals do not develop colon tumors (Tuveson, 2004). When combined with the loss of APC, high grade adenocarcinomas are formed (Haigis, 2008).

In previous reports FABP1-Cre was used to drive oncogenic K-RAS expression specifically in the colon (Tuveson, 2004). Compound heterozygous *K-ras*$^{LSL\text{-}12D}$*;Fabp1-Cre* mice were generated; however, gross and microscopic analysis of the colon revealed no increase in tissue mass or cell number compared to *K-ras*$^{LSL\text{-}12D}$ and *Fapb1-Cre* littermates. Recombination could not be detected in the colon suggesting that Cre was not appropriately expressed (data not shown). *Villin-Cre* animals have been successfully used in our laboratory to drive Cre expression in the small and large intestine. Compound heterozygous *K-ras*$^{LSL\text{-}12D}$*;Villin-Cre* mice were generated and showed recombination in the small and large intestine (Figure 2.10A). Consistent with previous reports, hypertrophy was clearly evident in the intestine of 2-month-old compound heterozygous *K-ras*$^{LSL\text{-}12D}$*;Villin-Cre* mice (Figure 2.11). Both small and large intestine of *K-ras*$^{LSL\text{-}12D}$*;Villin-Cre* mice were 20% longer than *K-ras*$^{LSL\text{-}12D}$ and *Villin-Cre* littermates (Table 2.8). The wet weight of intestines expressing oncogenic K-RAS was twice that of wild-type, and the cross sectional diameter of intestines were increased (Table 2.8; Figure 2.11). In the small intestine villus length and

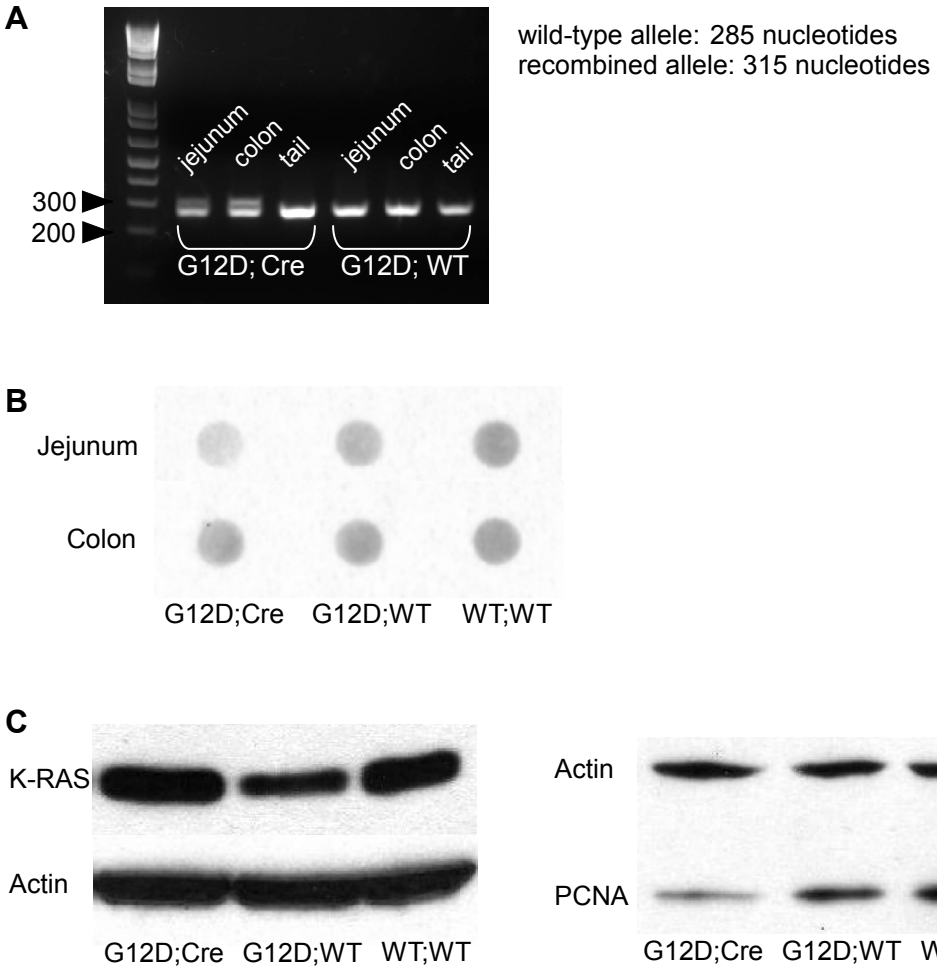

Figure 2.10 K-RAS^{G12D} expression in intestine.
(A) Multiplex PCR analysis of DNA from the indicated tissue was performed using primers that detect wild-type *K-ras* and recombined *K-ras*$^{LSL-G12D}$ alleles. **(B)** Mice of the indicated genotype were treated for 2 hours with 100 mg/kg BrdUrd by intraperitoneal injection. DNA was extracted from intestines and BrdUrd incorporation determined by immunoblotting. **(C)** Immunoblot analysis of whole colon protein lysates from a single animal of the indicated genotype. 4-month-old male littermates were used in the experiments shown in B and C.

Table 2.8
K-RAS^{G12D} phenotypes in intestine and adipose.

Parameter	control[1]	K-RAS^{G12D}
small intestine length (cm)	38.5 ±0.6	48.3* ±0.4
large intestine length (cm)	8.7 ±0.2	10.7* ±0.1
intestine wet weight (% of body weight)	5.8 ±0.4	12.1* ±0.7
epididymal fat pad weight (% of body weight)	4.1 ±0.4	2.0* ±0.3

[1] Littermates of *K-ras$^{LSL-G12D}$*;*Villin-Cre* mice harboring either *Villin-Cre* or *K-ras$^{LSL-G12D}$* alleles were used as controls. All animals were 8-10 month old males.
* $p < 0.001$ relative to control.

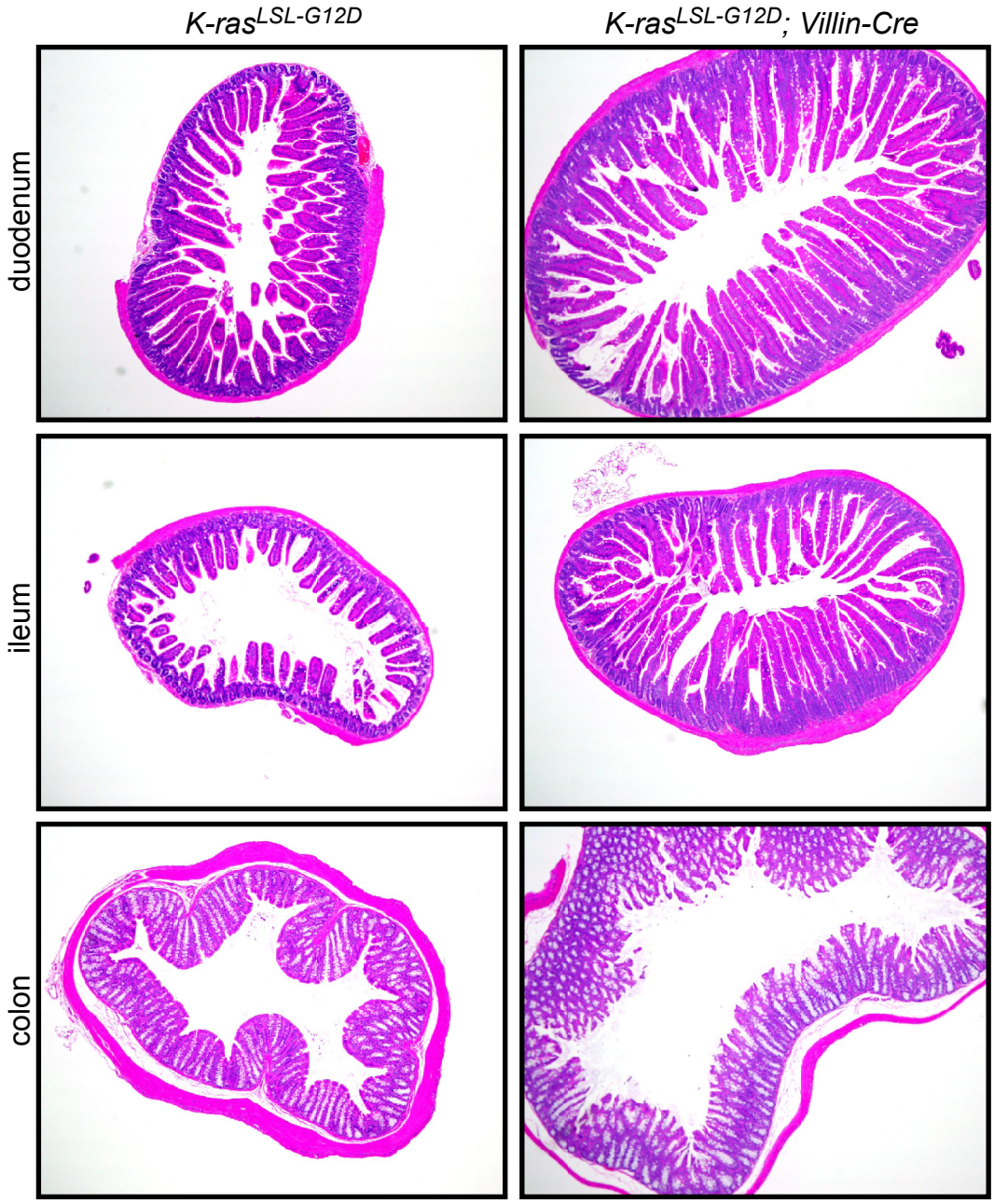

Figure 2.11 Intestinal hypertrophy in *K-ras*^{G12D} mice.
Intestines from mice of the indicated genotypes were fixed in formalin and paraffin embedded. Photos of H&E stained sections for all regions of the intestine were taken at the same magnification.

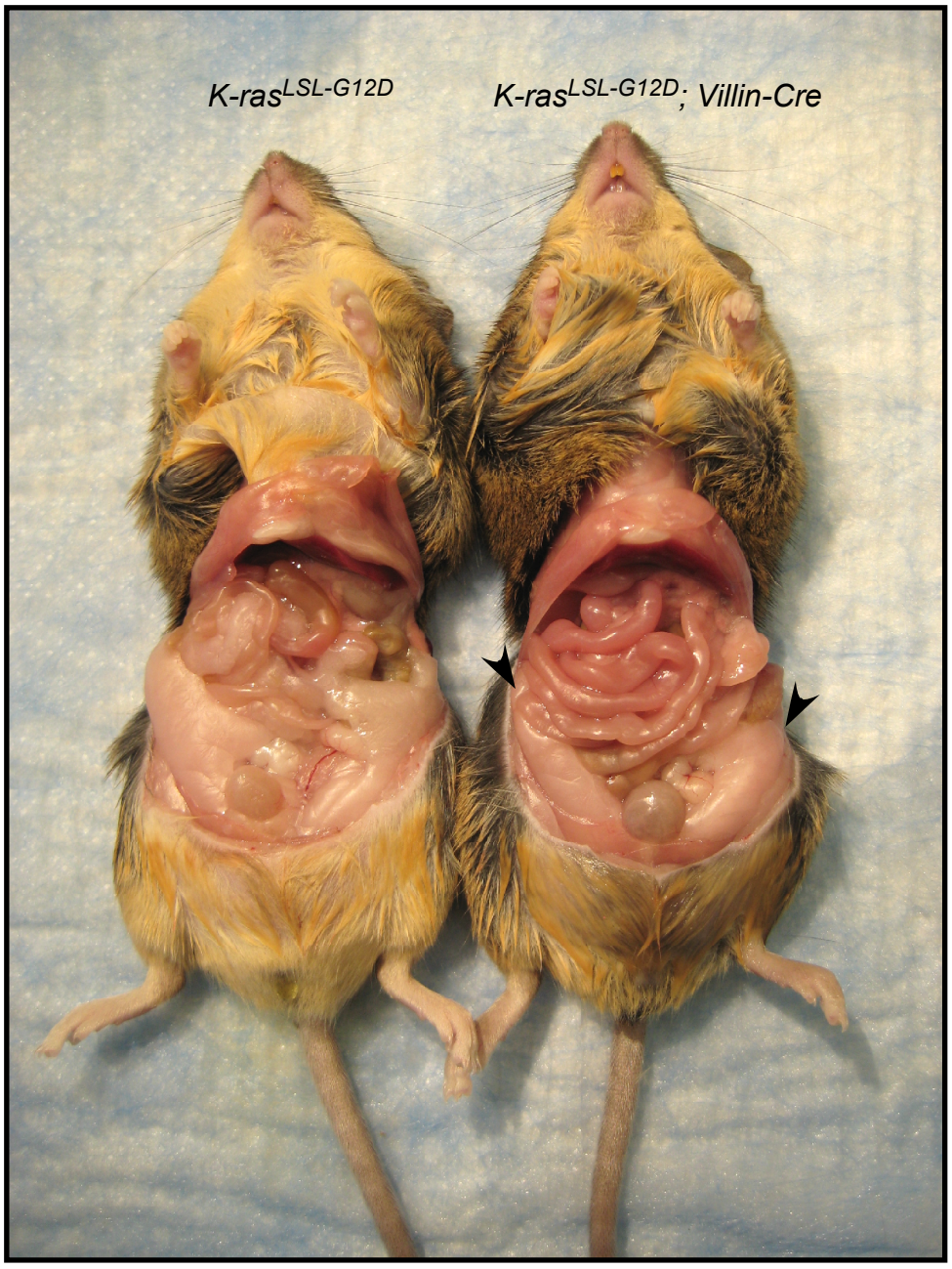

Figure 2.12 Effects of oncogenic K-RAS expression in the intestine on adiposity. Appearance of viscera from 9-month-old male littermates of the indicated genotype. Black arrows indicate epipidymal fat pads.

the number of villi and crypts per cross sectional area was increased (Figure 2.11). In the colon, the number of crypts and crypt height was increased. Apart from increased cell mass, no additional changes in tissue architecture were observed. Dysplasia was not evident. Surprisingly analysis of proliferation in 4-month-old male mice by bromodeoxyuridine (BrdUrd) incorporation demonstrated that intestines expressing K-RAS^{G12D} did not have increased proliferation (Figure 2.10B). In addition, levels of proliferating cell nuclear antigen (PCNA) were decreased in the colon of *K-ras$^{LSL-12D}$;Villin-Cre* mice (Figure 2.10C). These results were unexpected given the obvious hypertrophy of intestines expressing K-RAS^{G12D} and previous reports of intestinal hyperproliferation. It is worthy to note that while previous reports demonstrated increased MEK and ERK phosphorylation, no experiments were done to directly measure proliferation (Tuveson, 2004; Haigis, 2008). Thus, is it possible that hypertrophy (increased tissue mass) in intestines expressing oncogenic K-RAS is caused by increased cell survival rather than hyperproliferation *per se*.

To test the effects of loss of FXR in a genetic model of intestinal hypertrophy, *K-ras$^{LSL-12D}$;Villin-Cre* mice were crossed with *Fxr–/–* mice to generate *K-ras$^{LSL-12D}$;Villin-Cre;Fxr–/–* mice and the relevant genetic controls. This study and bile acid feeding studies in *K-ras$^{LSL-12D}$;Villin-Cre* mice are currently ongoing. It is expected that comparison of *K-ras$^{LSL-12D}$;Villin-Cre;Fxr–/–* with *K-ras$^{LSL-12D}$;Villin-Cre;Fxr+/+* mice will provide the necessary data to determine whether FXR plays a role in preventing progression of intestinal hyperplasia to dysplasia. In addition, these studies are the first to investigate potential effects of FXR on K-RAS signaling.

Two obvious phenotypes unrelated to the intestine were noted in *K-ras$^{LSL-12D}$;Villin-Cre* mice. As shown in Table 2.8 and Figure 2.12, these mice have a marked decrease in visceral adiposity. Epididymal fat pad weight was decreased

approximately 2-fold (Table 2.8). Since expression of oncogenic K-RAS is purportedly limited to the intestinal epithelium, effects in adipose tissue may be caused by altered endocrine signals. Future studies to address this phenotype should begin by measuring food intake, nutrient absorption, and energy expenditure. In addition, younger mice should be evaluated to investigate the possibility of a developmental phenotype.

The second observed phenotype was spontaneous formation of vulvar tumors in *K-ras*$^{LSL\text{-}12D}$*;Villin-Cre* mice. The analogous organ in male mice, the glans penis, was not affected (Figure 2.13A). These large exophytic tumors appeared to be of epithelial origin (Figure 2.13B). Keratinizing structures suggested involvement of epidermal tissue. PCR analysis confirmed recombination in tumor tissue and intestine, but not in other female reproductive tissues (Figure 2.13C). Tumors generally appeared at 2-4 months of age and grew slowly. Tumor incidence in mixed-strain 129S;C57BL/6 mice was 54% (26 out of 48 animals). Tumor incidence appears to be lower in mice extensively backcrossed to 129S. These animals may be useful to study the pathogenesis and treatment of vulvar cancer. In humans, vulvar cancer in young women is most often associated with human papilloma virus (HPV); while in older women, acquired mutations are believed to be the major cause (van der Avoort, 2006). Currently the primary treatment is surgical, but treatment of metastatic disease is problematic (Ghurani, 2001).

2.3.7 Effects of Secondary Bile Acids and Synthetic FXR Agonists on Tumor Incidence in *Smad3*–/– Mice

The AOM study described above and studies from other laboratories have shown that loss of FXR increases susceptibility to colon cancer in mouse models. To test whether FXR agonists decrease susceptibility to cancer, *Smad3*–/– mice were treated with two potent FXR agonists, INT-747 and INT-767. In addition,

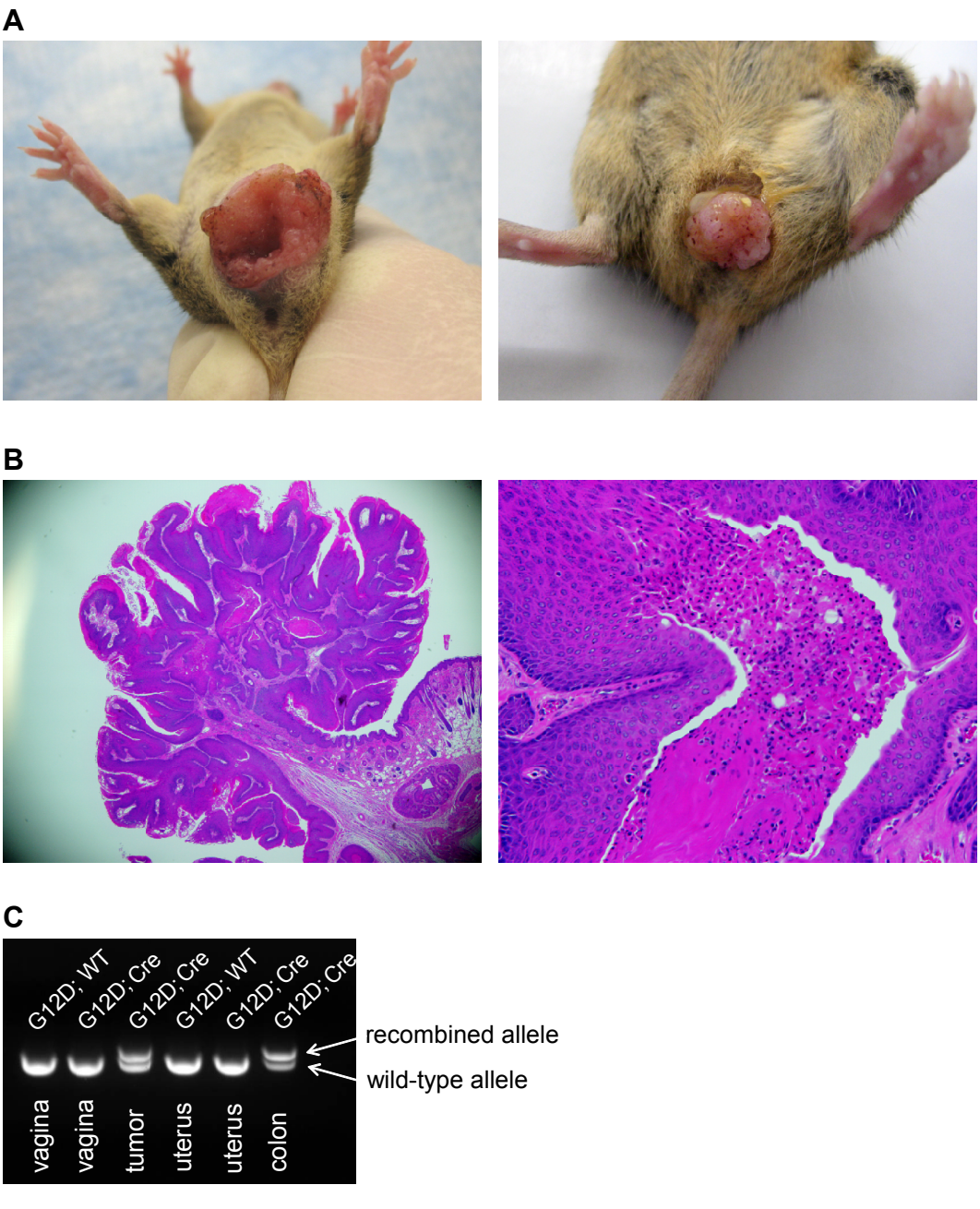

Figure 2.13 Oncogenic K-RAS induces vulvar tumors in mice.
(A) Vulvar tumors in 4-month-old female *K-ras*$^{LSL\text{-}G12D}$*;Villin-Cre* mice. **(B)** H&E stained section of vuvar tumors at low (left) and high (right) magnification. **(C)** Multiplex PCR analysis of DNA from the indicated tissue was performed using primers that detect wild-type *K-ras* and recombined *K-ras*$^{LSL\text{-}G12D}$ alleles.

mice were treated with the two most common secondary bile acids, DCA and LCA. Both bile acids have been shown to promote CRC in carcinogen-induced tumor studies in rats (Reddy, 1977a; Reddy, 1979).

Smad3–/– mice develop highly malignant tumors in the cecum, proximal colon, and rectum (Zhu, 1998). The mechanism of tumorigenesis is not fully understood; however, it is known that genetic background and changes in the intestinal flora affect tumor incidence (Zhu, 1998; Maggio-Price, 2006). I have found that colon tumors in *Smad3*–/– mice on the mixed 129;C57BL/6 background typically develop when animals are approximately 3-5 months old. In some cases (<5%) tumors develop early and animals become moribund at 3-4 months. These mice have co-morbid phenotypes such as splenomegaly, skeletal abnormalities of one or both forelimbs, and periorbital desquamation. These mice were excluded from the current study.

Initially I had also hoped to include *Fxr*–/–;*Smad3*–/– mice in this study; however, attempts to obtain double knock-out mice by crossing *Smad3*–/– with *Fxr*–/– (either 129S or C57BL/6 background) were unsuccessful. While a small number of viable *Fxr*–/–;*Smad3*–/– were obtained, none of them were capable of breeding.

Pilot studies showed that diets containing 0.2% (w/w) DCA and 0.2% (w/w) LCA were well tolerated when fed to mice for more than 6 months. Infrequent side affects included cholelithiasis, liver fibrosis, and bladder stones. To determine an optimal dose for INT-747 and INT-767, mice were fed diets containing increasing doses of each compound. FXR target genes in the liver and intestine were consistently increased by 0.005% (w/w) INT-747 and 0.0125% (w/w) INT-767 (Figure 2.14A and B). These doses also decreased *Cyp7a1* expression in the liver (i.e. suppressed bile acid synthesis) and were not hepatotoxic (Figure 2.14B and Figure 2.15). Based on chow consumption, it was

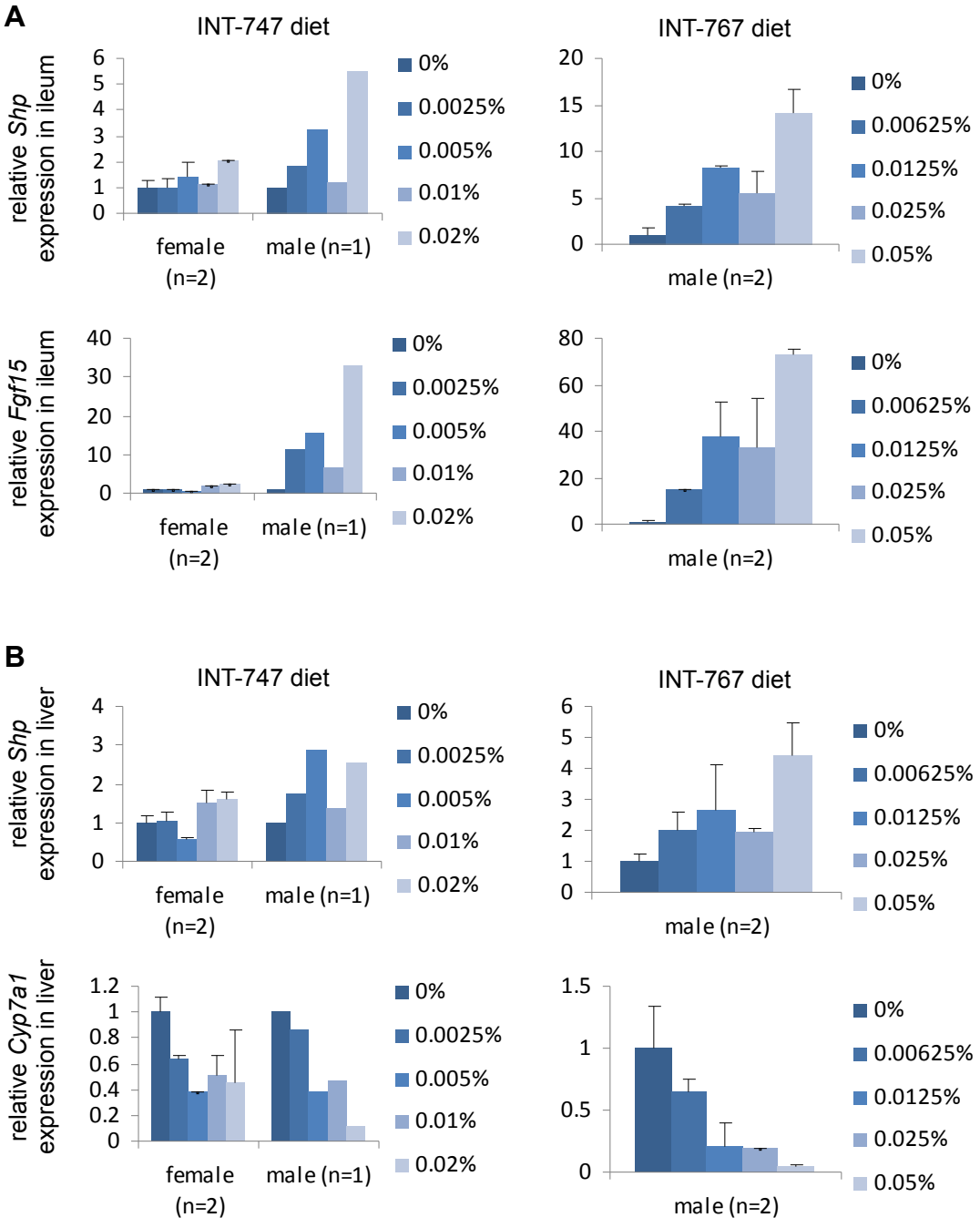

Figure 2.14 ***In vivo*** **dose-response of synthetic FXR agonists.**
Wild-type mice were treated for four days with diets containing synthetic FXR agonists, INT-747 and INT-767. Compounds were admixed in the diet at the indicated concentration (w/w). mRNA expression in ileum **(A)** and liver **(B)** was determined by QPCR, normalized to *U36b4*, and graphed relative to control diet. Data represent the mean ± SD.

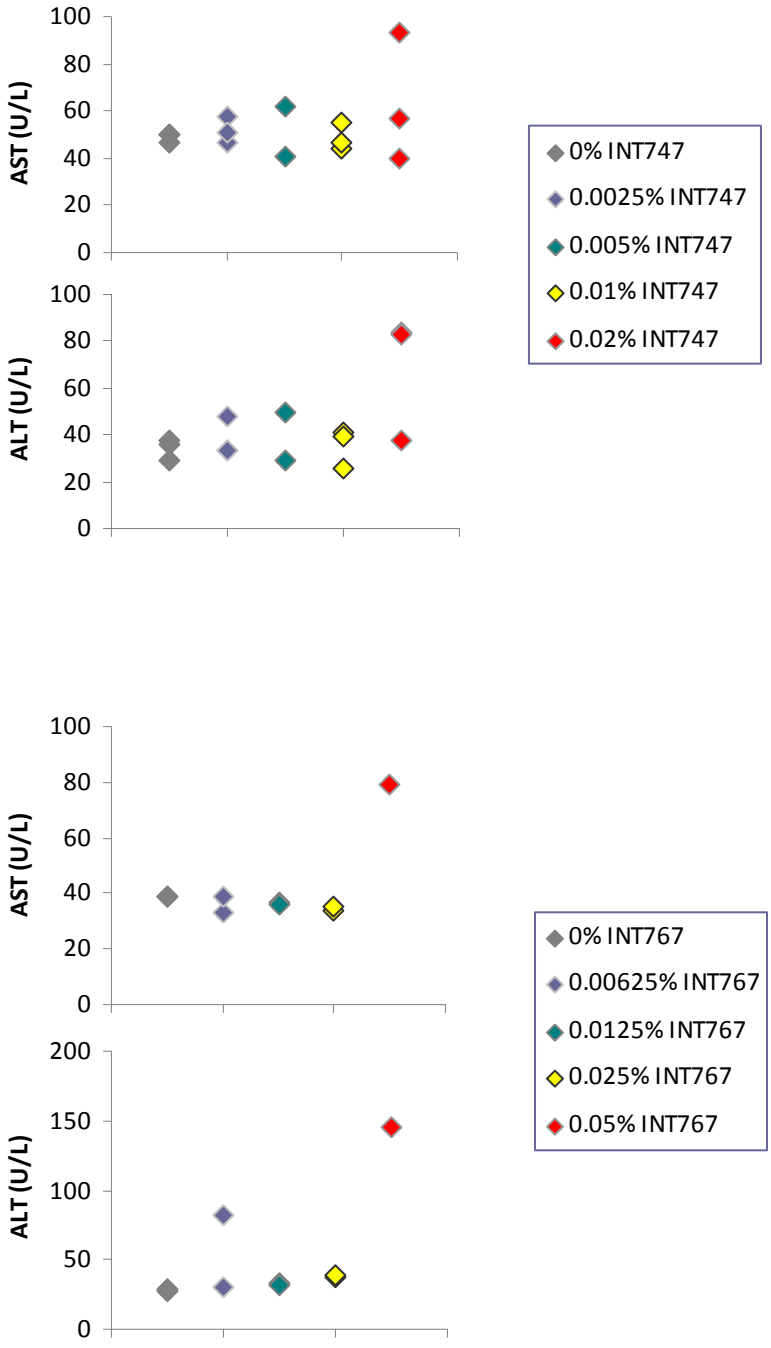

Figure 2.15 Determination of the maximum tolerated dose of FXR agonists. Aspartate aminotransferase (AST) and alanine aminotransferase (ALT) were measured in serum of animals treated with the indicated dose of INT-747 or INT-767. See Figure 14 for description of experiment.

calculated that the daily dose for was 8.87 mg/kg for INT-747 and 20.36 mg/kg for INT-767. These numbers are close to the recommended oral gavage doses of 10 mg/kg INT-747 and 30 mg/kg INT-767 used by Intercept Pharma in mouse studies (personal communication).

Bile acid metabolizing enzymes in mice are not fully expressed until two months of age (Schwarz, 1996). With that in mind, wild-type and *Smad3*–/– mice were fed diets containing DCA, LCA, INT-747, and INT-767 beginning at 2.5-3 months of age. At six months, intestinal tumor burden was quantitated. Animals that became moribund at greater than 4 month of age were necropsied and included in the study. None of the wild-type animals developed colon tumors (Table 2.9). 27% of *Smad3*–/– mice maintained on control diet presented with tumors, this number increased to 41% and 47% in DCA and LCA diet groups respectively (Table 2.9). The increase caused by LCA was statistically significant. In contrast, INT-767 significantly reduced the number of animals that developed tumors to 14%, and INT-747 did not affect tumor incidence. *Smad3*–/– mice typically develop one or two large mucinous adenocarcinomas in the cecum and proximal colon and one or no tumors in the rectum (Maggio-Price, 2006). Similar findings were observed in the current study; therefore, no differences in tumor multiplicity were noted for any of the treatment groups (Table 2.9). Tumor volume was significantly reduced in DCA, INT-747 and INT-767 groups, with the greatest decrease seen in the INT-767 group (Table 2.10).

Reduced tumor incidence in *Smad3*–/– mice treated with INT-767 suggested that this compound may have potential as a chemopreventive agent for CRC. Surprisingly, INT-747, although also an FXR agonist, did not affect tumor incidence. Hepatic enzymes conjugate INT-747, while INT-767 contains a chemical group that prevents conjugation. Differences in catabolism by intestinal bacteria may also exist and could provide an explanation for why INT-767, but

Table 2.9
SMAD3 study: Tumor incidence and statistical significance.

Parameter	control	DCA	LCA	INT-747	INT-767
Smad3+/+ animals in study	33	34	31	37	39
Smad3+/+ animals with tumor	0	0	0	0	0
Smad3+/+ tumor incidence	0%	0%	0%	0%	0%
Smad3–/– animals in study	73	69	66	68	66
Smad3–/– animals with tumor	20	28	31	18	9
Smad3–/– tumor incidence	27%	41%	47%	26%	14%
p (χ^2 test)[§]		0.10	0.02	0.89	0.05
risk ratio[§]		1.48	1.71	0.97	0.50
total number of tumors	29	46	44	26	16
tumor multiplicity[1]	1.5	1.6	1.4	1.4	1.8

[§] For *Smad3*–/– mice: treatment relative to control group.
[1] tumor number/number of animals with tumor.
Bile acid diets were begun at 3 months of age. Tumor incidence was determined at 6 months of age.

Table 2.10
SMAD3 study: Tumor volume.

Diet	# of Tumors	Tumor Volume (mm^3)
control	29	2614 ±730
0.2% DCA	46	758 ±250*
0.2% LCA	44	2189 ±737
0.005% INT-747	26	513 ±178*
0.015% INT-767	16	263 ± 92*

* $p < 0.02$ relative to control.

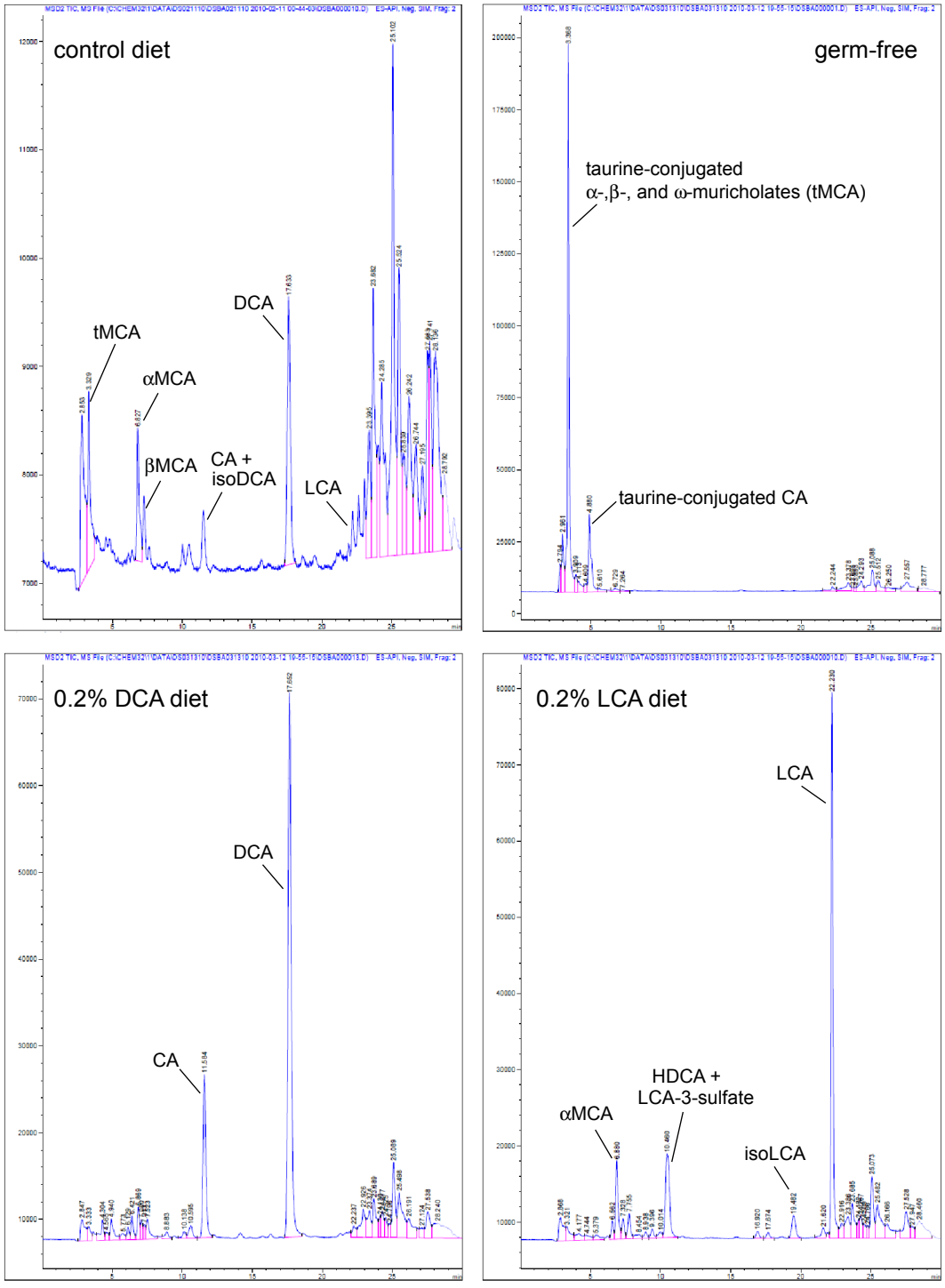

Figure 2.16A Bile acid feeding affects cecal bile acid composition.
For legend see Figure 16B.

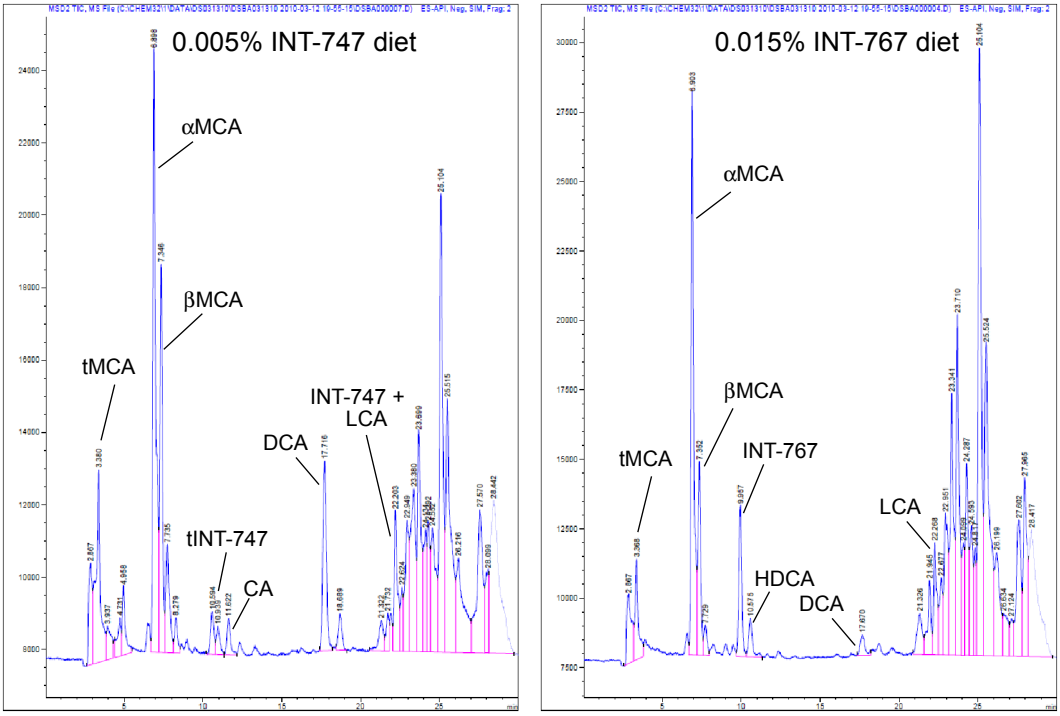

Figure 2.16B Bile acid feeding affects cecal bile acid composition.
Bile acids were extracted from cecal contents of germ-free or conventional mice treated with the indicated bile acid or control diets. Extracts were resolved by reverse phase chromatography and analyzed by mass spectometry using single ion monitoring (SIM) in negative ion mode. 19 ions, representing the most common bile acids and their metabolites were monitored. Selected peaks of known identity (through comparison to authentic standards) are labeled. Data shown is MS analysis of bile acids extracted from a single cecum and is representative of 3-6 samples per treatment group.

not INT-747, reduced tumor risk. To determine the concentration of these compounds in the intestine, bile acids were extracted from cecal contents and analyzed by LC/MS. In conventional mice fed control diet, conjugated bile acids were virtually absent from the cecum, tri-hydroxylated bile acids were present a low concentrations, and the major bile acid present was DCA (Figure 2.16A). These results are consistent with other studies (Hagio, 2009). In contrast, bile acids in the cecum of germ-free mice were exclusively conjugated and no secondary bile acids were present (Figure 2.16A). As expected, animals fed DCA and LCA had high concentrations of these bile acids and their metabolites (Figure 2.16A). INT-747 and low levels of taurine-conjugated INT-747 were present in the cecum of animals on this diet (Figure 2.16B). Compared to animals in the control group there was also a relative increase in muricholates. Amazingly, DCA was almost absent in the cecum of mice treated with INT-767 (Figure 2.16B). The major bile acids in these mice were muricholates. It is tempting to speculate that these changes in cecal bile acid composition are responsible for the chemopreventive effects of INT-767 in the current study. Future analysis of FXR target gene expression in the colon will be useful to determine the efficacy of INT-747 and INT-767 as FXR agonists in this organ.

2.4 Discussion

Secondary bile acids are thought to act as intestinal tumor promoters. They are also natural ligands for FXR. The current study has shown that loss of FXR increases susceptibility to intestinal cancer in mice; furthermore, it was demonstrated that a potent FXR agonist reduced the risk of developing cancer, while another had no effect on tumor incidence. These results effectively rule out FXR signaling as the mechanism responsible for tumor promotion by bile acids. Instead these results suggest that FXR may play a role in the prevention of CRC.

These conclusions are consistent with recent reports in the literature that loss of FXR increases the risk of intestinal cancer in mice (Modica, 2009; Maran, 2009).

A number of mechanisms may be responsible for the anti-tumor effects of FXR. Studies from the laboratory of Dr. Moschetta at the University of Bari suggest that FXR induces the transcription of pro-apoptotic genes (Modica, 2009). In the absence of normal levels of apoptosis, genetic mutations accumulate, ultimately resulting in cancer. Studies from the laboratory of Dr. Guo at the University of Kansas Medical Center showed increased tumor incidence in carcinogen-treated *Fxr*–/– mice and mice lacking both FXR and the tumor suppressor APC (Maran, 2009). They reported increased levels of β-catenin, c-MYC, and CyclinD1 in the intestine of *Fxr*–/– mice; however, no explanation was given for how these effects might be caused by the absence of FXR.

Given that secondary bile acids promote tumorigenesis, probably the simplest explanation for why *Fxr*–/– mice have increased risk of intestinal cancer is that decreased bile acid feedback regulation caused by the absence of FXR results in increased levels of bile acids, and ultimately bile acid-associated toxicity in the colon. In addition, FXR may regulate expression of genes that detoxify bile acids in the intestine, as has been shown for lithocholic acid detoxification by VDR and xenobiotic detoxification by PXR. The absence of such FXR-regulated bile acid detoxifying mechanisms together with increased bile acid levels in *Fxr*–/– mice would compound exposure of the intestinal mucosa to the toxic effects of bile acids. The major difficulty in testing these ideas is that the "toxic" effects of bile acids responsible for tumor promotion are not known. It has been suggested that tumor promotion by bile acids is a function of their ability to induce intestinal proliferation (DeRubertis, 1984), others contend that increased apoptosis caused by bile acids promotes the selection of apoptosis-resistant cells (Bernstein, 1999). It has also been reported that bile

acids increase DNA damage either by acting directly as mutagens, or more likely, through the generation of reactive oxygen species (Wilpart, 1983; Bernstein, 2009). A better understanding how and which of these deleterious properties of bile acids are relevant to the pathogenesis of CRC would greatly facilitate the study of mechanisms responsible for the protective effects of FXR. *In vitro* and *in vivo* studies to investigate the proliferative effects of bile acids are described in Chapters 4 and 5.

Ongoing studies in the oncogenic K-RAS mouse model will provide important information about the function of FXR in early stages of cancer progression. For example, if loss of FXR increased susceptibility to genotoxic insults then it would be expected that oncogenic K-RAS combined with the absence of FXR would facilitate progression from hyperplasia to dysplasia and possibly even malignancy.

While INT-747 did not decrease tumor incidence in the *Smad3–/–* model, one can clearly conclude from this study that, unlike secondary bile acids, long-term administration of INT-747 at a therapeutic dose does not promote tumorigenesis. Future studies will need to address whether INT-747 and INT-767 had similar effects on FXR target gene expression in the colon. Since INT-767 is a dual agonist for FXR and the G-protein coupled receptor, TGR5, it will be important to determine if activation of TGR5 is responsible for the reduction in tumor incidence in *Smad3–/–* mice by INT-767. Alternatively, activation of both FXR and TGR5 may be important for the chemopreventive effects of INT-767. Qualitative changes in luminal bile acids induced by long-term INT-767 administration significantly decreased the hydrophobicity of the bile acid pool in this compartment. Such changes presumably decreased bile acid toxicity in the colon and may have slowed the rate of tumor progression. Future analysis of biomarkers of proliferation and DNA damage in tissues from this study should

provide additional insight into the mechanism INT-767 mediated chemoprevention.

In summary, my studies have shown that FXR is expressed in terminally-differentiated cells of the colonic epithelium where it functions to regulate expression of genes involved in bile acid transport. Furthermore, loss of FXR increases susceptibility to colorectal cancer, while long-term administration of the dual FXR/TGR5 agonist, INT-767, reduced levels of secondary bile acids and decreased tumorigenesis in a mouse model of colorectal adenocarcinoma. I have also confirmed the tumor promoting effects of secondary bile acids by showing that they increase tumorigenesis in genetic and chemical-induced models of colon cancer in mice. These data will aid in the design of studies to elucidate the mechanism of tumor promotion by bile acids and determine strategies to prevent and treat CRC.

2.5 Acknowledgements

INT-747, INT-767, and conjugated species of INT-747 were provided by Intercept Pharma. I thank Dr. Mark Pruzanski and Dr. Luciano Adorini for making sufficient quantities of these compounds available for long-term animal studies. Assistance with histologic analysis of tumor specimens was provided by Dr. James Richardson. John Shelton assisted with the *in situ* expression analysis. Blood chemistry analysis was performed by Laura Brulé in the Mouse Metabolic Phenotyping Core Facility at UT Southwestern, Dallas, TX.

CHAPTER 3
AKR1B7 Metabolizes Bile Acids and is Regulated by FXR

3.1 Introduction

As described in Chapter 2, *Fxr*–/– mice have increased susceptibility to colorectal cancer. To determine the mechanism underlying this phenotype I initially focused on the effects of FXR on cell cycle regulators. VDR decreases proliferation and increases differentiation in human colon cancer cells by down-regulating cyclins and up-regulating cell cycle inhibitors such as p21 and p27 (reviewed in Buillon, 2006). Other nuclear receptors, such as androgen and estrogen receptors, also affect proliferation through direct transcriptional regulation of cell cycle regulators (Sabbah,1999; Liu, 2002; Balk, 2008). Given these examples, it seemed reasonable that FXR might play a related role in the intestine; however, while DCA (a natural FXR agonist) induced FXR target genes in the colon it did not affect expression of candidate cell cycle regulators (Chapter 2). It was decided that transcriptional profiling was necessary to gain insight into the function of FXR in the colon. Indeed, such experiments have led to the discovery of novel functions of FXR in the small intestine (Inagaki, 2005).

I begin this chapter by describing the design, results, and analysis of a transcriptional profiling experiment comparing mouse colon treated *in vivo* with both a natural and a synthetic FXR agonist. This experiment led to the identification of aldo-keto reductase family 1, member b7 (*Akr1b7*), also known as mouse vas deferens protein (*Mvdp*), as a novel FXR target gene. The enzymatic activity of AKR1B7 on bile acid substrates was investigated and biological properties of the products were tested. Results of these studies

demonstrate that AKR1B7 reduces 3-keto bile acids in a stereospecific manner, promoting the formation of iso bile acids. These products are less toxic than regular bile acids. Based on these results I propose that AKR1B7 contributes to bile acid detoxification in the intestine. Since *Akr1b7* is induced by FXR, this system provides a mechanism for FXR to increase bile acid detoxification, which may contribute to the anti-tumorigenic effects of FXR in the colon.

AKR1B7 has previously been proposed to function in the detoxification of lipid peroxides and toxic byproducts of steroid hormone biosynthesis. These data and pertinent background on AKR1B7 is described in the following paragraphs.

Aldo-keto reductases (AKRs) comprise a large group of cytoplasmic and microsomal enzymes that catalyze the reduction of a wide variety aliphatic and aromatic aldehydes and ketones (Jez, 1997). Several members of the aldo-keto reductase superfamily are classified as hydroxysteroid dehydrogenases (HSDs) due to their documented effects on steroid metabolism (Penning, 1997). Several AKRs play a key role in bile acid biosynthesis (Russell, 2003). *Akr1b7* is highly expressed in the mouse vas deferens epithelium and zona fasciculata of the adrenal cortex (Lau, 1995). Expression is also significant in the eye, intestine, seminal vesicle, kidney, liver, testis and lung. High expression has also been reported in the ovary exclusively during proestrus (Bauman, 2007). Adrenocorticotropic hormone (ACTH) stimulates expression of the gene in both mouse and rat adrenal, while androgens regulate vas deferens expression only in the mouse (Martinez, 1999; Val, 2002). In addition, luteinizing hormone (LH) and human chorionic gonadotropin (hCG) strongly induce its expression in thecal and interstitial cells of the ovary (Brockstedt 2000).

Biochemical analysis identified isocaproaldehyde (a product of cholesterol side chain cleavage) and 4-hydroxynonenal (a lipid peroxidation product) as preferred substrates for AKR1B7 (Lefrançois-Martinez, 1999). Given its high

level of expression in steroidigenic tissues and its substrate specificity, a putative role of AKR1B7 in the detoxification of byproducts of steroid biosynthesis has been proposed (Martinez, 2001). Its role in non-steroidigenic tissues, including the vas deferens, is unclear. Recently it has been shown that expression of AKR1B7 is regulated by LXR in intestine and by PXR and CAR in both liver and intestine (Volle, 2004; Liu, 2009). A high-fat diet is associated with increased levels of oxysterols and lipid peroxides, and since LXR is activated by oxysterols, it has been hypothesized that AKR1B7 may play a role in the detoxification of lipid peroxides in the intestine (Volle, 2004). Global *Akr1b7*–/– mice are viable and have no obvious reproductive phenotype (Bauman, 2007).

3.2 Methods

3.2.1 Animals and Animal Husbandry

Male C57BL/6 mice were purchased from Charles River Laboratories. *Fxr*+/+ and *Fxr*–/– mice were obtained from heterozygous breeders on a pure 129S background. All animals were housed in the same specific-pathogen-free facility. Animals were maintained under a temperature controlled environment and 12 hour light/dark cycles with ad lib access to water and irradiated rodent chow (TD.2916, Harlan-Teklad). Mice were euthanized by isofluorane inhalation and exsanguinated via the descending vena cava prior to tissue collection. All animal experiments were approved by the Institutional Animal Care and Research Advisory Committee at the University of Texas Southwestern Medical Center.

3.2.2 Animal Treatment

30 mg/kg GW4064 in DMSO was administered by intraperitoneal injection four hours before sacrifice. 100 mg/kg GW4064 in 1% Tween80, 1% methylcellulose, 25mM HEPES were administered by oral gavage at the

beginning and end of the dark cycle (fifteen and five hours before sacrifice). 2% (w/w) cholestyramine was admixed in the diet (custom diet TD.07658, Harlan-Teklad). 0.2% (w/w) deoxycholic acid was admixed in the diet (custom diet, Harlan-Teklad). GW4064 (GlaxoSmithKline) and T0901317 (Tocris) were admixed in the diet (500 mg/kg and 250 mg/kg diet respectively) and provided ad lib for twelve hours before sacrifice. LG268, in 0.25% Tween 80, 1% methylcellulose was administered by oral gavage twelve hours before sacrifice at a dose of 30 mg/kg. In all cases animals in the vehicle group received the appropriate vehicle solutions and diets in a manner identical to the treatment groups.

3.2.3 Transcriptional Profiling Analysis.

Preparation of *in vitro* transcription products, oligonucleotide array hybridization, and scanning were performed by using Affymetrix high-density oligonucleotide array mouse genome 430A 2.0 chips according to Affymetrix protocols. To minimize discrepancies due to variables, the raw expression data were scaled by using Affymetrix MICROARRAY SUITE 5.0 software, and pairwise comparisons were performed. The trimmed mean signal of all probe sets was adjusted to a user-specified target signal value (200) for each array for global scaling. No specific exclusion criteria were applied. Additional analysis was performed by using the freeware program BULLFROG 7.

3.2.4 RNA Extraction and Quantitative RT-PCR

These methods are described in Chapter 2.

3.2.5 Expression Plasmids

Akr1b7 and *Akr1b8* were cloned from mouse adrenal cDNA, and *Crad2* was a gift from David Russell at UT Southwestern Medical Center, Dallas, TX.

All genes were subcloned into pCMX and p3xFLAG-CMV-10 vectors containing the constitutive CMV promoter. The coding regions of all plasmids were verified by DNA sequencing, which was done at the McDermott Sequencing Core Facility at UT Southwestern, Dallas, TX.

3.2.6 Cell Culture

HEK293 cells were cultured in six-well plates at 37°C and 5% CO_2 in DMEM (containing 4 g/L glucose and L-glutamine, Gibco) supplemented with 10% charcoal-stripped, heat-inactivated FBS. Cell were transfected with 1 ug DNA and 6 uL Fugene 6 (Roche) per well. After 12-16 hours cells were treated with 25 mM bile acids. Culture media was collected 24 and 48 hours after treatment.

3.2.7 Bile Acid Extraction and Analysis by LC/MS

Culture media was combined with 10 volumes of acetonitrile and centrifuged at 16,000 x *g*. Supernatant was dried at 50°C in a vacuum oven. Bile acids were resuspended in 25% methanol. Bile acids were resolved by reverse-phase liquid chromatography (C8 pre-column, C18 analytical column) and quantified by mass spectrometry with electrospray ionization in negative ion mode. Samples were run in single ion monitoring (SIM) mode with the following ions being monitored simultaneously: 373, 375, 387, 389, 391, 393, 401, 403, 405, 407, 419.

3.2.8 Cotransfection and Luciferase Assay

HEK293 cells were grown at 37°C, 5% CO_2 in 96-well plates in DMEM (containing 4 g/L glucose and L-glutamine, Gibco) supplemented with 10% charcoal-stripped, heat-inactivated FBS and transfected by calcium phosphate coprecipitation as previously described (Makishima, 1999). Following 16-hour

treatment with bile acids, luciferase and β-galactosidase activities were measured as previously described (Lu, 2000). Luciferase activity was normalized for transfection efficiency using β-galactosidase activity and expressed as relative luciferase units (RLU). For each experiment all conditions were tested in triplicate and all experiments were repeated 3 times. Data shown is mean ± SD of triplicate assays from one representative experiment.

3.2.9 MTS Assay

This method is described in Chapter 4.

3.2.10 Statistical Analysis

Data are presented as mean ± SEM and were analyzed by two-tailed, unpaired Student's t-test. P values less than 0.05 were considered significant.

3.3 Results

3.3.1 Foreword

Throughout this section, various structural elements of bile acids are discussed. For reference, the chemical structures of some of these bile acids are shown at the end of this chapter (Figure 3.6 and 3.7).

3.3.2 Transcriptional Profiling to Identify FXR Target Genes in the Colon

The advantage of transcriptional profiling by microarray is that it represents a relatively unbiased analysis of changes in the global transcriptome. The major disadvantage is that data generated by microarray, unlike QPCR, is often not representative of actual quantitative changes in gene transcripts. This results in a high incidence of false positives that can make the validation of targets identified by microarray a time consuming and frustrating process. A number of steps were taken to reduce the frequency of false positives and thus improve

chances of identifying true FXR target genes in the colon. First, 4-5 animals were used for each treatment group. Second, RNA samples were pooled into two assay groups (RNA from 2-3 animals/assay group) and two independent microarray assays were run per treatment group. Finally, both natural and synthetic FXR agonists were used as well as *Fxr*–/– animals. Comparing results from these groups aided in ruling out hits that were not true transcriptional targets of FXR.

The platform used for transcriptional profiling was the GeneChip® Mouse Genome 430A 2.0 Array from Affymetrix. This array includes approximately 14,000 well-characterized mouse genes. Of these, 75 genes were significantly changed 2-fold or more in GW4064 (synthetic FXR agonist) treated mice, 103 in DCA treated mice, and 155 in *Fxr*–/– *mice* (Table 3.1). Comparison of these results resulted in the selection of eight putative FXR target genes (Table 3.2). Two genes on this list, *Ibabp* (also known as *Fabp-6*) and *Ostα*, were already known FXR target genes. After *Ibabp*, the gene with the greatest fold-increase in the GW4064 group was *Akr1b7*.

These results were initially disappointing because I had hoped to identify FXR targets involved in cell cycle regulation and mucosal immunity, the latter being another biological process in which FXR involvement has been implicated (Inagaki, 2006).

3.3.3 *Akr1b7* is Regulated by FXR in the Intestine

Since the most promising novel FXR target identified by microarray was *Akr1b7*, further analysis was done to confirm that this gene is indeed regulated by FXR in the intestine. QPCR analysis showed 9-fold induction of *Akr1b7* by GW4064 and 3-fold induction by DCA (Figure 3.1A). Evaluation of the relative expression of *Akr1b7* in mouse tissues confirmed previous reports of high expression in the adrenal and lower levels in the small intestine (Figure 3.1B).

Table 3.1
Summary of microarray results.[1]

group	↑	↓
GW4064	18	57
DCA	24	79
Fxr–/–	83	72

[1] Number of genes in the colon significantly increased or decreased 2-fold or greater in the indicated treatment group relative to control group.

Table 3.2
Genes induced by natural (DCA) and synthetic (GW4064) FXR agonists in the colon.[1]

Locus	Description	GW4064	DCA	*Fxr–/–*
Fabp6	fatty acid binding protein 6, ileal	173.9	5.5	1.8
Akr1b7	aldo-keto reductase family 1, member B7	6.2	1.8	1.2
Osta	organic solute transporter alpha	3.3	1.2	0.6
Sod3	superoxide dismutase 3, extracellular	2.4	3.1	1.4
Pde9a	phosphodiesterase 9A	2.4	1.4	1.2
Man2b1	mannosidase 2, alpha B1	2.3	2.0	1.7
Slc38a10	solute carrier family 38, member 10	2.1	2.7	1.6
Dapp1	dual adaptor for phosphotyrosine and 3-phosphoinositides 1	2.0	1.4	1.4

100 mg/kg GW4064 was administered by oral gavage 15 and 5 hours before sacrifice. DCA diet (0.2% w/w) was fed ad libitum for 10 days. All animals received either GW4064 or vehicle gavage and were fed matched control diet. All *Fxr*+/+ and *Fxr–/–* animals used in this study were 3-month-old 129/S males. Total RNA extracted from a 3 cm segment of the mid-colon (4-5 animals/group) was used for transcriptional profiling.
[1] Criteria for inclusion were > 2-fold increase in GW4064 group and < 2-fold increase in *Fxr–/–* group. Data represents fold-increase in mRNA for a given gene in the indicated group relative to control group.

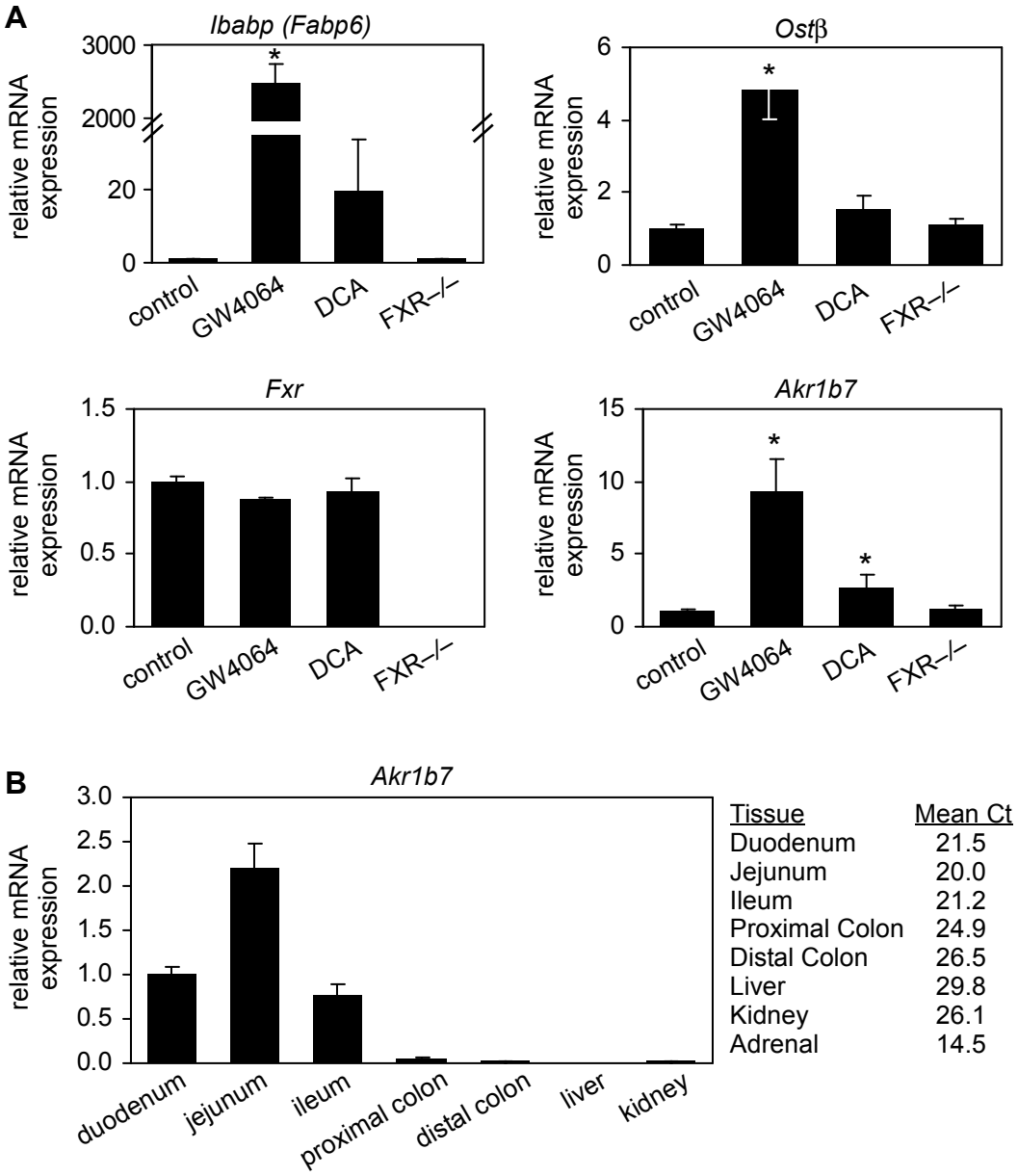

Figure 3.1 Expression profile of *Akr1b7* and induction by GW4064.
(A) Results from the transcriptional profiling study shown in Table 2 were validated by QPCR, normalized to *U36b4*, and graphed relative to wild-type, vehicle-treated control. Data represent the mean ± SEM of 4-5 animals per group. * $p < 0.05$ compared to control group.
(B) Expression of *Akr1b7* was determined by QPCR, normalized to *U36b4*, and graphed relative to duodenum. Mean cycle time (Ct) is shown.

Compared to ileum, 15- to 20-fold lower levels of expression were observed in colon and kidney and expression was reduced another 10-fold in liver (Figure 3.1B). *Akr1b7* has previously been identified as an LXR target gene in the intestine, where it is thought to play a role in the detoxification of lipid peroxides (Volle, 2004). To better characterize the extent to which *Akr1b7* is regulated by FXR, its expression was determined by QPCR in tissues from several independent experiments involving FXR activation. Results showed that *Akr1b7* was not induced by GW4064 in the adrenal gland, nor was FXR required for its expression in this tissue (Figure 3.2A). Induction of a known FXR target gene, *Ostβ*, confirmed that FXR was activated in adrenal (Figure 3.2A). In contrast, in the ileum *Akr1b7* was induced by GW4064 and expression was lower in *Fxr*–/– *mice* (Figure 3.2B). Furthermore, *Akr1b7* levels were decreased following treatment with the bile acid binding resin cholestyramine (Figure 3.2B). LXR and FXR activation in ileum produced comparable increases in *Akr1b7* expression (Figure 3.2C). In addition, activation of the common heterodimer partner, RXR, also increased *Akr1b7* expression (Figure 3.2C). It has recently been reported that intestinal *Akr1b7* is increased by ligands for PXR and CAR (Liu, 2009). These results demonstrate that *Akr1b7* is induced by a number of nuclear receptors in the intestine. Importantly, while FXR appears to be required for the basal expression of *Akr1b7* in ileum, this has not been shown for LXR, PXR, or CAR. In fact, higher levels of Akr1b7 are present in Lxrα–/– mice (Volle, 2004). In summary, these data demonstrated a direct correlation between FXR activity and *Akr1b7* expression and suggested a possible role for AKR1B7 in bile acid metabolism.

3.3.4 AKR1B7 Metabolizes 3-keto Bile Acids

Since other aldo-keto reductases are involved in the conversion of cholesterol to bile acids in liver, I hypothesized that bile acids might be substrates for AKR1B7 in the intestine. To test this, *Akr1b7* and a closely related gene,

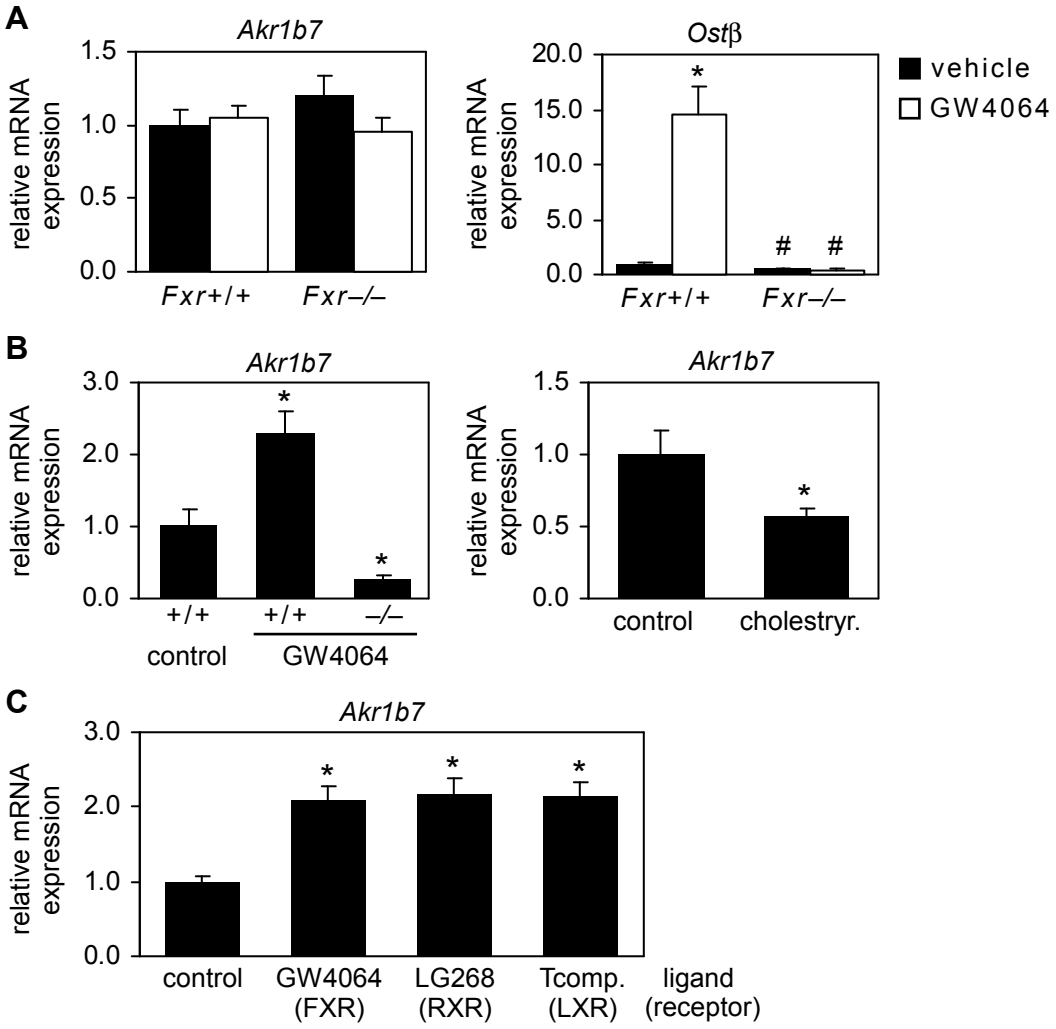

Figure 3.2 Transciptional regulation of *Akr1b7 in vivo.*
(A) M ice of the indicated genotype were treated for 4 hours with 30 mg/kg GW4064 by intraperitoneal injection. *Akr1b7* and *Ost*β expression in adrenal was determined by QPCR, normalized to *cyclophilin*, and graphed relative to vehicle-treated wild-type group. Data represent the mean ± SEM of 5 animals per group.
* $p < 0.05$ compared to vehicle of the same genotype. # $p < 0.05$ compared to wild-type of the same treatment group. **(B)** Wild-type and *Fxr–/–* animals were treated with 100 mg/kg GW4064 by oral gavage 5 and 15 hours before sacrifice or 10 days with 2% (w/w) cholestyramine admixed in diet. *Akr1b7* expression in ileum was determined by QPCR, normalized to *cyclophilin*, and graphed relative to vehicle-treated control. Data represent the mean ± SEM of 4 animals per group. * $p < 0.05$ compared to wild-type control. **(C)** Wild-type animals were treated for 12 hours with the indicated ligands. *Akr1b7* expression in ileum was determined by QPCR, normalized to *U36b4*, and graphed relative to vehicle-treated control. Data represent the mean ± SEM of 5 animals per group.
* $p < 0.05$ compared to control.

Akr1b8, were cloned and expressed in HEK293 cells. Following treatment with bile acids, culture media was collected and analyzed for bile acid metabolites by LC/MS. The primary method to determine whether bile acids are substrates for AKR1B7 was to compare bile acid metabolites from cells expressing AKR1B7 with metabolites from cells transfected with a control vector. It was found that a variety of 3-keto bile acids were reduced to 3-hydroxy bile acid in cells expressing AKR1B7 (Table 3.3). Significant conversion was apparent 24 hours after treatment and prolonged incubation resulted in greater than 50% of the substrate being metabolized (Figure 3.3A and B). Interestingly, reduction of the 3-keto group occurred in a stereospecific manner, such that only 3β-hydroxy bile acids were formed. In contrast, an endogenous enzyme in HEK293 cells produced the 3α-hydroxy epimer. Specifically, Figure 3.3A (24-hour treatment) and Figure 3.3B (48-hour treatment) show conversion of 3-keto lithocholic acid (3-keto LCA) to 3α-hydroxy lithocholic acid (LCA) by HEK293 cells transfected with control vector, and conversion to 3β-hydroxy lithocholic acid (iso LCA) by cells expressing AKR1B7 (note that in both figures the scale in the lower panel is different from the upper two panels, thus while the LCA to 3-keto LCA ratio is increased in the lower panel relative to the middle panel, this is the result of increased conversion of 3-keto LCA to iso LCA and not LCA). AKR1B7 did not oxidize the 3-hydroxy group of regular bile acids or iso bile acids, indicating that it selectively increases the rate of the reducing reaction (Table 3.3). Furthermore, reduction of 6-keto, 7-keto, and 12-keto bile acids did not occur, indicating specificity of AKR1B7 for the 3-keto group.

Some of the more abundant 3-keto bile acids present in colon, such as 3-keto DCA and 3-keto CDCA, are not commercially available. To test whether these are substrates for AKR1B7, heterologous co-expression of AKR1B7 with *cis*-retinol/androgen dehydrogenase 2 (CRAD2) was followed by treatment with

Table 3.3
Bile acids metabolized by AKR1B7.

bile acid[1] tested	detected metabolites
3-keto-5β-cholanic acid (3-keto LCA)	3β-hydroxy-5β-cholanic acid (iso LCA)
3,6-diketo-5β-cholanic acid	monohydroxy-monoketo-5β-cholanic acid*
3,7-diketo-5β-cholanic acid	monohydroxy-monoketo-5β-cholanic acid*
3,12-diketo-5β-cholanic acid	monohydroxy-monoketo-5β-cholanic acid*
3,7,12-triketo-5β-cholanic acid (dehyro CA)	monohydroxy-diketo-5β-cholanic acid*
3-keto-7α,12α-dihydroxy-5β-cholanic acid	3β,7α,12α-dihydroxy-5β-cholanic acid (iso CA)
3α-hydroxy-5β-cholanic acid (LCA)	none
3α,7α-dihydroxy-5β-cholanic acid (CDCA)	none
3α,12α-dihydroxy-5β-cholanic acid (DCA)	none
3α,7α,12α-trihydroxy-5β-cholanic acid (CA)	none
3α-hydroxy-6-keto-5β-cholanic acid	none
3α-hydroxy-7-keto-5β-cholanic acid	none
3α-hydroxy-12-keto-5β-cholanic acid	none
3β-hydroxy-5β-cholanic acid (iso LCA)	none
3β,12α-dihydroxy-5β-cholanic acid (iso DCA)	none

[1] common name is shown in parentheses.
* no authentic standard available for identification.
HEK293T cells were transfected with *Akr1b7*, *Akr1b8*, or control vector and treated with the indicated bile acids (25 mM). Bile acids were extracted from culture media collected 24 and 48 hours after treatment. Extracts were resolved by reverse phase chromatography and analyzed by mass spectometry using single ion monitoring (SIM) in negative ion mode. Monitored ions included all combinations of mono- di- and tri-hydroxy and keto bile acids. AKR1B8 yielded the same results as shown for AKR1B7.

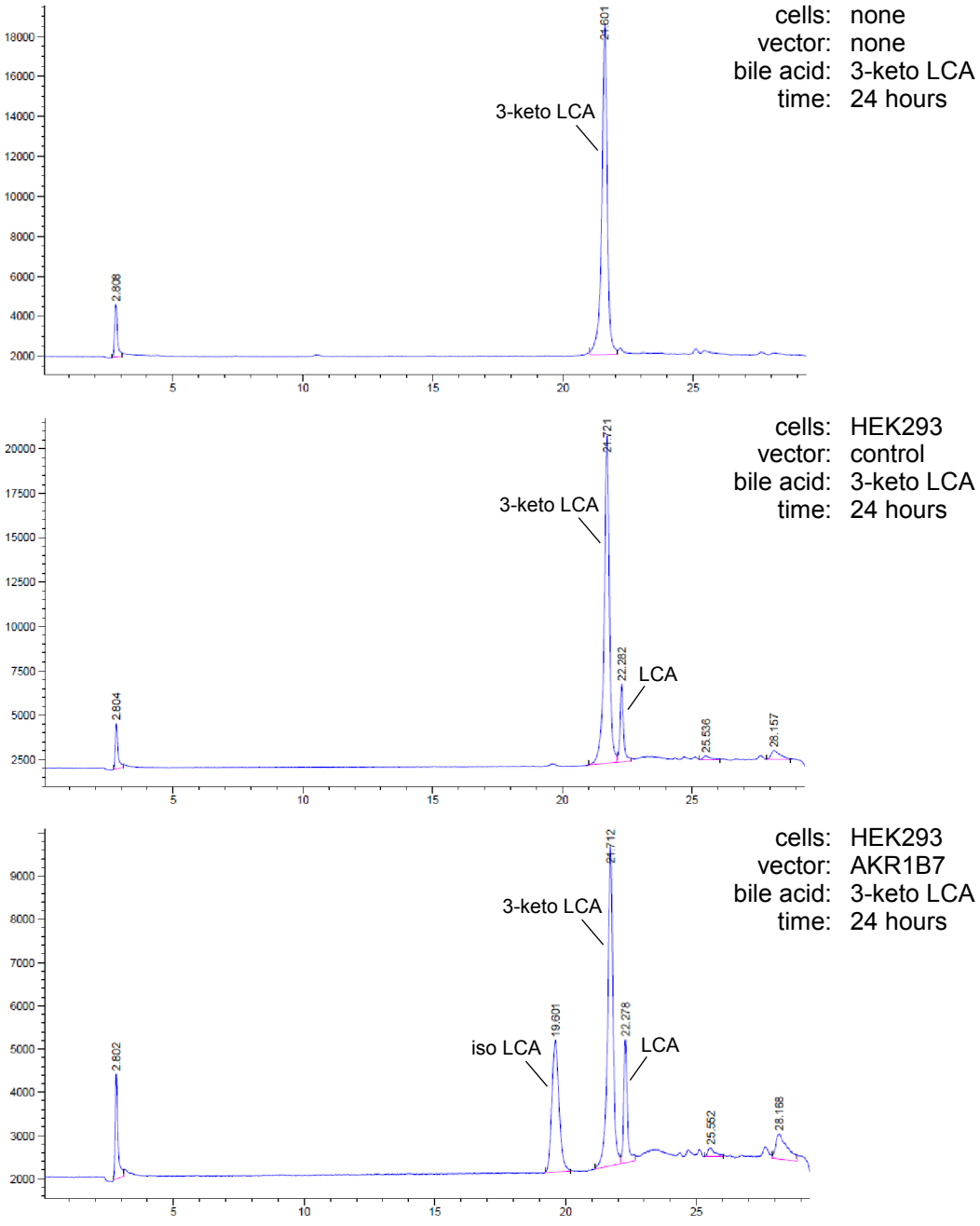

Figure 3.3A AKR1B7 metabolizes 3-keto LCA to iso LCA.
HEK293 cells or culture media alone was treated as indicated. Bile acids were extracted from culture media, resolved by reverse phase chromatography and analyzed by mass spectometry using single ion monitoring (SIM) in negative ion mode. Monitored ions included all combinations of mono- di- and tri-hydroxy and keto bile acids.

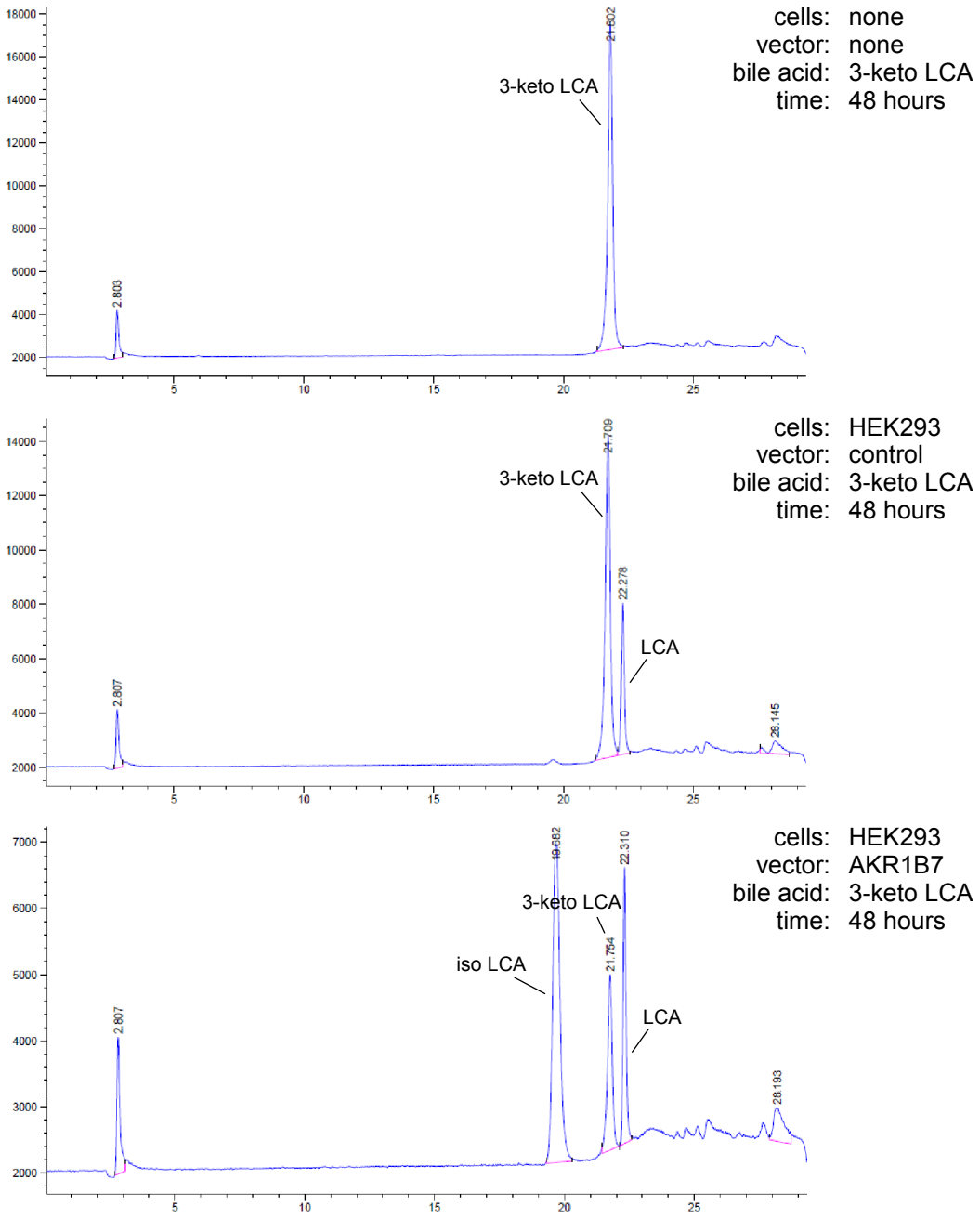

Figure 3.3B AKR1B7 metabolizes 3-keto LCA to iso LCA.
HEK293 cells or culture media alone was treated as indicated. Bile acids were extracted from culture media, resolved by reverse phase chromatography and analyzed by mass spectometry using single ion monitoring (SIM) in negative ion mode. Monitored ions included all combinations of mono- di- and tri-hydroxy and keto bile acids.

DCA and CDCA. CRAD2 has been shown to oxidize 3α-hydroxy bile acids, generating 3-keto bile acids (Cheng, 2003). Cells expressing AKR1B7 did not metabolize DCA, while cells expressing CRAD2 produced 3-keto DCA and smaller amounts of iso DCA (Figure 3.4). Interestingly, co-expression of AKR1B7 and CRAD2 resulted in production of mainly iso DCA (Figure 3.4). In ancillary studies I found that CRAD2 also oxidizes 3β-hydroxy groups and reduces 3-keto groups (conversion to α-hydroxy highly favored over β-hydroxy) (Table 3.4). These data suggest that some of the 3-keto DCA and DCA still present in the AKR1B7/CRAD2 co-expression samples may be formed by concomitant conversion of iso DCA to these species by CRAD2, thus underestimating the efficacy of AKR1B7 to convert 3-keto DCA to iso DCA. Comparable results were obtained for conversion of CDCA to iso CDCA by co-expression of AKR1B7 with CRAD2 (data not shown). These results indicate that AKR1B7, together with an enzyme such as CRAD2, may function to convert regular bile acids to iso bile acids.

3.3.5 Pharmacology and Biology of Iso Bile Acids

Although iso bile acids represent 27% of bile acids in normal human cecal contents, not much is known about their biological function (Hamilton, 2007). In the absence of 3β-hydroxy steroid dehydrogenase type 7 (HSD3B7), mice do not produce 3α-hydroxy bile acids, instead primarily iso bile acids are made and secreted by the liver (Shea, 2007). Although comparable levels of bile acids are formed, severe lipid malabsorption in these mice results in death at an early age. These results indicate that the conformation of the 3α-hydroxyl group is essential for the detergent properties of bile acids. It was also found that FXR target gene expression was reduced in *Hsd3b7*–/– mice, indicating that iso bile acids may not be ligands for FXR. Together with the finding that FXR induced *Akr1b7*, and that AKR1B7 in turn produced iso bile acids, these data suggested the possibility of a

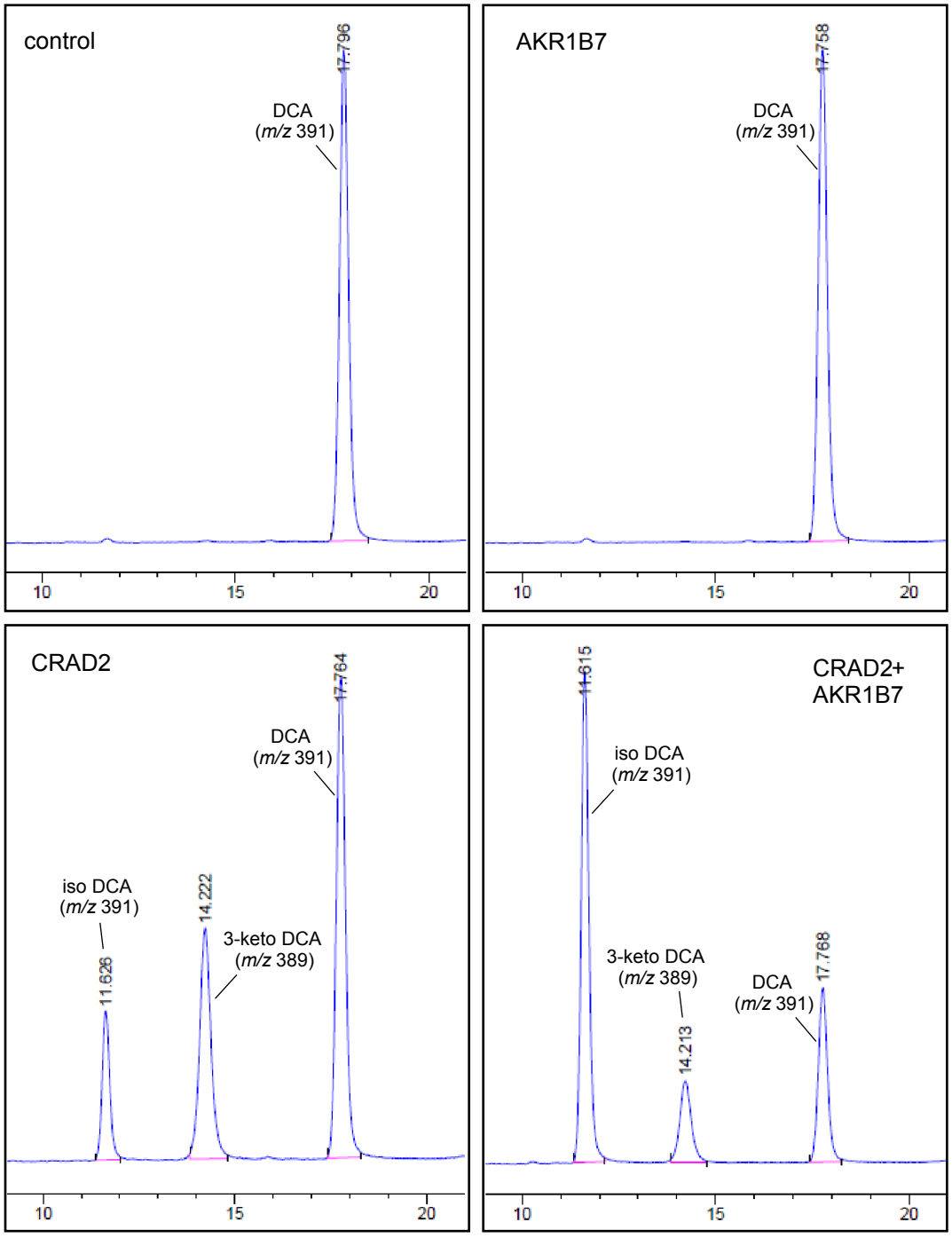

Figure 3.4 CRAD2 + AKR1B7 convert DCA to iso DCA.
HEK293 cells were transfected as indicated and treated for 48 hours with 25 mM DCA. Bile acids were extracted from culture media, resolved by reverse phase chromatography and analyzed by mass spectometry using single ion monitoring in negative ion mode. Monitored ions included all combinations of mono- di- and tri-hydroxy and keto bile acids.

Table 3.4
Bile acids metabolized by CRAD2.

bile acid[1] tested	detected metabolites
3α-hydroxy-5β-cholanic acid (LCA)	3-keto-5β-cholanic acid (3-keto LCA)
3-keto-5β-cholanic acid (3-keto LCA)	3α-hydroxy-5β-cholanic acid (LCA)
3β-hydroxy-5β-cholanic acid (iso LCA)	3-keto-5β-cholanic acid (3-keto LCA) and 3α-hydroxy-5β-cholanic acid (LCA)
3,6-diketo-5β-cholanic acid	monohydroxy-monoketo-5β-cholanic acid*
3,7-diketo-5β-cholanic acid	monohydroxy-monoketo-5β-cholanic acid*
3α,7α-dihydroxy-5β-cholanic acid (CDCA)	monohydroxy-monoketo-5β-cholanic acid*
3α,12α-dihydroxy-5β-cholanic acid (DCA)	monohydroxy-monoketo-5β-cholanic acid*

[1] common name is shown in parentheses.
* no authentic standard available for identification.
HEK293T cells were transfected with *Crad2* or control vector and treated with the indicated bile acids (25 mM). Bile acids were extracted from culture media collected 24 and 48 hours after treatment. Extracts were resolved by reverse phase chromatography and analyzed by mass spectometry using single ion monitoring (SIM) in negative ion mode. Monitored ions included all combinations of mono- di- and tri-hydroxy and keto bile acids.

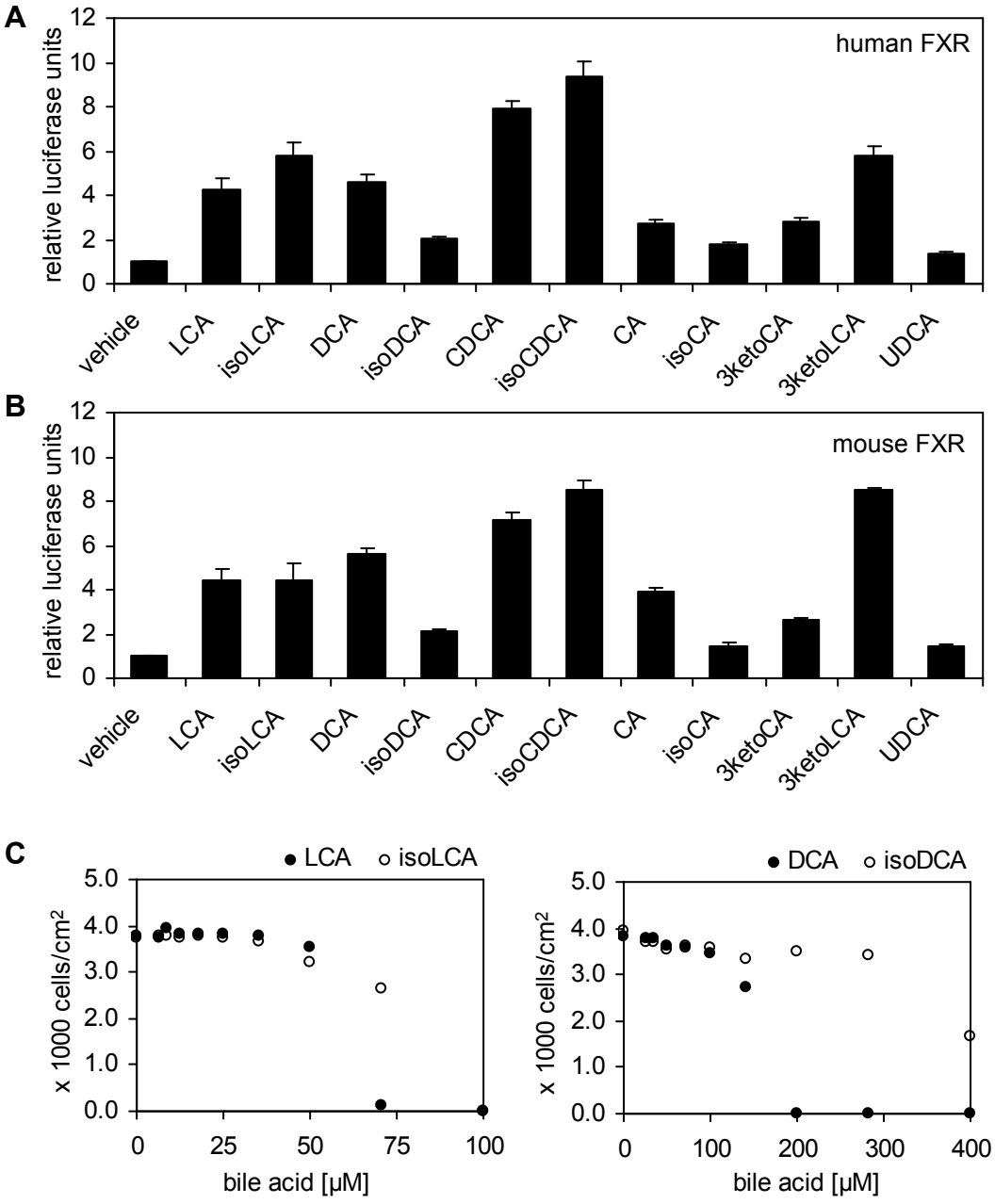

Figure 3.5 Iso bile acids activate FXR and are less toxic than regular bile acids. HEK293 cells were cotransfected with β-galactosidase, FXRE-luciferase, hIBAT, hRXR, and either hFXR **(A)** or mFXR **(B)**. Following treatment with 20 μM bile acids or vehicle, luciferase activity was quantitated and normalized to ß-galactosidase activity. Data are graphed relative to the first data point and represent the mean ± SD of 3 replicates. **(C)** IEC-18 cells were treated with bile acids for 72 hours. Cell number was determined by MTS assay.

negative feedback loop to regulate FXR activity. Unfortunately, a reporter-gene assay failed to show major differences between FXR transactivation by standard bile acids and iso bile acids (Figure 3.5A and 3.5B). Of note, decreased induction was seen for iso bile acids with a 12-hydroxy group (CA and DCA) while slightly higher induction occurred with bile acids without this group (LCA and CDCA), suggesting that the two groups of bile acids likely bind FXR in slightly different conformations.

Given that iso bile acids are poor detergents, I hypothesized that they might be less toxic than their 3α-hydroxy epimers. As described in Chapter 4, mono- and di-hydroxylated bile acids with hydroxyl groups in the α conformation induce apoptosis in cultured cells when present at high micromolar concentrations. MTS assay was used to quantitate viability of immortalized rat intestinal epithelial cells (IEC-18) treated with bile acids. These experiments showed that both iso LCA and iso DCA were less toxic than LCA and DCA respectively (Figure 3.5C). Thus conversion of bile acids to iso bile acids may be a mechanism for bile acid detoxification.

3.4 Discussion

Loss of FXR has been shown to increase the risk of developing cancer in the liver and intestine (Chapter 2). The mechanism underlying these effects is not known. Many tumor suppressor genes function by regulating the cell cycle or by inducing DNA repair mechanisms. These events prevent the propagation of genetic insults that might otherwise lead to cancer. Since FXR is a transcription factor, its effects on a biological process are likely to be evident at the level of the transcriptome. The main objective of the transcriptional profiling study described in this chapter was to provide mechanistic information about the anti-tumor effects of FXR in the colon.

While it was initially expected that this study might reveal transcriptional targets of FXR that play a role in regulating the cell cycle, no such association was found. In retrospect, it appears unlikely that FXR plays a role in regulating the cell cycle, particularly in light of new information regarding the location of FXR expression in the intestine (Chapter 2). In most organs the delineation between replication-competent cells and post-mitotic cells is not as clear as in the colon. Colonic epithelium is organized into discrete crypts. Stem cells reside exclusively at the base of these crypts, transient proliferating cells are present in the lower half, while the upper half and the surface epithelium are populated exclusively by terminally differentiated cells. Given that FXR expression appears to be limited to the terminally differentiated compartment (Chapter 2), a role for FXR in regulating the cell cycle in colonocytes would be irrelevant since cells would already have exited the cell cycle. It has been reported that FXR contributes to the mechanism of bile acid-induced liver regrowth following hepatectomy in mice (Huang, 2006). This conclusion was based on the observation that liver regrowth is blunted in *Fxr*–/– mice. No clear mechanism was proposed for how FXR might be inducing proliferation in the liver, and it is possible that the observed effects were secondary to preexisting inflammation or bile acid-induced toxicity. Nonetheless, it is possible that FXR may play a role in regulating the cell cycle in liver, but not intestine.

A particularly exciting result of this study is the finding that FXR regulates expression of an enzyme that appears to play a role in bile acid detoxification. *Akr1b7* is transcriptionally regulated *in vivo* by multiple members of the nuclear receptor superfamily; however, only FXR appears to be required for its expression in the intestine. Previously, two other enzymes have been implicated in the detoxification of bile acids, CYP3A4, which catalyzes hydroxylation of position 6, and SULT2A1 which adds a sulfo moiety to the

hydroxyl group at position 3 (Araya, 1999; Echchgadda, 2004). As described in Chapter 1, both of these enzymes are regulated by nuclear receptors. The findings of the current study provide further evidence that members of the enteric nuclear receptor clade (see Chapter 1) play a role in the regulation of bile acid/xenobiotic detoxification in the intestine.

Three phases of xenobiotic detoxification have been defined. In the first phase, a substrate is typically modified by the addition of a hydroxyl group by a cytochrome P450. The reactions carried out by this family of monooxygenases include oxidation, reduction, and hydrolysis. In phase II, the chemically activated moiety is further modified by conjugating enzymes that add a larger, more hydrophilic group such as glucuronic acid, glutathione, sulfate, glycine, taurine, or acetate. Finally phase III involves transporting the modified and typically more water-soluble compound out of the cell. As bile acids travel between the intestine and liver, these same reactions also function to maintain a healthy bile acid pool. In the liver, bile acids are conjugated to glycine or taurine and are normally di- or tri-hydroxylated (in mice >95% are tri-hydroxylated). In the intestine, bile acids are deconjuated and dehydroxylated resulting in a more hydrophobic steroid nucleus. These reactions are carried out by enzymes expressed by intestinal bacteria. After returning to the liver bile acids are repaired (rehydroxylated and reconjugated) before they are again secreted and stored in the gallbladder (Hofmann, 1999a). Little is known about the role of the intestine in this process. The major function of bile acids is to facilitate lipid absorption; however, once they are absorbed by intestinal cells, the detergent properties of bile acids are no longer desirable. The conversion of bile acids to iso bile acids by AKR1B7 may be a way to decrease such detergent effects. Future studies to examine the types of bile acids present in portal circulation under postprandial

conditions may provide a better understanding of bile acid metabolism by the intestine.

The endogenous source and prevalence of substrates for AKR1B7 is an important question that has not been addressed in this study. Intestinal bacteria are known to produce 3-keto bile acids (Kang, 2008). Alternatively, an intestinal enzyme with a function similar to CRAD2 may be the source. Indeed, data presented in the current study demonstrate that AKR1B7 and CRAD2 together were capable of efficient conversion of 3α-hydroxy bile acids to iso bile acids.

Unlike AKR1B7, CRAD2 increases the rate of both oxidation and reduction of the hydroxy/keto group at position 3. The biological function of CRAD2 is not known. Given its high level of expression in liver, it is likely to function in regulating the balance between 3-keto and 3α-hydroxy bile acids in this organ.

As shown in Figure 3.6, the therapeutic bile acid UDCA has a hydroxyl group on the β-side of the steroid nucleus, and like iso bile acids it is less toxic than its epimer, CDCA (see Chapter 4). These observations suggest that the presence of a β-hydroxyl group may be a general feature of bile acids with low toxicity. Interestingly, UDCA has been shown to prevent carcinogen-induced colon cancer in rats (Earnest, 1994; Narisawa, 1999). Unlike humans and rats, a large proportion of bile acids in mice have β-hydroxyl groups, including α-, β-, and ω-muricholates. The presence of muricholates may partially explain why the incidence of spontaneous colon cancer is rare in mice.

Data presented in this chapter provide evidence that AKR1B7 metabolizes 3-keto bile acids. Many other 3-keto steroids play important roles in endocrine biology. Cortisol, produced in the adrenal gland, functions in regulating blood glucose levels; in the adult, male sex steroids are essential for growth and virility; and a major function of progesterone is to support gestation.

These steroids may also be substrates for AKR1B7. Preliminary results suggest that androstenedione is metabolized by AKR1B7 (communication with Dr. Richard Auchus). Interestingly, ACTH stimulates both glucocorticoid production and AKR1B7 expression in the zona fasciculata of the adrenal. In the ovary, AKR1B7 is highly expressed in thecal cells which produce androstenedione. Moreover, 3-keto steroids may affect sperm transport within the vas deferens, where AKR1B7 is highly expressed. Thus, AKR1B7 is expressed in several organs exposed to 3-keto steroids. It will be interesting to see if steroid hormone metabolism is regulated by AKR1B7 in these organs.

3.5 Acknowledgements

Samuel Schmidt cloned *Akr1b7* and *Akr1b8*, and performed all the experiments to identify substrates of these enzymes including transfections, bile acid treatments, and bile acid extractions. Thus, he contributed significantly to the studies described in this chapter. Tissues from animals treated with RXR and LXR ligands were obtained from an experiment designed and organized by Klementina FonTacer and Angie Bookout. Microarray studies were done in collaboration with Ruth Yu at the Salk Institute for Biological Sciences, La Jolla, CA.

3α,7α-dihydroxy-5β-cholanic acid (CDCA)

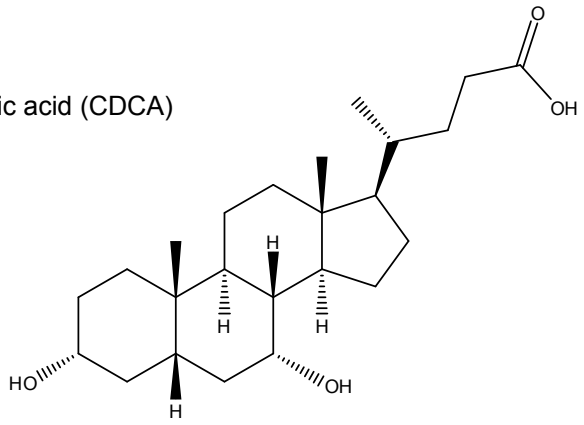

3β,7α-dihydroxy-5β-cholanic acid (iso CDCA)

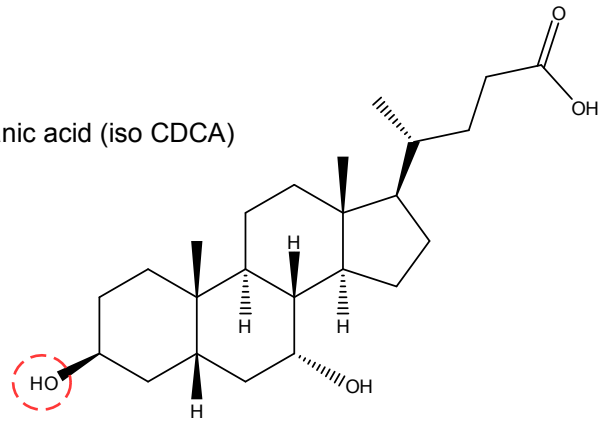

3α,7β-dihydroxy-5β-cholanic acid (UDCA)

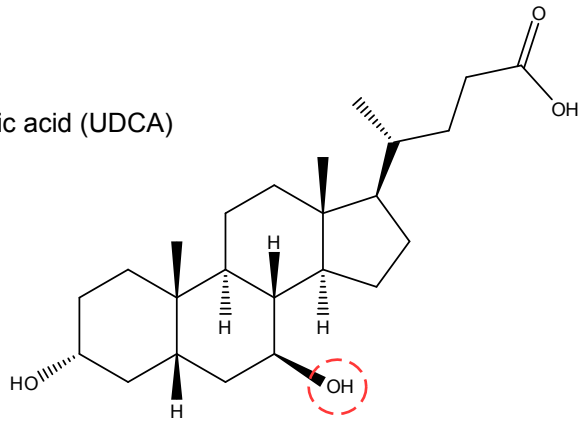

Figure 3.6 Bile acid structures.

3α-dihydroxy-5β-cholanic acid (LCA)

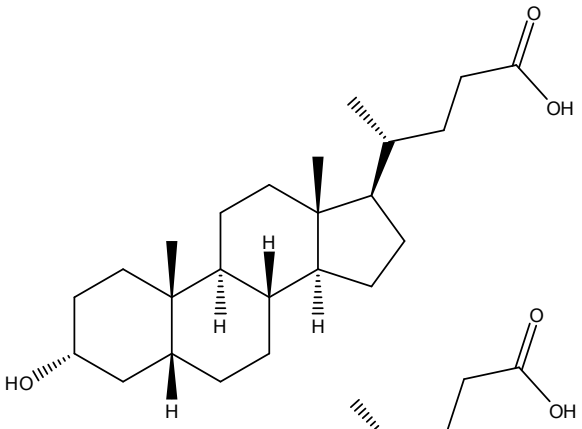

3β-dihydroxy-5β-cholanic acid (iso LCA)

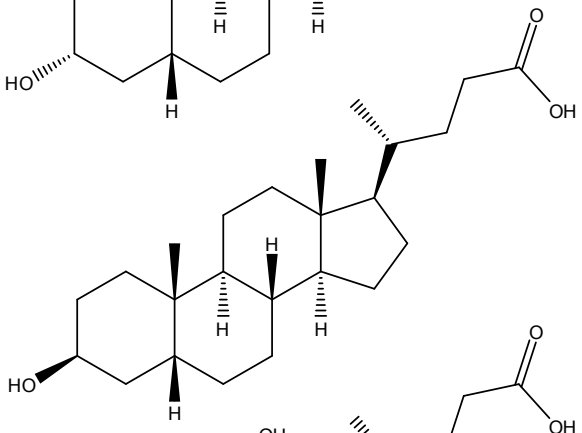

3α,12α-dihydroxy-5β-cholanic acid (DCA)

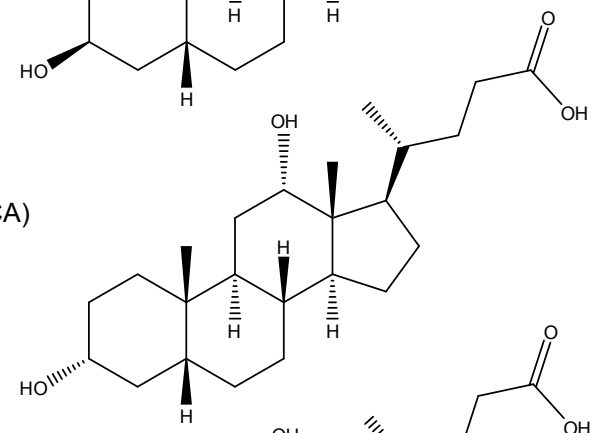

3β,12α-dihydroxy-5β-cholanic acid (iso DCA)

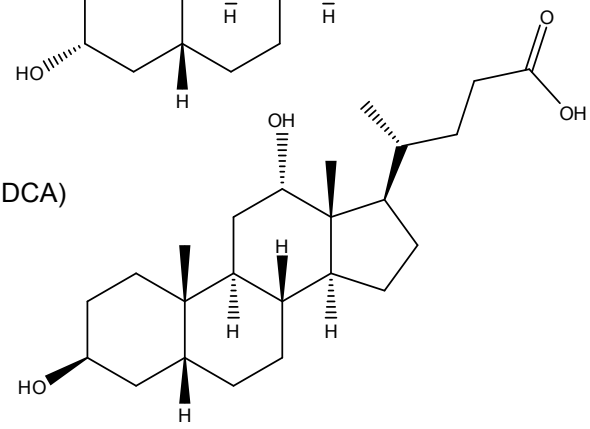

Figure 3.7 Bile acid structures.

CHAPTER 4
Biological Effects of Bile Acids on Cultured Cells

4.1 Introduction

At millimolar and high micromolar concentrations, bile acids induce apoptosis in liver cells *in vitro* and *in vivo* (Graf, 2002a; Graf 2002b). Some reports suggested that low millimolar concentrations of DCA induce proliferation in colon cancer cells (Milovic, 2002; Peiffer, 1997). Such concentrations also activate FXR in cell lines. Preliminary data from our lab had shown that select bile acids and a synthetic FXR agonist, GW4064, induced proliferation in colon cancer cells. Thus, it was hypothesized that signaling by FXR might be responsible for the proliferative effects of bile acids in colon cancer cells.

The experiments described in this chapter tested the hypothesis that bile acid-induced proliferation *in vitro* was the result of FXR-mediated changes in gene transcription. Ultimately, a large number of bile acids and GW4064 were tested in numerous cell lines; however, no increase in proliferation was seen under any condition. At higher concentrations bile acids induced cell cycle arrest and apoptosis. These results were documented using a several methods to measure proliferation. Interestingly, it was found that bovine serum albumin ameliorated the toxic effects of bile acids. It is hypothesized that these effects are due to chelation of bile acids by albumin.

4.2 Methods

4.2.1 Cell Lines and Culture Conditions

Caco2 cells were purchased from ATCC (Number HTB-37) and propagated in DMEM (containing 4 g/L glucose and L-glutamine, CellGro) supplemented with 20% heat-inactivated FBS. HCT-116 and HT-29 cells were provided by Dr. John Minna at UT Southwestern Medical Center, Dallas, TX. Both cell lines were propagated in McCoy's 5a Medium (ATCC) supplemented with 20% heat-inactivated FBS. IEC-18 cells were purchased from ATCC and propagated in DMEM (containing 4 g/L glucose and L-glutamine, CellGro) supplemented with 5% heat-inactivated FBS and 10 μg/mL bovine insulin (Sigma). All cell lines were cultured at 37°C in ambient air adjusted to 5% carbon dioxide. Unless otherwise indicated in figure legends, the culture conditions for all experiments performed with these cell lines are as indicated above. Bile acids were purchased from Sigma or Steraloids. Bile acid enantiomers were kindly provided by Dr. Douglas Covey.

4.2.2 Cell Counts

Cells cultured in 6-well or 12-well plates were trypsinized and diluted in trypan blue solution (Sigma). Trypan blue negative cells were counted using a hemocytometer.

4.2.3 Thymidine Incorporation Assay

Cells grown in 12-well plates were exposed for two hours to 1 μCi/mL tritiated thymidine (Amersham, TRK328). Media was removed and cells were rinsed with cold PBS. DNA was precipitated with 10% TCA solution for two hours. Following a 95% ethanol rinse, cells were dissolved with 0.2N sodium hydroxide. Lysates diluted in 10 mL scintillation cocktail were analysed in triplicate using a scintillation counter (Beckman LS 6500).

4.2.4 MTS Assay

Cells were grown in 96-well plates, in 50 μL culture media at a starting density of 1000 or 5000 cells per well. On each plate with 5000 cells per well, dilutions of 4000, 3000, 2000, and 0 cells per well were also plated. On each plate with 1000 cells per well, dilutions of 750, 500, 250, and 0 cells per well were also plated. 24 hours after plating, cells were treated by the addition of 50 μL media containing the treatment condition. Wells containing cell dilutions were treated with the control condition. 3 days after treatment, plates were assayed using CellTiter 96™ (Promega). The assay was performed as recommended by the manufacturer. Following determination of absorbance at 490 nm, cells in wells containing cell dilutions were trypsinized and counted. Cell counts and absorbance values were used to generate a standard curve allowing conversion of absorbance to cell number for all treatment conditions.

4.2.5 RNA Extraction and Quantitative RT-PCR

Prior to RNA extraction, culture media was removed and cells were rinsed briefly with PBS. Total RNA was extracted using RNA STAT-60™ (IsoTex Diagnostics) as recommended by the manufacturer. Four micrograms of RNA from each sample were DNAse treated and reverse transcribed using random hexamers. The resulting complementary DNA (cDNA) was analyzed by quantitative RT-PCR using a protocol using a protocol previously described in detail (Bookout, 2003). Briefly, quantitative PCR reactions containing 25 ng of cDNA, 150 nmol of each primer, and SYBR® GreenER TM PCR Master Mix (Invitrogen) were carried out in triplicate in 384-well format using an ABI PRISM® 7900HT instrument (Applied Biosystems). Relative mRNA levels were calculated using the comparative CT method normalized to *cyclophilin*. The primer sequences used for gene expression analyses are listed in Appendix A.

They were designed using Primer Express® software (Applied Biosystems) and validated as previously described (Bookout, 2003).

4.2.6 Analysis of Apoptosis by FACS

Cells grown in 6-well plates were trypsinized and prepared using the Annexin V-FITC Apoptosis Detection Kit and Protocol (BD Biosciences Cat. # 556547). Propidium iodide was used to control for nonviable cells. Following staining, cells were immediately analyzed by flow cytometry at the UT Southwestern FACS core facility.

4.2.7 Immunodetection of Cleaved PARP

Cells grown in 6-well plates were scraped in Laemmli sample buffer containing protease inhibitors (complete-Mini™, Roche) and sonicated at 30% intensity with 15 one-second pulses. Soluble proteins were quantitated by Bradford assay, resolved by SDS-PAGE, and transferred to Hybond-P membrane (GE). PARP was detected using an antibody from Cell Signaling (#9542). Membranes were subsequently reprobed with an α-actin antibody (Sigma A5316).

4.2.8 Transcriptional Profiling of Cell Cycle Genes

Analysis of cell cycle gene expression was performed using the Human Cell Cycle PCR Array from SABiosciences™ (PAHS-020). RNA was extracted and reverse-transcribed using the reagents and protocol recommended by SABiosciences. cDNA quantitation was performed using PCR Array reagents (SABiosciences) and ABI PRISM® 7900HT instrument (Applied Biosystems). Results were analyzed using a data analysis patch for Microsoft Excel® provided by SABiosciences.

4.2.9 Statistical Analysis

Data were analyzed by two-tailed, unpaired Student's t-test. P values less than 0.05 were considered significant.

4.3 Results

4.3.1 Colon Cancer Cell Lines Differentially Express *FXR*

A large number of well-characterized human colon cancer cell lines have been used to study various aspects of cell growth, differentiation, and metabolism in transformed cells derived from the intestinal epithelium. Of the eight cell lines I initially analyzed, three were chosen for further analysis based on their growth properties and gene expression profiles (Figure 4.1). Caco2 cells grow relatively slow, and upon reaching confluency they begin to express markers of differentiation. Studies have shown that changes in gene expression in differentiating Caco2 cells are similar to migrating intestinal cells as they differentiate *in vivo* (properties of colon cell migration and differentiation are described in Chapters 2 and 3) (Saaf, 2007). HT-29 cells have a shorter doubling time and are also more tumorigenic in orthotopic implantation models (Figure 4.1A) (Flatmark, 2003). HCT-116 cells are poorly differentiated, divide rapidly, and are highly tumorigenic (Figure 4.1A) (Flatmark, 2003). In preconfluent (undifferentiated) Caco2 cells, *FXR* expression was low, but increased dramatically when the cells differentiate (Figure 4.1B). Expression of the FXR target gene, *IBABP*, also increased upon differentiation; while expression of another FXR target, *FGF19*, was not changed. In contrast, both preconfluent and postconfluent HT-29 cells express moderate levels of *FXR*, high levels of *FGF19*, and no *IBABP* (Figure 4.1B). HCT-116 cells do not express any of these genes and have the highest level of *CyclinD1* expression (Figure 4.1B).

A

cell line	doubling time	tumorigenicity	other features
Caco2	3-4 days	low	differentiate when confluent
HT-29	2 days	medium	mutated *p53*
HCT-116	1-2 days	high	oncogenic *KRAS*

B

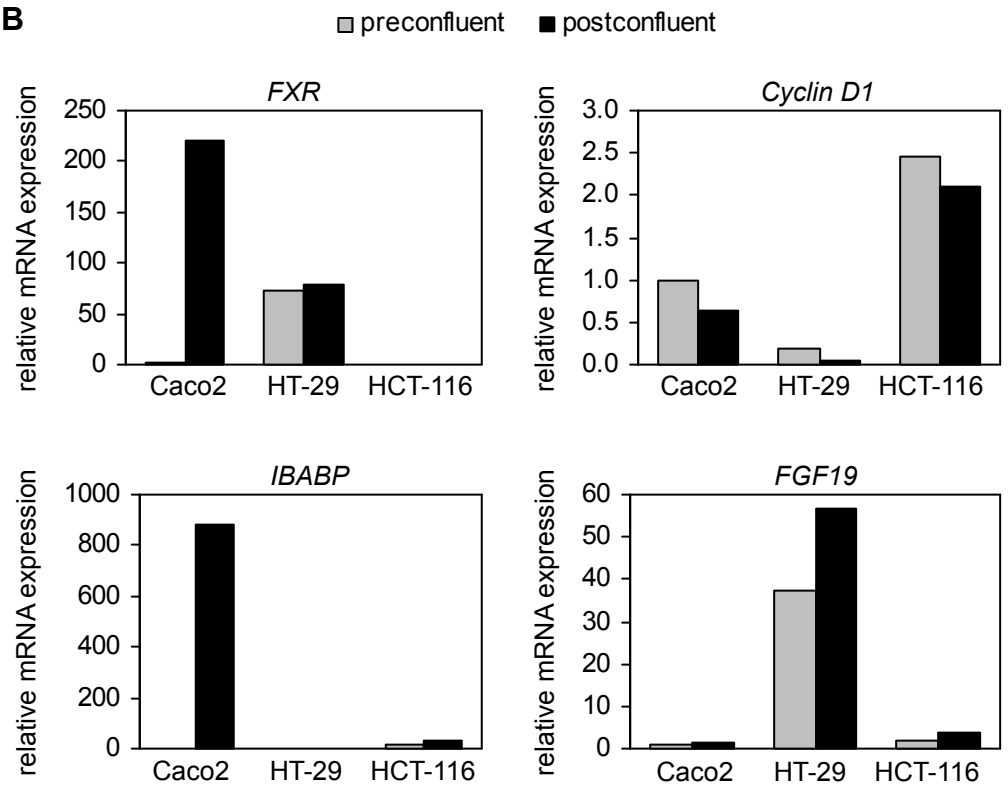

Figure 4.1 Colon cancer cell lines: growth properties and gene expression.
(A) Growth properties of colon cancer cell lines. Doubling time was measured in standard culture media supplemented with 10% FBS. Tumorigenicity indicates the potential to form tumors in mice. **(B)** Total RNA was extracted from the indicated cell lines during log growth (preconfluent) and one week after reaching confluency (postconfluent). The level of mRNA expression was determined by QPCR, normalized to *cyclophilin,* and graphed relative to preconfluent Caco2.

4.3.2 Bile Acids and GW4064 Do Not Induce Proliferation

Given the high expression of *FXR* in differentiated Caco2 cells, experiments were done to determine the optimal time point to activate FXR and induce proliferation. Three days after reaching confluency, *FXR* expression was detected and both CDCA and GW4064 increased expression of *IBABP* (Figure 4.2A and 4.2B). At this time point cells were also actively dividing (log growth phase) (Figure 4.2A). Three-day postconfluent Caco2 cells were treated with primary bile acids (CA and CDCA), secondary bile acids (DCA, LCA, and UDCA), and enantiomers of CDCA and LCA (eCDCA and eLCA). While CDCA is a potent activator of FXR, its enantiomer has no such effect; thus it was included in these experiments as an indicator of ligand-independent detergent effects. Under these conditions bile acids and GW4064 did not induce proliferation (Figure 4.2C). Caco2 cells were also tested in the stationary growth phase (18-days postconfluent) and again no increased proliferation was observed (data not shown). Caco2 cells are normally cultured in the presence of 20% serum. It was possible, that bile acid-induced proliferation might be more apparent in the absence of other growth factors. To reduce the presence of growth factors, cells were cultured in 10% and 0.2% serum; however, even under serum-starved conditions bile acids did not induce proliferation (Figure 4.3A). In previous reports, 20 μM DCA induced proliferation in Caco2 and HT-29 cells (Milovic, 2002). To compare growth induced by this concentration of DCA to growth induced by serum factors, Caco2 cells grown in 10% serum were treated with either 20 μM DCA or an additional 10% serum. HCT-116 cells do not express FXR and were used as a control. While high serum conditions induced growth, no increase was seen with 20 μM DCA (Figure 4.3B). If the effects of bile acids on proliferation were transient, they would not be detected by an end point assay such as cell counts. In addition, increased apoptosis could mask the

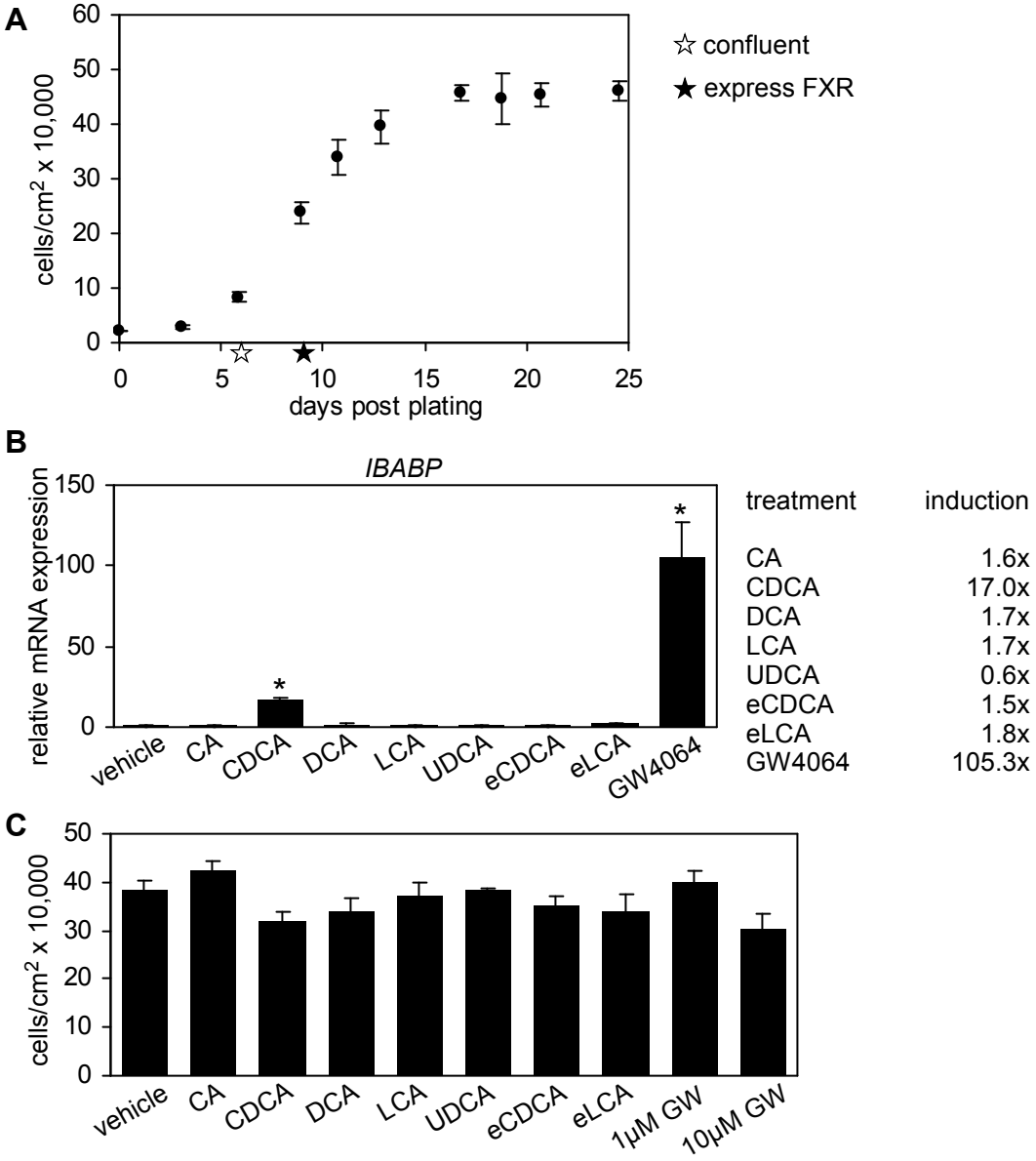

Figure 4.2 FXR agonists do not increase proliferation in Caco2 cells.
(A) Caco2 cells were grown in 12-well plates. At the indicated time points cells were trypsinized and trypan blue-negative cells were counted. The onset of confluency and FXR expression are indicated. **(B)** Postconfluent Caco2 cells were treated for 8 hours with 20 μM bile acids or 1 μM GW4064. mRNA expression was determined by QPCR, normalized to *cyclophilin*, and graphed relative to vehicle-treated control. Fold-induction of *IBABP* in treated cells relative to control is shown. Data represent the mean ± SD of three experiments. * $p < 0.05$ compared to vehicle. **(C)** Postconfluent Caco2 cells were treated for 5 days as in B. Following treatment, cells were trypsinized and trypan blue-negative cells were counted. Data represent the mean ± SD of three experiments.

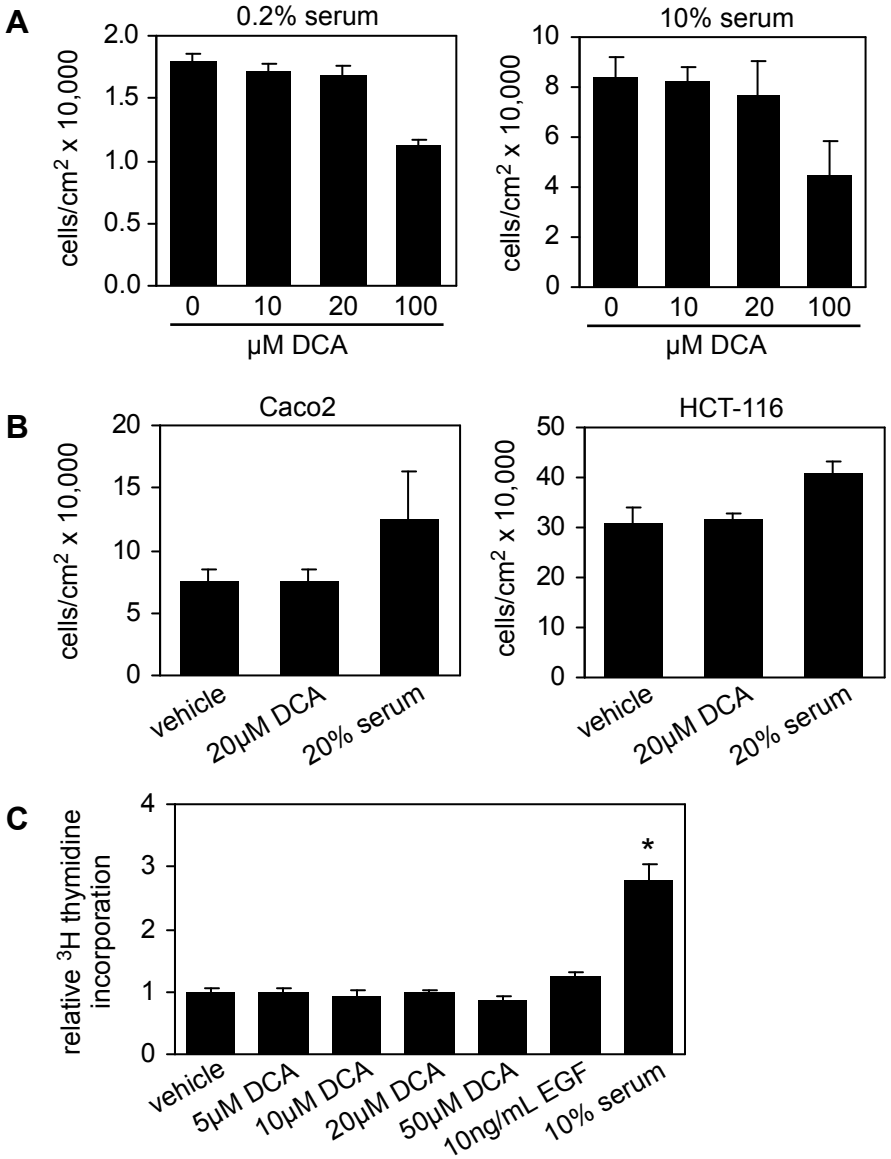

Figure 4.3 DCA does not induce proliferation in colon cancer cell lines.
(A) Caco2 cells were grown in media supplemented with the indicated amount of serum. Following 3-day treatment with the indicated concentrations of DCA, cells were trypsinized and trypan blue-negative cells were counted. Data represent the mean ± SD of two experiments. **(B)** Caco2 and HCT-116 cells grown in 10% serum were treated for 3 days as indicated, trypsinized, and trypan blue-negative cells were counted. Data represent the mean ± SD of two experiments. **(C)** HT-29 cells grown in 0.2% serum were treated for 24 hours as indicated. Data represent the mean ± SD of three experiments. * $p < 0.05$ compared to vehicle.

effect of increased proliferation in an end point assay. Incorporation of tritium-labeled thymidine was used to determine whether bile acids induced acute changes in cell proliferation. HT-29 cells were used in these experiments because Caco2 cells detached from the culture plate during wash steps of the thymidine incorporation assay. Following a period of serum starvation, cells were stimulated with 5 to 50 μM DCA, epidermal growth factor (EGF), or serum. Results showed that DCA did not acutely increase proliferation (Figure 4.3C).

4.3.3 High Bile Acid Concentrations Induce Growth Arrest and Apoptosis

In order to test a larger number of conditions, cells were grown in 96-well plates and a colorimetric assay (MTS) was used to evaluate cell growth. These experiments showed that at higher concentrations mono-hydroxylated (e.g. LCA) and some di-hydroxylated (e.g. DCA and CDCA) bile acids appeared to decreased proliferation, while similar concentrations of tri-hydroxylated (e.g. CA) and some di-hydroxylated (e.g. UDCA) bile acids had no effect (Figure 4.4 and data not shown). These effects were not specific to colon cell lines since they also occurred in human embryonic kidney (HEK293) cells (Figure 4.4). The effects were more pronounced in non-transformed cells (IEC-18, immortalized rat intestine epithelial cells), while highly malignant cells (HCT-116) were more resistant to these effects (Figure 4.4). Decreased cell numbers measured by MTS assay could be the result of growth inhibition or increased apoptosis. Indeed, at the highest concentrations tested, bile acids caused similar effects as the apoptosis-inducing agents, camptothecin and staurosporine (Figure 4.4).

Additional experiments in IEC-18 and HT-29 cells indicated that 100-200 μM DCA and CDCA induced growth inhibition (decreased proliferation) rather than apoptosis. While cells treated with camptothecin and staurosporine showed classic signs of apoptosis (nuclear condensation and membrane blebbing) no such changes were seen in bile acid treated cultures (Figure 4.5 and 4.6). Cleavage and

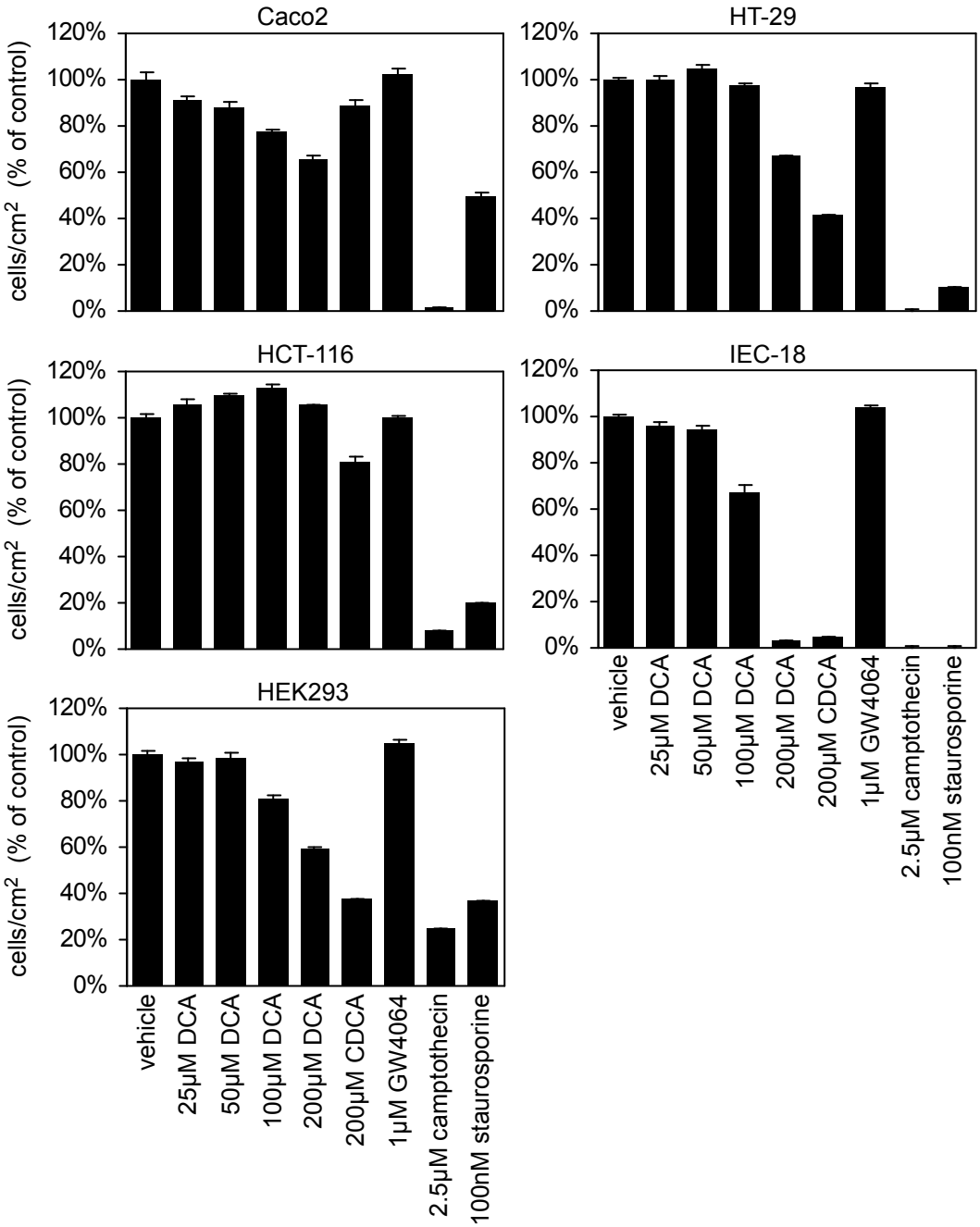

Figure 4.4 DCA and CDCA decrease growth in colon cancer cell lines.
Cells were grown in 96-well plates. Following 3-day treatment, cell density was determined by MTS assay. To generate a plot of cell density relative to absorbance, each plate was set up with cell dilutions which were counted with a hemocytometer following MTS assay. From the resulting standard curve, cell density for all conditions was calculated. Data represent the mean ± SEM of three experiments.

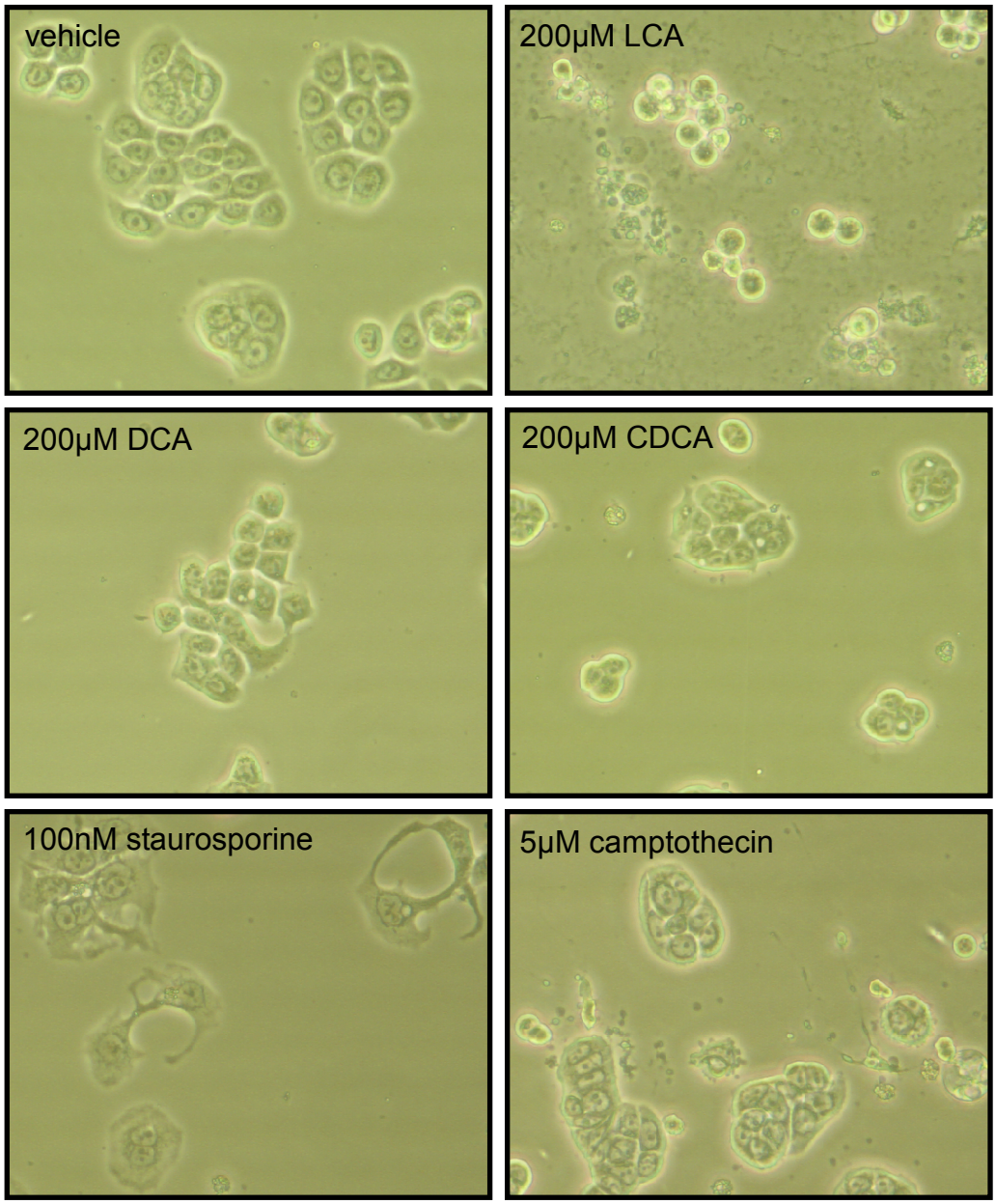

Figure 4.5 Effect of bile acids and inducers of apoptosis in HT-29 cells.
HT-29 cells were grown in media supplemented with 5% serum and were treated for 24 hours with the indicated agents. Note: LCA precipitates in culture media at concentrations > 100 μM.

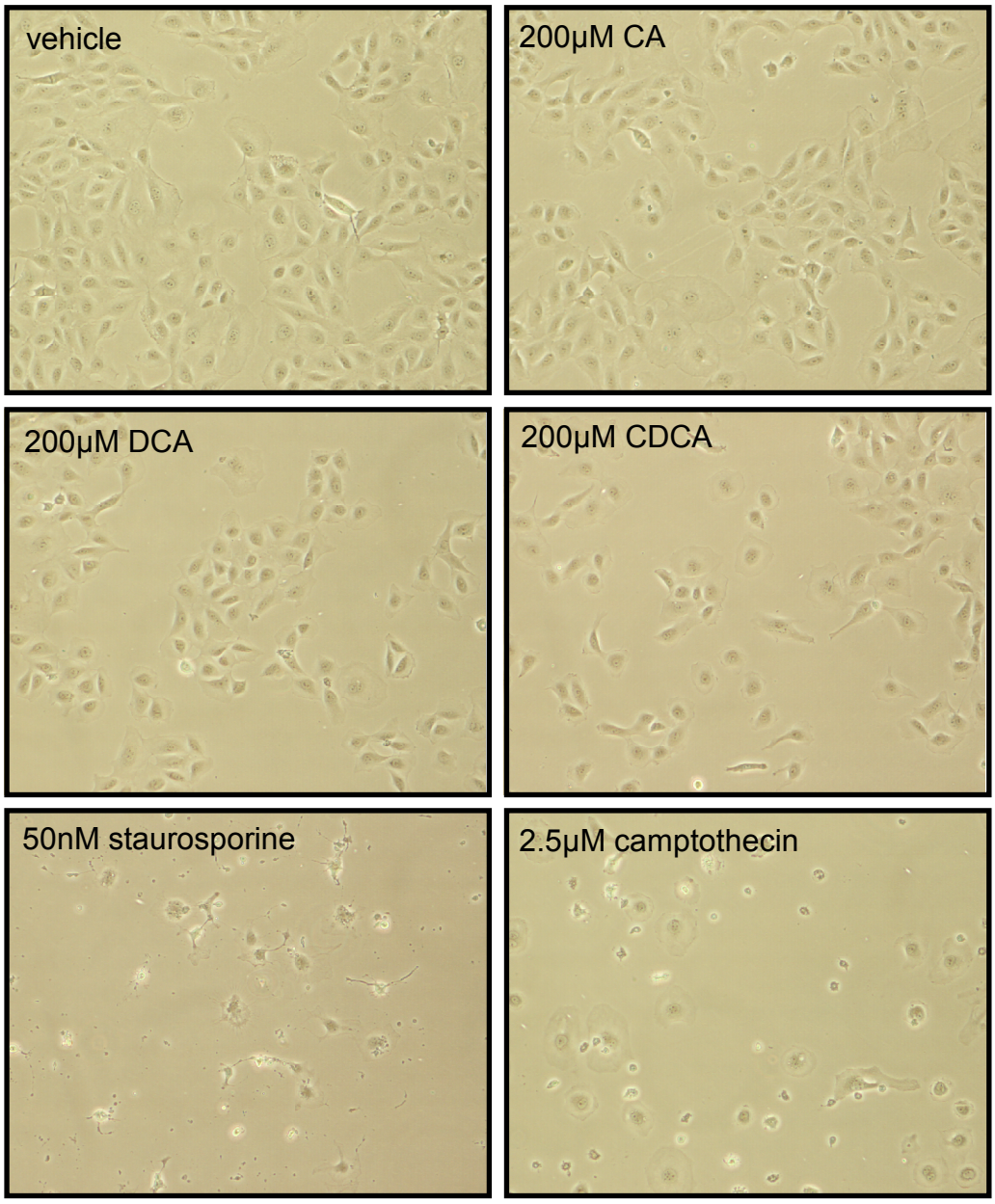

Figure 4.6 Effect of bile acids and inducers of apoptosis in IEC-18 cells.
IEC-18 cells were grown in media supplemented with 5% serum and were treated for 24 hours with the indicated agents.

activation of caspases is a hallmark of apoptosis. Extrinsic and intrinsic apoptosis pathways activate caspase 3, and poly ADP-ribose polymerase (PARP) is one of the main cleavage products of caspase 3. Notably, cleaved PARP was only detected in cells treated with >200 μM DCA (Figure 4.7A). Low levels of apoptosis might escape detection by methods that measure average cell responses. To evaluate apoptosis in individual cells at the molecular level, annexin V positive cells were immunolabeled and quantitated by fluorescent activated cell sorting (FACS). Consistent with visual evaluation of cell cultures, no apoptotic cells were detected in cultures treated with 200 μM DCA, CDCA, or CA (Figure 4.7B). These experiments indicate that 100-200 μM DCA or CDCA induce growth arrest that does not result in apoptosis.

The growth-inhibitory effects of DCA occurred over a remarkably narrow range in HT-29 cells. While 100 μM DCA was largely without effect, cell growth was halted at 150 μM (Figure 4.8). When serum concentrations were decreased from 10% to 2.5%, growth arrest occurred at 100 μM DCA (reasons discussed below). To gain insight into the mechanism of growth arrest induced by DCA, targeted transcriptional profiling of cell cycle regulators was performed using a quantitative RT-PCR (QPCR) platform (PCR Superarray). Expression of 89 genes involved in cell cycle regulation was measured in cells treated with 100 μM DCA for 4, 8, and 24 hours. The earliest changes were seen in the expression cyclins required for the G1/S transition. Within 4 hours of DCA treatment >2-fold reduction in Cyclin D1 and CyclinE1 occurred (Table 4.1). This was followed by increased expression of negative regulators of the G1/S transition (p21 and p15) at 8 hours, and further increases at 24 hours. Genes involved in the initiation of DNA replication and markers of proliferating cells were not decreased until 24 hours.

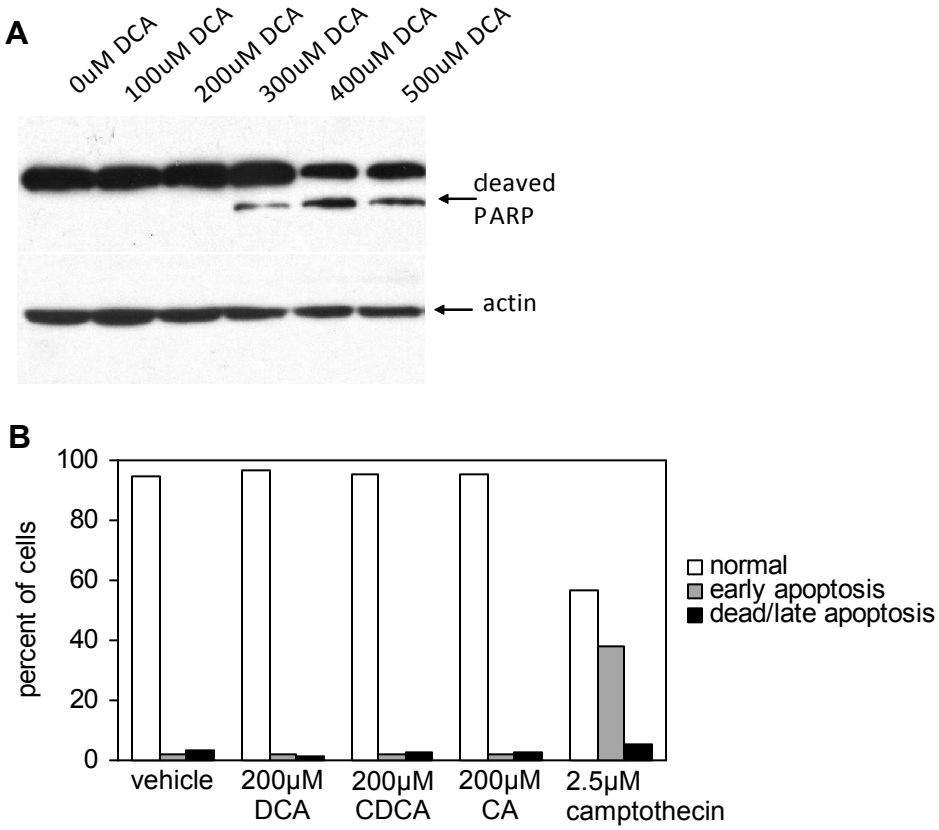

Figure 4.7 Bile acids do not induce apoptosis at intermediate concentrations. **(A)** HT-29 cells grown in 2.5% serum were treated for 4 hours with the indicated concentrations of DCA. Whole cell lysates were resolved by SDS-PAGE and immunoblotted for PARP and actin. **(B)** IEC-18 cells grown in 5% serum were treated for 48 hours as indicated. Cells were labeled with a fluorescent α-annexin V antibody, and stained with propidium iodide (PI). Cells in early apoptosis (annexin V positive, PI negative), late apoptosis/dead cells (annexin V positive, PI positive), and normal cells (annexin V negative, PI negative) were quantitated by FACS.

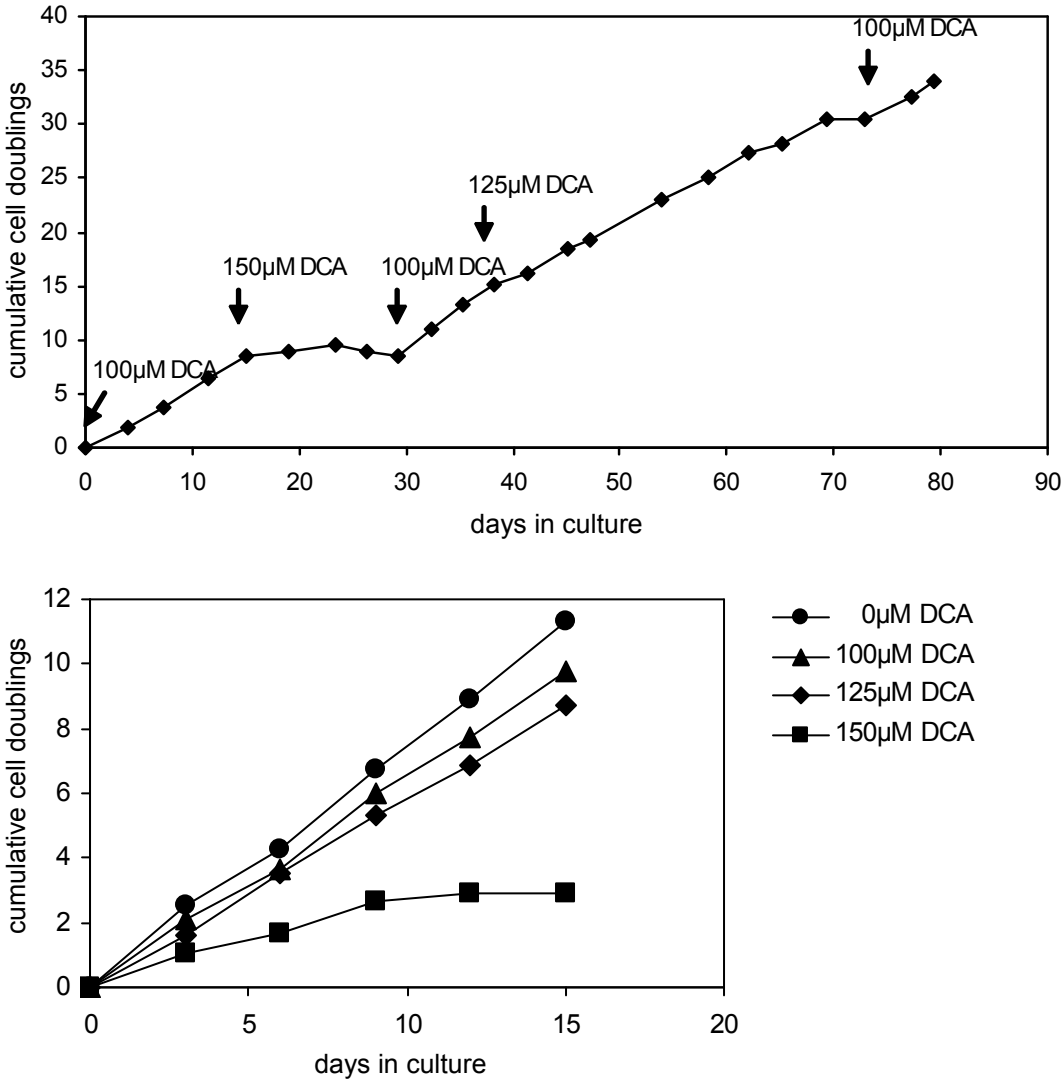

Figure 4.8 Effect of DCA on HT-29 cell growth.
HT-29 cells were propagated in culture media supplemented with 10% serum and the indicated concentrations of DCA. Trypan blue-negative cells were counted to determine cell density at the time of splitting. Cell doublings were calculated from the number of cells plated and cell number determined at splitting.

Table 4.1
DCA-induced changes in cell cycle gene expression.

		fold-change relative to control			
gene	Ct*	4 hrs	8 hrs	24hrs	gene function
CyclinD1	25	**-3.5**	-1.1	1.4	induce G1/S transition
CyclinE1	24	**-2.1**	-2.2	-4.1	induce G1/S transition
p15	27	1.5	2.6	**6.3**	block G1/S transition
p21	26	1.9	2.1	**7.6**	block G1/S transition
MCM2	24	1.4	-1.3	**-20.0**	initiation of DNA replication
MCM3	22	-1.3	-1.9	**-4.0**	initiation of DNA replication
MCM4	22	-1.2	-2.3	**-7.0**	initiation of DNA replication
MCM5	24	-1.3	-1.5	**-4.8**	initiation of DNA replication
Ki67	22	-1.2	-1.2	**-5.1**	marker of replicating cells
GTSE-1	26	-1.5	-1.6	**-5.5**	marker of replicating cells

* Average cycle time in the control condition, as determined by QPCR.
HT-29 cells cultured in 2.5% serum were treated with vehicle or 100 μM DCA for the indicated time periods. mRNA expression was determined by QPCR array. Data shown is fold-change in gene expression for the treated condition relative to control.

4.3.4 Albumin Reverses the Effect of Bile Acids on Cell Growth

In the course of performing these experiments it was noted that decreasing the amount of serum in culture media increased bile acid toxicity. When serum concentration was reduced to 2.5%, the growth of HT-29 cells was decreased with concentrations of DCA as low as 50 μM (Figure 4.9A). In contrast, 100 μM DCA in the presence of 10% serum had no effect on the growth of HT-29 cells (Figure 4.4 and Figure 4.8). Similar effects were seen in HCT-116 and IEC-18 cells (Figure 4.9B). These data suggested that a component present in serum could overcome the growth inhibitory effects of bile acids. I initially hypothesized that a growth factor, such as insulin, might be responsible for these effects; however, increasing insulin did not affect cell growth in the presence of bile acids (Figure 4.10A). Albumin accounts for approximately 50-60% of total protein in human serum (40 mg/mL). In the blood, free lipids such as fatty acids are bound by albumin, which facilitates their transport and decreases their toxic effects. To determine whether such chelating effects of albumin could account for the observed effects, cultures treated with bile acids were supplemented with bovine serum albumin (BSA). Amazingly, purified BSA, at concentrations comparable to those present in serum, was more effective than serum at decreasing the toxic effects of bile acids on cell growth (Figure 4.10B and 4.11).

4.4 Discussion

In summary, I have found that neither bile acids nor synthetic FXR agonists increase proliferation of several colon cancer cell lines. At low micromolar concentrations bile acids activate FXR. Ten-fold higher concentrations induce growth arrest and further increases are needed to induce apoptosis. Thus, it appears that FXR is designed to sense bile acids levels well

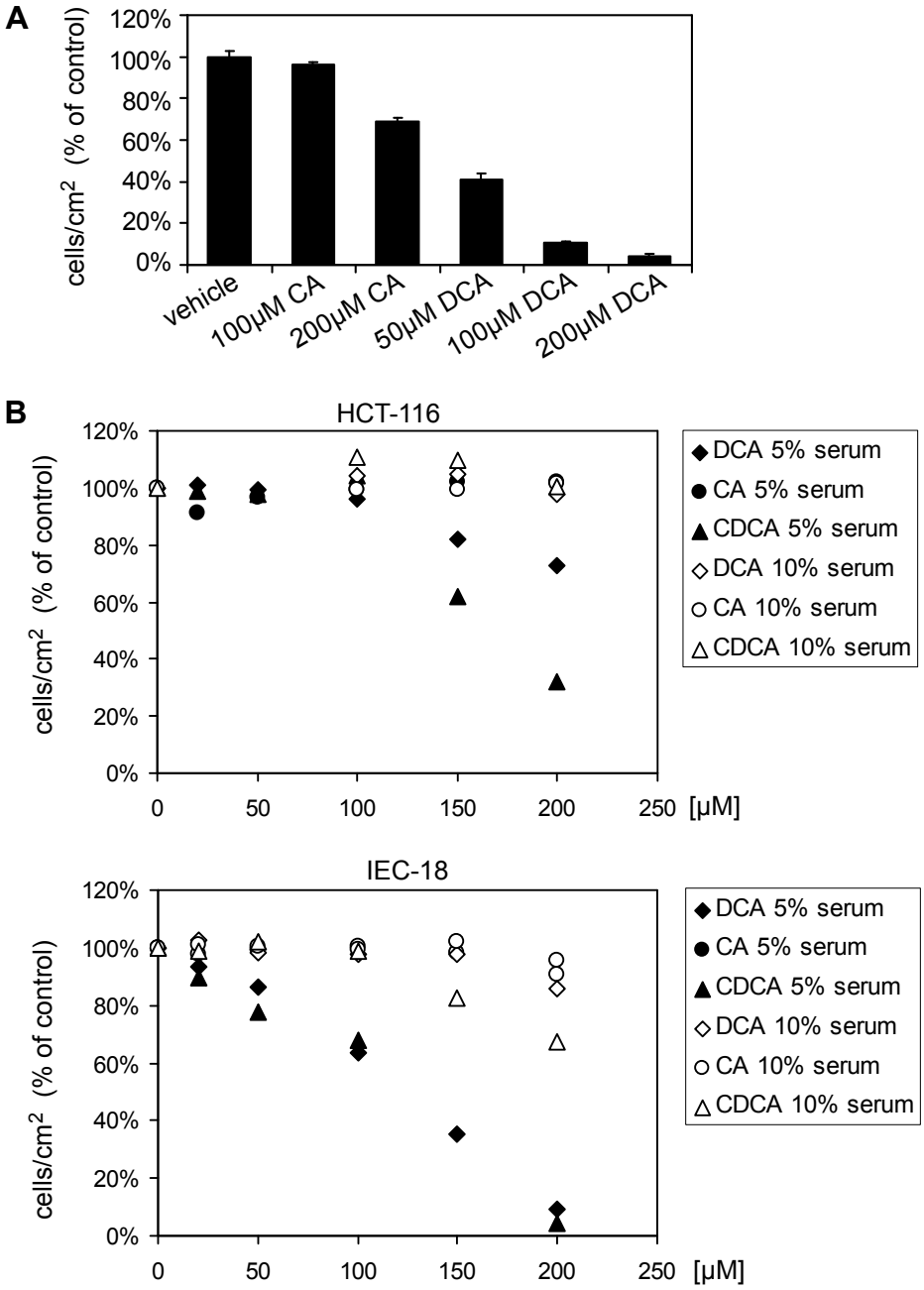

Figure 4.9 Serum decreases the toxic effects of bile acids.
(A) HT-29 cells were grown in media supplemented with 2.5% serum. Following 3-day treatment as indicated, cells were trypsinized and trypan blue-negative cells were counted. Data represent the mean ± SEM of three experiments. **(B)** HCT-116 and IEC-18 cells grown in 5% or 10% serum were treated for 3 days with the indicated concentrations of DCA, CDCA, and CA. Cell number was quantitated by MTS assay as described in Figure 4.

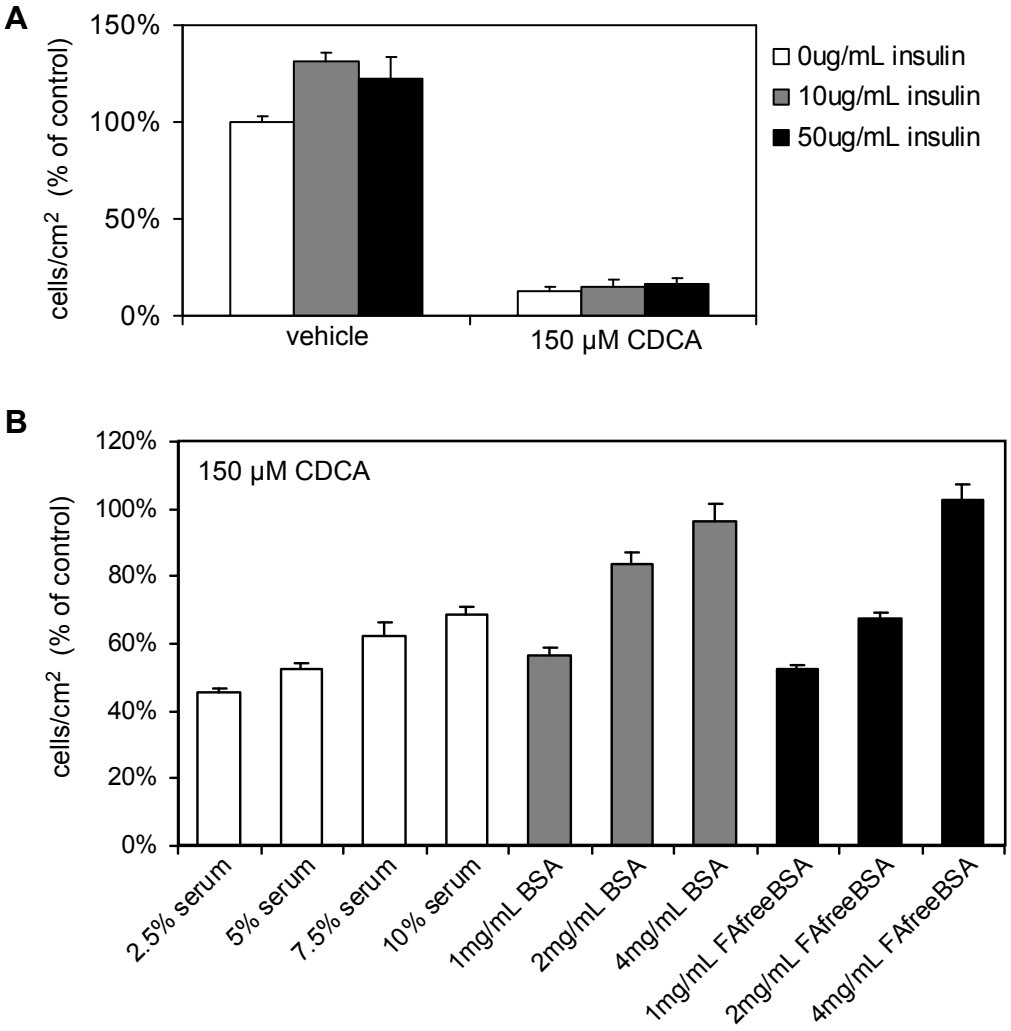

Figure 4.10 BSA decreases the toxic effects of CDCA on HT-29 cells while insulin has no effect.
(A) HT-29 cells were grown in media supplemented with 2.5% serum and the indicated concentrations of insulin. Following 3-day treatment with 100 µM CDCA or vehicle, cells were trypsinized and trypan blue-negative cells were counted. Data represent the mean ± SEM of three experiments. **(B)** HT-29 cells grown in 2.5% serum and 150 µM CDCA, were treated with increased amounts of serum, bovine serum albumin (BSA), or fatty acid-free BSA (FAfreeBSA) as shown. Three days after plating, cells were trypsinized and trypan blue-negative cells were counted. Data represent the mean ± SEM of three experiments.

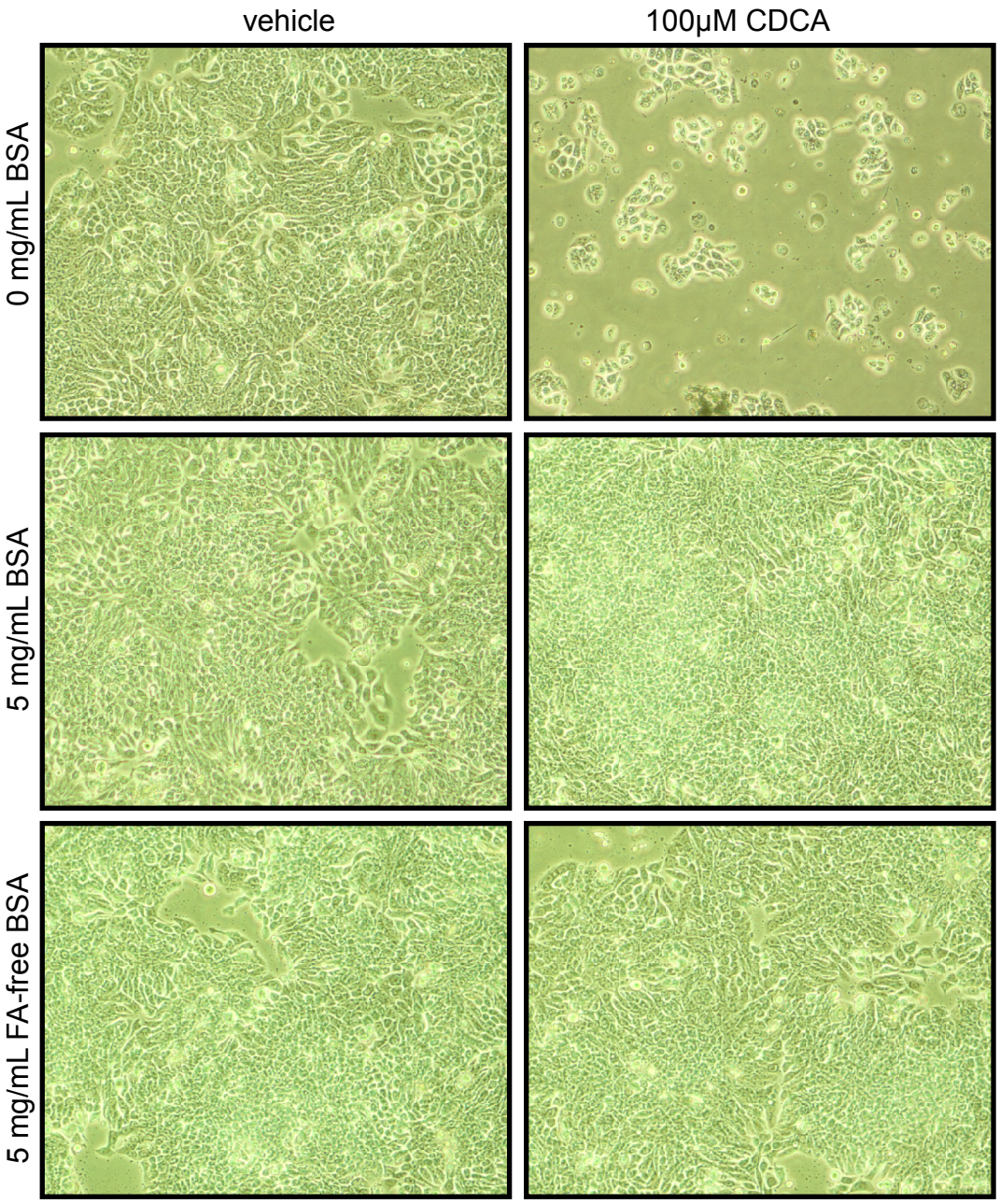

Figure 4.11 BSA decreases the toxic effect of CDCA on HT-29 cells.
HT-29 cells grown in media supplemented with 2.5% serum. At the time of plating cells were treated with CDCA, bovine serum albumin (BSA), and fatty acid-free BSA (FA-free BSA) as indicated. Images were taken 3 days after treatment.

Effects of bile acids in colon cancer cell lines:

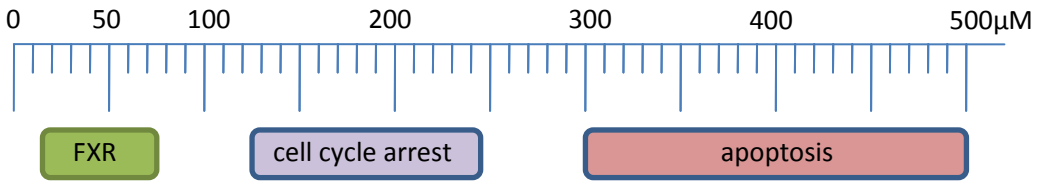

Figure 4.12 Relationship between bile acid concentration and biological effects *in vitro*.
Summary of biological and pharmacologic effects of DCA and CDCA observed in colon cancer cell lines cultured in 10% serum.

below concentrations that induce toxic effects. These conclusions are summarized in Figure 4.12.

Hydrophobicity of bile acids roughly parallels their potency to induce toxic effects. Increasing the number of hydroxyl groups (e.g. CA > CDCA = DCA > LCA) decreases bile acid toxicity. In addition, the presence of hydroxyl groups on both faces of the steroid nucleus further decreases toxicity. For example, CDCA and UDCA both have two hydroxyl groups; however, CDCA has both on the same side of the steroid nucleus while UDCA has one on either side (see Figure 3.6 and 3.7). Much higher concentrations of UDCA are needed to achieve similar effects on growth arrest as lower concentrations of CDCA. Since hydrophilic bile acids such as UDCA and CA do not easily diffuse through cell membranes, these data suggest that diffusion into or through membranes is required for bile acid toxicity *in vitro*.

The observation that therapeutic concentrations of GW4064 (FXR agonist) do not induce growth arrest or apoptosis, and that these effects are observed after bile acid treatment in cell lines that do not express FXR, indicate that FXR is not responsible for bile acid-induced growth arrest or apoptosis. The results I obtained from expression analysis of cell cycle regulators following DCA treatment suggest that transcriptional suppression of G1/S phase cyclins is likely an early event in the induction of growth arrest by bile acids. Future experiments will need to address the signaling pathways responsible for these changes in gene transcription.

The dramatic effects of albumin on the potency and efficacy of bile acids *in vitro* underscore the importance of developing controlled conditions when quantitating the biological and pharmacologic effects of lipids such as bile acids. In addition, these data suggest that the pharmacology of lipids *in vitro* may not be representative of their pharmacologic effects *in vivo*.

4.5 Acknowledgements

Genevieve Armstrong assisted in the [^{3}H]-thymidine incorporation experiments. I am grateful for her perseverance in optimizing this assay. Bryson Katona synthesized the bile acid enantiomers in the laboratory of Dr. Douglas Covey at Washington University School of Medicine, St. Louis, MO.

CHAPTER 5
Mechanism of Bile Acid-Induced Intestinal Proliferation

5.1 Introduction

Nearly thirty years have passed since the first report of bile acid-induced proliferation in rat colon (Deschner, 1981). Since then, numerous studies in rats have confirmed this observation and numerous correlative findings have been proposed as possible mechanisms including: induction of apoptosis and reactive proliferation; production of the lipoxygenase product, 12-hydroxyeicosatetraenoic acid; and production of reactive oxygen species (Bull, 1983; DeRubertis, 1984; Craven, 1986a; Craven, 1986b; Craven, 1992; Barone, 2002) A positive correlation between fasting serum DCA levels and proliferation in human colon has also been reported (Ochsenkühn, 1999). To my knowledge, no *in vivo* studies have described a molecular mechanism for bile-acid induced proliferation. Several *in vitro* studies (mainly in hepatocytes) have shown that a myriad of signaling pathways and molecules are activated by bile acids, including protein kinase C (PKC), extracellular signal-regulated kinase (ERK, also known as MAPK), activator protein 1 (AP-1, includes c-Jun and c-Fos), protein kinase B (PKB, also known as AKT), and jun N-terminal kinase (JNK) (Craven, 1987; Fitzer 1987; Branting, 1995; Qiao, 2000; Gupta, 2001; Dent, 2005). In general, the most active bile acids in these studies have been DCA and CDCA. Since none of these studies evaluated proliferation, it is difficult to ascertain whether these signaling pathways are relevant to proliferation in the intestine.

The initial goal of the studies described in this chapter was to determine whether FXR was involved in the mechanism of bile acid-induced intestinal proliferation. To this end, a variety of assays were developed to evaluate

intestinal proliferation. Subsequently, optimal experimental conditions were identified to investigate the mechanism of bile acid-induced proliferation *in vivo*. In summary, it was found that FXR and the bile acid-activated G-protein coupled receptor, TGR5, are dispensable for proliferative effects of bile acids; instead, phosphoinositide 3-kinase (PI3K) signaling was required for intestinal proliferation induced by bile acids.

5.2 Methods

5.2.1 Animals and Animal Husbandry

Wild-type 129S mice were purchased from Jackson Laboratories and bred in house. Unless otherwise indicated, 129S mice were used for all experiments. *Fxr*+/+ and *Fxr*–/– mice were obtained from heterozygous breeders on a pure 129S background. *Tgr5*+/+ and *Tgr5*–/– were obtained from heterozygous breeders on a mixed C57BL/6;129S background. All conventional animals were housed in the same specific-pathogen-free facility. Animals were maintained under a temperature controlled environment and 12 hour light/dark cycles with ad libitum access to water and irradiated rodent chow (TD.2916, Harlan-Teklad). All experiments were done with 2.5 to 6 month-old (age-matched) male mice sacrificed at the same time of day. Mice were euthanized by isofluorane inhalation and exsanguinated via the descending vena cava prior to tissue collection. Experiments involving germ-free animals were performed in the gnotobiotic facility of Dr. Jeffrey Gordon at Washington University School of Medicine, St. Louis, MO. These animals were sacrificed by cervical dislocation. All animal experiments were approved by the Institutional Animal Care and Research Advisory Committee at the University of Texas Southwestern Medical Center.

5.2.2 Animal Treatment

CA, CDCA, DCA and LCA were from Steraloids. All taurine conjugates and UDCA were from Sigma. 0.5% and 1% (w/w) DCA was admixed in the diet and provided ad libitum. For oral gavages, bile acids were dissolved in 1% Tween 80, 1% methylcellulose. For enemas, bile acids were dissolved in 1% Tween 80, 1% methylcellulose, 25 mM HEPES, and pH was adjusted to 7.4 with sodium hydroxide. For all gavage and enema experiments involving a time course, the time of treatment was staggered and animals were sacrifice at the same time of day.

2% (w/w) cholestyramine was admixed in the diet (custom diet TD.07658, Harlan-Teklad) and provided ad libitum. For bromodeoxyuridine (BrdUrd) labeling studies, mice received an intraperitoneal injection of BrdUrd (10mg/mL in PBS) at a dose of 100 mpk (10 uL/g body weight) two hours before sacrifice.

5.2.3 RNA Extraction and Quantitative RT-PCR

This method is described in Chapter 2.

5.2.4 DNA Dot Blot

DNA was extracted from crushed whole intestine or isolated colon crypts using DNeasy Blood & Tissue Kit (Qiagen). DNA was denatured by incubation in 0.4N NaOH for 30 minutes at room temperature, neutralized with equal volume 1M Tris HCl (pH 6.8) and blotted on nitrocellulose membrane. Immunoblotting was performed using mouse anti-BrdU (Roche, 11170376001) and sheep anti-mouse HRP (Amersham, NA931V).

5.2.5 Protein Extraction and Immunoblotting

Frozen and crushed colon was homogenized in lysis buffer containing 10 mM Tris HCl (pH 7.5), 150 mM NaCl, 0.5% NP40, 10% glycerol, 5 mM EDTA,

50 mM NaF, 10 mM β-Glycerol Phosphate, 1 mM Na_3VO_4 1 mM PMSF and a protease inhibitor cocktail (complete-Mini™, Roche). Homogenates were centrifuged at 13,000 rpm for 10 minutes and the supernatants were used as whole cell lysates. Protein was quantitated by Bradford assay (Bio-Rad) and resolved by SDS-PAGE (30 μg of protein/sample). Nitrocellulose membrane was used for blotting. Primary antibody incubation was performed in TBS containing 0.05% Tween (TBS-T) and 5% BSA. For secondary antibody incubation, TBS-T containing 5% milk was used. For visualization of the results, either SuperSignal (West Pico) or ECL western blotting substrates (Pierce) were used.

Immunoblotting was performed using the following antibodies: phospho-GSK3a (Cell Signaling #9331), GSK3a/b (Invitrogen 44-610), phosphor-GSK3b (Cell Signaling #9336), phospho-JNK (Cell Signaling #9251), JNK (Cell Signaling #9252), phospho-ERK (Cell Signaling #9101), ERK (Cell Signaling #4695), phospho-AKT (Cell Signaling #9271), AKT (Cell Signaling #9272), phospho-p38 (Cell Signaling #92115), p38 (Santa Cruz A-12 clone), c-myc (Cell Signaling #9402).

5.2.6 Isolation of Colon Crypts and Quantitation of BrdUrd Incorporation

Colon crypts were isolated by chelation with 5 mM EDTA and fixed in 70% ethanol. Isolated crypts were denatured in 2N HCl for 30 minutes at 37°C, permeabilized in 0.5% Triton X-100 for 10 minutes at room temperature, and blocked with normal goat serum for 1 hour at room temperature. Crypts were incubated with monoclonal mouse anti-bromodeoxyuridine (Roche, 11170376001) in PBS + 1 mg/mL BSA for 2 hours at 4°C. They were then incubated with FITC-conjugated goat anti-mouse (Jackson Immuno, 115-095-166) for 30 minutes at room temperature, and counterstained with propidium iodide for 10 minutes. Stained crypts were wet-mounted with 20% Vectashield (Vector Labs) and analyzed for BrdUrd incorporation by fluorescence microscopy

within 24 hours. The total number of BrdUrd-labeled cells per crypt was determined for a minimum of 30 crypts per sample.

5.2.7 TUNEL Assay

Formalin-fixed, paraffin-embedded sections of mouse colon were deparaffinized and labeled with terminal deoxynucleotidyl transferase for detection of apoptotic cells using the ApopTag Peroxidase *In Situ* Apoptosis Detection Kit and Protocol (Chemicon, Cat# S7100). Sections were incubated with peroxidase substrate for two times five minutes, and were counterstained with hematoxylin. Mouse thymus was used as a positive control and showed adequate labeling of apoptotic cells.

5.2.8 Statistical Analysis

Data are presented as mean ± SEM and were analyzed by two-tailed, unpaired Student's t-test. P values less than 0.05 were considered significant.

5.3 Results

5.3.1 DCA Induces Proliferation in the Intestine, Liver, and Biliary Epithelium

Previous attempts to demonstrate bile acid-induced proliferation in colon cancer cell lines were unsuccessful (Chapter 4). Studies in rats have shown that 1% CA feeding for 3 days increases intestinal proliferation *in vivo* (Deschner, 1981). To determine whether similar effects occurred in mice, animals were fed diets containing 0.5% and 1% DCA or control diet for 6 days followed by an overnight fast. To label proliferating cells, bromodeoxyuridine (BrdUrd) was administered two hours before sacrifice. BrdUrd incorporates into the DNA of actively replicating cells and can be detected in tissues or tissue extracts using a variety of immunologic methods. Results from this study demonstrated that both

concentrations of DCA induced proliferation in the liver and intestines; however, while 1% DCA was more effective that 0.5% DCA in the liver, the converse was true in the intestine (Figure 5.1). Changes in body weight suggested a possible explanation for these findings. While animals on the control diet gained weight (8±2%), no weight gain was observed in the 0.5% DCA group (0±2%), and animals in the 1% DCA group lost weight (12±3%). It is well established that feeding increases intestinal proliferation, while long-term fasting (>24 hours) decreases proliferation. Thus, the effects on proliferation in the intestine may have been confounded by differences in food intake.

To establish a better system to evaluate intestinal proliferation, animals were treated with bile acids by oral gavage. Since the dose could be easily adjusted to body weight this also allowed better comparison of animals of different ages and weights. To determine the minimal effective dose, animals were gavaged once daily for 3 days with 500, 1000, and 2000 mg/kg DCA. On the second day, animals that received the highest dose demonstrated signs of toxicity, including reduced food intake and activity. These animals were not administered a third dose. The liver of animals treated with either 500 or 1000 mg/kg DCA showed increased proliferation of hepatocytes (Figure 5.2A). In contrast, animals treated with 2000 mg/kg DCA had less hepatocyte proliferation but dramatically increased proliferation of intrahepatic biliary epithelial cells (Figure 5.2A). It is possible that the highest DCA dose exceeded the capacity of the biliary system, resulting in toxic effects within this compartment. It is likely that such high concentrations would ultimately result in intrahepatic cholestasis. Histologic analysis of the colon showed that animals treated with 1000 mg/kg DCA had significantly reduced mucous droplets, while epithelial mucus was completely absent in animals treated with 2000 mg/kg DCA (Figure 5.3). While no obvious differences were noted at necropsy, microscopic analysis revealed

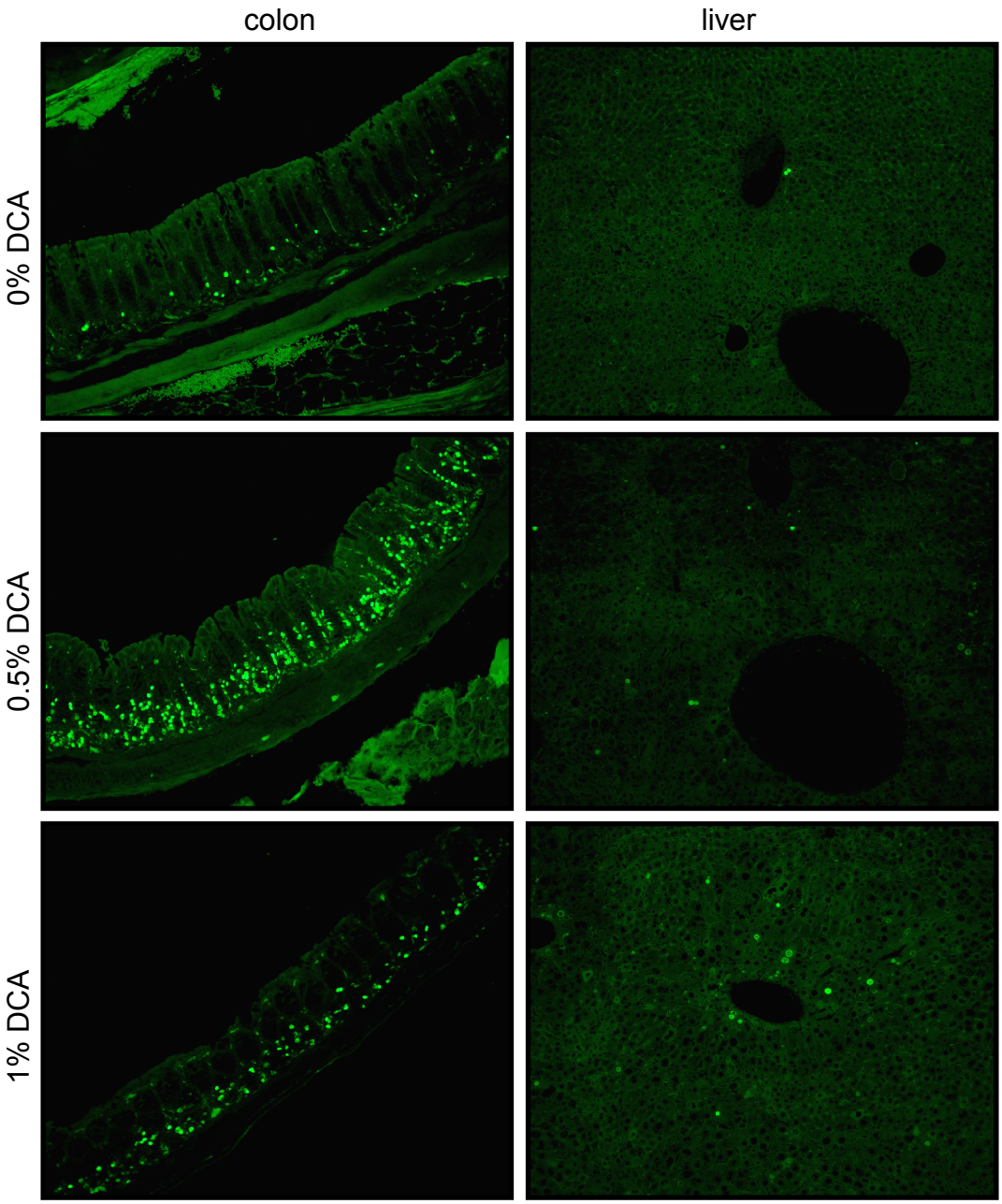

Figure 5.1 DCA induces proliferation in colon and liver.
Wild-type male mice were treated with diets containing the indicated amount of DCA (w/w) for 6 days. 100 mg/kg BrdUrd was administered by intraperitoneal injection 2 hours before sacrifice. Immunohistochemical detection of BrdUrd was performed on formalin-fixed, paraffin-embedded tissues.

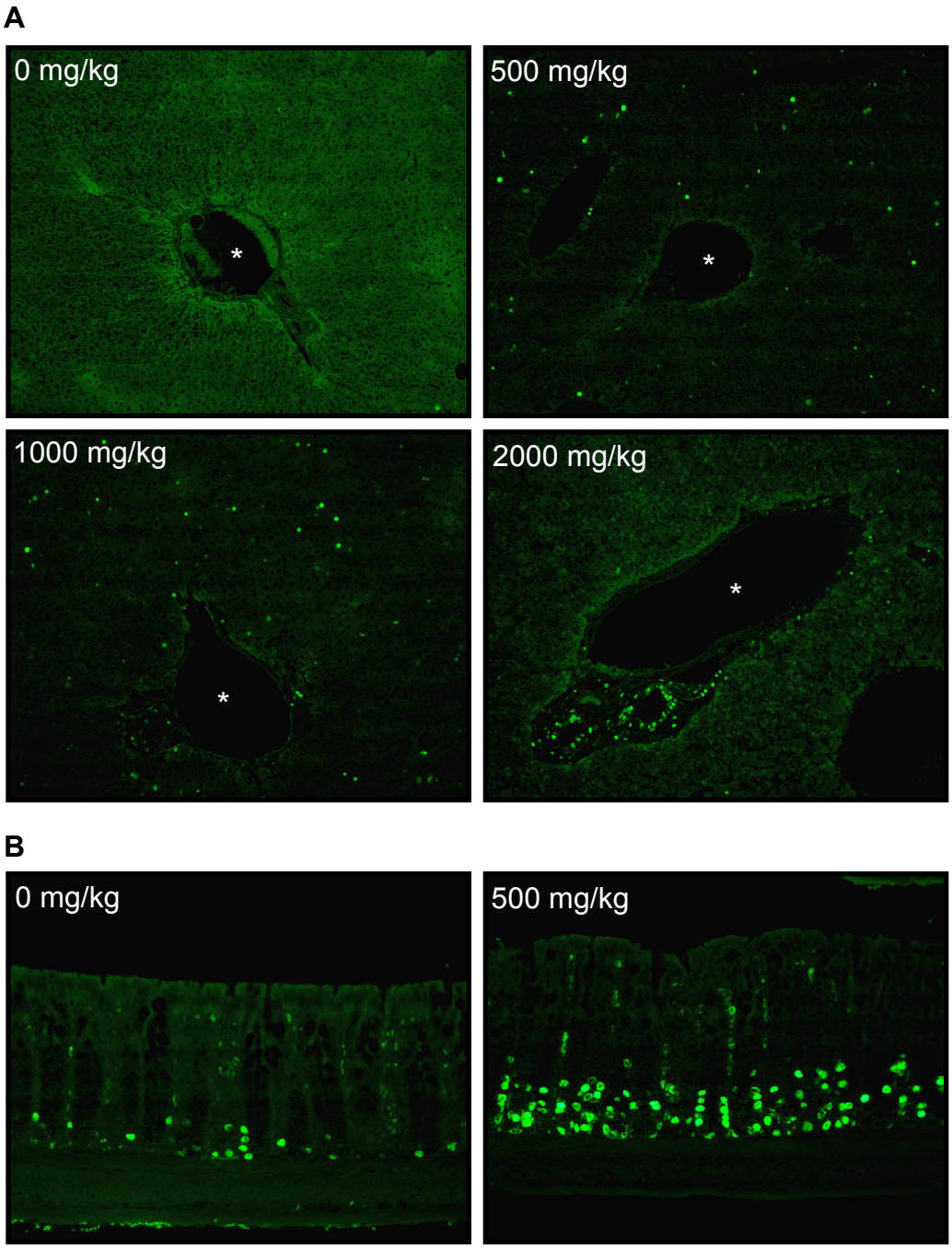

Figure 5.2 DCA gavage induces proliferation in liver and colon.
Wild-type male mice were treated with the indicated dose of DCA by oral gavage. See text for details. 100 mg/kg BrdUrd was administered by intraperitoneal injection 2 hours before sacrifice. Immunohistochemical detection of BrdUrd was performed on formalin-fixed, paraffin-embedded liver **(A)** and colon **(B)**. * indicates portal vein

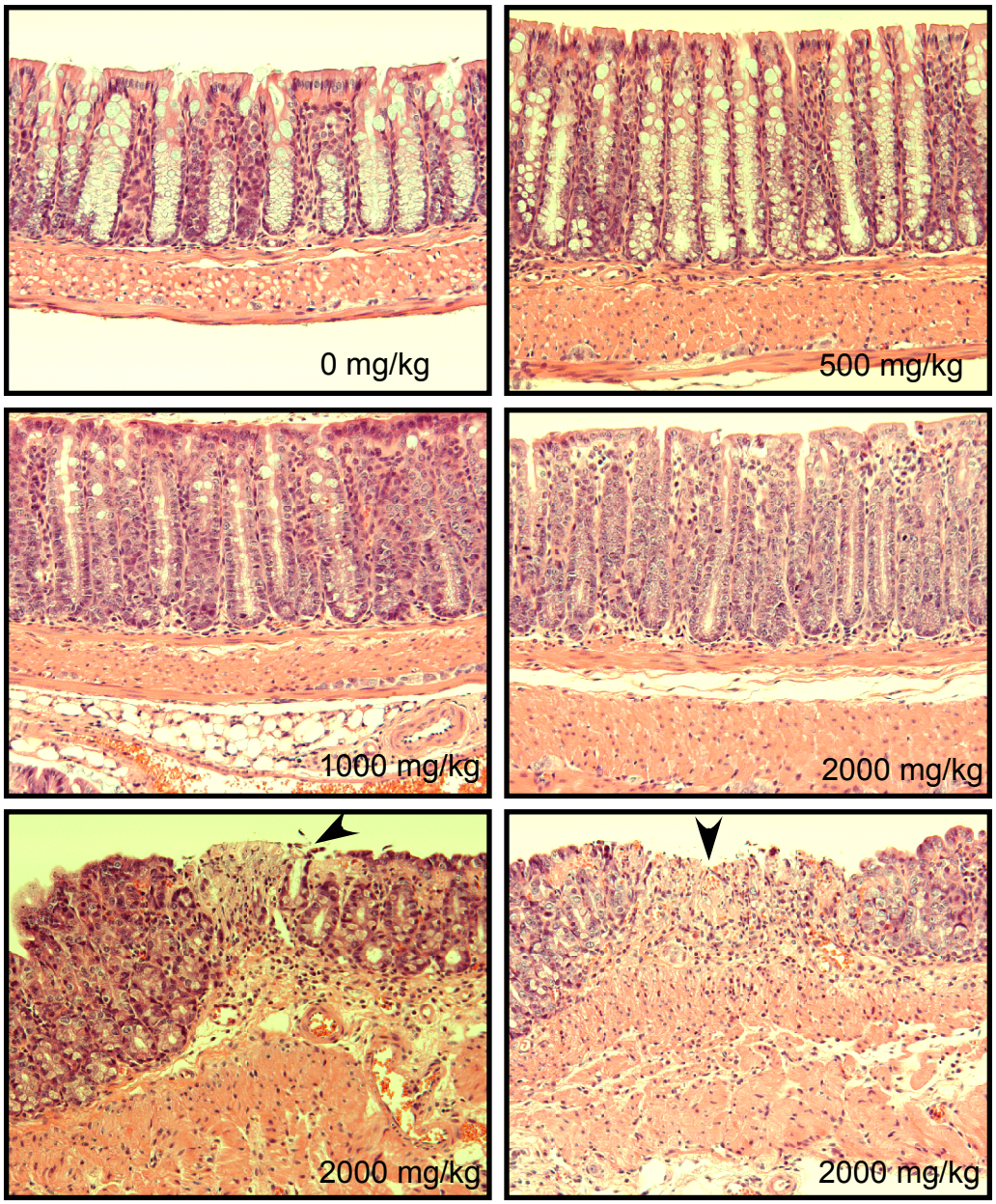

Figure 5.3 High dose DCA depletes mucous and induces mucosal damage in the colon.
H&E stained formalin-fixed, paraffin-embedded sections of mouse colon. Wild-type male mice were treated with the indicated dose of DCA by oral gavage. See text for details. Arrows indicate mucosal ulceration.

small areas of ulceration in the colon from this latter group (Figure 5.3). These data indicate that high concentrations of DCA also induce acute toxicity in the colon. Evaluation of BrdUrd incorporation showed significant increases in the group treated with 500 mg/kg DCA, while no toxic effects were seen at the gross or microscopic level (Figure 5.2B and Figure 5.3). Thus, for all subsequent experiments bile acids were administered by oral gavage at a dose of 500 mg/kg.

5.3.2 Improved Methods for Measuring Proliferation

Quantitation of BrdUrd incorporation by immunohistochemistry using paraffin sections is costly and time-consuming. It was found that colonic crypts could be isolated and separated from adjacent submucosa using calcium chelating solutions (Figure 5.4A). Crypts collected in this manner could be fixed and labeled using modified immunocytochemical methods (Figure 5.4B and C). Not only was this approach more efficient than standard immunohistochemistry it also improved data collection and analysis since the total number of BrdUrd positive cells per crypt could be determined rather than only the number of cells present in a 5 μm section. An additional challenge with paraffin-embedded sections was optimal orientation of the tissue to allow visualization of whole crypts from base to opening. These problems were not encountered with isolated crypts that were easily examined microscopically using a wet-mount technique. DNA extracted from isolated crypts and immobilized on nitrocellulose could also be used for detection of BrdUrd by immunoblot (DNA "dot blot"). Since DNA was collected exclusively from epithelial cells, BrdUrd signals from DNA dot-blots accurately represented proliferation in the colonic epithelial compartment (Figure 5.5). This method allowed rapid screening of many conditions for effects on intestinal proliferation *in vivo*.

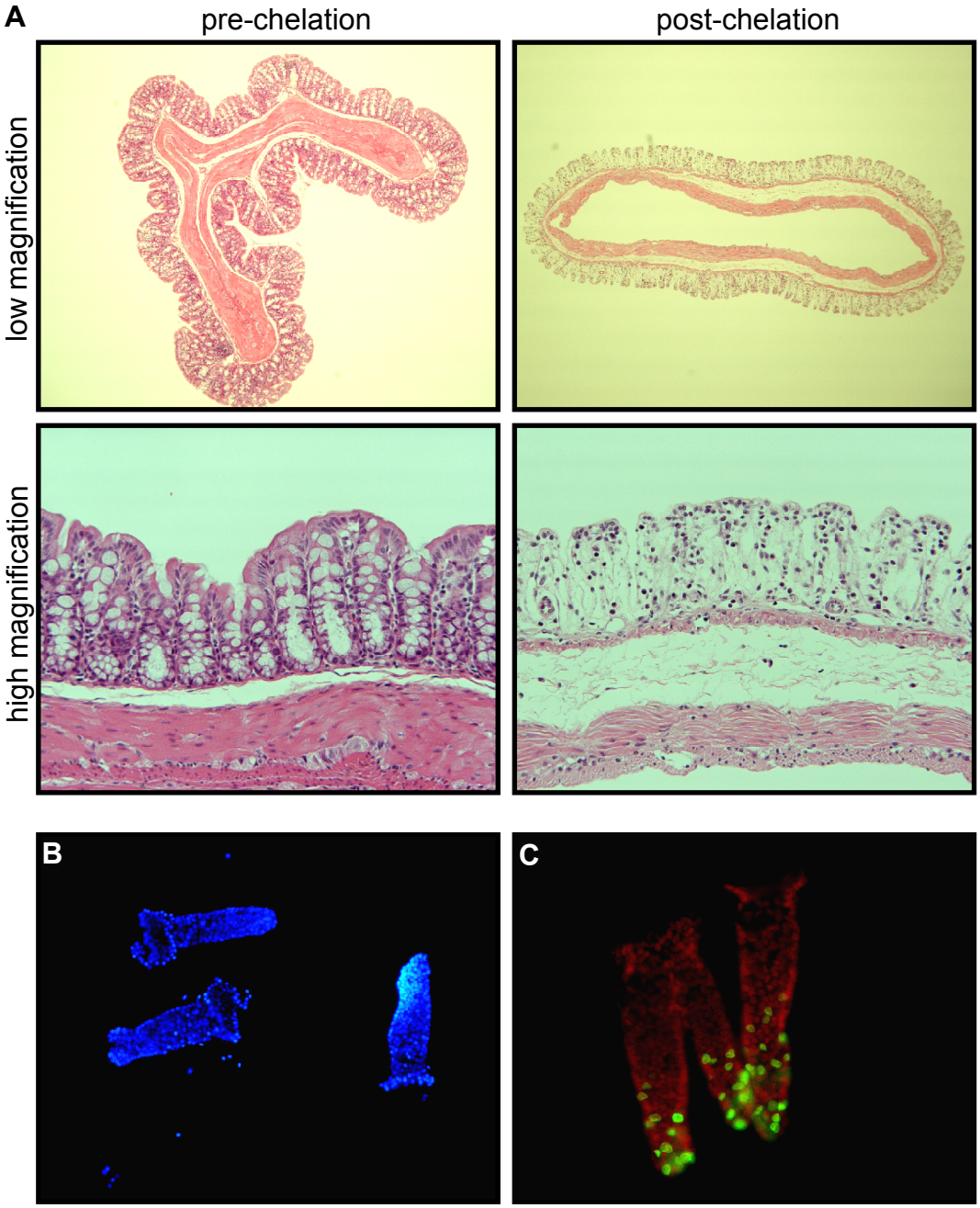

Figure 5.4 Isolation of colon crypts.
(A) H&E stained formalin-fixed, paraffin-embedded colon. Images show colon pre-chelation (before removal of colon crypts) and post-chelation (after removal of colon crypts). In the upper images the colon has been inverted. **(B)** Hoechst-stained isolated colon crypts. **(C)** Immunocytochemical detection of BrdUrd (green) with propidium iodide (red) counter-stain.

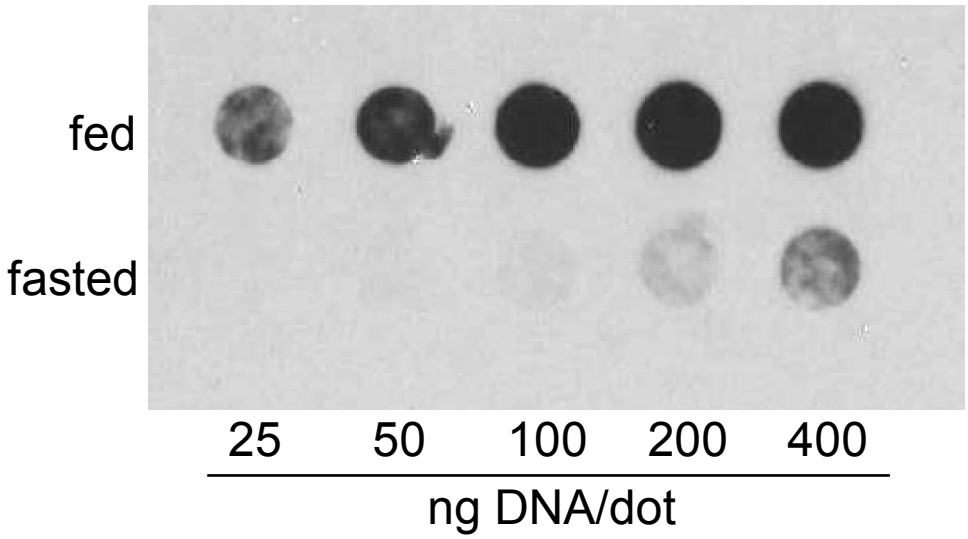

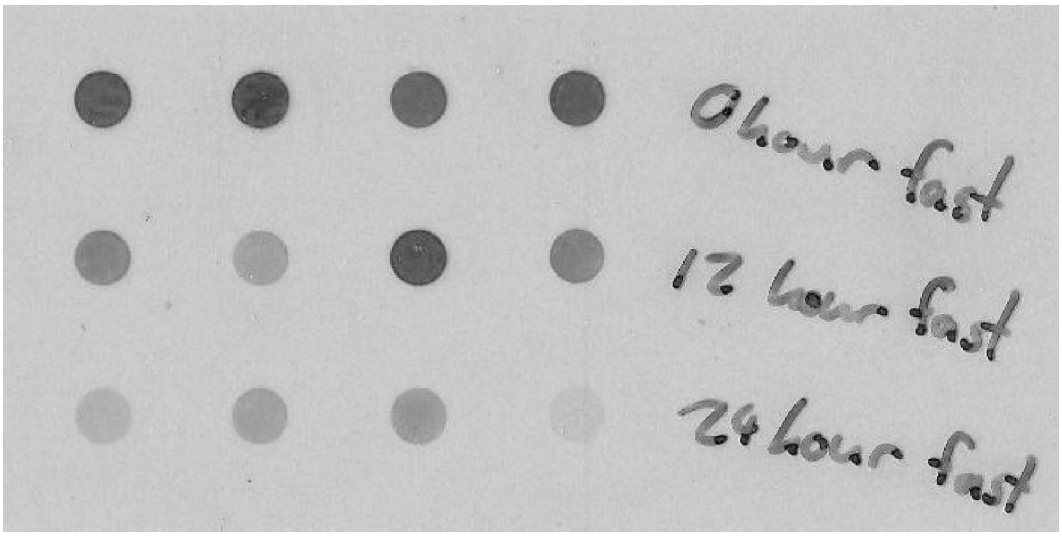

Figure 5.5 DNA dot blot.
Fed or fasted animals were treated for 2 hours with 100 mg/kg BrdUrd. DNA extracted from colon crypts was immobilized on nitrocellulose and immunoblotted for BrdUrd. Top panel: the indicated amounts of DNA from a single fed or fasted animal were used. Bottom panel: each dot is 25 ng colon crypt DNA from an individual animal, n = 4 per group.

5.3.3 Comparison of CA and DCA Administered by Gavage

DNA dot blots were used to confirm the effect of 0.5% DCA diet on intestinal proliferation and show that a single day of feeding followed by an overnight fast was sufficient to elicit the proliferative response (Figure 5.6A). It was also found that two DCA gavages administered 38 and 14 hours before sacrifice induced proliferation, while a single treatment for 14 hours did not (Figure 5.6A). To determine whether these effects were due to dosing or timing, gavages were administered 16 hours, 40 hours, or 40 and 16 hours before sacrifice. It was found that a single dose of DCA was sufficient, but more than 16 hours were required for the proliferative response to occur (Figure 5.6B). Interestingly, while proliferation was seen 40 hours but not 16 hours after DCA gavage, the converse was true for CA (Figure 5.6B and C). These results indicated that the onset of proliferation with CA was more rapid than DCA and that the effects were transient (being absent 40 hours after CA gavage). It was noted that animals treated with DCA had a significant portion of the gavage solution remaining in the stomach at time of sacrifice while animals in the CA group did not. Based on this observation it was hypothesized that DCA might affect gastric emptying and thus account for the delayed proliferative response. Indeed, using carmine red (a non-absorbable red dye) it was found that intestinal transit time in the CA group was no different from vehicle, but was significantly slowed in the DCA group (data not shown). Therefore, delayed gastric emptying and/or prolonged intestinal transit time was likely responsible for the later onset of proliferation seen in DCA treated animals relative to the CA treated group. Of note, glycoCDCA has been shown to inhibit motility and delay transit in the jejunum and ileum in humans (Penagini, 1989). Thus, it appears that dihydroxy bile acids affect intestinal motility while the trihydroxy bile acid CA does not.

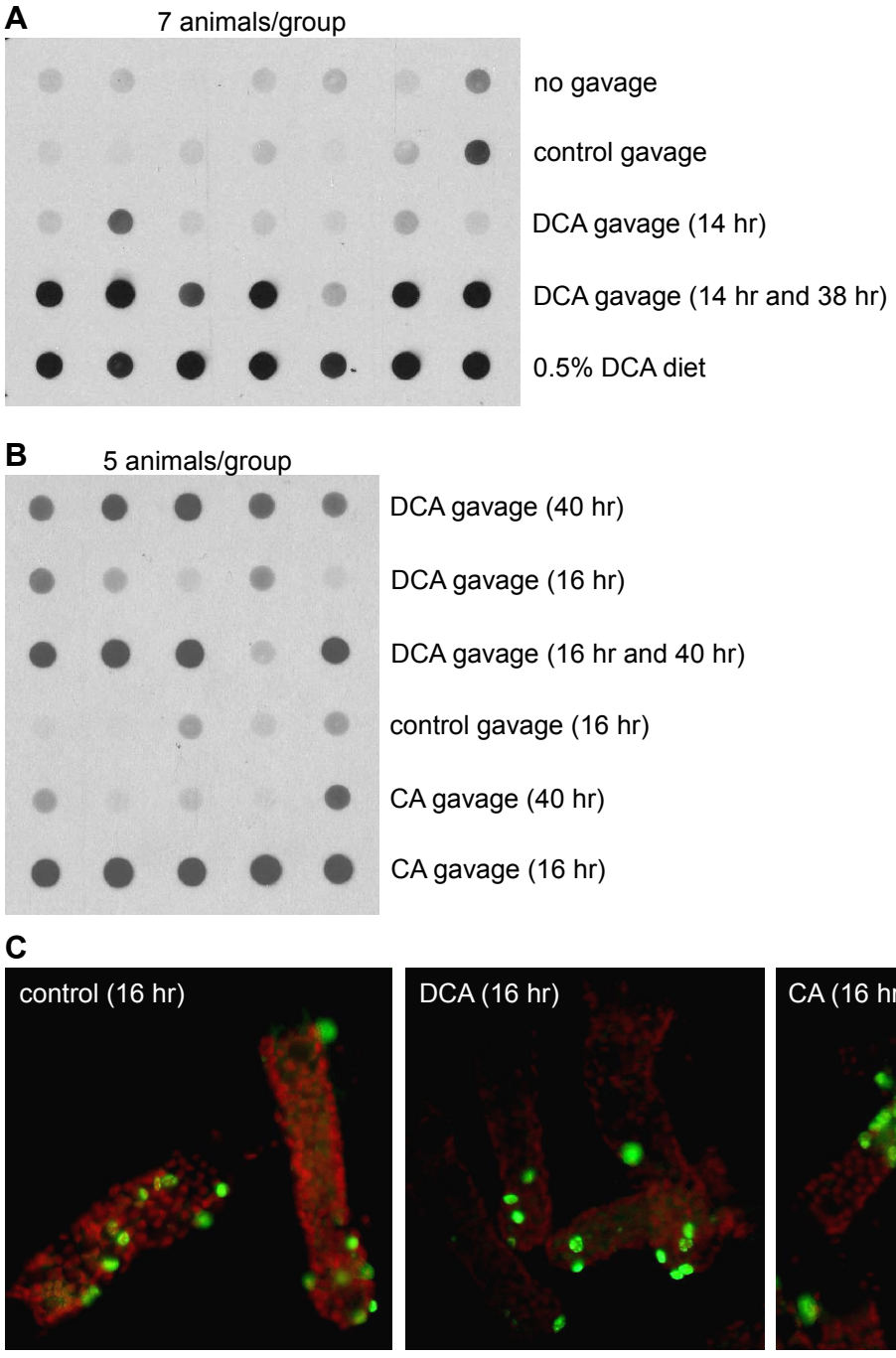

Figure 5.6 Onset of proliferation is more rapid with CA than DCA.
Wild-type mice were gavaged with 500 mg/kg DCA or CA at the indicated time points, or fed 0.5% DCA diet. Two hours prior to sacrifice animals received 100 mg/kg BrdUrd by intraperitoneal injection. **(A and B)** DNA extracted from colon crypts was immobilized on nitrocellulose and immunoblotted for BrdUrd. **(C)** BrdUrd (green) staining of colon crypts.

5.3.4 Kinetics of the Proliferative Response to CA Gavage

In order to study the mechanism of proliferation, the chronology of events leading up to increased DNA synthesis (the parameter measured by BrdUrd incorporation) had to be determined. Given that CA gavage induced proliferation within 16 hours, a time course was done to determine the onset of proliferation in all segments of the intestine. Tissues from the duodenum, jejunum, ileum, and colon were collected for BrdUrd incorporation and RNA expression analysis. In the colon DNA synthesis was increased at 10 hours and further increases were seen at 14 and 18 hours after gavage (Figure 5.7A and B). DNA synthesis in the ileum began at 6 hours and peaked around 10 to 14 hours (Figure 5.7B). Similarly, increases in Ki67 (proliferation marker) mRNA levels in the ileum preceded increases in the colon by approximately four hours (Figure 5.7C). Results for the duodenum and jejunum were similar to the ileum (data not shown). These data indicate that proliferation is not induced by a systemic response to bile acids, but rather occurs sequentially as each segment of the intestine is exposed to bile acids during intestinal transit.

Germ-free mice were used to confirm that CA, and not a bacterial metabolite of CA, induced proliferation (Figure 5.7D). Interestingly, taurine-conjugated cholic acid was not capable of inducing proliferation in the intestine.

To gain insight into the mechanism of proliferation, the expression of a number of genes was evaluated, including cell cycle regulators, FXR target genes, stress factors, and factors described in the literature to either be involved in or drive intestinal proliferation (Figure 5.8A-C). These data showed that G1/S phase cyclins were among the first genes to be induced, followed by FXR target genes and S phase cyclins (Figure 5.8A and B). Notably, changes in candidate genes putatively involved in regulating intestinal proliferation, including RAS target genes, β-catenin pathway regulators, and select growth factors were either not

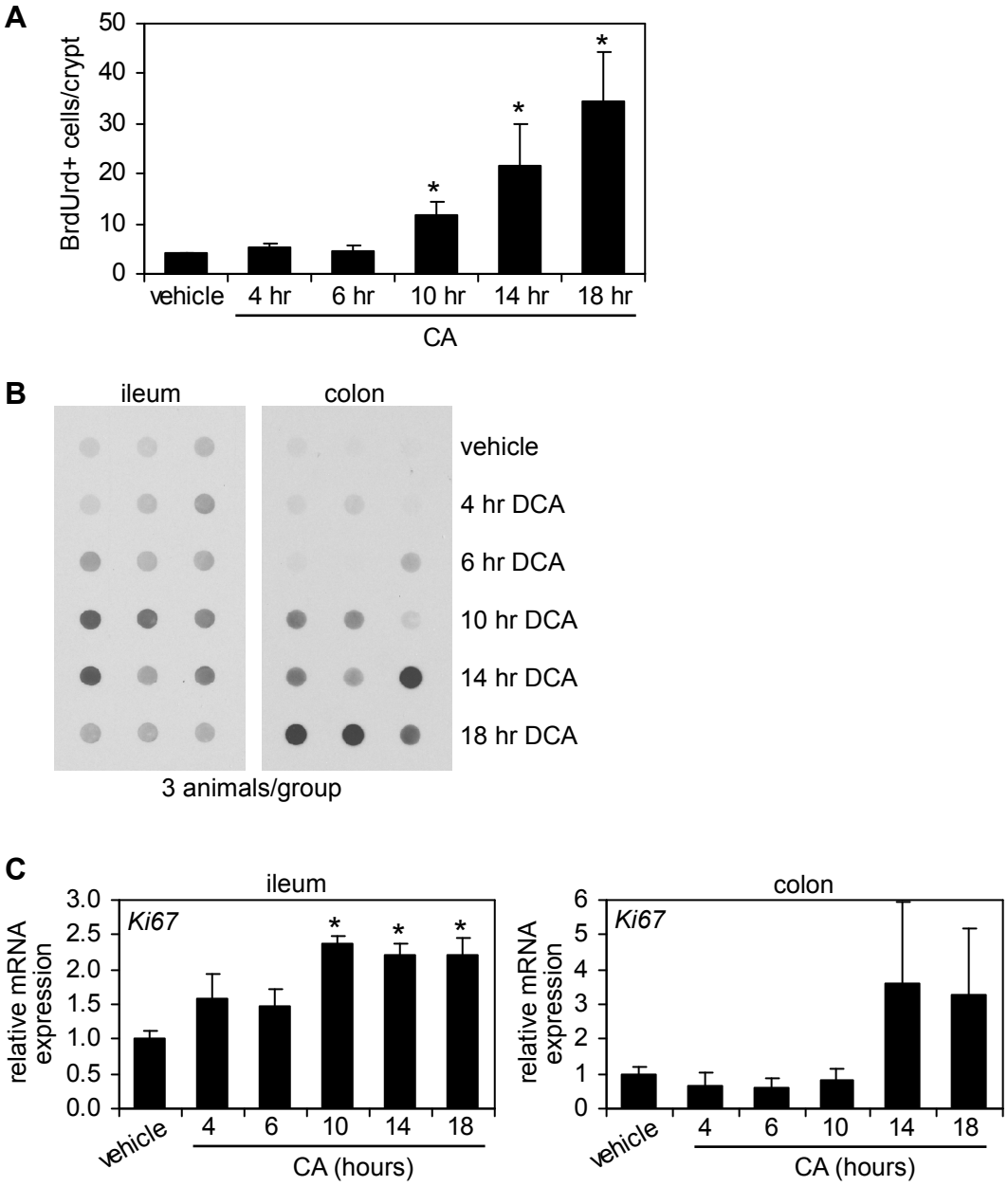

Figure 5.7A-C Proliferation in ileum precedes proliferation in colon.
Wild-type mice were treated with 500 mg/kg CA by oral gavage for the indicated time points. Vehicle group includes two animals gavaged at 4 hours and one animal at 18 hours. Two hours prior to sacrifice animals received 100 mg/kg BrdUrd by intraperitoneal injection. **(A)** Average number of BrdUrd positive cells per colon crypt. **(B)** DNA extracted from whole ileum and colon crypts was immobilized on nitrocellulose and immunoblotted for BrdUrd. **(C)** mRNA expression of *Ki67* in the ileum and colon was determined by quantitative RT-PCR, normalized to *U36b4*, and graphed relative to vehicle-treated control. For A and C data represent the mean ± SEM of 3 animals per group. * $p < 0.05$ compared to vehicle.

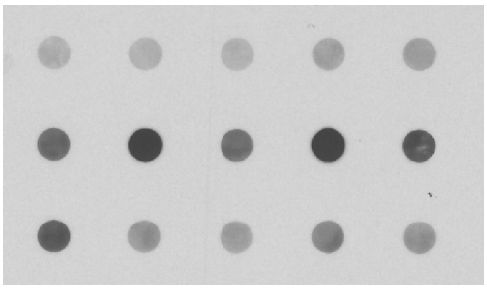

Figure 7D CA but not tauroCA induces proliferation in germ-free mice.
Germ-free mice (5 animals/group) were treated with 500 mg/kg CA or tauroCA by oral gavage for 14 hours. Two hours prior to sacrifice animals received 100 mg/kg BrdUrd by intraperitoneal injection. DNA extracted from whole isolated ileum epithelium was immobilized on nitrocellulose and immunoblotted for BrdUrd.

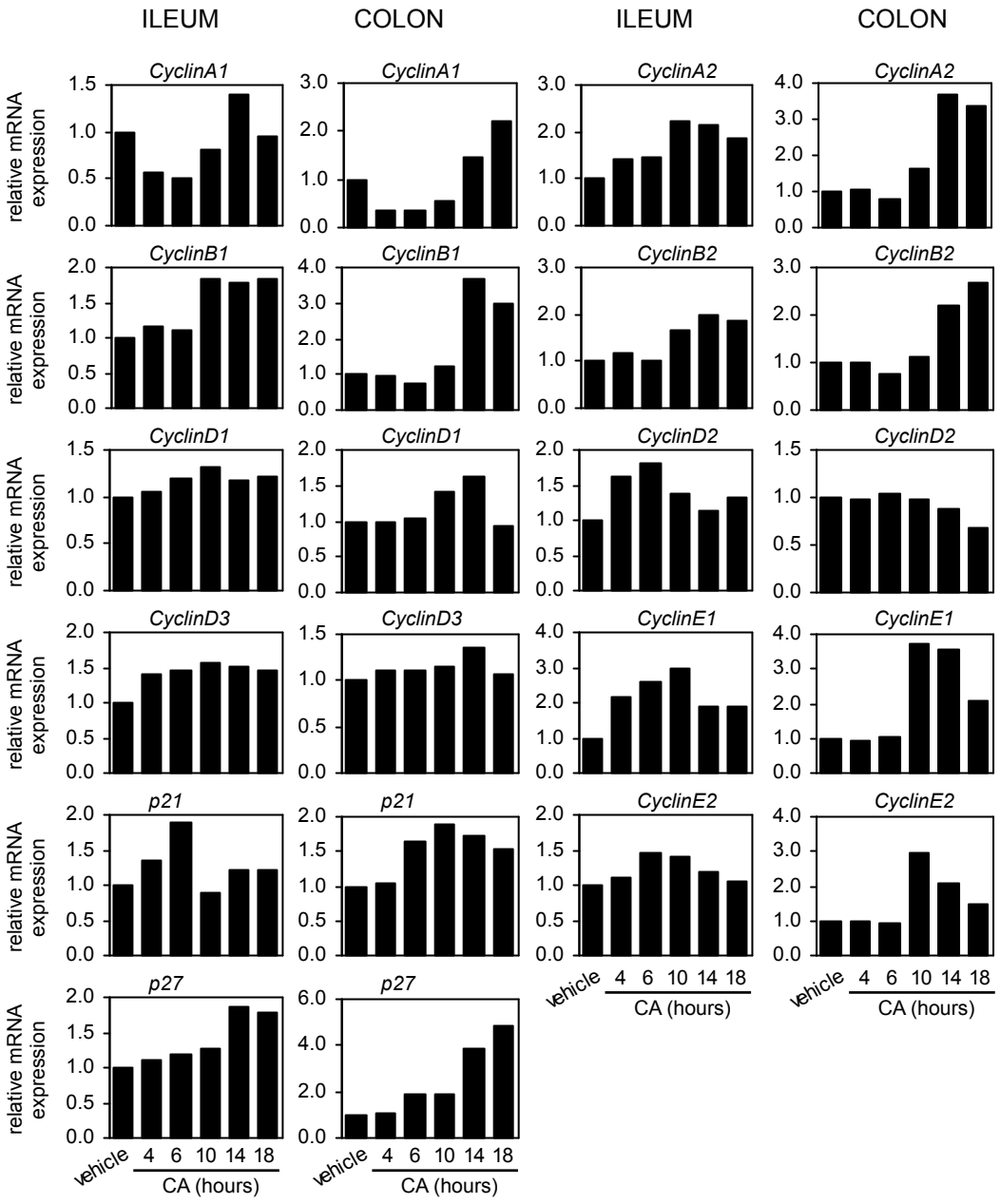

Figure 5.8A Gene expression in ileum and colon following CA gavage.
Wild-type mice were treated with 500 mg/kg CA by oral gavage for the indicated time points. Vehicle group includes two animals gavaged at 4 hours and one animal at 18 hours. Equal quantities of RNA extracted from the colon were pooled from 3 animals per group. mRNA expression in the ileum and colon was determined by quantitative RT-PCR, normalized to *U36b4*, and graphed relative to vehicle-treated control.

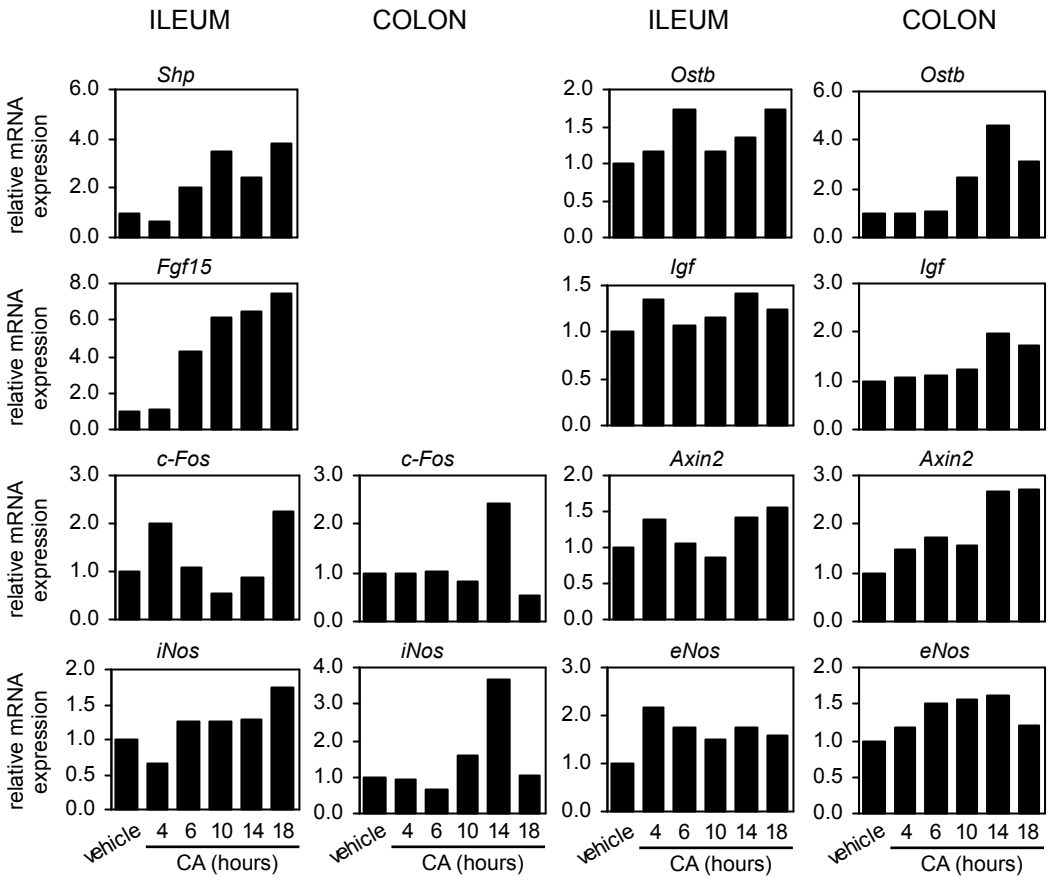

Figure 5.8B Gene expression in ileum and colon following CA gavage.
Wild-type mice were treated with 500 mg/kg CA by oral gavage for the indicated time points. Vehicle group includes two animals gavaged at 4 hours and one animal at 18 hours. Equal quantities of RNA extracted from the colon were pooled from 3 animals per group. mRNA expression in the ileum and colon was determined by quantitative RT-PCR, normalized to *U36b4*, and graphed relative to vehicle-treated control.

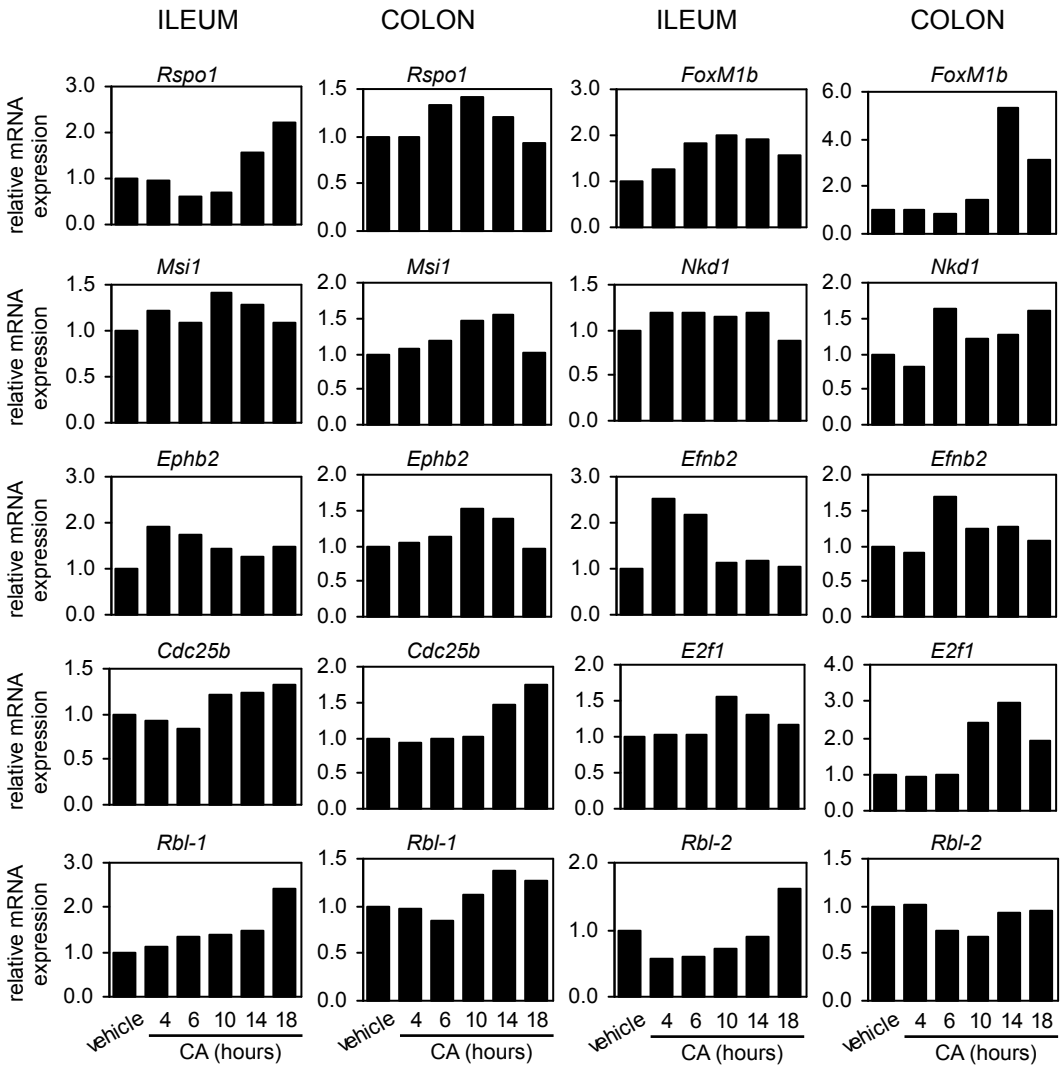

Figure 5.8C Gene expression in ileum and colon following CA gavage.
Wild-type mice were treated with 500 mg/kg CA by oral gavage for the indicated time points. Vehicle group includes two animals gavaged at 4 hours and one animal at 18 hours. Equal quantities of RNA extracted from the colon were pooled from 3 animals per group. mRNA expression in the ileum and colon was determined by quantitative RT-PCR, normalized to *U36b4*, and graphed relative to vehicle-treated control.

changed or they increased hours after the induction of G1/S phase cyclins (Figure 5.8B and C). The most significantly induced G1/S- phase cyclin was *CyclinE1*, while *CyclinA2* was the most induced S phase cyclin (Figure 5.8A). Thus, expression of these two genes and *Ki67* (the expression of which appeared to coincide with S phase cyclins) were subsequently used as biomarkers of proliferation.

5.3.5 FXR and TGR5 Are Not Required for Bile Acid-Induced Proliferation

Gene expression analysis suggested that signaling pathways that regulate G1/S phase cyclins would likely be involved in the mechanism of bile acid-induced proliferation. Given that FXR and TGR5 are bile acid sensors, I sought to determine whether they were involved in the proliferative response. To test this, wild-type and knock-out animals were treated for 16 hours by CA gavage and proliferation in the colon was evaluated. Results showed that CA-induced proliferation occurred in both *Fxr–/–* and *Tgr5–/–* mice, indicating that the mechanism of bile acid-induced proliferation does not require FXR or TGR5 (Figure 5.9).

5.3.6 Evaluation of CA Administered by Enema

Oral gavage studies were useful to determine the kinetics of bile acid-induced proliferation; however, an oral gavage dose-response study to determine the effective bile acid concentration was not practical. In addition, bile acids such as DCA and CDCA appeared to affect intestinal transit time (data not shown), making it difficult to draw conclusions regarding a bile acid/proliferation structure-activity relationship. To circumvent these problems, CA was administered by enema in a time course study. Results showed that *CyclinE1* was increased at 6 hours while *CyclinA2* and *Ki67* were increased by 10 hours (Figure 5.10A). Interestingly *c-Myc* was found to be induced as early as 2 hours after the

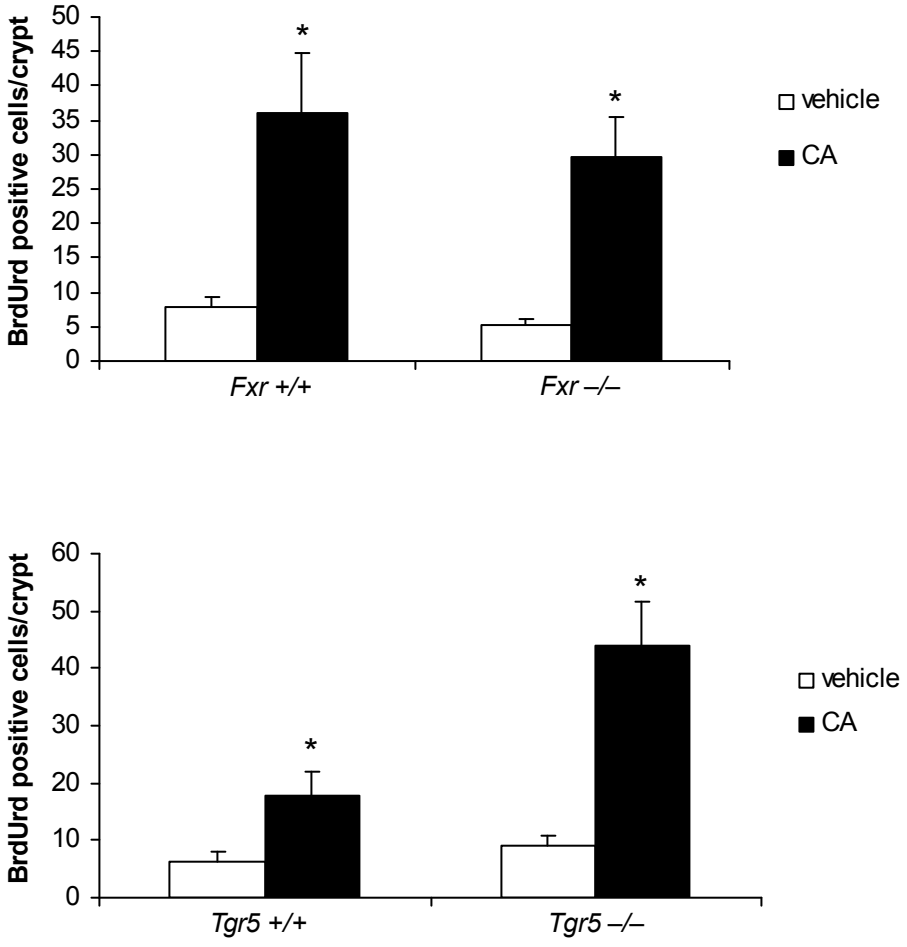

Figure 5.9 FXR and TGR5 are not required for bile acid-induced proliferation.
Mice of the indicated genotype were treated for 16 hours with 500 mg/kg CA by oral gavage. Colon crypts were isolated and immunostained for BrdUrd. The average number of BrdUrd positive cells per colon crypt were counted. A minimum of 30 crypts were counted per animal. Data represent the mean ± SEM of 6 animals per group. * $p < 0.05$ compared to vehicle of the same genotype.

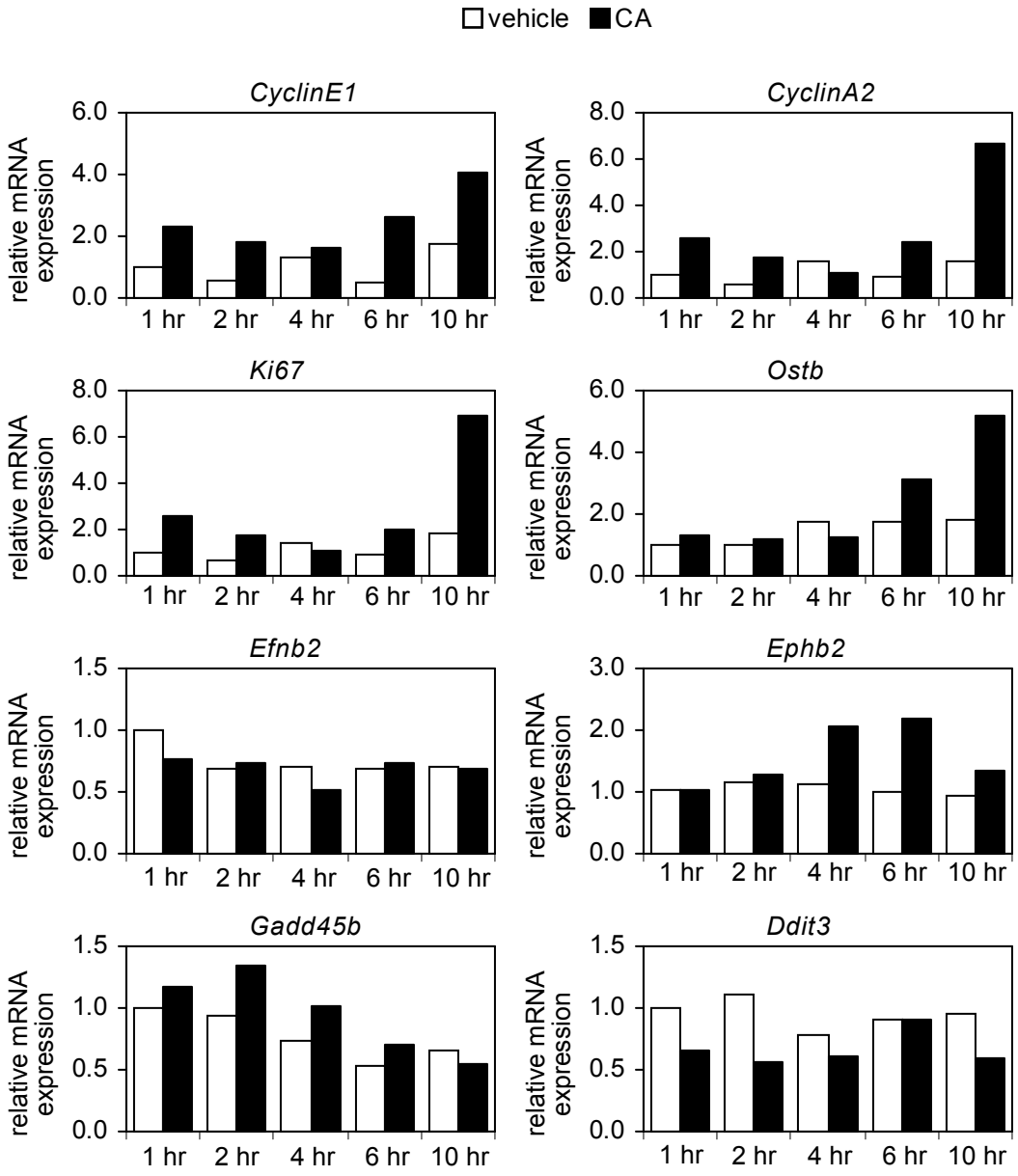

Figure 5.10A Proliferation in the colon induced by CA enema.
Wild-type mice were treated for the indicated times with 100 mM CA or vehicle by enema. Equal quantities of RNA extracted from the colon were pooled from 2-3 animals per group. mRNA expression was determined by quantitative RT-PCR, normalized to *U36b4*, and graphed relative to the 1 hour vehicle treatment group.

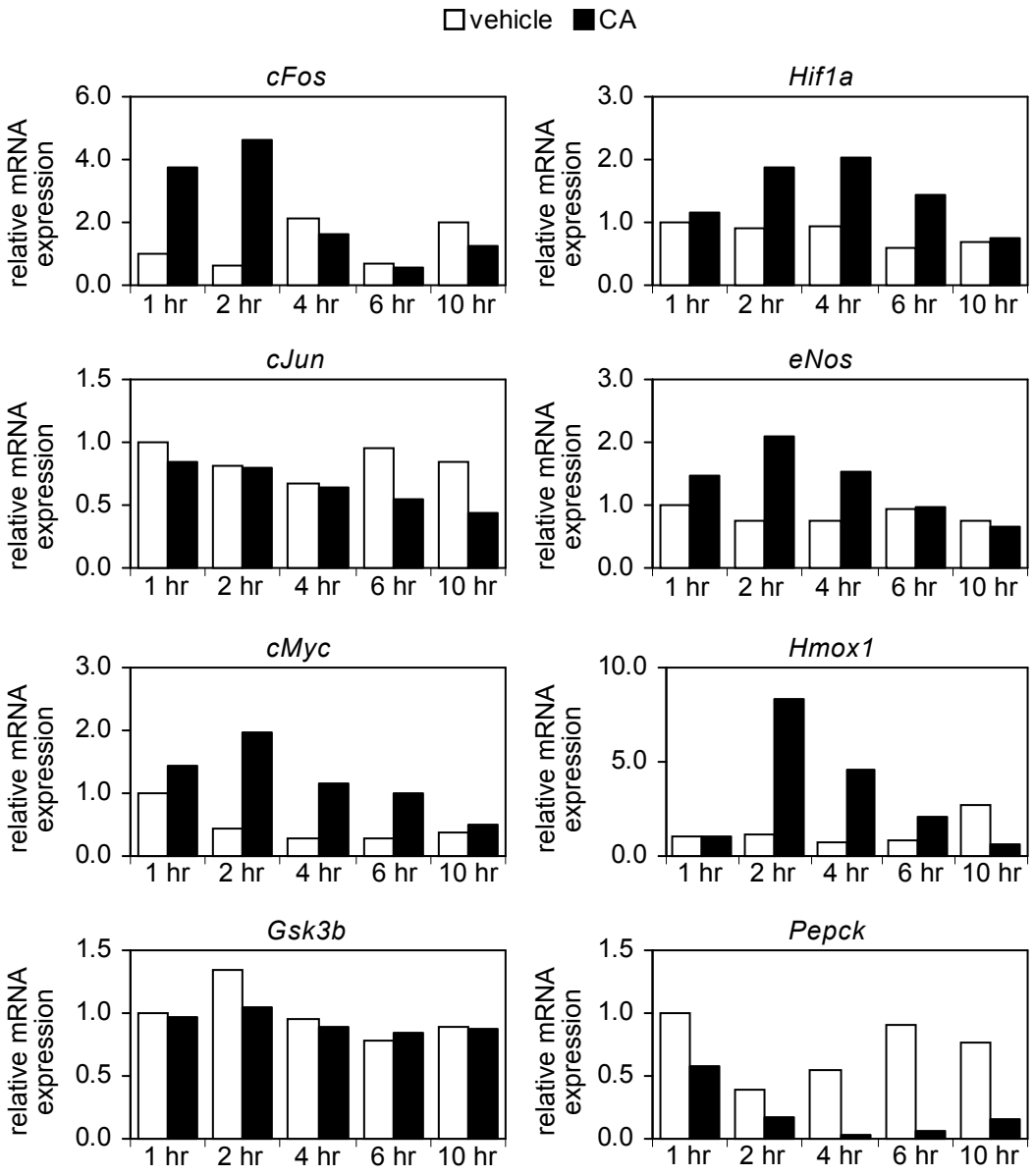

Figure 5.10B Proliferation in the colon induced by CA enema.
Wild-type mice were treated for the indicated times with 100 mM CA or vehicle by enema. Equal quantities of RNA extracted from the colon were pooled from 2-3 animals per group. mRNA expression was determined by quantitative RT-PCR, normalized to *U36b4*, and graphed relative to the 1 hour vehicle treatment group.

enema was administered (Figure 5.10B). This event preceded the increase in cyclins. In addition, *Pepck* expression was dramatically reduced (Figure 5.10B). No increase was seen in DNA damage genes (*Gadd45g* and *Ddit3*) that are induced by high concentrations of bile acid *in vitro*; however, expression of *Hif1a* was increased, as were two HIF1A target genes, *Hmox1* and *eNos* (Figure 5.10A and B). *cFos* expression was also increased at early time points, but rapidly normalized (Figure 5.10B).

5.3.7 Proliferative Effects Occur When Bile Acids Are at Their Critical Micellar Concentration

To determine the minimum bile acid concentration required to induce proliferation, a number of dose-response experiments were performed with CA and DCA. Interestingly, it was found that 5 mM DCA was sufficient to induce proliferation; however, 25 mM CA was needed to see a similar response (Figure 5.11). The critical micellar concentration (CMC) of DCA is estimated to be around 5 mM, while the CMC for CA is approximately 10 mM. Thus, these data indicate that bile acids must be present at or above their CMC in order to induce intestinal proliferation. It is important to note that *Ostβ* expression was also not increased at levels below the CMC, suggesting that at such concentrations bile acids may not be getting into mucosal cells to activate FXR (Figure 5.11). Clearly the milieu of the colon *in vivo* is significantly different from cell culture systems in which micromolar concentrations of bile acids are sufficient to activate FXR (see Chapter 4).

5.3.8 Bile Acid Structure-Activity Relationship

Both DCA and CA were found to induce proliferation, while studies in germ-free mice showed that taurine-conjugated CA did not induce proliferation (Figure 5.7D). These data indicate that specific structural properties of bile acids

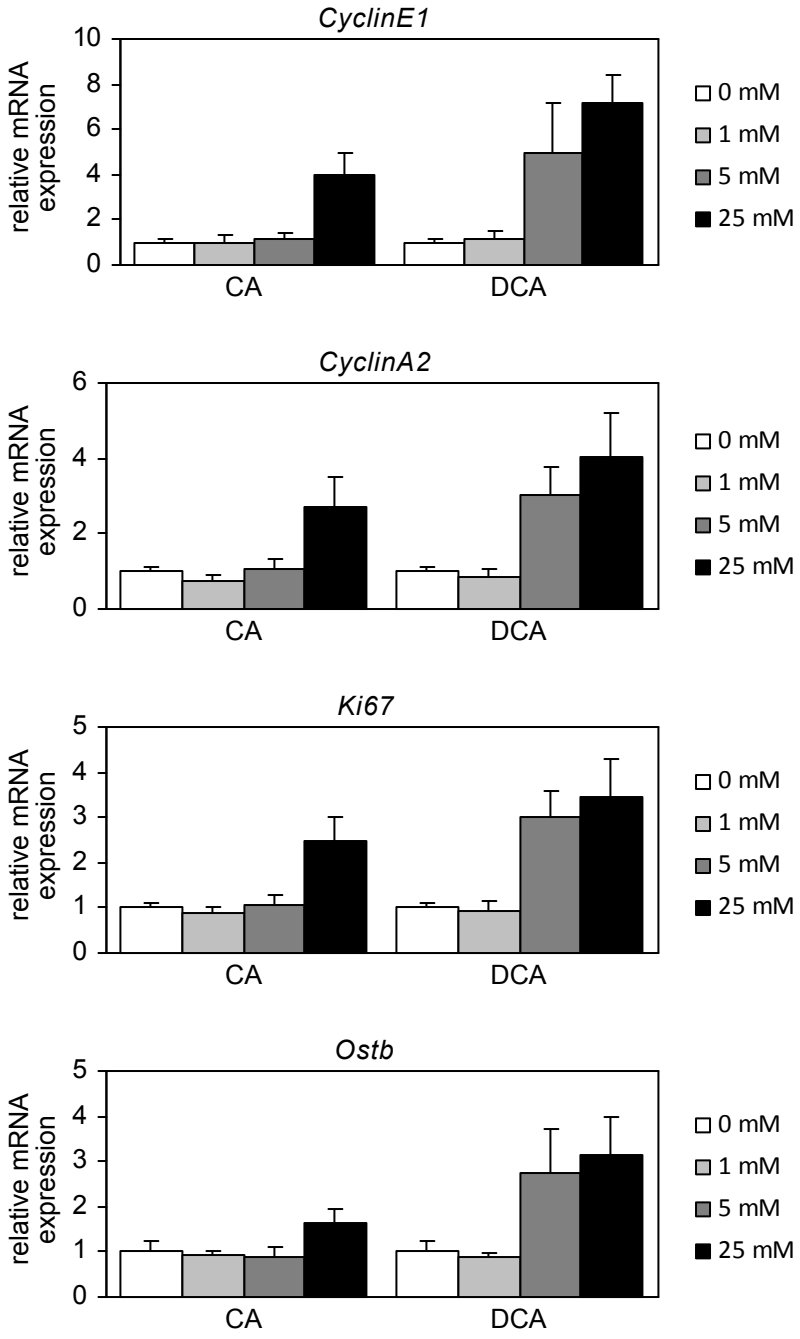

Figure 5.11 CA and DCA dose-response profile.
Wild-type mice were treated for 10 hours with the indicated concentrations of CA or DCA by enema. mRNA expression was determined by quantitative RT-PCR, normalized to *U36b4*, and graphed relative to vehicle treatment group. Data represent the mean ± SEM of 4 animals per group.

are important for determining their ability to activate proliferation. One possibility is that intestinal proliferation is regulated by a receptor or sensor that is only activated by select bile acids. To determine a structure-activity relationship between bile acids and proliferation, the major bile acids and their taurine-conjugates were tested at a concentration of 25 mM. This concentration is greater than the CMC of these bile acids. Results showed that at this concentration DCA and CDCA produced the greatest effect, while other bile acids (e.g. UDCA) had no effect (Figure 5.12). Conjugated bile acids were significantly less effective, although the trends were similar with tauroDCA being most effective (Figure 5.12). Importantly, these results confirmed the data from germ-free mice showing that the primary bile acid produced by the liver, tauroCA, does not induce proliferation or activate FXR target genes in the intestine.

5.3.9 DCA Does Not Induce Apoptosis *in vivo*

High concentrations of bile acids induce apoptosis *in vitro* (see Chapter 4). One possible explanation for bile-acid induced proliferation *in vivo* is that the surface epithelium is first induced to undergo apoptosis and this is followed by a so-called "reactive proliferation" within the crypts. Since proliferation occurs within hours after bile acid administration, it seems unlikely that it is caused by increased apoptosis and subsequent reactive proliferation. Nevertheless, to rule out this possibility, apoptosis was evaluated by TUNEL assay. Little apoptosis was seen in vehicle treated animals, and no increase occurred with DCA treatment (Figure 5.13).

5.3.10 Signaling Pathways Involved in Bile Acid-Induced Proliferation

The previously described CA enema time-course study identified a number of genes whose expression was rapidly changed and preceded the increase in G1/S phase cyclins (Figure 5.10A and B). To confirm and extend

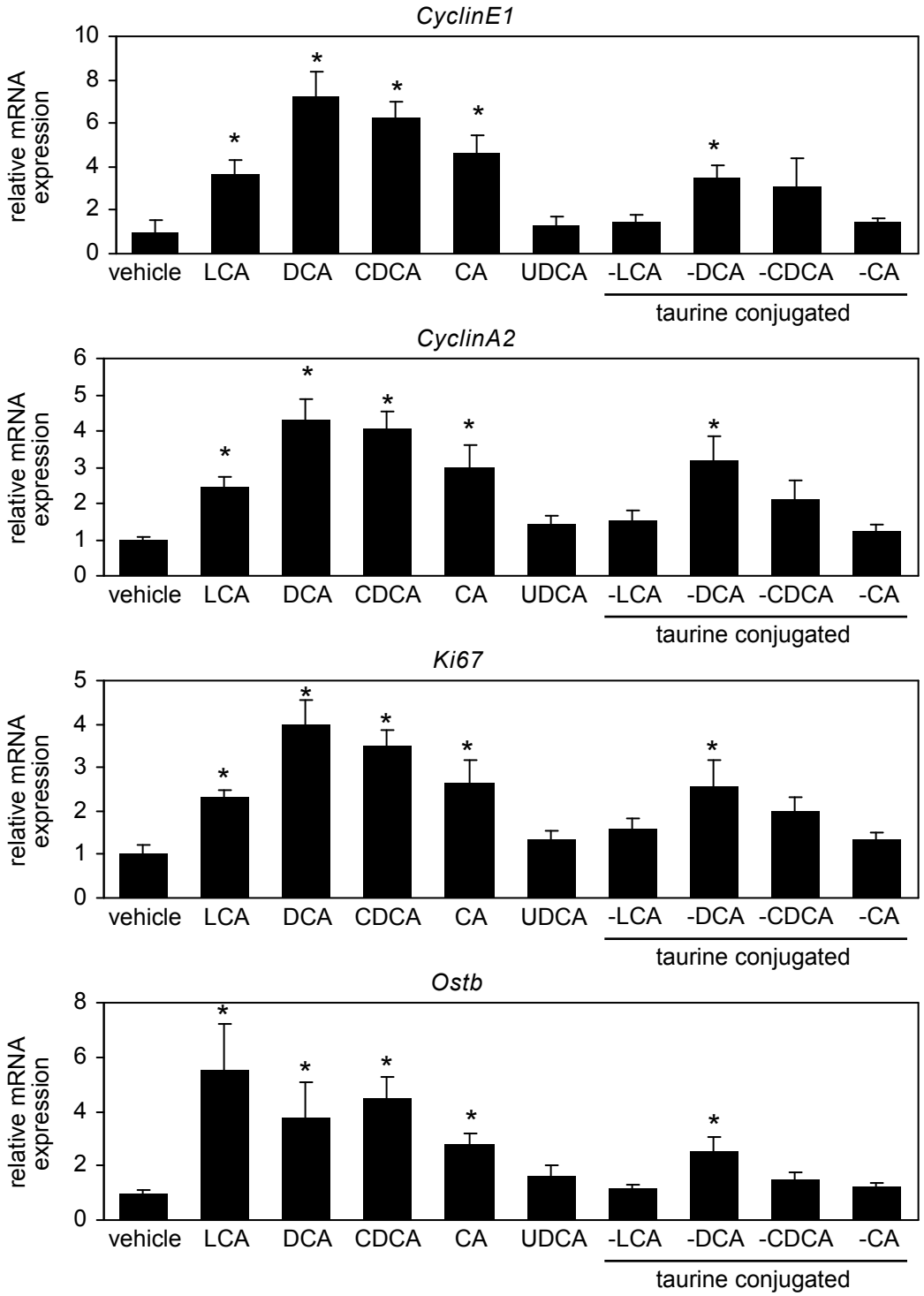

Figure 5.12 Bile acid structure-activtiy relationship.
25 mM bile acid treatment by enema for 10 hours. * $p < 0.05$ compared to vehicle.

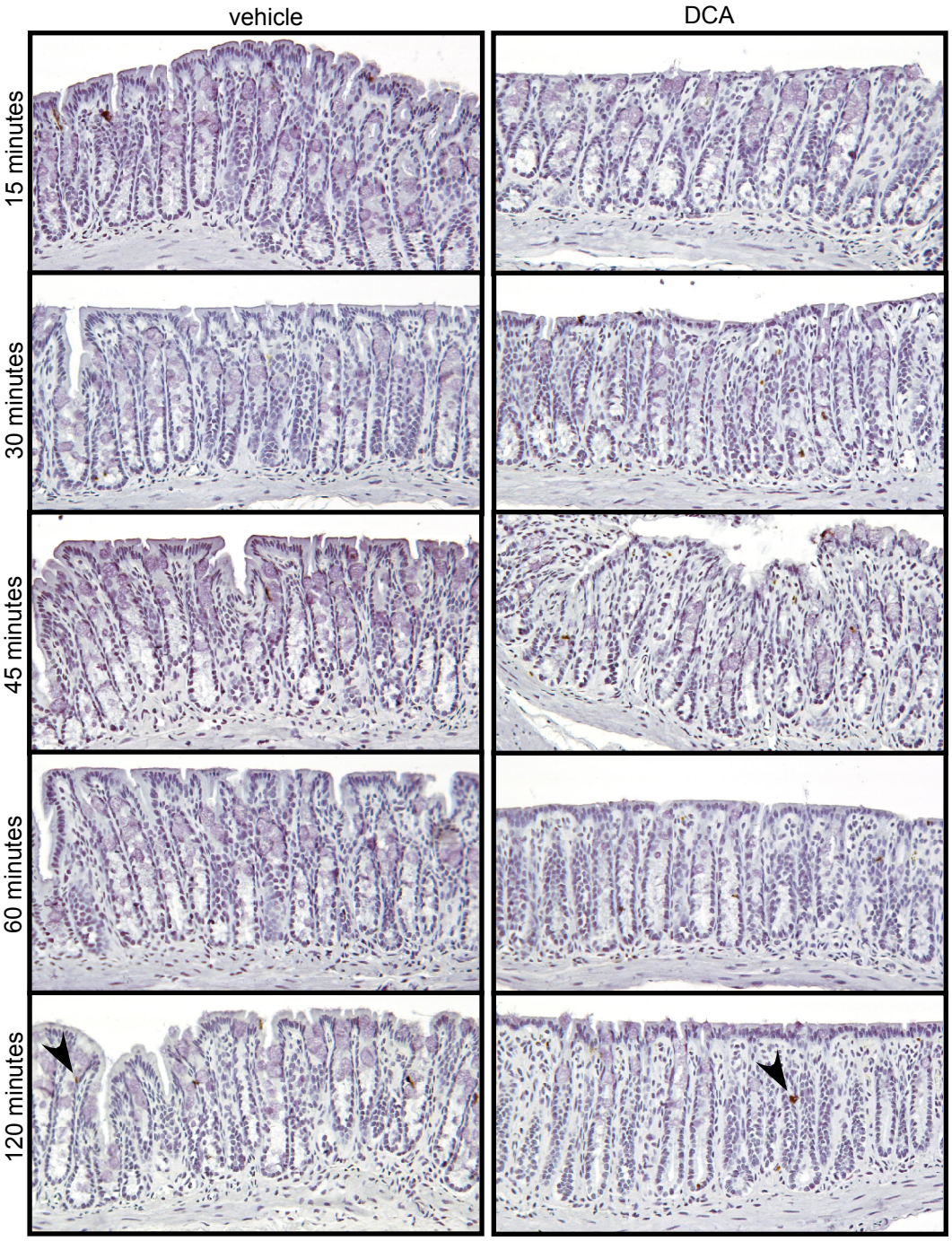

Figure 5.13 DCA enema does not induce apoptosis.
Wild-type mice were treated for the indicated times with 25 mM DCA or vehicle by enema. Images show TUNEL DAB-staining of formalin-fixed, paraffin-embedded sections. Arrow indicates apoptotic cells.

these studies, the effects of DCA on proliferation were tested at different time points. While the effect of DCA administered by oral gavage was delayed relative to CA, no difference was observed between DCA and CA administered by enema. Similar to CA, increased proliferation with DCA was seen at 10 hours, and by 12 hours *CyclinE1* had already begun to decline (Figure 5.14 and 5.15A). Furthermore, gene expression analysis at the 2-hour time point confirmed the previous finding that *cMyc* was induced while *Pepck* was suppressed (Figure 5.15B). Around the 4-hour time point, *Hifa* and *Hmox1* (a HIF1A target gene) were induced (Figure 5.15C). Attempts were made to evaluate HIF1A protein levels; however, HIF1A could not be detected by western blot in either vehicle or DCA treated colon (data not shown).

Activation of AKT through its effects on FOXO and other downstream transcription factors is known to produce a similar profile of gene expression changes; thus, I hypothesized that AKT may be activated by and mediate the proliferative effects of bile acids in the colon. To determine whether the PI3K/AKT pathway was activated, the phophorylation status of AKT and other signaling kinases was evalauated in mouse colon treated with DCA. Indeed, it was found that AKT was phosphorylated as early as 15 minutes after DCA treatment and phosphorylation remained high at all time points tested (up to two hours) (Figure 5.16). ERK phosphorylation was also increased while p38 was not. JNK phosphorylation was slightly increased by DCA treatment only at the 15 minute time point; however, total JNK levels were increased with both vehicle and DCA enema. No increase in GSK3a/b phosphorylation was detected, suggesting that this downstream target of AKT was not involved in the signaling of proliferation. Consistent with gene expression analysis, c-MYC levels were dramatically increased at the two hour time point.

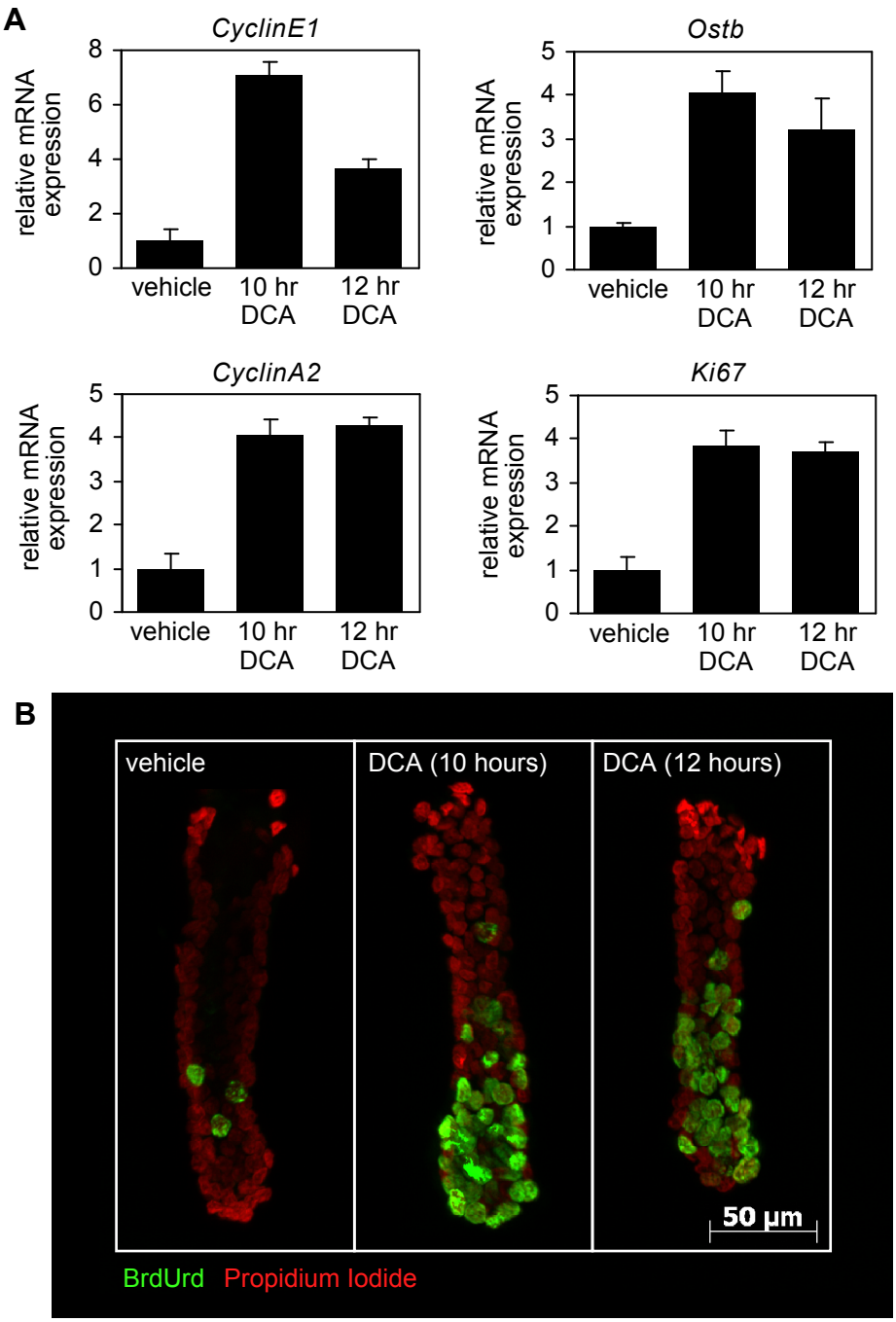

Figure 5.14 Proliferation in the colon induced by DCA enema.
Wild-type mice were treated for the indicated times with 25 mM DCA or vehicle by enema. **(A)** mRNA expression was determined by quantitative RT-PCR, normalized to *U36b4*, and graphed relative to vehicle treatment group. Data represent the mean ± SEM of 3 animals per group.**(B)** BrdUrd (green) staining of colon crypts.

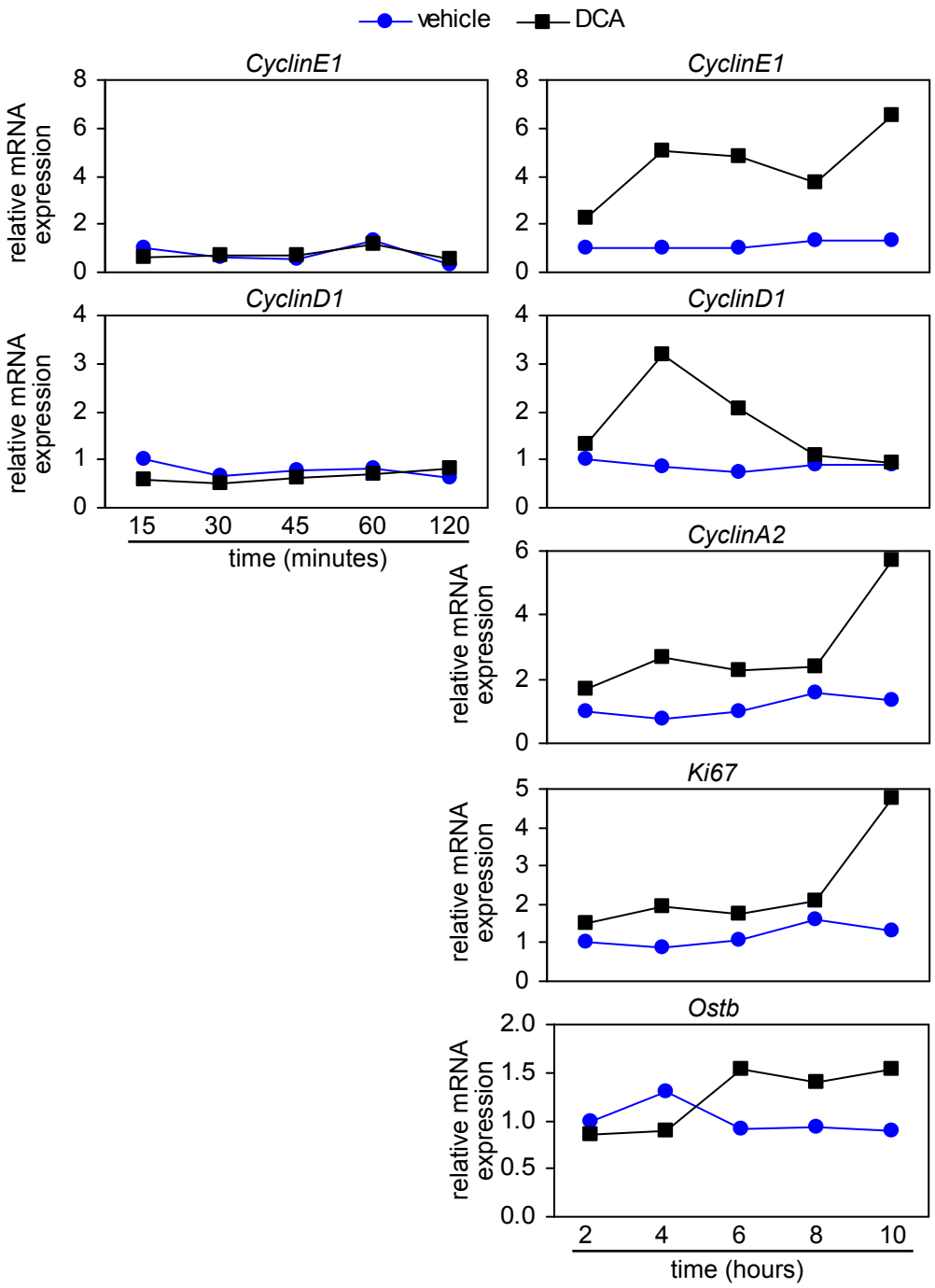

Figure 5.15A DCA time-course.
Wild-type mice were treated for the indicated times with 25 mM DCA or vehicle by enema. mRNA expression was determined by quantitative RT-PCR, normalized to *U36b4*, and graphed relative to the first vehicle point.

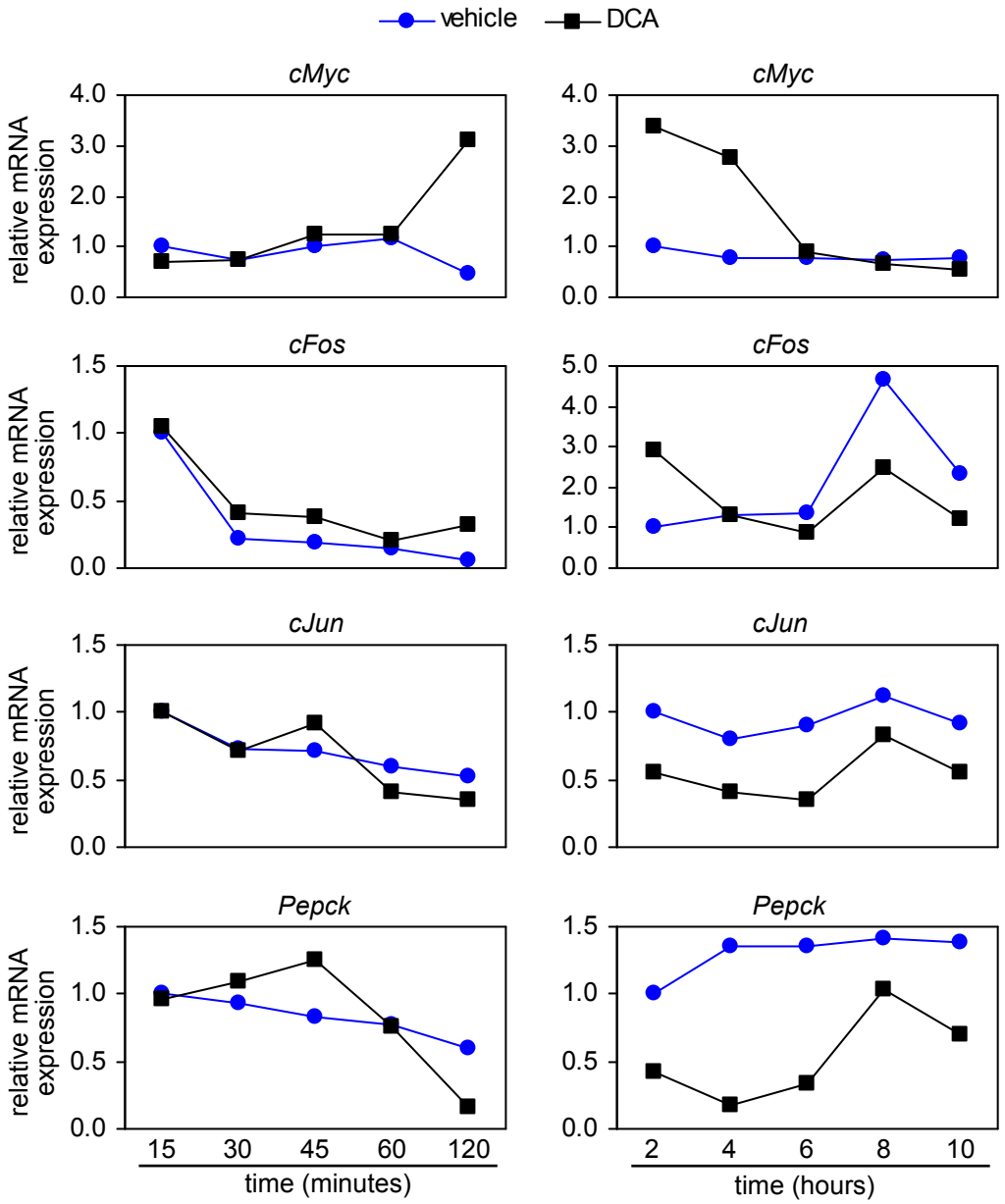

Figure 5.15B DCA time-course.
Wild-type mice were treated for the indicated times with 25 mM DCA or vehicle by enema. mRNA expression was determined by quantitative RT-PCR, normalized to *U36b4*, and graphed relative to the first vehicle point.

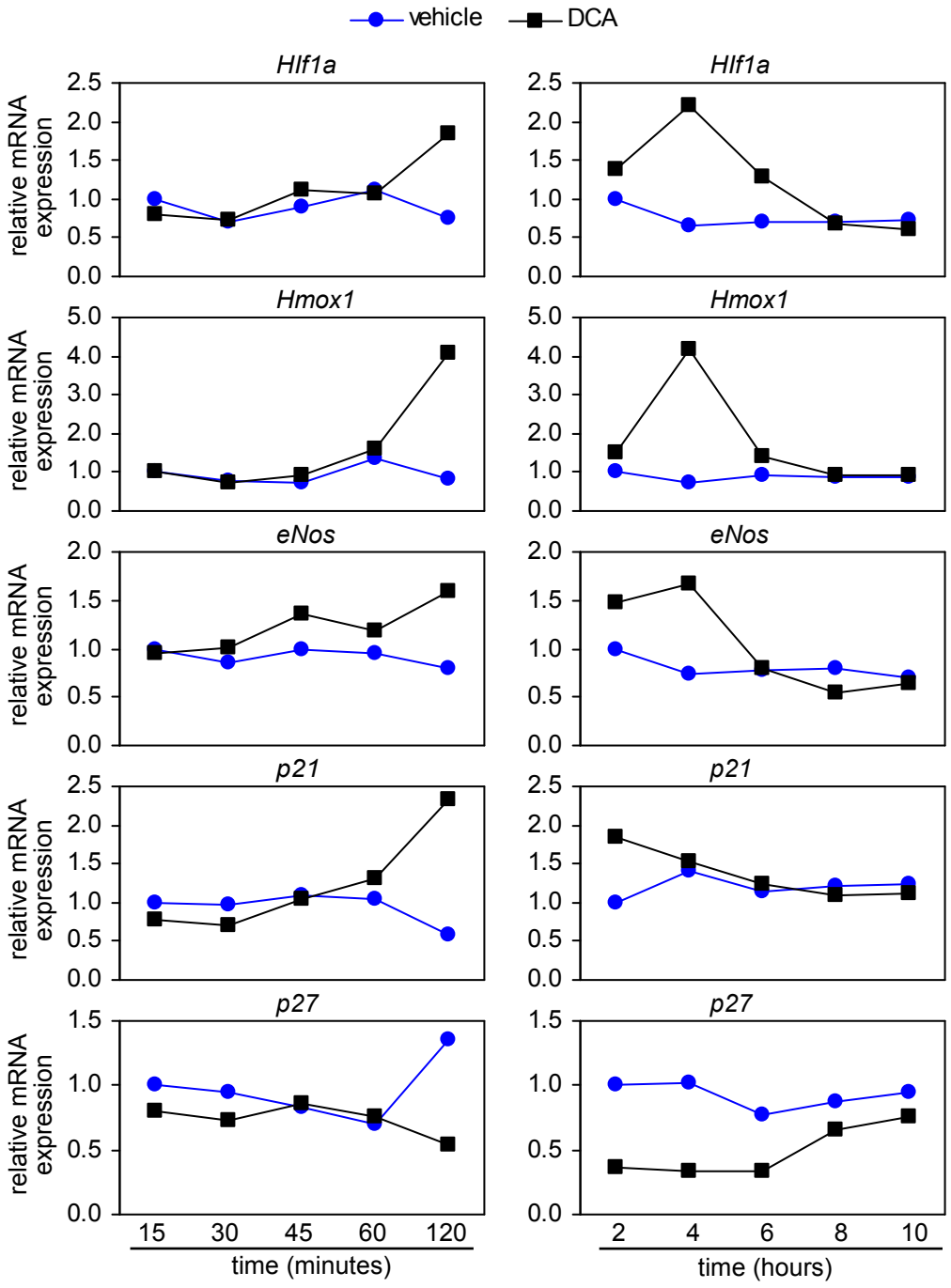

Figure 5.15C DCA time-course.
Wild-type mice were treated for the indicated times with 25 mM DCA or vehicle by enema. mRNA expression was determined by quantitative RT-PCR, normalized to *U36b4*, and graphed relative to the first vehicle point.

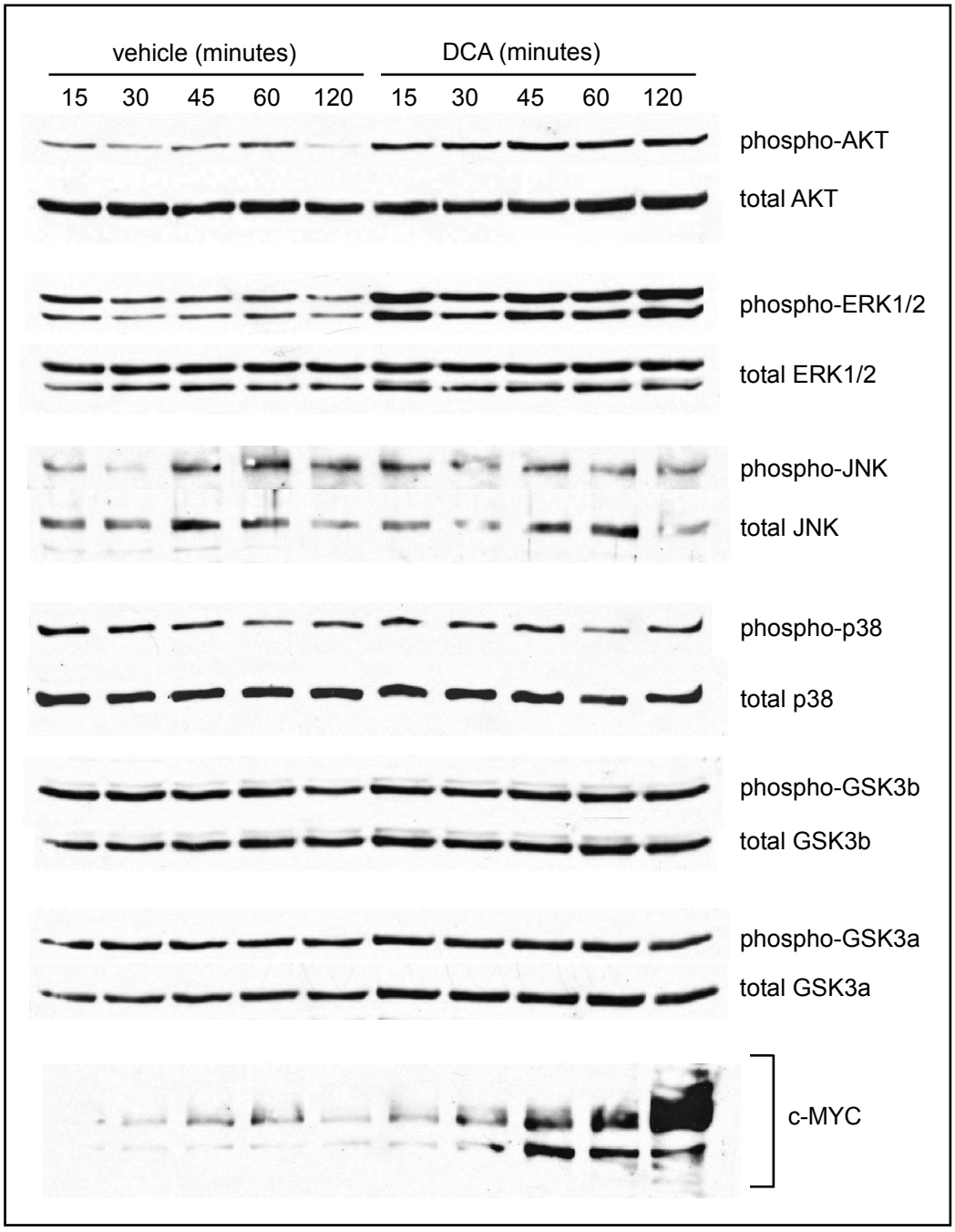

Figure 5.16 Signaling pathways activated by DCA *in vivo*.
Wild-type mice were treated for the indicated times with 25 mM DCA or vehicle by enema. Whole colon lysates were resolved by SDS-PAGE and immunoblotted for the indicated proteins.

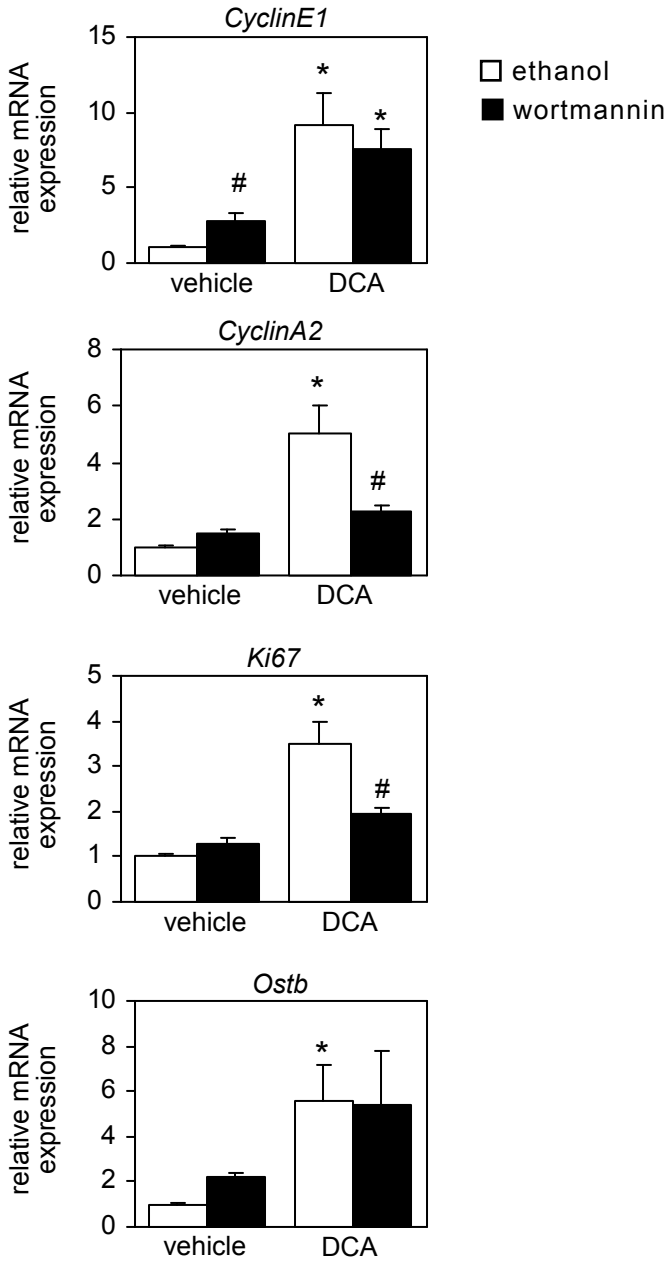

Figure 5.17 Wortmannin blocks bile acid-induced proliferation.
Wild-type mice were treated for 10 hours by enema with 25 mM DCA or vehicle and either 100 μM wortmannin or ethanol. mRNA expression was determined by quantitative RT-PCR, normalized to *U36b4*, and graphed relative to the vehicle/ethanol group. Data represent the mean ± SEM of 3 animals per group. * $p < 0.05$ compared to vehicle, # $p < 0.05$ compared to ethanol.

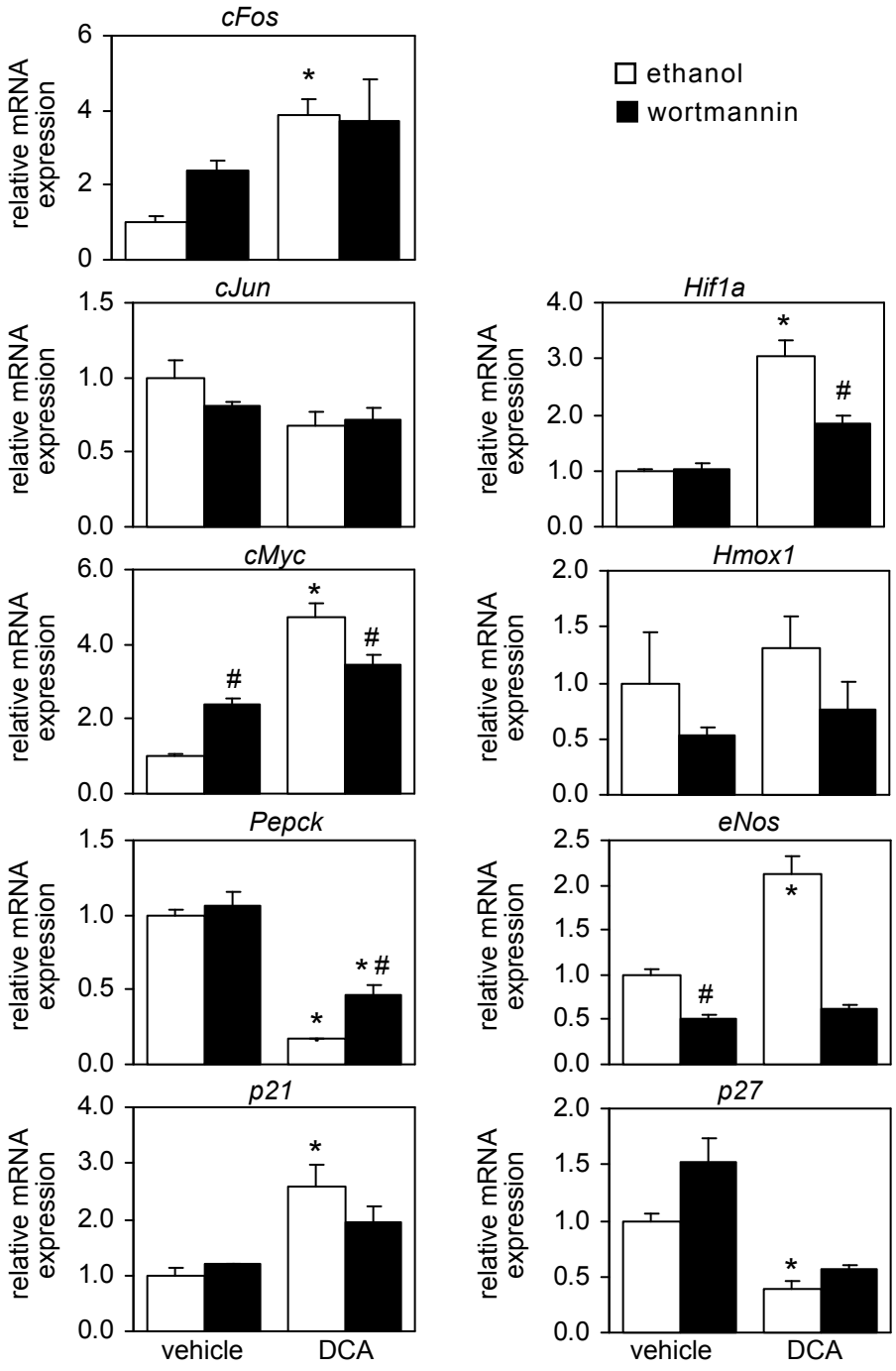

Figure 5.18 Effects of wortmannin on early gene expression.
Wild-type mice were treated for 2 hours by enema with 25 mM DCA or vehicle and either 100 μM wortmannin or ethanol. mRNA expression was determined by quantitative RT-PCR. Data represent the mean ± SEM of 3 animals per group. * $p < 0.05$ compared to vehicle, # $p < 0.05$ compared to ethanol.

To determine whether AKT phosphorylation was relevant to bile acid-induced proliferation, a PI3K inhibitor (wortmannin) was co-administed with the DCA enema, and biomarkers of proliferation were evaluated. Although *CyclinE1* was not significantly changed, both *Ki67* and *CyclinA2* were reduced to near-normal levels by the inhibitor (Figure 5.17). The effects of blocking PI3K signaling on early gene expression were also evaluated, and wortmannin was found to partially block the inductions of *cMyc* and *Hif1a* (Figure 5.18). These results support the hypothesis that bile acids induce proliferation in the intestine by activating the PI3K/AKT pathway.

5.4 Discussion

It has previously been reported that bile acids induce proliferation in the intestine. Furthermore, it has been suggested that the proliferative effects of bile acids underlie their ability to promote intestinal tumorigenesis. Thus far, no molecular mechanism has been shown to explain these effects. The current study was undertaken to confirm these effects and determine the mechanism of bile acid-induced proliferation.

Results of this study demonstrate that bile acids induce proliferation in the small and large intestine through local (not systemic) effects. These effects are independent of (and thus not mediated by) the presently known bile acid sensors, FXR and TGR5. Instead it appears that PI3K signaling is required for the proliferative effects of bile acids.

Futhermore, I have found that bile acids induce proliferation in the intestine only when present at or above their critical micelle concentration. Such concentrations induce phosphorylation of AKT and ERK1/2; however, they do not induce phosphorylation of the stress-activated kinase p38, and they also do not activate apoptosis. While micellar concentrations of bile acid in the small

intestine are necessary to allow fat absorbtion, 95% of bile acids are reabsorbed in the distal small intestine, such that normally only submicellar concentrations exist in the colon. In the proximal ileum, total bile acid concentrations exceed 10 mM, but only 10% of these are unconjugated (Northfield, 1973). Total bile acid concentrations in human cecum are in the 0.5-1 mM range, almost all are unconjugated, and 30% are 3β-hydroxy bile acids (Hamilton, 2007). Thus, in healthy adults unconjugated bile acids are not present at concentrations that have been shown in this study to induce proliferation (i.e. above the CMC); however, under conditions of bacterial overgrowth in the small intestine, unconjugated bile acid concentrations are likely higher. Furthermore, a high fat diet has been shown to increase both fecal bile acid concentration as well as proliferation in the colon (Rafter, 1987; Stadler, 1988; Hori, 1998). It is unclear whether increases in bile acids under these pathologic/abnormal conditions are substantial enough to account for increased proliferation. To my knowledge no studies exist that demonstrate unconjugated bile acid concentrations in excess of their CMC in human intestine.

Future studies are needed to elucidate upstream events leading to the activation of PI3K. It is possible that bile acids, when present at or above their CMC, cause changes in plasma membrane structure that result in activation of growth promoting receptor tyrosine kinases such as epidermal growth factor receptor (EGFR) or the ephrin-B receptors. The classic EGF signaling cascade involves activation of both AKT and ERK/MAPK pathways. In addition, EGF signaling has been shown to increase *Hif1a* expression (Zhong, 2000). The fact that all three events occur following bile acid treatment strongly suggests that the most proximal event is activation of the EGF receptor.

Finally, the suppression of *Pepck* and induction of *Hif1a* suggest that proliferating cells in the intestine are programmed for glycolytic metabolism,

reminiscent of the Warburg effect in cancer cells. The experiments described in this chapter provide an *in vivo* model to further investigate the relationship between cell metabolism and proliferation in this context.

5.5 Acknowledgements

I thank Klementina FonTacer for optimizing the DNA dot-blot assay, and Serkan Kir for immunoblot analysis of the intracellular signaling pathways described above. David O'Donnell assisted with experiments involving germ-free mice in the laboratory of Dr. Jeffrey Gordon at the Center for Genome Science, Washington University School of Medicine, St. Louis, MO.

CHAPTER 6
Regulation of Bile Acid Synthesis by Vitamins A and D

6.1 Introduction

Lipid-soluble vitamins are essential for human health and must be obtained from the environment. They exist in four major groups (A, D, E and K), each of which comprises a series of structurally related compounds with multiple biological functions. Members of the nuclear receptor family of transcription factors are central to the mechanism of action of the lipid-soluble vitamins A and D. Metabolites of vitamin A regulate gene transcription by binding to and activating the retinoic acid receptors (RARs) and the retinoid X receptors (RXRs) (Mangelsdorf, 1995). Similarly, the genomic actions of vitamin D are mediated by the vitamin D receptor (VDR) (Haussler, 1997).

Retinol, the basic form of vitamin A, is obtained from foods of animal origin where it is present in the form of retinyl esters. Vitamin A can also be synthesized in the liver from beta-carotene, which is present in foods of plant origin. In the body, retinol is converted to several metabolites that function as signaling molecules in various biological processes including vision, development, growth, metabolism, and cell differentiation (Ross, 1993; Zile, 1998; Blomhoff, 2006; Mark, 2009). Most of the transcriptional actions of vitamin A *in vivo* have been shown to require the RXR/RAR heterodimer (Mark, 2009).

Vitamin D is synthesized in the skin from 7-dehydrocholesterol through a process that requires sunlight, or it can be obtained directly from the diet. Dietary sources include cholecalciferol (vitamin D3, animal origin) and ergocalciferol

(vitamin D2, plant origin). Whether obtained from the diet or photo-activation in skin, vitamin D must be converted to its bioactive form, 1α,25-dihydroxyvitamin D3 by the action of cytochrome P450 enzymes in the liver and kidney (Prosser, 2004). Vitamin D is best known for its essential role in regulating calcium and phosphate homeostasis (Pannabecker, 1995; Jones, 1998; Amling 1999; Hoenderop, 1999; Van Cromphaut, 2001; Bouillon 2003; Okano, 2004; reviewed in DeLuca, 2004). Recently, the repertoire of physiological systems regulated by vitamin D and its receptor has been expanded to include both innate and adaptive immunity and bile acid detoxification (Piemonti, 2000; reviewed in DeLuca, 2001; Gregori, 2001; Mangelsdorf, 2005; Liu, 2006; Moro, 2008).

The absorption of lipid-soluble vitamins from the diet requires the detergent actions of bile acids. Bile acids are amphipathic sterols synthesized from cholesterol in the liver and secreted into the intestine where, when present at high concentrations, they function to emulsify dietary lipids (Hofmann, 1999a). Cholesterol 7α-hydroxylase (CYP7A1), which catalyzes the rate-limiting step in bile acid biosynthesis, is tightly regulated at the transcriptional level by bile acids and other signaling molecules (Gilardi, 2007). Positive transcriptional regulators of *Cyp7a1* include orphan nuclear receptors, liver-related homologue-1 (LRH-1) and hepatocyte nuclear factor 4α (HNF4α) (Crestani, 1998; Nitta, 1999). Negative feedback regulation of *Cyp7a1 in vivo* involves two complementary mechanisms. First, bile acids activate the nuclear bile acid receptor (FXR) in intestine to induce expression of fibroblast growth factor 15 (*Fgf15*, *FGF19* in humans), which signals from the intestine to repress hepatic *Cyp7a1* through a mechanism that involves the atypical nuclear receptor, small heterodimer partner (SHP), and the membrane receptor, fibroblast growth factor receptor 4 (FGFR4) (Holt, 2003; Inagaki, 2005; Lundasen, 2006). Second, bile acids activate FXR in liver to induce transcription of SHP, which subsequently binds to LRH-1 and

HNF4α, resulting in the repression of *Cyp7a1* (Goodwin, 2000; Lee, 2000; Lu, 2000). How these two FXR-regulated pathways interact to control *Cyp7a1* expression is not clear, albeit both are required for the FXR-mediated feedback repression of bile acid biosynthesis (Kim, 2007a). In addition, activation of c-Jun N-terminal kinase (JNK) signaling by bile acids has been reported to repress *Cyp7a1* expression in cultured hepatocytes (Chiang, 2009; Hylemon, 2009). Thus, multiple signaling pathways activated by bile acids and other signaling molecules converge on CYP7A1 transcriptional regulation to maintain normal levels of bile acids.

While it is well established that bile acids are essential for the absorption of lipid-soluble vitamins, it is not known whether lipid-soluble vitamins affect bile acid biosynthesis. The studies described in this chapter demonstrate that vitamins A and D both regulate bile acid synthesis by overlapping, but distinct mechanisms.

6.2 Methods

6.2.1 Animals and Animal Husbandry

Male C57BL/6 mice were purchased from Charles River Laboratories and used for all experiments involving only wild-type animals. *Vdr*+/+ and *Vdr*–/– mice were obtained from heterozygous breeders on a pure 129T2 background. *Fxr*+/+ and *Fxr*–/– mice were obtained from heterozygous breeders on a pure 129S background. *Fgf15*+/+ and *Fgf15*–/– were obtained from homozygous breeders on a mixed C57BL/6;129S background. *Shp*+/+ and *Shp*–/– were obtained from homozygous breeders on a pure 129S background. All animals were housed in the same specific-pathogen-free facility. Animals were maintained under a temperature controlled environment and 12 hour light/dark cycles with ad lib access to water and irradiated rodent chow (TD.2916, Harlan-

Teklad). The expression of metabolic genes analyzed in this study is affected by circadian and feeding cycles, therefore the following steps were taken to ensure a synchronous feeding cycle. On the day prior to sacrifice chow was removed ten hours before the dark cycle, replaced at the onset of the dark cycle, and removed four hours after the onset of the dark cycle. The change in body weight between the beginning and end of the dark cycle was less than five percent for all animals. For food entrainment experiments, animals were given access to chow only during the first four hours of the dark cycle. All experiments were done with 3 to 6 month-old (age-matched) male mice sacrificed between four and six hours after the beginning of the light cycle. Mice were euthanized by isofluorane inhalation and exsanguinated via the descending vena cava prior to tissue collection. All animal experiments were approved by the Institutional Animal Care and Research Advisory Committee at the University of Texas Southwestern Medical Center.

6.2.2 Animal Treatment

Vitamin D (1α,25-dihydroxycholecalciferol, Sigma) in sterile saline was administered by intraperitoneal injection at the end of the dark cycle and four hours before sacrifice. Vitamin A (retinyl palmitate, ~1,800 USP units/mg, Sigma) and vitamin E (d-α-tocopherol acetate, ~1,360 IU/g, Sigma) in 1% Tween80, 1% methylcellulose, 25mM HEPES were administered by oral gavage at the beginning and end of the dark cycle (sixteen and four hours before sacrifice). Cholestyramine was admixed in the diet (custom diet TD.07658, Harlan-Teklad). GW4064 (GlaxoSmithKline) and TTNPB (Sigma) were admixed in the diet (500 mg/kg and 0.25 mg/kg diet respectively) and provided ad lib for twelve hours before sacrifice. LG268, in 0.25% Tween 80, 1% methylcellulose was administered by oral gavage twelve hours before sacrifice at a dose of 30 mg/kg. INT-747 (6-ethyl-CDCA, Intercept), in 1% Tween 80, 1% methylcellulose was administered by oral gavage at the beginning and end of the

dark cycle (sixteen and four hours before sacrifice) at a dose of 10 mg/kg. For the bile pool size study, INT-747 was administered once daily (six hours after the beginning of the light cycle) for 12 days. In all cases animals in the vehicle group received the appropriate vehicle solutions and diets in a manner identical to the treatment groups.

6.2.3 Measurement of Liver Enzymes

Blood was collected in heparinized tubes and immediately centrifuged at 4°C, 500 g for 30 minutes. Plasma was stored for maximum 24 hours at 4°C. AST and ALT levels were measured using a VITROS® 250 chemistry analyzer (Johnson & Johnson).

6.2.4 Mouse Ileum Explant Culture

Following euthanasia, 5 cm of the terminal ileum was collected and flushed with phosphate-buffered saline (PBS) to remove contents. 1×3 mm segments of the ileum were cultured at 37°C and 95% oxygen for six hours in DMEM (containing 4 g/L glucose and L-glutamine, Gibco) supplemented with 10% charcoal-stripped, heat-inactivated FBS, 25 mM HEPES, 100 U/mL penicillin, 100 μg/mL streptomycin and either vitamin D (1α,25-dihydroxycholecalciferol, Sigma) or 0.1% ethanol (vehicle). Each condition contained four 1×3 mm segments of ileum from which total RNA was extracted at the end of the six-hour culture period.

6.2.5 Bile Acid Extraction and Analysis by LC/MS

Bile acid pool size measurements were performed as previously described with minor modifications (Lee, 2008). The following is a brief description of the protocol including modified parameters. Liver, gallbladder, intestines, and attached mesentery were removed en bloc and homogenized in ethanol.

Homogenates were heating to boiling, cooled, and then filtered. This step was repeated twice. Filtrates were combined and adjusted to a constant volume. Bile acids were resolved by reverse-phase liquid chromatography (C8 pre-column, C18 analytical column) and quantified by mass spectrometry with electrospray ionization in negative ion mode. Unconjugated and taurine-conjugated bile acids used as calibration standards are listed in Chapter 2. Deuterium-labeled cholic acid (5β-cholanic acid-3α,7α,12α-triol-2,2,4,4-d4) and chenodeoxycholic acid (5β-cholanic acid-3α,7α-diol-2,2,4,4-d4) were used as recovery controls. Nor-cholic acid (23-nor-5β-cholanic acid-3α,7α,12α-triol) was used as the sample loading control.

6.2.6 RNA Extraction and Quantitative RT-PCR

Following euthanasia, the left-lateral lobe of the liver and distal ileum (5 cm proximal to the ileocecal junction, flushed with PBS) was collected and frozen immediately in liquid nitrogen. RNA Extraction and Quantitative RT-PCR were done as described in Chapter 2.

6.2.7 ChIP Analysis

Following euthanasia, ileum was collected, flushed with PBS, and frozen immediately in liquid nitrogen. Samples of 4-5 mice were pulverized and pooled. 300 mg from each pool were fixed in PBS with 1% formaldehyde for ten minutes and quenched with glycine for five minutes. Samples were then dounce homogenized in a hypotonic buffer (10 mM HEPES pH 7.9, 1.5 mM MgCl2, 10 mM KCl, 0.2% NP40, 1 mM EDTA, 5% sucrose) and layered over cushion buffer (10 mM Tris HCl pH 7.5, 15 mM NaCl, 60 mM KCl, 1 mM EDTA, 10% sucrose) followed by centrifugation at 200 g to collect the crude nuclear pellet. Subsequent ChIP steps were done using ChIP EZ Kit (Upstate) materials and methods. 3 ug of protein from sonicated chromatin was used for pull down with either rabbit IgG

(Santa Cruz), anti-VDR (Santa Cruz, C-20x), or anti-RXR (Santa Cruz, ΔN-197x). Primers scanning -1500 to +3000 of the *Fgf15* locus were designed and used for analyzing VDR and RXR binding by QPCR as previously described (Bookout, 2003). Primer sequences are listed in Appendix B.

6.2.8 Expression Plasmids

CMX-hFXR, CMX-hVDR, and CMX-hRXRα plasmids expressing full-length nuclear receptors under control of the constitutive CMV promoter have been previously described (Lu, 2000; Makishima, 2002; Makishima, 1999).

6.2.9 *Fgf15* Promoter and Intron 2 Cloning

Total DNA was isolated from mouse colon using the DNeasy Blood & Tissue Kit (Qiagen) and protocol. A 2338 nucleotide region of the *Fgf15* promoter including 6 nucleotides downstream of the transcriptional start site was amplified using the following primers containing restriction endonuclease sites (shown underlined): forward (CCTAAACC<u>AAGCTT</u>CTGGCCATCTG) and reverse (AGAGTTACTGC<u>GTCGAC</u>AGTGG). This product was inserted upstream of the thymidine kinase (Tk) promoter sequence in the Tk-LUC plasmid (Willy, 1995) to generate p2300Fgf15+TATA_TkLUC. This plasmid was used to amplify shorter regions of the *Fgf15* promoter, which were likewise inserted into Tk-LUC. Promoter regions were amplified using distinct forward primers (CTGCGAAAGCTTGCTAAAGGAGAG for p400Fgf15+TATA_TkLUC; CCACCAAGCTTCTGTGCATTGAAC for p230Fgf15+TATA_TkLUC; CCTGTCGACGCATCAAGTCTCC for p100Fgf15+TATA_TkLUC) and a common reverse primer (GGATCCTCTAGAGTCGACAGTGG). p230Fgf15+TATA_TkLUC was amplified using the following overlapping primers containing two altered nucleotides (shown underlined): forward (GGCCTGGGCGGG<u>AC</u>CACTGGGTTGGGG) and reverse

(CCCAACCCAGTGGTCCCGCCCAGGCC). The *Fgf15* promoter region containing the two nucleotide mutation was re-inserted into Tk-LUC to generate p230(mut-145)Fgf15+TATA_TkLUC. A 2460 nucleotide region encompassing the second intron of Fgf15 was amplified using the following primers containing restriction endonuclease sites (shown underlined): forward (GAGCGCGGTCGACAAGATATACG) and reverse (AAGGTACAGTCGACCTCCGAGTAG). The product was inserted in reverse orientation upstream of the thymidine kinase (Tk) promoter sequence in Tk-LUC to generate pFgf15intron2rev_TkLUC. The modified regions of all plasmids were verified by DNA sequencing.

6.2.10 Cotransfection and Luciferase Assay

HEK293 cells were grown at 37°C, 5% CO_2 in 96-well plates in DMEM (containing 4 g/L glucose and L-glutamine, Gibco) supplemented with 10% charcoal-stripped, heat-inactivated fetal bovine serum and transfected by calcium phosphate coprecipitation as previously described (Makishima, 1999). Following 16-hour treatment with GW4064 (GlaxoSmithKline) and vitamin D (1α,25-dihydroxycholecalciferol, Sigma), luciferase and β-galactosidase activities were measured as previously described (Lu, 2000). Luciferase activity was normalized for transfection efficiency using β-galactosidase activity and expressed as relative luciferase units (RLU). For each experiment, all conditions were tested in triplicate and all experiments were repeated 3 times. Data shown is mean ± SD of triplicate assays from one representative experiment.

6.2.11 Statistical Analysis

Data are presented as mean ± SEM and were analyzed by two-tailed, unpaired Student's t-test. P values less than 0.05 were considered significant.

6.3 Results

6.3.1 Bile Acid Metabolism is Dysregulated in *Vdr–/–* Mice

Previous studies from our lab and others have shown that activation of the vitamin D receptor in the intestine by 1α,25-dihydroxyvitamin D3 or lithocholic acid results in the induction of bile acid detoxifying genes such as *CYP3A4* (Makishima, 2002; Jurutka, 2005; Nehring, 2007). The contribution of VDR to bile acid metabolism *in vivo* has not been extensively evaluated. During necropsy I noted that the gallbladder of *Vdr–/–* mice appeared larger than that of their heterozygous and wild-type littermates (Figure 6.1A). I hypothesized that this phenotype was the result of an expansion of the bile acid pool size. Indeed, *Vdr–/–* mice had ~30 percent larger bile acid pool size at three months of age and more than twice the amount of bile acids at 6 months of age as their wild-type littermates (Figure 6.1B). The loss of VDR also increased the hydrophobicity of the bile acid pool due to a greater increase in taurocholic acid relative to tauromuricholic acids (Figure 6.1B).

To determine the mechanism underlying the perturbation of bile acid homeostasis caused by the loss of VDR, I analyzed the expression of genes in the liver known to play a role in bile acid metabolism. In humans and rodents, bile acids are synthesized from cholesterol in the liver via two pathways (Russell, 2003). CYP7A1 catalyzes the first and rate-limiting step in the classic (neutral) pathway of bile acid synthesis, while CYP27A1 catalyzes the first step in the alternative (acidic) pathway. Under normal physiologic conditions the majority of bile acids are produced via the classic pathway. Consistent with an increased rate of bile acid synthesis, I found that *Vdr–/–* mice had 3-fold higher expression of *Cyp7a1* (Figure 6.2A). In addition, the enzyme that catalyzes the final step in the synthesis of cholic acid, *Cyp8b1*, was increased. These changes were accompanied by a 2-fold decrease in *Shp* mRNA and more modest changes in

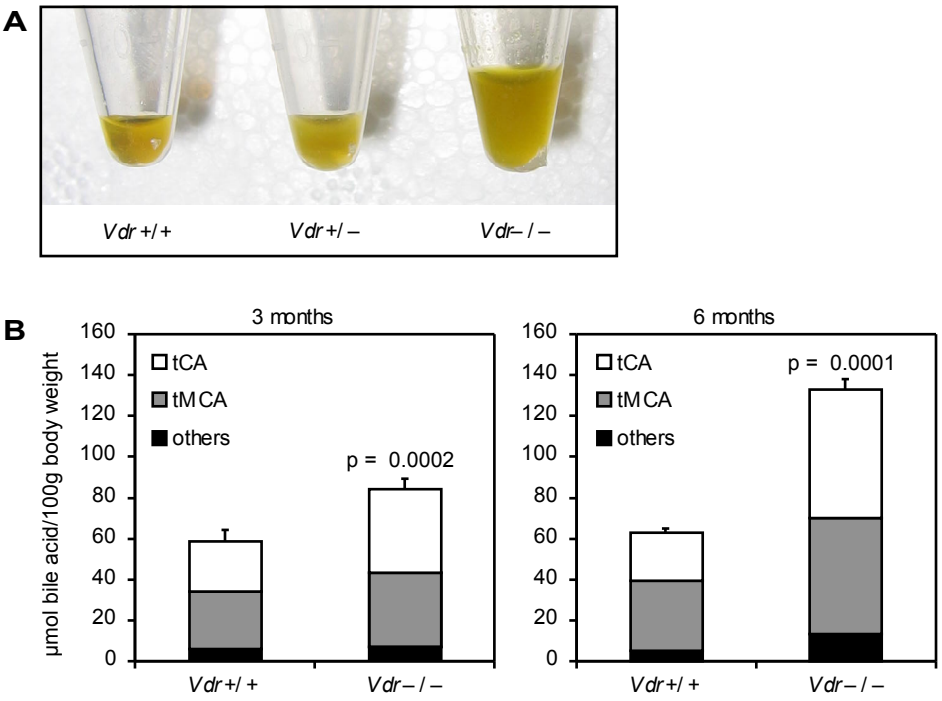

Figure 6.1 Bile acid metabolism is dysregulated in *Vdr–/–* mice.
(A) Total volume of gallbladder bile from a representative 6 month-old male mouse of the indicated genotype. **(B)** Total bile acids were extracted from gallbladder, liver, intestine, and portal blood and quantitated by LC/MS. Results shown are bile acid pool size and composition in 3 month-old (n = 7) and 6 month-old (n = 4) male mice of the indicated genotype. Taurocholate (tCA) and tauromuricholates (tMCA, includes α-,β- and ω-muricholate) comprise the majority of bile acids in the mouse. See methods for a complete list of bile acids grouped as "others". Data represent the mean ± SEM.

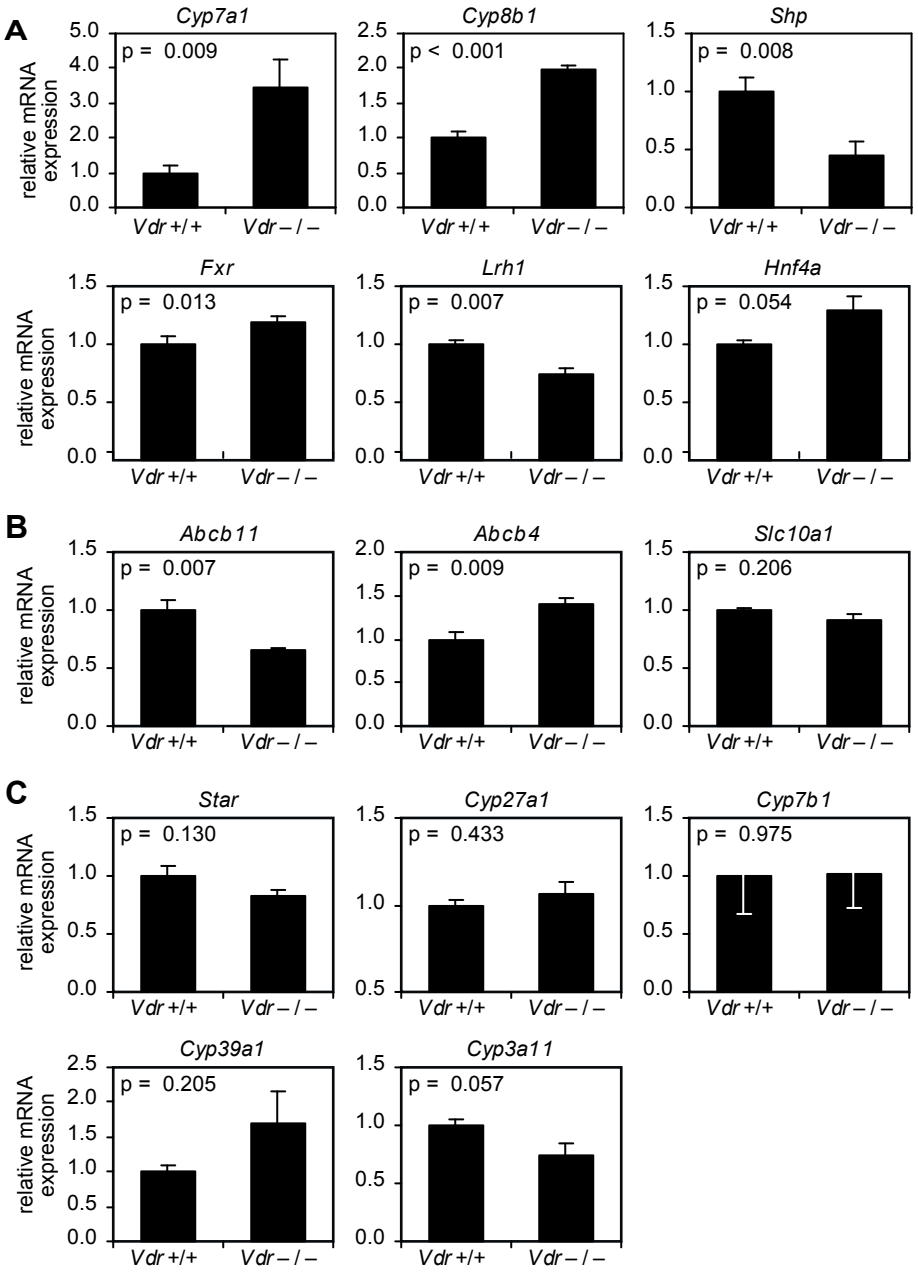

Figure 6.2 Gene expression is altered in the liver of *Vdr–/–* mice.
Hepatic mRNA expression of bile acid synthesis enzymes and nuclear receptors that regulate *Cyp7a1* transcription **(A)**, bile acid transporters **(B)**, and genes involved in the alternative bile acid synthesis pathway **(C)**. *Vdr* expression in the liver was undetectable in either genotype (data not shown). The level of mRNA expression was normalized to *U36b4* and graphed relative to wild-type control. Data represent the mean ± SEM of 7 animals per group.

Fxr, *Hnf4α*, and *Lrh-1* expression. Expression analysis of the major bile acid transporters revealed decreased expression of the canalicular bile acid export pump, *Abcb11*, a small increase in the phospholipid exporter, Abcb4, and no change in the expression of the sinusoidal sodium taurocholate import pump, *Slc10a1* (Figure 6.2B). In contrast to enzymes of the classic bile acid synthesis pathway, no change was seen in expression of genes encoding enzymes of the alternative bile acid synthesis pathway (Figure 6.2C). These alterations in gene expression in livers of *Vdr–/–* mice were somewhat surprising given that VDR is not expressed in hepatocytes, and suggested that the changes were either secondary to alterations in the bile acid pool size and composition or were caused by perturbation of vitamin D signaling outside the hepatocyte.

I next examined gene expression in the terminal small intestine (ileum), which is the major site of bile acid reabsorption and thus plays an integral role in maintaining bile acid homeostasis. Here, bile acid activation of FXR induces expression of bile acid transporters and *Fgf15* (Dawson, 2009; Inagaki, 2005). As previously described, FGF15 is essential for FXR-mediated feedback repression of *Cyp7a1* and bile acid synthesis. Surprisingly, despite normal levels of FXR and bile acid transporters, the expression of *Fgf15* was decreased markedly in *Vdr–/–* mice (Figure 6.3).

6.3.2 Vitamin D Induces FGF15 to Suppress *Cyp7a1*

Since VDR is expressed in enterocytes and *Fgf15* expression was lower in *Vdr–/–* mice, I hypothesized that VDR might regulate *Fgf15* at the transcriptional level. Indeed, treatment of wild-type but not *Vdr–/–* mice with 1α,25-dihydroxyvitamin D3 (hereafter referred to as vitamin D) for four hours increased *Fgf15* expression in intestine and decreased *Cyp7a1* in liver (Figure 6.4A). Intestinal bile acid transporters were also decreased, while the gene encoding the ileal bile acid binding protein (*Ibabp*, an FXR target gene also known as *Fabp-6*)

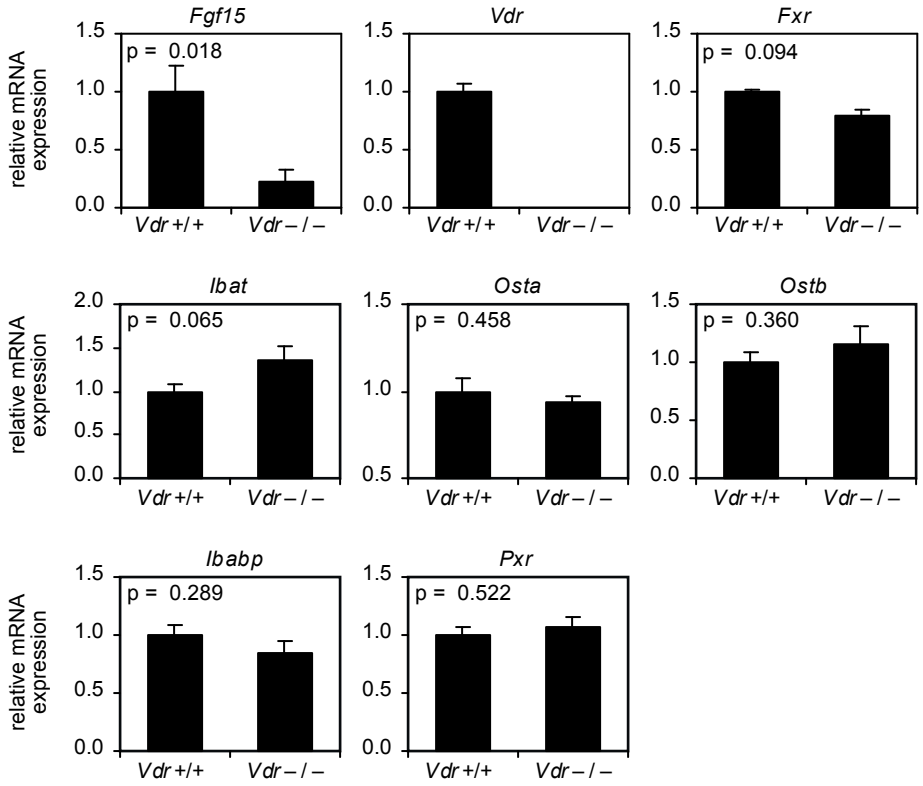

Figure 6.3 Gene expression is altered in the ileum of *Vdr–/–* mice.
Intestinal mRNA expression of select nuclear receptors and genes involved in bile acid homeostasis. The level of mRNA expression was normalized to *U36b4* and graphed relative to wild-type control. Data represent the mean ± SEM of 7 animals per group.

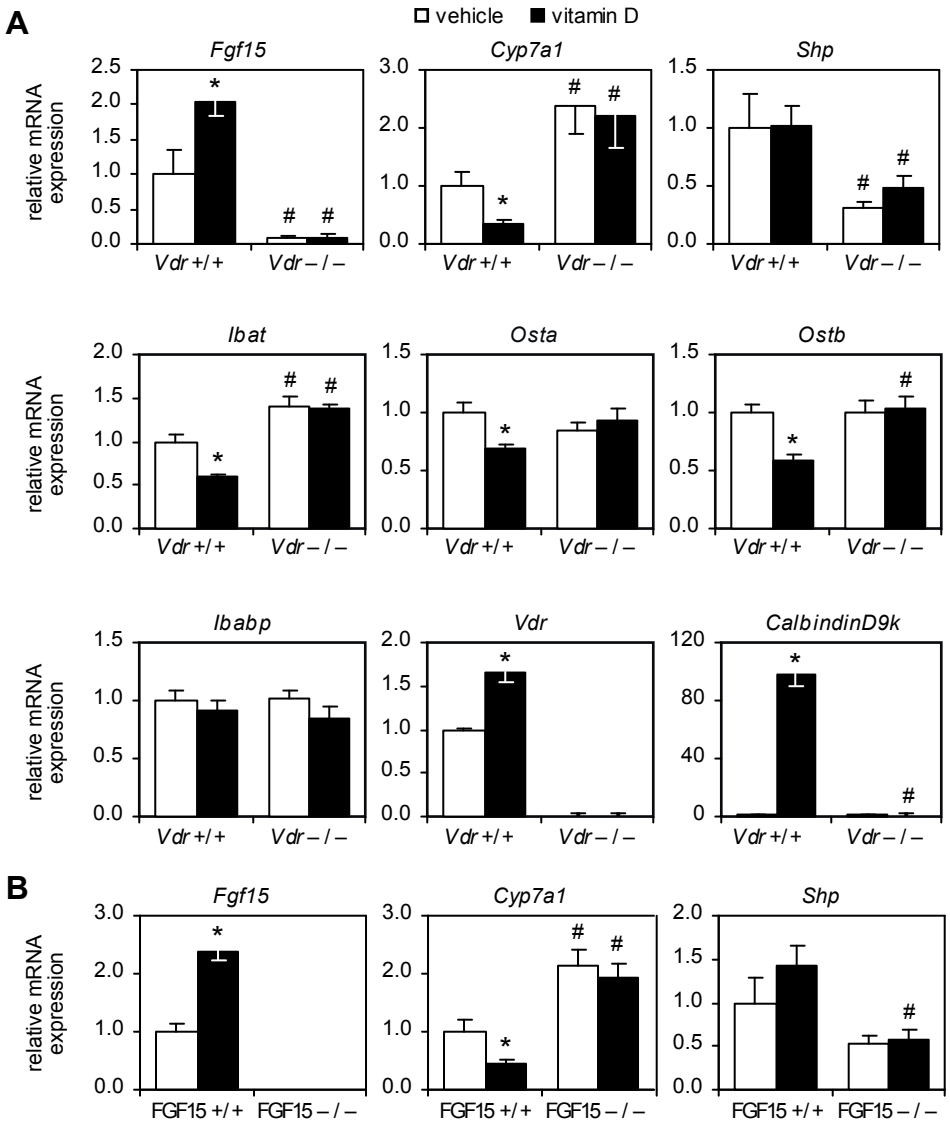

Figure 6.4 VDR induces *Fgf15* to suppress *Cyp7a1*.
Mice of the indicated genotype were treated for four hours by intraperitoneal injection with 75 μg/kg 1α,25-dihydroxyvitamin D3 **(A)**, or 50 μg/kg 1α,25-dihydroxyvitamin D3 **(B)**. mRNA expression in the liver (*Cyp7a1* and *Shp*) and ileum (all other genes) was determined by quantitative RT-PCR, normalized to *U36b4*, and graphed relative to wild-type, vehicle-treated control. Data represent the mean ± SEM of 5-6 animals per group. * $p < 0.05$ compared to vehicle of the same genotype. # $p < 0.05$ compared to wild-type of the same treatment group.

was not changed. Importantly, the repression of *Cyp7a1* by vitamin D was absent in *Fgf15* null mice (*Fgf15–/–*), demonstrating that FGF15 is required for vitamin D-dependent suppression of *Cyp7a1* (Figure 6.4B).

To determine whether physiologic levels of vitamin D contribute to the regulation of *Fgf15*, I compared the induction of *Fgf15* to that *CalbindinD9k* (a known VDR target gene) in ileum explants. Notably, both genes were induced by vitamin D in a comparable, dose-dependent manner (Figure 6.5). Taken together with the finding that VDR is required for normal expression of *Fgf15*, these data provide evidence that the transcriptional regulation of *Fgf15* by vitamin D is physiologically relevant.

Previous work has shown that FXR directly regulates *Fgf15* expression by binding to an FXR/RXR response element in the second intron of the gene (Inagaki, 2005). Given the rapid effect of vitamin D treatment on *Fgf15* expression it seemed likely that the regulation of *Fgf15* by VDR was also direct. ChIP analysis was performed to identify VDR/RXR binding sites in the regulatory regions of *Fgf15*. As expected, a strong RXR binding site was detected in the second intron, and an additional binding site was found in the proximal promoter near the transcriptional start site (Figure 6.6A). VDR binding was also detected at both sites. Interestingly, analysis of the *Fgf15* regulatory regions by reporter-gene assay showed that VDR transactivation occurred exclusively through the proximal promoter site while FXR transactivation occurred exclusively at the second intron (Figure 6.6B). Promoter truncations localized the vitamin D-responsive *cis*-acting element to a region between 100 and 200 nucleotides upstream of the transcriptional start site. Analysis of this region revealed a DR3 site with similarity to known VDR response elements (VDREs), and transactivation of the *Fgf15* promoter by VDR was eliminated by mutating two nucleotides within this site (Figure 6.6B). These results

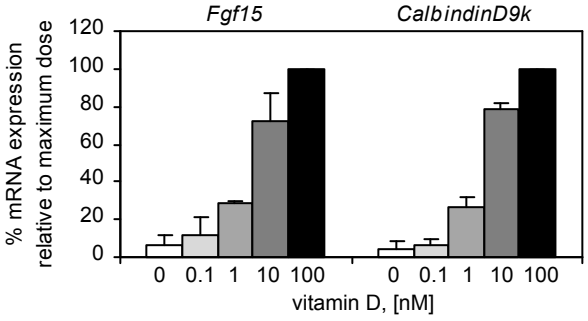

Figure 6.5
Induction in Explants.
Ileum explants were treated for 6 hours with the indicated concentration of 1α,25-dihydroxyvitamin D3. The level of mRNA expression was normalized to *U36b4* and graphed relative to the highest treatment dose. Data represent the mean ± SD of two independent experiments.

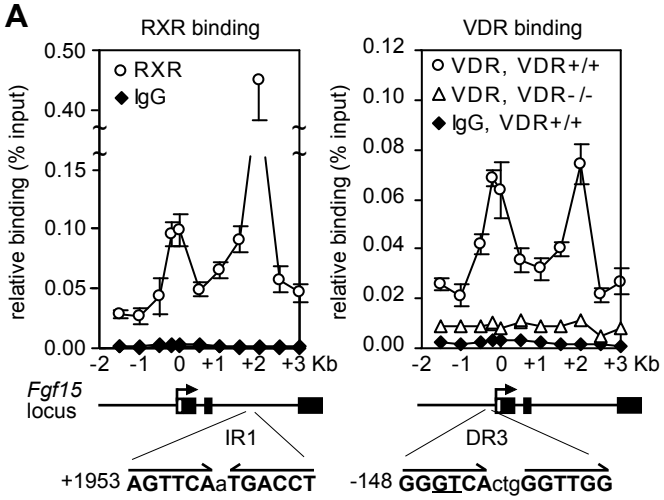

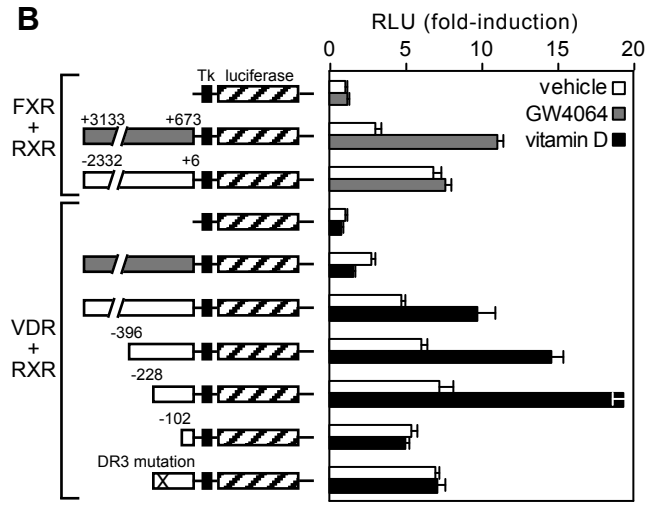

Figure 6.6
Promoter Regulation.
(A) Pooled ileum from 3-4 *Vdr*+/+ and *Vdr*–/– mice treated for 2 hours with 50 µg/kg 1a,25-dihydroxyvitamin D3 was analysed by ChIP using specific antibodies for VDR and RXR and an isotype-matched IgG control antibody. Bound DNA was quantitated by QPCR and normalized to input. Data represent the mean ± SEM of 4 independent experiments. The location and sequence of the IR1 FXR/RXR response element (FXRE) and putative DR3 VDR/RXR response element (VDRE) are shown below the graph. Nucleotides mutated in the promoter analysis shown in F are underlined.
(B) *Fgf15* promoter (-2332 to +6) and intron 2 (+673 to +3133) were cloned upstream of the thymidine kinase promoter (Tk) and luciferase gene as shown. HEK293 cells were cotransfected with the indicated reporter constructs, βgal, hRXR, and either hFXR or hVDR. Following treatment with 1 µM GW4064 (FXR agonist), 100 nM 1α,25-dihydroxyvitamin D3, or vehicle, luciferase activity was quantitated and normalized to βgal activity. Data are graphed relative to the first data point and represent mean ± SD of 3 replicates. X indicates mutated DR3 site.

demonstrate that VDR binds directly to the *Fgf15* promoter and regulates *Fgf15* expression through a direct transcriptional mechanism.

Given that both VDR and FXR induce *Fgf15*, I reasoned that VDR could substitute for FXR in mediating repression of bile acid synthesis in *Fxr–/–* mice. While the fold induction of *Fgf15* by vitamin D was similar in wild-type and *Fxr–/–* mice, the absolute levels of *Fgf15* in vitamin D treated *Fxr–/–* mice remained below those in vehicle-treated wild-type mice (Figure 6.7A). Notably, the repression of *Cyp7a1* by vitamin D was absent in *Fxr–/–* mice. Additional experiments in food-entrained animals showed that wild-type mice fasted more than 20 hours also did not repress *Cyp7a1* upon vitamin D treatment despite significant induction of *Fgf15* (Figure 6.7B). These findings indicate that vitamin D-dependent induction of *Fgf15* is not by itself sufficient to cause repression of *Cyp7a1*. Of note, FXR-mediated repression of bile acid synthesis has been shown to require FXR activation in both liver and intestine, suggesting that repression of *Cyp7a1* requires appropriate hepatic and intestinal signals as would occur during normal enterohepatic circulation of bile acids (Kim, 2007a). These data indicate that transcriptional regulation of *Fgf15* by VDR is not dependent on FXR; however, FXR is required for the induction of *Fgf15* to levels that suppress *Cyp7a1*.

The ability of a potent FXR agonist, INT-747 (6-ethyl-CDCA), to correct increased bile acid synthesis in *Vdr–/–* mice was also tested. Despite increases in *Fgf15* levels induced by INT-747, the absolute levels of *Fgf15* remained lower in *Vdr–/–* mice (Figure 6.7C). Furthermore, 12-day treatment with INT-747 reduced bile acids levels in both wild-type and *Vdr–/–* mice; however, bile acid levels remained higher in INT-747 treated *Vdr–/–* mice than in vehicle-treated wild-type mice (Figure 6.7D). These data indicate that maximum activation of FXR is not

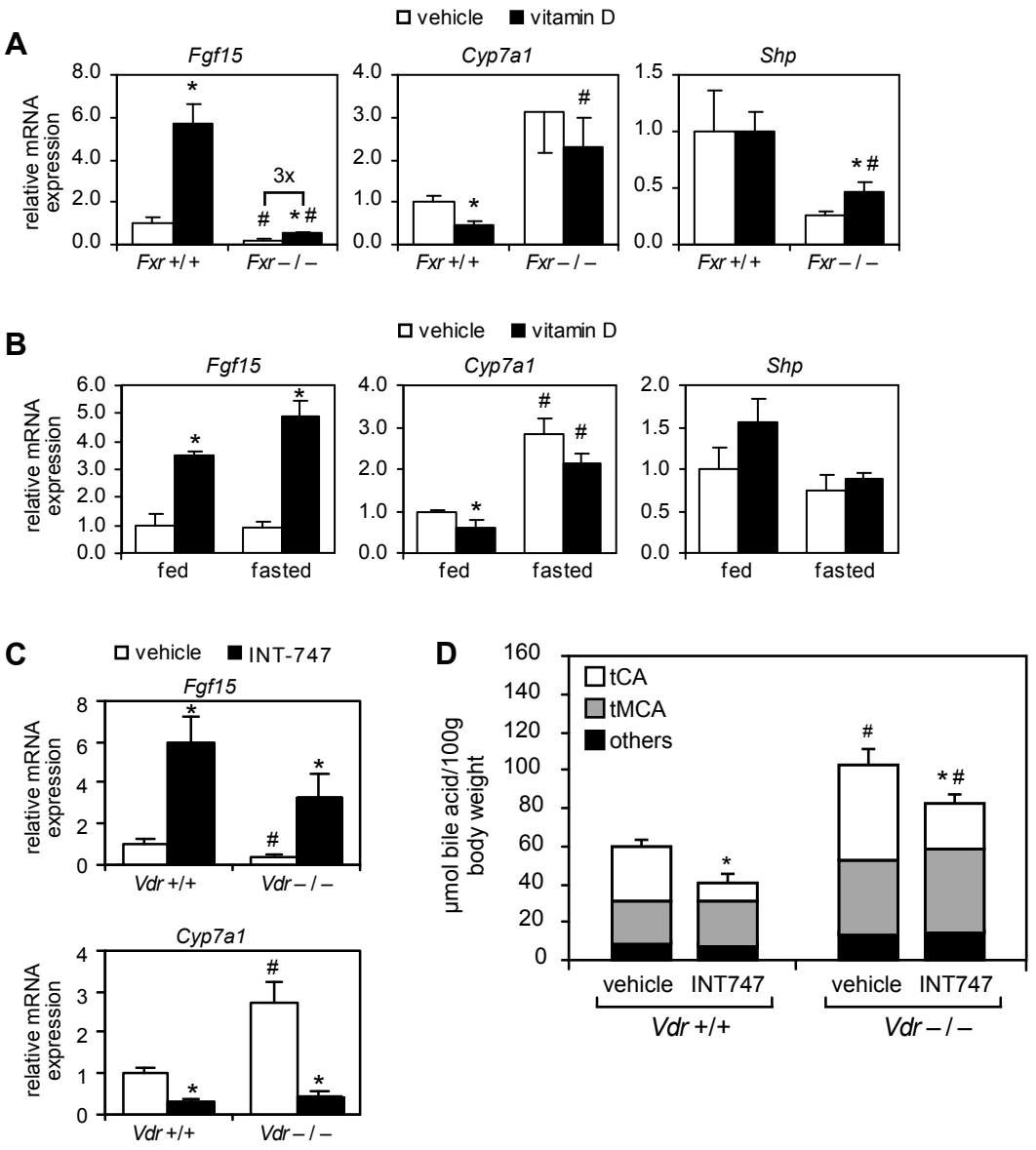

Figure 6.7 Both VDR and FXR are required to maintain bile acid homeostasis. Mice of the indicated genotype were treated for 4 hours by intraperitoneal injection with 50 µg/kg 1α,25-dihydroxyvitamin D3 **(A and B)**, or 16 and 4 hours 10mg/kg INT-747 by oral gavage **(C)**. Animals in B were food entrained for 10 days and sacrificed 8 hours (fed state) or 20 hours (fasted state) after a 4 hour meal. mRNA expression in the ileum (*Fgf15*) and liver (*Cyp7a1* and *Shp*) was determined by quantitative RT-PCR, normalized to *U36b4*, and graphed relative to wild-type, vehicle-treated control. **(D)** Bile acid pool size in mice of the indicated genotype treated for 12 days with vehicle or 10mg/kg/day INT-747 by oral gavage. For all panels data represent the mean ± SEM of 3-6 animals per group. * $p < 0.05$ compared to vehicle of the same genotype. # $p < 0.05$ compared to wild-type of the same treatment group.

sufficient to overcome deficiencies in bile acid homeostasis caused by the loss of VDR.

6.3.3 Vitamin A Induces FGF15 and SHP to Suppress *Cyp7a1*

Given the effects of vitamin D on *Fgf15* and *Cyp7a1* regulation, I sought to determine whether other lipid-soluble vitamins also caused repression of bile acid synthesis. While d-α-tocopherol (i.e., vitamin E) had no effect on *Cyp7a1* or any other genes analyzed, retinyl palmitate (i.e., vitamin A) dramatically increased *Fgf15* expression in intestine and suppressed *Cyp7a1* in liver (Figure 6.8A). Furthermore, vitamin A increased expression of *Shp* in liver.

In vivo, vitamin A may be metabolized to all-trans retinoic acid, which activates RAR, and 9-*cis* retinoic acid, which activates both RAR and RXR. To determine which nuclear receptor was mediating the transcriptional effects of vitamin A on *Fgf15*, *Cyp7a1*, and *Shp*, I analyzed hepatic and intestinal gene expression in wild-type mice treated with the synthetic ligands TTNPB (selective for RAR) and LG268 (selective for RXR). Both RAR and RXR induced *Shp* and suppressed *Cyp7a1*; however, *Fgf15* was only induced by RXR (Figure 6.8B). Since the VDR/RXR heterodimer is not activated by RXR ligands (Shulman, 2004), Davo suggested that the induction of *Fgf15* by RXR ligand might occur through activation of the FXR/RXR heterodimer. To test this idea, I treated *Fxr–/–* mice with vitamin A and found that in the absence of FXR vitamin A had no effect on *Fgf15* expression (Figure 6.9A). Taken together, these data suggest that *Fgf15* was induced by vitamin A through the RXR partner of the FXR/RXR heterodimer complex.

Interestingly, despite the absence of *Fgf15* induction, vitamin A still efficiently repressed *Cyp7a1* in *Fxr–/–* mice, indicating that additional vitamin A-dependent mechanisms exist to suppress *Cyp7a1* (Figure 6.9A). Further analysis of hepatic gene expression demonstrated that despite lower basal levels of *Shp* in

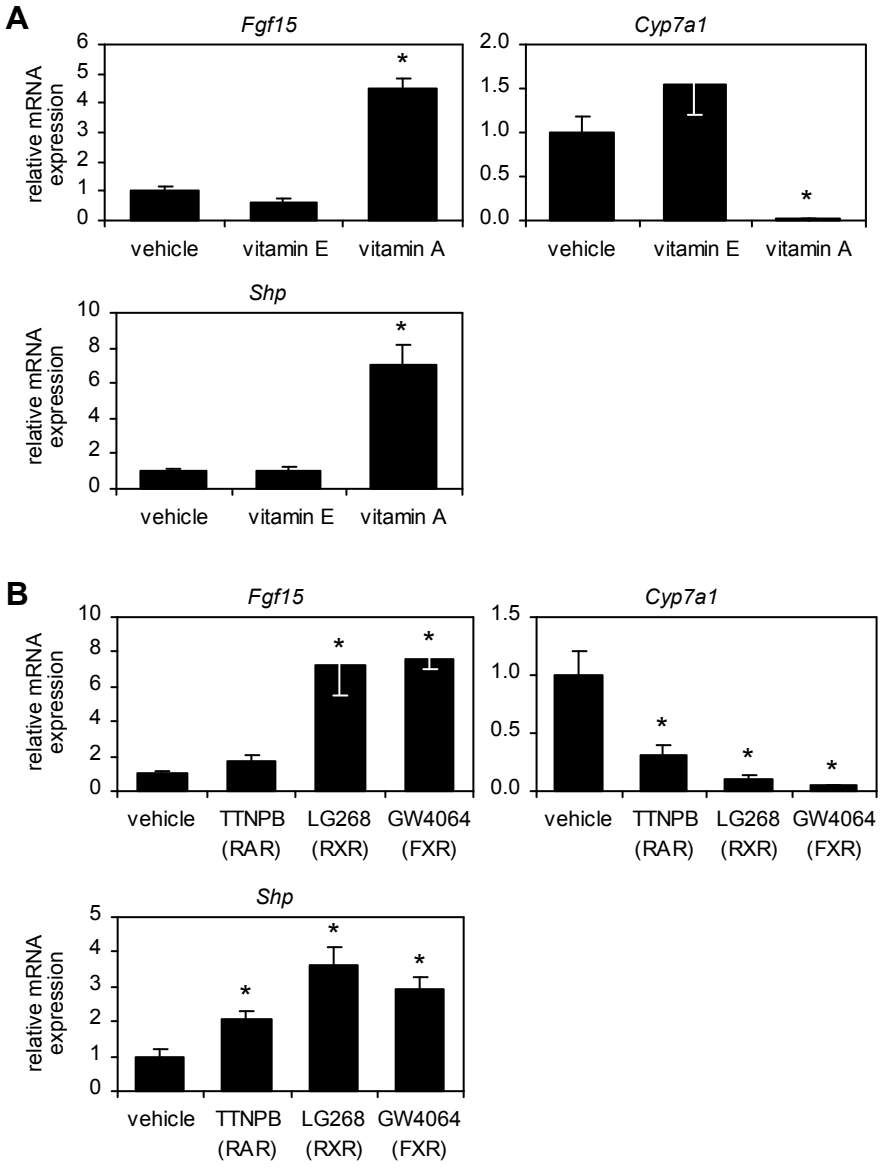

Figure 6.8 Vitamin A induces FGF15 and SHP to suppress *Cyp7a1*.
(A) Wild-type mice were treated for 16 hours by oral gavage with 500 mg/kg d-α-tocopherol (vitamin E) or 100 mg/kg retinyl palmitate (vitamin A). **(B)** Wild-type mice were treated for one day with diets containing the indicated synthetic ligands. Target nuclear receptor is shown in parentheses. mRNA expression in the ileum (*Fgf15*) and liver (*Cyp7a1* and *Shp*) was determined by quantitative RT-PCR, normalized to *U36b4*, and graphed relative to vehicle-treated control. Data represent the mean ± SEM of 5 animals per group. * $p < 0.05$ compared to vehicle of the same genotype.

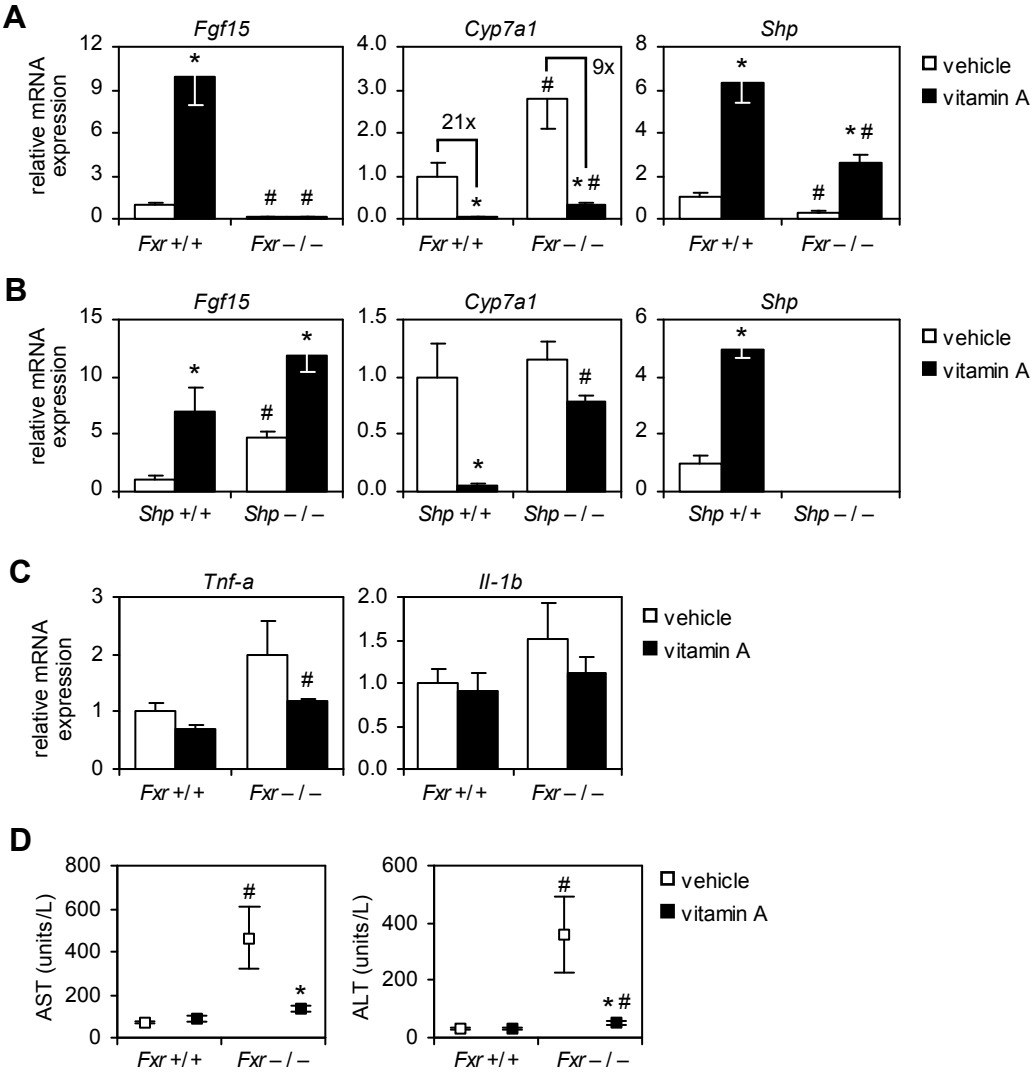

Figure 6.9 FXR and SHP are required for *Cyp7a1* suppression by vitamin A.
(A-C) Mice of the indicated genotype were treated for 16 hours by oral gavage with 100 mg/kg retinyl palmitate (vitamin A). mRNA expression in the ileum (*Fgf15*) and liver (*Cyp7a1*, *Shp*, *TNF*α, and *Il-1*β) was determined by quantitative RT-PCR, normalized to *U36b4*, and plotted relative to wild-type, vehicle-treated control. **(D)** AST and ALT levels were measured in plasma samples from the experiment shown in C. For all panels, data represent the mean ± SEM of 5 animals per group. * $p < 0.05$ compared to vehicle of the same genotype. # $p < 0.05$ compared to wild-type of the same treatment group.

Fxr–/– mice, FXR was not required for induction of *Shp* by vitamin A, suggesting that *Shp* induction contributed to *Cyp7a1* repression by vitamin A. In support of this idea, I found that repression of *Cyp7a1* by vitamin A was greatly reduced in the absence of SHP (Figure 6.9B).

Bile acids have been shown to suppress *CYP7A1* in cells through FXR-independent mechanisms involving induction of proinflammatory cytokines, TNF-α and IL-1β, and activation of JNK signaling (Miyake 2000, Gupta 2001, Li 2006). To determine whether this pathway contributes to the suppression of *Cyp7a1* by vitamin A, I measured hepatic cytokine expression and the level of liver enzymes (aminotransferases) in blood. No increase was seen in the expression of proinflammatory cytokines in the liver (Figure 6.9C). In addition, vitamin A did not affect aminotransferase levels in wild-type mice (Figure 6.9D). Interestingly, however, significantly lower AST and ALT levels were seen in vitamin A treated *Fxr–/–* mice compared to vehicle-treated littermates.

Taken together, these results demonstrate that vitamin A represses *Cyp7a1* through both FXR-dependent and FXR-independent mechanisms. In the intestine vitamin A metabolites appear to activate the FXR/RXR heterodimer to induce *Fgf15* expression, while in liver vitamin A metabolites induce *Shp* expression through a mechanism that may involve transcriptional regulation of *Shp* by RAR. Both events appear to be required for vitamin A-dependent *Cyp7a1* repression.

6.3.4 Vitamin A Rescues *Fgf15* and *Shp* Expression and Suppresses *Cyp7a1* When Bile Acid Feedback is Impaired

The finding that vitamin A could repress *Cyp7a1* expression by inducing bile acid feedback regulatory genes in both liver and intestine suggested that vitamin A analogs might be useful therapeutically in pathologic conditions in which feedback repression of bile acid synthesis is interrupted. One such condition is bile acid malabsorption, which is characterized by decreased

intestinal bile acid reabsorption, resulting in low FGF19 levels (human ortholog of FGF15) and excessive bile acid synthesis by the liver (Hofmann *et al.*, 2009). The effects of bile acid malabsorption on expression of bile acid feedback regulatory genes can be mimicked by administering the bile acid binding resin, cholestyramine. As expected, cholestyramine treatment of wild-type mice dramatically decreased *Fgf15* and *Shp* expression and increased *Cyp7a1* (Figure 6.10). Amazingly, vitamin A completely rescued *Fgf15* and *Shp* expression and reversed the de-repression of *Cyp7a1* caused by interrupted bile acid reabsorption in cholestyramine-treated animals. Consistent with my previous results, in the absence of bile acids vitamin D modestly induced *Fgf15* but did not change *Shp* or *Cyp7a1* expression. These data highlight the potential of vitamin A analogs to correct disrupted feedback repression of bile acid biosynthesis.

6.4 Discussion

Owing to their unique physicochemical properties, bile acids are essential structural components of lipid micelles (Hofmann, 1999a). In this capacity, bile acids promote the intestinal absorption of lipids and lipid-soluble vitamins. The studies described in this chapter have revealed an unexpected link between lipid-soluble vitamins and bile acid biosynthesis. Surprisingly, vitamin A and D exerted negative feedback on bile acid synthesis *in vivo* by decreasing *Cyp7a1* expression. FGF15 and SHP play a central role in the feedback regulation of bile acid synthesis by bile acids and FXR (Chiang, 2009). Based on the results of the current studies, I conclude that FGF15 is integral to the mechanism of *Cyp7a1* regulation by vitamin D and both FGF15 and SHP are important for the regulation of bile acid synthesis by vitamin A.

I found that VDR transcriptionally regulated *Fgf15* in the intestine and that this pathway was essential for the repression of bile acid synthesis by

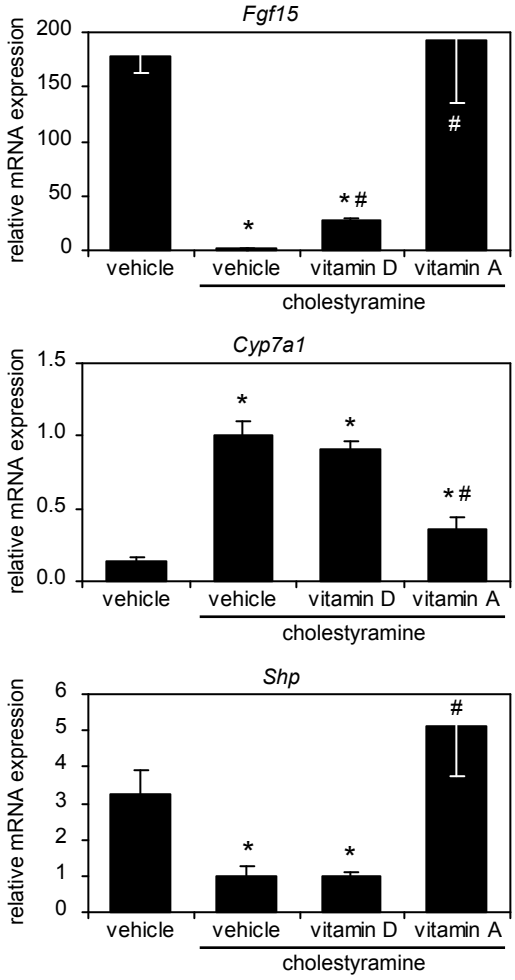

Figure 6.10 Vitamin A rescues *Fgf15* and *Shp* expression and suppresses *Cyp7a1* when bile acid feedback is impaired.
Wild-type mice were treated treated for two days with a 2% (w/w) cholestyramine diet and either 50 µg/kg 1α,25-dihydroxyvitamin D3 (vitamin D) or 100 mg/kg retinyl palmitate (vitamin A). Vitamin D and A treatments were administered as described in previous figures. The control group received standard chow and the appropriate vehicle treatments. mRNA expression in the ileum (*Fgf15*) and liver (*Cyp7a1* and *Shp*) was determined by quantitative RT-PCR, normalized to *U36b4*, and plotted relative to vehicle-treated control. Data represent the mean ± SEM of 3 animals per group. * $p < 0.05$ compared to control. # $p < 0.05$ for vitamin treatment compared to cholestyramine alone.

vitamin D. Surprisingly, VDR was required to maintain normal *Fgf15* expression and bile acids levels *in vivo*. Together, these results demonstrate that vitamin D and its receptor contribute to the feedback regulation of bile acid synthesis by controlling expression of the endocrine hormone FGF15.

Interestingly, *Cyp7a1* repression by vitamin D required an intact FXR signaling pathway, indicating that VDR activation alone is not sufficient to suppress bile acid synthesis. There are at least two possible explanations for this finding. First, activation of both VDR and FXR may be required to induce *Fgf15* to the level required for *Cyp7a1* suppression. Second, as has recently been shown for FXR (Kim, 2007a), feedback repression of bile acid synthesis may require corresponding signals in the intestine and liver, the latter of which does not occur upon activation of VDR alone. The fact that a potent FXR ligand did not normalize *Fgf15* levels nor correct the defect in bile acid synthesis in *Vdr–/–* mice strongly suggests that both FXR and VDR are required for maintaining normal levels of *Fgf15*, and consequently normal bile acid levels. From a mechanistic standpoint, it will be interesting to determine whether the two *cis*-regulatory elements bound by VDR and FXR cooperate to facilitate *Fgf15* transcription. Additional ChIP studies would be useful to investigate changes in chromatin structure at the *Fgf15* locus in wild-type, *Fxr–/–*, and *Vdr–/–* mice.

Vitamin A repressed *Cyp7a1* through both FXR-dependent and FXR-independent mechanisms. Ligands for RXR, but not RAR, induced *Fgf15*, and FXR was required for the induction of *Fgf15* by vitamin A. These results indicate that induction of *Fgf15* expression by vitamin A occurred through RXR as the obligate heterodimeric partner of the FXR/RXR complex. This finding provides evidence that RXR functions as a vitamin A receptor *in vivo*, and demonstrates that the FXR/RXR heterodimer can serve as a sensor for dietary vitamin A. In contrast to its effects on *Fgf15* expression, vitamin A-dependent induction of *Shp*

expression did not require FXR. Interestingly, I found that the RAR ligand, TTNPB induced *Shp* and suppressed *Cyp7a1*, suggesting that *Shp* induction by RAR may be an FXR-independent mechanism whereby vitamin A suppresses *Cyp7a1*. Taken together, these results point to two distinct nuclear receptor-mediated mechanisms by which vitamin A regulates bile acid synthesis.

Fxr–/– mice have increased expression of inflammatory genes and present with liver tumors at 12-15 months of age (my own observation and Yang, 2007). Liver damage, inflammation, and increased proliferation precede tumor formation. Importantly, tumor number is reduced by cholestyramine treatment, indicating that elevated bile acid levels contribute to the mechanism of hepatocarcinogenesis in *Fxr–/–* mice (Yang, 2007). The surprising result that vitamin A normalized liver enzymes in *Fxr–/–* mice implies that hepatocyte damage caused by the loss of FXR can be acutely ameliorated. Vitamin A is known to decrease expression of TNFα as well as other inflammatory cytokines in macrophages (Moro, 2008; Pino-Lagos, 2008). It is plausible that both reduced bile acid levels and decreased inflammatory cytokines contributed to the improved liver health in *Fxr–/–* mice following vitamin A treatment. Future studies will need to address how the protective effects of vitamin A in the liver of *Fxr–/–* mice are related to its bile acid-lowering and anti-inflammatory properties.

Under normal physiologic conditions bile acids are efficiently reabsorbed in the ileum (Hofmann, 1999a). Bile acid malabsorption is a pathologic condition often seen in patients with Crohn's disease or ileal resection and is characterized by reduced ileal bile acid reabsorption and delivery of large quantities of bile acids to the colon (Hofmann *et al.*, 2009). Increased luminal concentrations of bile acids in the colon induce fluid secretion, resulting in cholorrheic enteropathy and the characteristic symptom of watery diarrhea. Bile acid sequestrants are currently the primary therapy and provide symptomatic relief but do not correct

bile acid overproduction and hypersecretion by the liver. The exciting finding that vitamin A induces *Fgf15* and suppresses bile acid synthesis under conditions of interrupted bile acid reabsorption suggests that vitamin A analogs may provide therapeutic benefit to patients with bile acid malabsorption and increased hepatic bile acid synthesis. Interestingly, a subset of patients with bile acid malabsorption has increased hepatic bile acid synthesis despite normal ileal bile acid transport. This condition, termed idiopathic bile acid malabsorption, has recently been shown to be associated with decreased plasma levels of FGF19 (Walters, 2009). It is not known why FGF19 levels are abnormally low in these patients. Based on the findings of the current study, I believe that vitamin A and D may be useful tools to examine the underlying cause of low FGF19 in these patients.

Elevated levels of bile acid in the colon may promote colon cancer while vitamin D is associated with reduced risk of colon cancer (Nagengast, 1995; Kallay, 2001; Lamprecht, 2003; Cross, 2005; Garland, 2009; Yin, 2009). Former members of the Mango Lab have shown that VDR is activated by lithocholic acid and induces enzymes that detoxify bile acids in the colon (Makishima, 2002; Ishizawa, 2008; Matsubara, 2008). My studies suggest that vitamin D-dependent regulation of bile acid synthesis may be an additional mechanism by which vitamin D protects against the tumor promoting effects of toxic bile acids (Figure 6.11).

With regard to the mechanism underlying the hormonal effects of vitamin D, an interesting parallel emerges between the regulation of bile acid synthesis by FGF15 and the role of FGF23 in renal phosphate metabolism. Previous studies have shown that vitamin D induces *Fgf23* in bone, and that FGF23 signals in a bone-kidney axis to control phosphate absorption and vitamin D metabolism in the kidney (Shimada, 2004; Fukagawa, 2005; Kolek, 2005; Saito, 2005; Barthel, 2007; Liu, 2007). In this study I show that vitamin D induces *Fgf15* in intestine,

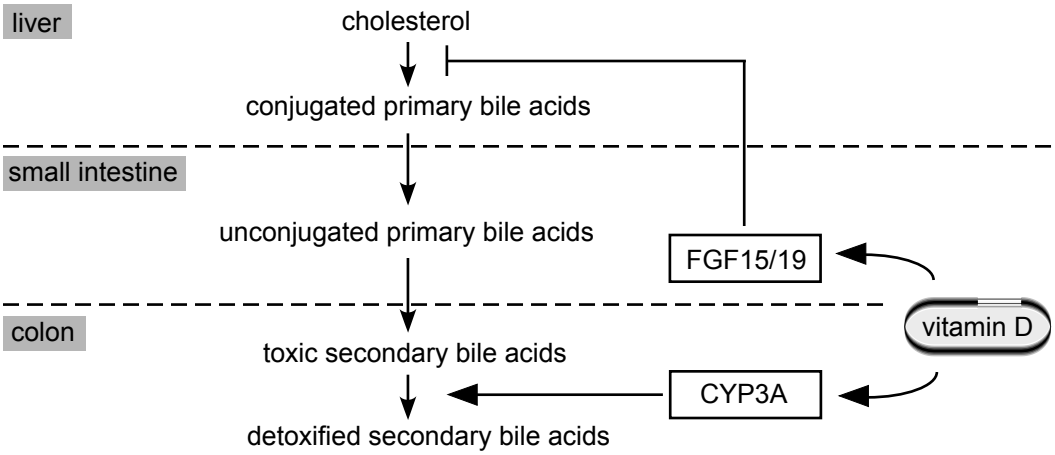

Figure 6.11 Role of vitamin D in bile acid metabolism.
Summary of known mechanisms by which vitamin D might decrease the toxic effects of bile acids. See text for details.

which signals in an intestine-liver axis to regulate bile acid synthesis in the liver. Thus, a paradigm emerges in which endocrine FGFs function as downstream messengers to mediate the homeostatic effects of vitamin D and coordinate vitamin D signaling between organ systems (Figure 6.12).

On a final note, while hepatocytes are the site of bile acid synthesis and are the most numerous cell type in the liver, other cells in the liver clearly play an important role in inflammation and the metabolism of lipid-soluble vitamins. Stellate cells are the major site of vitamin A storage and may affect bile acid synthesis through paracrine signaling to hepatocytes (Song, 2007). Kupffer cells play a central role in inflammation and the hepatic response to liver damage. Both stellate and Kupffer cells also reportedly express VDR (Gascon-Barre, 2003). Thus, paracrine signals might also contribute to VDR-dependent regulation of bile acid synthesis. Future research should address the contribution of non-parenchymal hepatic cells to the effects of vitamin A and D on bile acid homeostasis.

In summary, the findings of this study highlight the importance of nuclear receptors in the regulation of bile acid metabolism and provide mechanistic insight into the elegant signaling pathways involving FGF15 and SHP that govern feedback repression of bile acid biosynthesis. Since bile acids promote absorption of lipid-soluble vitamins, it is tempting to speculate that the mechanisms allowing vitamin A and D to control feedback repression of bile acid synthesis evolved to protect the organism from exposure to potentially toxic levels of lipid-soluble vitamins in the diet or to allow increased absorption of lipid-soluble vitamins from a vitamin deficient environment (Figure 6.13). I propose that multiple dietary factors, functioning through their cognate sensors, regulate the basic molecular mechanisms that control bile acid synthesis. In this system, each sensor would be capable of adjusting bile acid synthesis to maintain levels that are

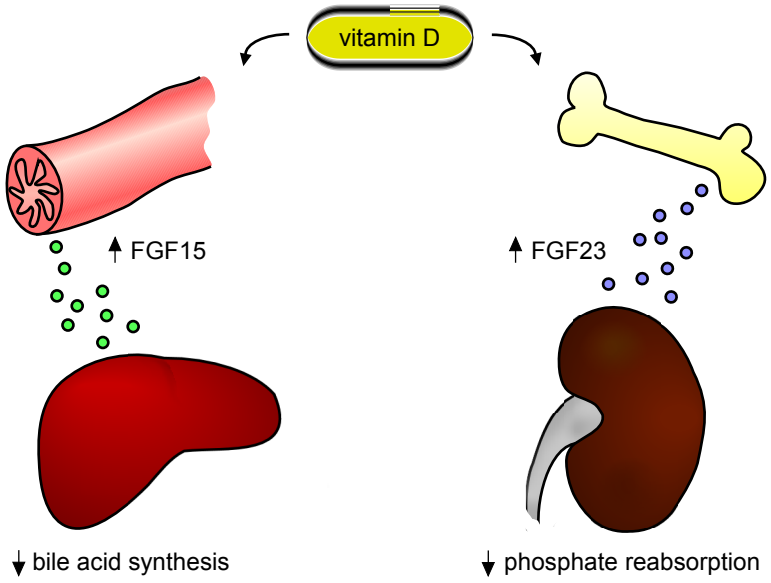

Figure 6.12 Endocrine FGFs as second messengers in the vitamin D signaling cascade.
Model depicting vitamin D-stimulated production of FGF15 in intestine and FGF23 in bone. These endocrine FGFs function as second messengers to mediate the homeostatic effects of vitamin D in the liver and kidney respectively.

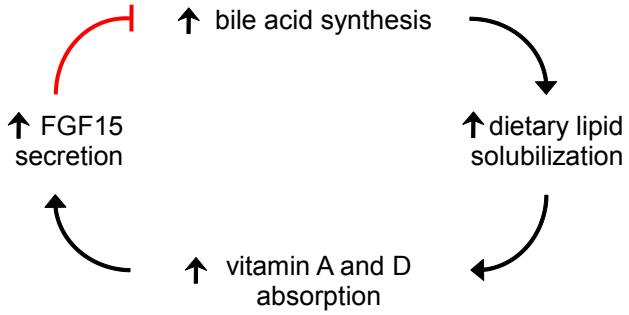

Figure 6.13 Vitamin feedback repression loop.
Proposed model of vitamin A and D induced feedback repression of bile acid synthesis via FGF15.

appropriate for existing dietary conditions. Under normal dietary conditions, multiples sensors fine tune the level of bile acid synthesis, while under conditions of maximal activation, a single sensor has the ability to dramatically affect bile acid synthesis (Figure 6.14).

6.5 Acknowledgements

Analysis of the *Fgf15* promoter by ChIP, and design of ChIP primers was done by Sam Holmstrom. Tissues from animals treated with RAR and RXR ligands were obtained from an experiment designed and organized by Klementina FonTacer and Angie Bookout. Unpublished results from the latter study were the first to show decreased expression of *Cyp7a1* in response to vitamin D treatment. I am grateful to Klementina and Angie for making this data available.

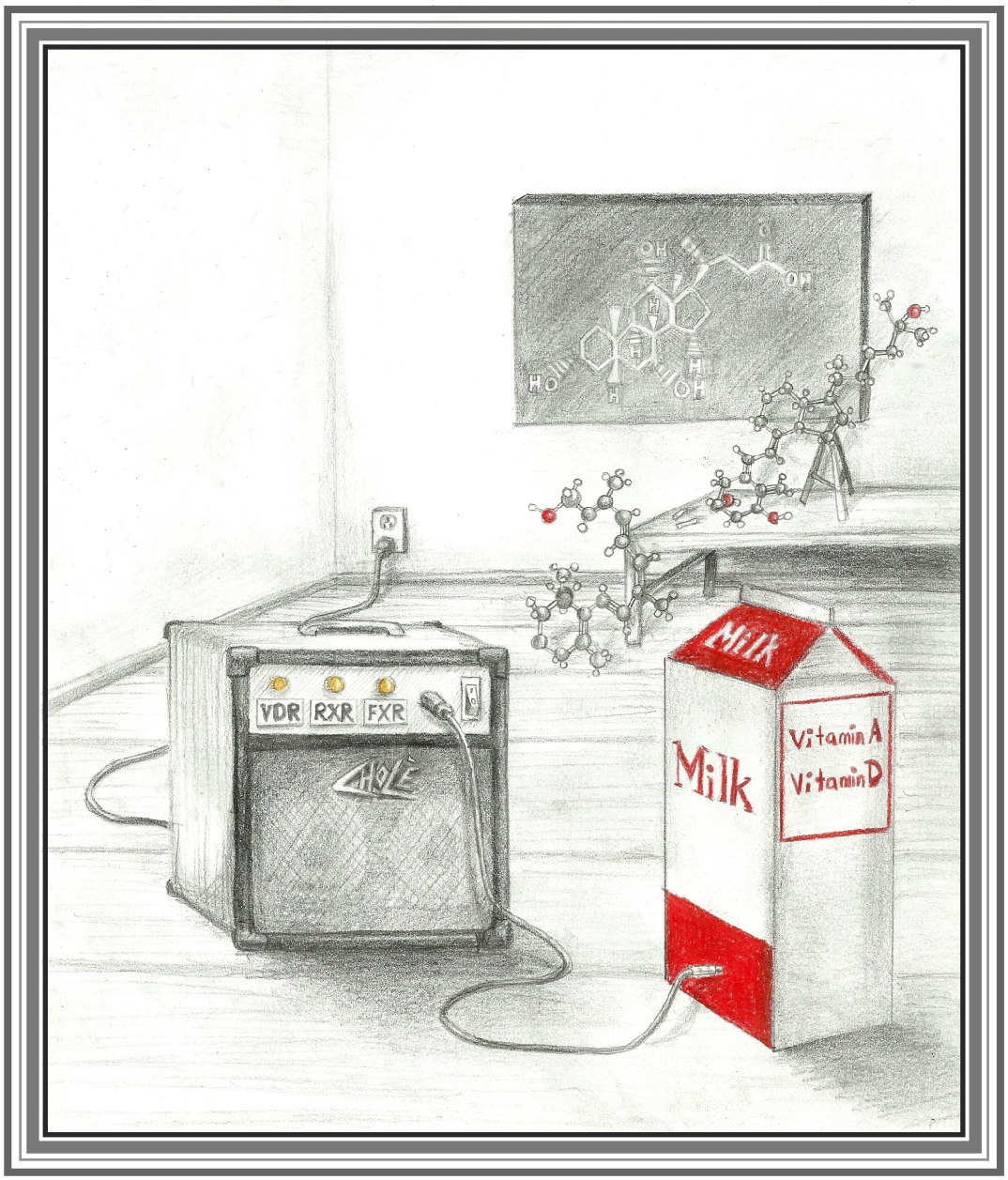

Figure 6.14 Artwork by Sara Schmidt.
Bile acid levels are regulated by controlling the rate of bile acid synthesis in the liver. The vitamin D receptor (VDR), retinoid X receptor (RXR), and bile acid receptor (FXR) control the rate of bile acid biosynthesis. Dietary vitamins A and D activate RXR and VDR respectively and contribute to the regulation of bile acid levels.

CHAPTER 7
Perspectives and Future Directions

7.1 Introduction

The "war on cancer" is said to have started with the signing of the National Cancer Act by Richard Nixon in 1971. Its goal was to find a cure for cancer. Although progress has been made, cancer still accounts for 1 in 4 deaths in the US, and it remains a major health problem worldwide (Jemal 2010). The complexity of cancer biology is arguably a major reason why no cure has yet been found. On the bright side, a major advance has been the realization that cancer is a genetic disease. With that knowledge comes the understanding that if we are to intervene in cancer growth and metastasis, it is essential to understand how these processes function at a molecular level. The goal of my thesis has been 1) to understand how lipid and xenobiotic metabolism in the intestine is regulated at the transcriptional level and 2) to determine how defects in these metabolic pathways contribute to the pathogenesis of colorectal cancer. The major discoveries described in this dissertation are summarized in Figure 7.1. The implications of these findings for human health and disease are the topic of this chapter. In addition, conclusions regarding further work needed to translate these discoveries into new therapeutic strategies are discussed.

7.2 Impact of the Environment on the Pathogenesis of Cancer

Genomic instability and enhanced tumor cell growth and survival are hallmarks of cancer that likely play a key role early in the development of tumors. Like other cancers of epithelial origin, colon cancer probably develops as a result

1) Bile acids promote tumorigenesis in both genetic and carcinogen-induced mouse models of colon cancer.

2) Loss of FXR increases susceptibility to colon and hepatocellular cancer.

3) FXR induces AKR1B7 in intestine, which in turn detoxifies bile acids.

4) Vitamins A and D regulate bile acid synthesis.

Figure 7.1 Summary of Key Findings

of chronic exposure to environmental agents that 1) cause mutational events to occur at an increased rate and 2) allow mutations to accumulate over time within the same cell, ultimately leading to cell transformation and cancer. Such environmental agents may either cause direct genotoxic damage (e.g. carcinogens) or may activate signaling pathways that allow cells to evade apoptosis and propagate despite having genomic mutations. In the colon, major environmental agents include bacteria, intestinal secretions, nutrients, and non-nutrient chemicals acquired in the diet.

7.3 The Role of FXR and Bile Acids in Colorectal Cancer

One of the major dietary problems currently affecting western nations is obesity. In the United States, the incidence of obesity has attained epidemic proportions. Overweight and obesity are associated with increased risk of developing cancer as well as increased mortality from cancer (Wolin 2010, Polednak 2008, Calle 2003). The greatest increase is for breast, endometrium, colon, rectum, esophagus, gallbladder, pancreas, kidney, and thyroid cancer. As discussed in Chapter 1, bacterial metabolites of bile acids are proposed to be responsible for increases in colon cancer caused by high fat diet. Briefly a high fat and high cholesterol diet increase circulating bile acids, which in turn promote colorectal cancer (Figure 7.2). Despite more than thirty years of animal studies showing tumor promotion by bile acids, the mechanism remains unclear. In line with previous studies, I have found that exogenously administered bile acids promote tumorigenesis only when co-administered with a carcinogen. I have also found that bile acids increase the incidence of colorectal cancer in animals that are homozygous null for the tumor suppressor, SMAD3. These studies suggest that bile acids are not directly genotoxic, but rather act as tumor promoters, accelerating the stepwise accumulation of mutations, likely through effects on

growth-promoting or anti-apoptotic signaling pathways. These findings lead me to conclude that the greatest risk of colorectal cancer occurs when both excess fat and carcinogens are present in the diet.

Interestingly, others and I have found that loss of FXR increases tumor incidence in both colon and liver (Chapter 2). Given the importance of FXR in regulating bile acid homeostasis, this result is perhaps not surprising. Of note, while liver tumors form spontaneously in *Fxr*–/– mice, colon cancer does not occur unless additional tumor suppressors are absent or chemical carcinogens are administered. Although several mechanisms have been proposed, I believe that the simplest explanation for how FXR functions as a tumor suppressor is by eliminating the tumor promoting effect of bile acids (Figure 7.2).

As discussed in Chapter 1, FXR and other members of the enteric nuclear receptor clade, including VDR, PXR, and CAR, function by regulating the transcription of genes involved in all phases of nutrient, bile acid, and xenobiotic metabolism. The data I have presented in this dissertation support and extend this concept. In addition to regulating FGF15 to control bile acid biosynthesis, I have found that intestinal FXR also induces AKR1B7, resulting in the catabolism of toxic secondary bile acids in the colon (Figure 7.3). The relative importance of this metabolic pathway to the tumor suppressive function of FXR is unclear. I suspect that the combination of impaired feedback repression of bile acid synthesis and the lack of bile acid detoxification in the colon is responsible for increased susceptibility to colon cancer in *Fxr*–/– mice. Future studies involving transgenic expression of AKR1B7 in an FXR null background would be helpful to determine the contribution of AKR1B7 to tumor suppression. More important, however, is the identification of a human homolog of AKR1B7 and determination of its role in intestinal bile acid metabolism.

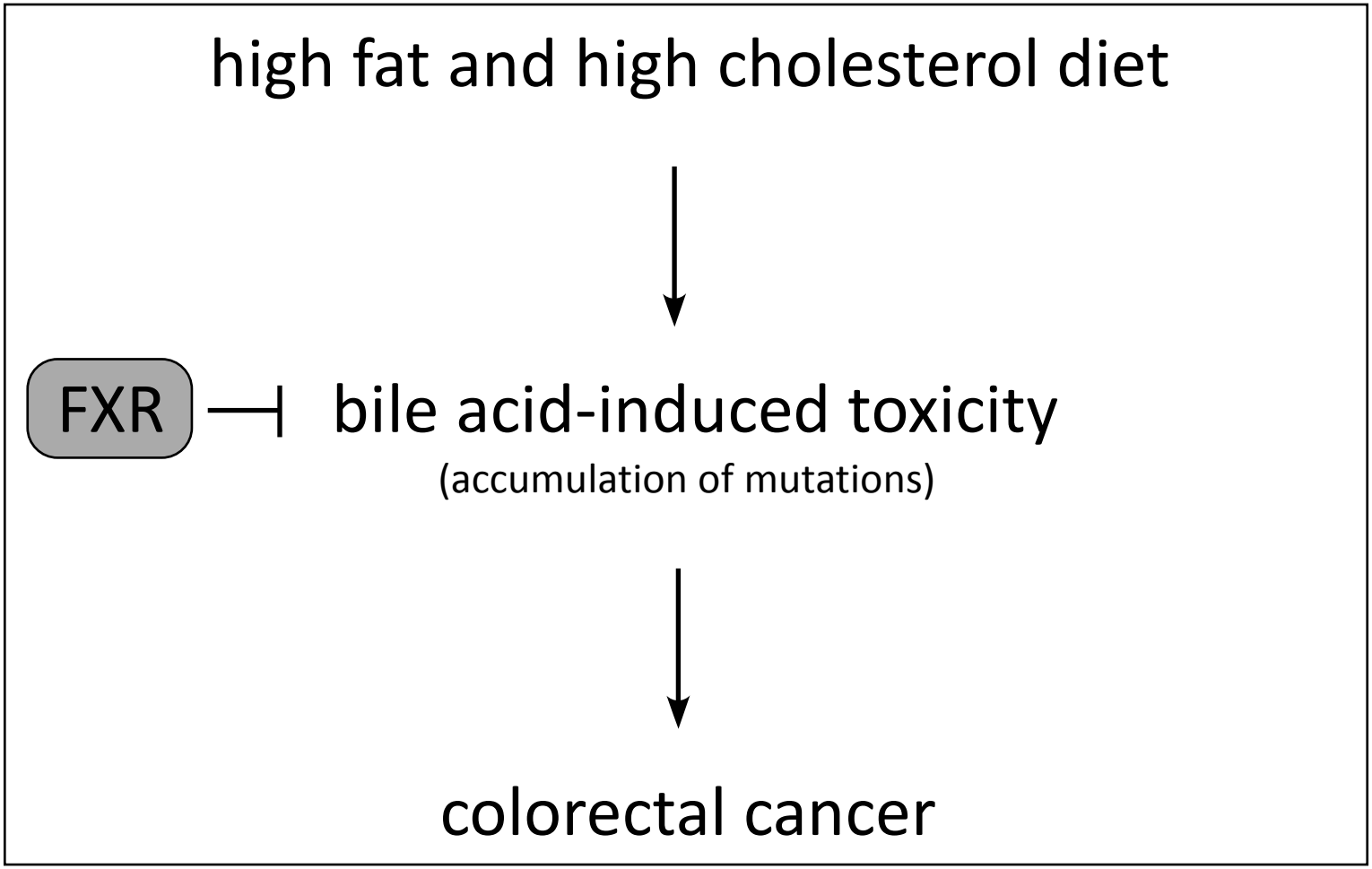

Figure 7.2 The role of diet, bile acids, and FXR in colorectal cancer.

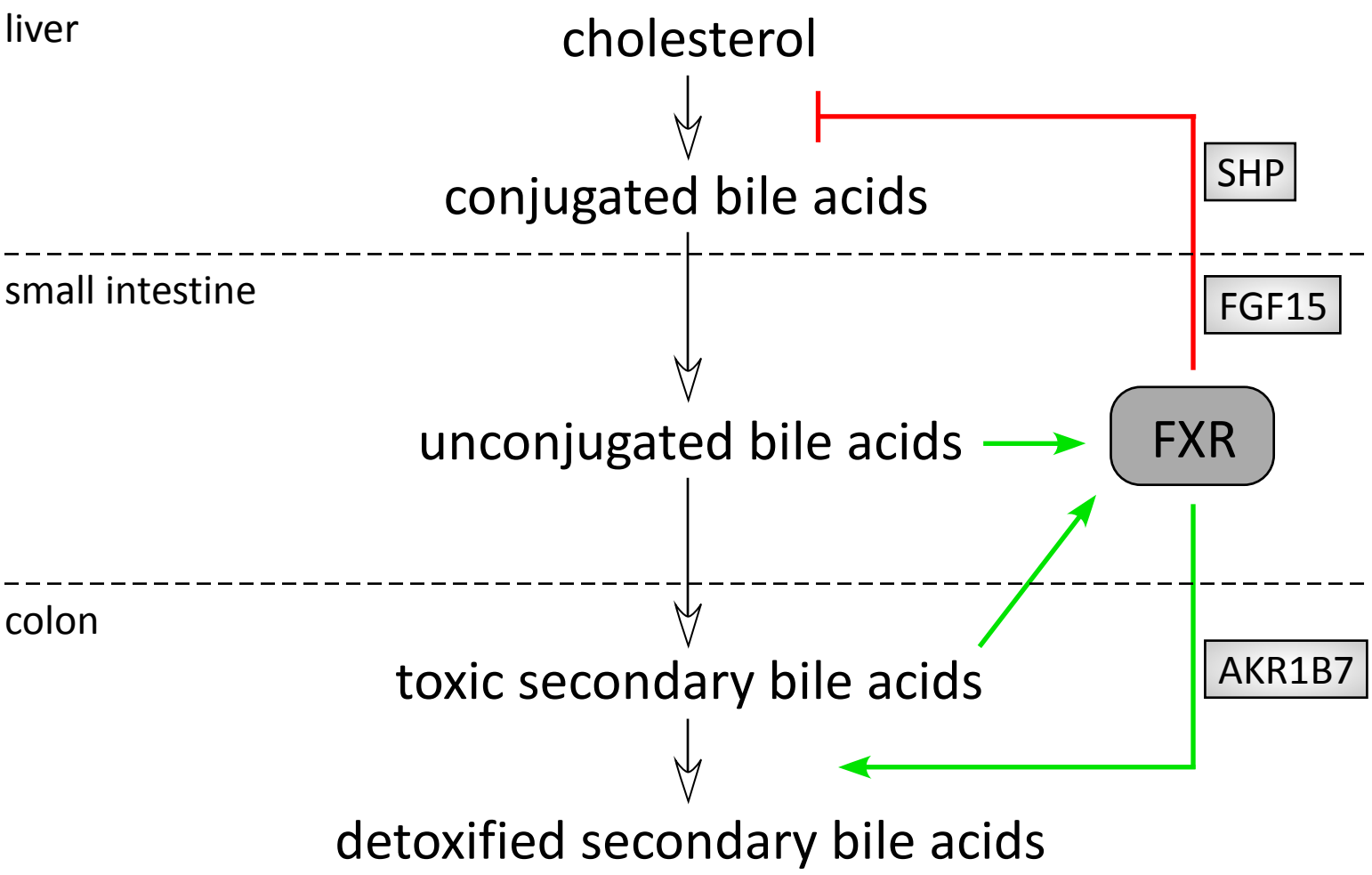

Figure 7.3 The role of FXR in bile acid metabolism.

One interesting question that my dissertation has not addressed is what role the intestinal immune system and bacterial flora play in the pathogenesis of colorectal cancer. Indeed, others in our laboratory have shown that loss of FXR alters intestinal flora and compromises antibacterial defenses (Inagaki 2006). Furthermore, bacteria are responsible for the conversion of primary bile acids to toxic secondary bile acids in the intestine (Ridlon 2006, Figure 3.16A). It is possible that alterations in the bacterial microenvironment in the intestine contribute to the heightened cancer risk phenotype of *Fxr*–/– mice. An ideal experiment to test this would be to generate *Fxr*–/– germ-free mice and evaluate their susceptibility to chemical carcinogens as I have done for conventional mice (Chapter 2). I suspect that part of the increased risk of colorectal cancer in *Fxr*–/– mice is due to changes in bacterial flora, intestinal inflammation, and host defense mechanisms.

7.4 Lipid Soluble Vitamins Regulate Bile Acid Synthesis

A particularly interesting and novel finding of my thesis is the discovery that vitamin A and D play a role in regulating bile acid synthesis (Chapter 6; Schmidt, 2010). The intestinal hormone FGF15 is central to the mechanism by which vitamin D represses bile acid synthesis (Figure 7.4). This explains why vitamin D decreases bile acid synthesis despite the fact that its receptor is not present in hepatocytes. An additional mechanism for protection from toxic bile acids by vitamin D was discovered by previous lab members who showed that vitamin D induces CYP3A4, an enzyme that detoxifies bile acids in the intestine (Figure 7.4). Thus, there are at least two distinct biochemical pathways involving bile acid metabolism that are regulated by vitamin D and its receptor. In contrast, vitamin A appears to work through activation of the FXR/RXR heterodimer in

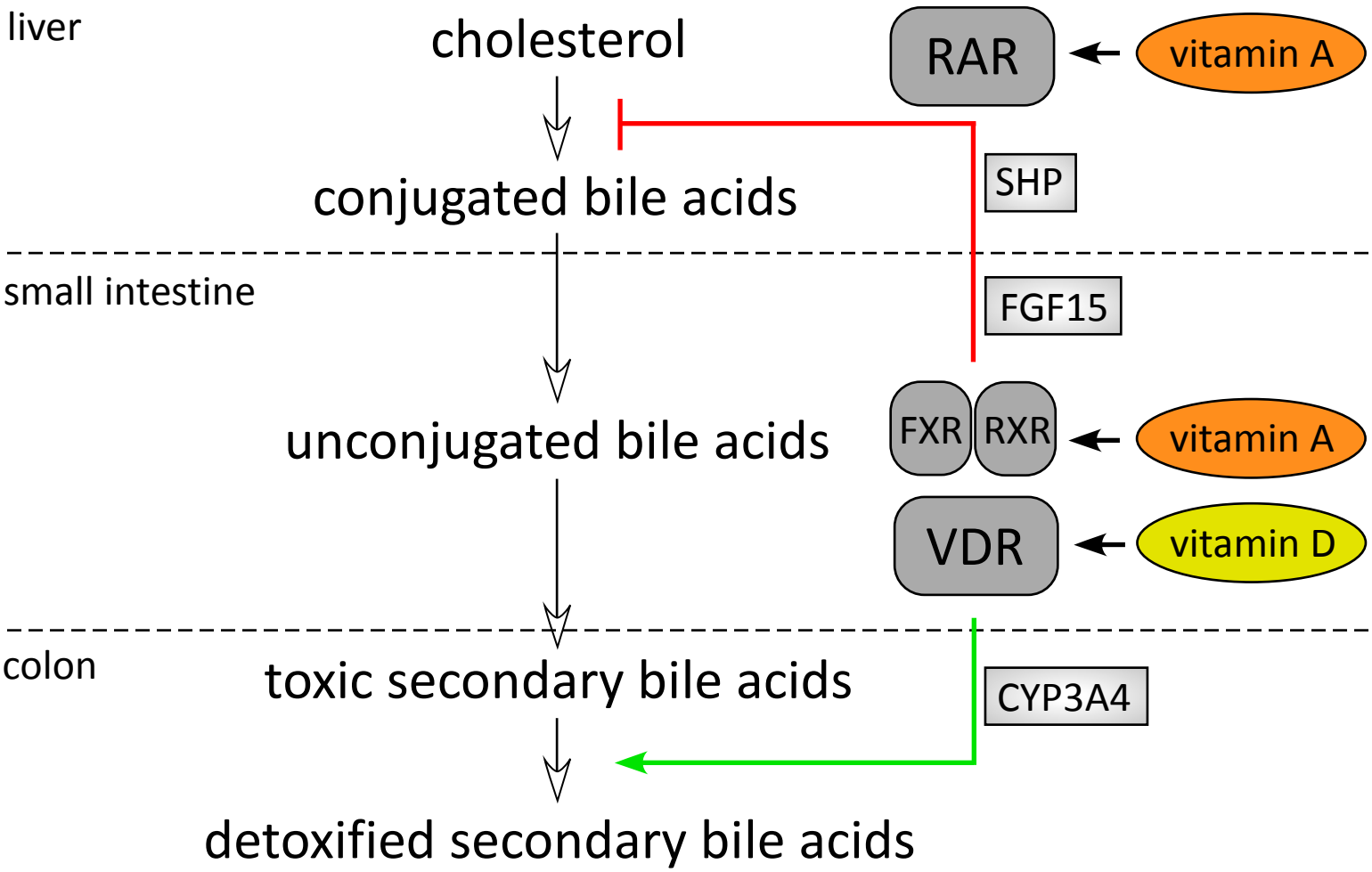

Figure 7.4 Effect of lipid soluble vitamins on bile acid metabolism.

intestine and RAR in liver, where it induces negative regulators of bile acid synthesis, FGF15 and SHP respectively (Figure 7.4).

Of note, low serum vitamin D levels are associated with increased risk of colorectal and other cancers (Garland 2009, Yin 2009). To my knowledge, vitamin A deficiency has not been linked to cancer; however, no studies have looked at the effect of vitamin A supplementation on cancer incidence. It is tempting to speculate that vitamins A and D might act as chemopreventive agents in patients at high risk for colorectal cancer. Future studies in humans are needed to look at the relationship between serum vitamin A and D levels and bile acid synthesis and excretion. Furthermore, given their safety as a dietary supplement, it is reasonable to investigate whether these vitamins affect colorectal cancer incidence and mortality in high risk populations.

7.5 Mechanism of Bile Acid-Induced Proliferation

As noted previously, the mechanism of tumor promotion by bile acids remains unclear. Prior studies in rodents showed that exogenous administration of bile acids induces intestinal proliferation (DeRubertis 1984, Craven 1986a). These studies suggested that increased proliferation, which in theory increases the rate at which mutations accumulate, underlies the tumor promoting effect of bile acids; however, the mechanism of bile acid-induced proliferation was unexplained. I have found that bile acids rapidly activate the PI3K/AKT and ERK pathways *in vivo*; furthermore PI3K signaling is required for the proliferative effect of bile acids (Chapter 5). Although, this is an exciting finding that provides a mechanism for bile acid-induced proliferation, its relevance to the pathogenesis of colorectal cancer in humans is not known. As discussed in Chapter 5, it is unclear whether a high fat, high cholesterol diet is sufficient to raise bile acid levels enough to cause activation of the PI3K/AKT pathway. Clearly, further

investigation is needed to determine whether bile acids contribute to the increased incidence of colorectal cancer in obese individuals.

7.6 Closing Remarks

In summary, thorough review of the literature and critical evaluation of my own data lead me to believe that nutrition plays an important role in the natural history of colorectal cancer. A diet composed of high fat and cholesterol and low vitamin/calorie ratio likely represents a significant risk factor for the development of colorectal cancer. Additional studies are needed to delineate the mechanism by which bile acids promote tumorigenesis such that chemopreventive strategies can be explored.

APPENDIX A

Quantitative PCR Primer Sequences

Gene	Common Name	Accesssion #	Primers
Abcb11	Bsep	NM_021022	aagctacatctgccttagacacagaa caatacaggtccgaccctctct
Abcb4	Mdr2	NM_008830	cttgaggcagcgagaaatg ggttgctgatgctgcctagt
Cyp27a1		NM_024264	gcctcacctatgggatcttca tcaaagcctgacgcagatg
Cyp39a1		NM_018887	tggccaatgctcctcctat tgtggatatcgggatgagaca
Cyp3a11		NM_007818	aaactgcaggatgagatcgatga tccaggtattccatctccatcac
Cyp7a1		NM_007824	agcaactaaacaacctgccagtacta gtccggatattcaaggatgca
Cyp7b1		NM_007825	tagccctctttcctccactcata gaaccgatcgaacctaaattcct
Cyp8b1		NM_010012	gccttcaagtatgatcggttcct gatcttcttgcccgacttgtaga
Fabp-6	Ibabp	NM_008375	ttgagagtgagaagaattacgatgagt tttcaatcacgtctcctggaa
Fgf15		NM_008003	acgggctgattcgctactc tgtagcctaaacagtccatttcct
Hnf4a		NM_008261	accaagaggtccatggtgttt gtgccgagggacgatgtag
Il1b	Il-1b	NM_008361	tgacggaccccaaaagatg tggacagcccaggtcaaag
Nr0b2	Shp	NM_011850	cgatcctcttcaacccagatg agggctccaagacttcacaca
Nr1h4	Fxr	NM_009108	tccggacattcaaccatcac tcactgcacatcccagatctc
Nr1i2	Pxr	NM_010936	caaggccaatggctacca cgggtgatctcgcaggtt
Nr5a2	Lrh-1	NM_030676	tgggaaggaagggacaatctt cgagactcaggaggttgttgaa
Osta		NM_145932	aacagaacatgggatccaagttt cagggcggtcaggatga

Ostb		NM_178933	gacaagcatgttcctcctgaga tgtcttgtggctgcttctttc
S100g	CalbindinD9k	NM_009789	gcctcctgaaggcttcaagt tccatcgccattcttatcca
Slc10a1	Ntcp	NM_011387	gaagtccaaaaggccacactatgt acagccacagagagggagaaag
Slc10a2	Asbt and Ibat	NM_011388	tgactcgggaacgattgtg ggaataacaagagcaaccagagaa
Star		NM_011485	cggagcagagtggtgtcatc tgagtttagtcttggagggacttc
Tnf	Tnf-a	NM_013693	ctgaggtcaatctgcccaagtac cttcacagagcaatgactccaaag
U36b4		NM_007475	cgtcctcgttggagtgaca cggtgcgtcagggattg
Vdr		NM_008361	ggcttccacttcaacgctatg atgctccgcctgaagaaac

Additional primer sets are on file in the Mango Lab.

APPENDIX B

ChIP Primer Sequences

Amplicon	Forward Primer	Reverse Primer
-1569 to -1498	gtcccattttctaccttgttcaga	gggccgccataagaacatt
-998 to -927	accacggagctaggccagta	ccccccaactcctgtatgtg
-704 to -619	tcaagggcctgatcatcga	gacttttgagaagggtggactga
-182 to -71	gctcctcctctgccagatct	tcagagcatttctcctcctaattg
+430 to +510	tcccttaggacccagaagca	cccagctccagtctggaagt
+921 to + 991	ggctaactgctgagtcccatt	aagccaggagaggaggcttt
+1515 to +1570	cccctgcctggctgaa	agatacaggcaggagatttgctt
+1932 to + 2002	agagccttatctgccaactgtct	caggctgtgtctgcctaagc
+2381 to +2451	agcagggttttggaaagttga	tgtgcaaatcttcctggttttt
+2900 to +2959	tgggatgagccaacaatctc	aggcaagaaatccagagttgaag

BIBLIOGRAPHY

Amling, M., Priemel, M., Holzmann, T., Chapin, K., Rueger, J. M., Baron, R., and Demay, M. B. (1999). Rescue of the skeletal phenotype of vitamin D receptor-ablated mice in the setting of normal mineral ion homeostasis: formal histomorphometric and biomechanical analyses. Endocrinology *140*, 4982-4987.

Ananthanarayanan, M., Balasubramanian, N., Makishima, M., Mangelsdorf, D. J., and Suchy, F. J. (2001). Human bile salt export pump promoter is transactivated by the farnesoid X receptor/bile acid receptor. J Biol Chem *276*, 28857-28865.

Araya, Z., and Wikvall, K. (1999). 6alpha-hydroxylation of taurochenodeoxycholic acid and lithocholic acid by CYP3A4 in human liver microsomes. Biochim Biophys Acta *1438*, 47-54.

Balk, S. P., and Knudsen, K. E. (2008). AR, the cell cycle, and prostate cancer. Nucl Recept Signal *6*, e001.

Barone, M., Berloco, P., Ladisa, R., Ierardi, E., Caruso, M. L., Valentini, A. M., Notarnicola, M., Di, L. A., and Francavilla, A. (2002). Demonstration of a direct stimulatory effect of bile salts on rat colonic epithelial cell proliferation. Scand J Gastroenterol *37*, 88-94.

Barthel, T. K., Mathern, D. R., Whitfield, G. K., Haussler, C. A., Hopper, H. A. t., Hsieh, J. C., Slater, S. A., Hsieh, G., Kaczmarska, M., Jurutka, P. W., Kolek, O. I., Ghishan, F. K., and Haussler, M. R. (2007). 1,25-Dihydroxyvitamin D3/VDR-mediated induction of FGF23 as well as transcriptional control of other bone anabolic and catabolic genes that orchestrate the regulation of phosphate and calcium mineral metabolism. J Steroid Biochem Mol Biol *103*, 381-388.

Baumann, C., Davies, B., Peters, M., Kaufmann-Reiche, U., Lessl, M., and Theuring, F. (2007). AKR1B7 (mouse vas deferens protein) is dispensable for mouse development and reproductive success. Reproduction *134*, 97-109.

Berggren, S., Gall, C., Wollnitz, N., Ekelund, M., Karlbom, U., Hoogstraate, J., Schrenk, D., and Lennernas, H. (2007). Gene and protein expression of P-glycoprotein, MRP1, MRP2, and CYP3A4 in the small and large human intestine. Mol Pharm *4*, 252-257.

Bernstein, C., Bernstein, H., Garewal, H., Dinning, P., Jabi, R., Sampliner, R. E., McCuskey, M. K., Panda, M., Roe, D. J., L'Heureux, L., and Payne, C. (1999). A bile acid-induced apoptosis assay for colon cancer risk and associated quality control studies. Cancer Res *59*, 2353-2357.

Bernstein, H., Bernstein, C., Payne, C. M., and Dvorak, K. (2009). Bile acids as endogenous etiologic agents in gastrointestinal cancer. World J Gastroenterol *15*, 3329-3340.

Bernstein, H., Bernstein, C., Payne, C. M., Dvorakova, K., and Garewal, H. (2005). Bile acids as carcinogens in human gastrointestinal cancers. Mutat Res *589*, 47-65.

Blomhoff, R., and Blomhoff, H. K. (2006). Overview of retinoid metabolism and function. J Neurobiol *66*, 606-630.

Bookout, A. L., Jeong, Y., Downes, M., Yu, R. T., Evans, R. M., and Mangelsdorf, D. J. (2006). Anatomical profiling of nuclear receptor expression reveals a hierarchical transcriptional network. Cell *126*, 789-799.

Bookout, A. L., and Mangelsdorf, D. J. (2003). Quantitative real-time PCR protocol for analysis of nuclear receptor signaling pathways. Nucl Recept Signal *1*, e012.

Bouillon, R., Eelen, G., Verlinden, L., Mathieu, C., Carmeliet, G., and Verstuyf, A. (2006). Vitamin D and cancer. J Steroid Biochem Mol Biol *102*, 156-162.

Bouillon, R., Van Cromphaut, S., and Carmeliet, G. (2003). Intestinal calcium absorption: Molecular vitamin D mediated mechanisms. J Cell Biochem *88*, 332-339.

Branting, C., Toftgard, R., Hallstrom, I. P., and Rafter, J. (1995). Role of protein kinase C in growth stimulation of primary mouse colonic epithelial cells. In Vitro Cell Dev Biol Anim *31*, 790-795.

Brockstedt, E., Peters-Kottig, M., Badock, V., Hegele-Hartung, C., and Lessl, M. (2000). Luteinizing hormone induces mouse vas deferens protein expression in the murine ovary. Endocrinology *141*, 2574-2581.

Bull, A. W., Marnett, L. J., Dawe, E. J., and Nigro, N. D. (1983). Stimulation of deoxythymidine incorporation in the colon of rats treated intrarectally with bile acids and fats. Carcinogenesis *4*, 207-210.

Calle, E. E., Rodriguez, C., Walker-Thurmond, K., and Thun, M. J. (2003). Overweight, obesity, and mortality from cancer in a prospectively studied cohort of U.S. adults. N Engl J Med *348*, 1625-1638.

Calvert, P. M., and Frucht, H. (2002). The genetics of colorectal cancer. Ann Intern Med *137*, 603-612.

Campbell, R. L., Singh, D. V., and Nigro, N. D. (1975). Importance of the fecal stream on the induction of colon tumors by azoxymethane in rats. Cancer Res *35*, 1369-1371.

Chawla, A., Repa, J. J., Evans, R. M., and Mangelsdorf, D. J. (2001). Nuclear receptors and lipid physiology: opening the X-files. Science *294*, 1866-1870.

Cheng, J., and Russell, D. W. (2003). Adolf Windaus Prize Lecture: The Enzymes and Genes of Bile Acid Synthesis. In Bile Acids: From Genomics to Disease and Therapy, G. Paumgartner, ed. (Dordrecht: Kluwer Academic), pp. 1-11.

Chiang, J. Y. (2002). Bile acid regulation of gene expression: roles of nuclear hormone receptors. Endocr Rev *23*, 443-463.

Chiang, J. Y. (2009). Bile acids: regulation of synthesis. J Lipid Res *50*, 1955-1966.

Choi, M., Moschetta, A., Bookout, A. L., Peng, L., Umetani, M., Holmstrom, S. R., Suino-Powell, K., Xu, H. E., Richardson, J. A., Gerard, R. D., Mangelsdorf, D. J., and Kliewer, S. A. (2006). Identification of a hormonal basis for gallbladder filling. Nat Med *12*, 1253-1255.

Cohen, B. I., and Raicht, R. F. (1981). Effects of bile acids on colon carcinogenesis in rats treated with carcinogens. Cancer Res *41*, 3759-3760.

Craven, P. A., and DeRubertis, F. R. (1992). Alterations in protein kinase C system of colonic epithelium during fasting-refeeding. Evidence for protein kinase C independent pathway of enhanced proliferative activity. Dig Dis Sci *37*, 1162-1169.

Craven, P. A., Pfanstiel, J., and DeRubertis, F. R. (1986a). Role of reactive oxygen in bile salt stimulation of colonic epithelial proliferation. J Clin Invest *77*, 850-859.

Craven, P. A., Pfanstiel, J., and DeRubertis, F. R. (1987). Role of activation of protein kinase C in the stimulation of colonic epithelial proliferation and reactive oxygen formation by bile acids. J Clin Invest *79*, 532-541.

Craven, P. A., Pfanstiel, J., Saito, R., and DeRubertis, F. R. (1986b). Relationship between loss of rat colonic surface epithelium induced by deoxycholate and initiation of the subsequent proliferative response. Cancer Res *46*, 5754-5759.

Crestani, M., Sadeghpour, A., Stroup, D., Galli, G., and Chiang, J. Y. (1998). Transcriptional activation of the cholesterol 7alpha-hydroxylase gene (CYP7A) by nuclear hormone receptors. J Lipid Res *39*, 2192-2200.

Cross, H. S. (2005). Vitamin D and Colon Cancer. In Vitamin D, D. Feldman, ed., p. 1709.

Dawson, P. A., Hubbert, M., Haywood, J., Craddock, A. L., Zerangue, N., Christian, W. V., and Ballatori, N. (2005). The heteromeric organic solute transporter alpha-beta, Ostalpha-Ostbeta, is an ileal basolateral bile acid transporter. J Biol Chem *280*, 6960-6968.

Dawson, P. A., Lan, T., and Rao, A. (2009). Bile acid transporters. J Lipid Res *50*, 2340-2357.

DeLuca, H. F. (2004). Overview of general physiologic features and functions of vitamin D. Am J Clin Nutr *80*, 1689S-1696S.

Deluca, H. F., and Cantorna, M. T. (2001). Vitamin D: its role and uses in immunology. Faseb J *15*, 2579-2585.

Denson, L. A., Sturm, E., Echevarria, W., Zimmerman, T. L., Makishima, M., Mangelsdorf, D. J., and Karpen, S. J. (2001). The orphan nuclear receptor, shp, mediates bile acid-induced inhibition of the rat bile acid transporter, ntcp. Gastroenterology *121*, 140-147.

Dent, P., Fang, Y., Gupta, S., Studer, E., Mitchell, C., Spiegel, S., and Hylemon, P. B. (2005). Conjugated bile acids promote ERK1/2 and AKT activation via a pertussis toxin-sensitive mechanism in murine and human hepatocytes. Hepatology *42*, 1291-1299.

DeRubertis, F. R., Craven, P. A., and Saito, R. (1984). Bile salt stimulation of colonic epithelial proliferation. Evidence for involvement of lipoxygenase products. J Clin Invest *74*, 1614-1624.

Deschner, E. E., Cohen, B. I., and Raicht, R. F. (1981). Acute and chronic effect of dietary cholic acid on colonic epithelial cell proliferation. Digestion *21*, 290-296.

Earnest, D. L., Holubec, H., Wali, R. K., Jolley, C. S., Bissonette, M., Bhattacharyya, A. K., Roy, H., Khare, S., and Brasitus, T. A. (1994). Chemoprevention of azoxymethane-induced colonic carcinogenesis by supplemental dietary ursodeoxycholic acid. Cancer Res *54*, 5071-5074.

Echchgadda, I., Song, C. S., Roy, A. K., and Chatterjee, B. (2004). Dehydroepiandrosterone sulfotransferase is a target for transcriptional induction by the vitamin D receptor. Mol Pharmacol *65*, 720-729.

Eloranta, J. J., and Kullak-Ublick, G. A. (2008). The role of FXR in disorders of bile acid homeostasis. Physiology (Bethesda) *23*, 286-295.

Fitzer, C. J., O'Brian, C. A., Guillem, J. G., and Weinstein, I. B. (1987). The regulation of protein kinase C by chenodeoxycholate, deoxycholate and several structurally related bile acids. Carcinogenesis *8*, 217-220.

Flatmark, K., Maelandsmo, G. M., Martinsen, M., Rasmussen, H., and Fodstad, O. (2004). Twelve colorectal cancer cell lines exhibit highly variable growth and metastatic capacities in an orthotopic model in nude mice. Eur J Cancer *40*, 1593-1598.

Flynn, C., Montrose, D. C., Swank, D. L., Nakanishi, M., Ilsley, J. N., and Rosenberg, D. W. (2007). Deoxycholic acid promotes the growth of colonic aberrant crypt foci. Mol Carcinog *46*, 60-70.

Fukagawa, M., Nii-Kono, T., and Kazama, J. J. (2005). Role of fibroblast growth factor 23 in health and in chronic kidney disease. Curr Opin Nephrol Hypertens *14*, 325-329.

Garland, C. F., Gorham, E. D., Mohr, S. B., and Garland, F. C. (2009). Vitamin D for cancer prevention: global perspective. Ann Epidemiol *19*, 468-483.

Gascon-Barre, M., Demers, C., Mirshahi, A., Neron, S., Zalzal, S., and Nanci, A. (2003). The normal liver harbors the vitamin D nuclear receptor in nonparenchymal and biliary epithelial cells. Hepatology *37*, 1034-1042.

Ghurani, G. B., and Penalver, M. A. (2001). An update on vulvar cancer. Am J Obstet Gynecol *185*, 294-299.

Gilardi, F., Mitro, N., Godio, C., Scotti, E., Caruso, D., Crestani, M., and De Fabiani, E. (2007). The pharmacological exploitation of cholesterol 7alpha-hydroxylase, the key enzyme in bile acid synthesis: from binding resins to chromatin remodelling to reduce plasma cholesterol. Pharmacol Ther *116*, 449-472.

Gnerre, C., Blattler, S., Kaufmann, M. R., Looser, R., and Meyer, U. A. (2004). Regulation of CYP3A4 by the bile acid receptor FXR: evidence for functional binding sites in the CYP3A4 gene. Pharmacogenetics *14*, 635-645.

Gong, Y. Z., Everett, E. T., Schwartz, D. A., Norris, J. S., and Wilson, F. A. (1994). Molecular cloning, tissue distribution, and expression of a 14-kDa bile acid-binding protein from rat ileal cytosol. Proc Natl Acad Sci U S A *91*, 4741-4745.

Goodwin, B., Gauthier, K. C., Umetani, M., Watson, M. A., Lochansky, M. I., Collins, J. L., Leitersdorf, E., Mangelsdorf, D. J., Kliewer, S. A., and Repa, J. J. (2003). Identification of bile acid precursors as endogenous ligands for the nuclear xenobiotic pregnane X receptor. Proc Natl Acad Sci U S A *100*, 223-228.

Goodwin, B., Jones, S. A., Price, R. R., Watson, M. A., McKee, D. D., Moore, L. B., Galardi, C., Wilson, J. G., Lewis, M. C., Roth, M. E., Maloney, P. R., Willson, T. M., and Kliewer, S. A. (2000). A regulatory cascade of the nuclear receptors FXR, SHP-1, and LRH-1 represses bile acid biosynthesis. Mol Cell *6*, 517-526.

Graf, D., Kurz, A. K., Fischer, R., Reinehr, R., and Haussinger, D. (2002a). Taurolithocholic acid-3 sulfate induces CD95 trafficking and apoptosis in a c-Jun N-terminal kinase-dependent manner. Gastroenterology *122*, 1411-1427.

Graf, D., Kurz, A. K., Reinehr, R., Fischer, R., Kircheis, G., and Haussinger, D. (2002b). Prevention of bile acid-induced apoptosis by betaine in rat liver. Hepatology *36*, 829-839.

Gregori, S., Casorati, M., Amuchastegui, S., Smiroldo, S., Davalli, A. M., and Adorini, L. (2001). Regulatory T cells induced by 1 alpha,25-dihydroxyvitamin D3 and mycophenolate mofetil treatment mediate transplantation tolerance. J Immunol *167*, 1945-1953.

Grober, J., Zaghini, I., Fujii, H., Jones, S. A., Kliewer, S. A., Willson, T. M., Ono, T., and Besnard, P. (1999). Identification of a bile acid-responsive element in the human ileal bile acid-binding protein gene. Involvement of the farnesoid X receptor/9-cis-retinoic acid receptor heterodimer. J Biol Chem *274*, 29749-29754.

Grubben, M. J., Nagengast, F. M., Katan, M. B., and Peters, W. H. (2001). The glutathione biotransformation system and colorectal cancer risk in humans. Scand J Gastroenterol Suppl, 68-76.

Gupta, S., Stravitz, R. T., Dent, P., and Hylemon, P. B. (2001). Down-regulation of cholesterol 7alpha-hydroxylase (CYP7A1) gene expression by bile acids in primary rat hepatocytes is mediated by the c-Jun N-terminal kinase pathway. J Biol Chem *276*, 15816-15822.

Hagio, M., Matsumoto, M., Fukushima, M., Hara, H., and Ishizuka, S. (2009). Improved analysis of bile acids in tissues and intestinal contents of rats using LC/ESI-MS. J Lipid Res *50*, 173-180.

Haigis, K. M., Kendall, K. R., Wang, Y., Cheung, A., Haigis, M. C., Glickman, J. N., Niwa-Kawakita, M., Sweet-Cordero, A., Sebolt-Leopold, J., Shannon, K. M., Settleman, J., Giovannini, M., and Jacks, T. (2008). Differential effects of oncogenic K-Ras and N-Ras on proliferation, differentiation and tumor progression in the colon. Nat Genet *40*, 600-608.

Hamilton, J. P., Xie, G., Raufman, J. P., Hogan, S., Griffin, T. L., Packard, C. A., Chatfield, D. A., Hagey, L. R., Steinbach, J. H., and Hofmann, A. F. (2007). Human cecal bile acids: concentration and spectrum. Am J Physiol Gastrointest Liver Physiol *293*, G256-263.

Handschin, C., and Meyer, U. A. (2003). Induction of drug metabolism: the role of nuclear receptors. Pharmacol Rev *55*, 649-673.

Haussler, M. R., Haussler, C. A., Jurutka, P. W., Thompson, P. D., Hsieh, J. C., Remus, L. S., Selznick, S. H., and Whitfield, G. K. (1997). The vitamin D hormone and its nuclear receptor: molecular actions and disease states. J Endocrinol *154 Suppl*, S57-73.

Heuman, D. M., Mills, A. S., McCall, J., Hylemon, P. B., Pandak, W. M., and Vlahcevic, Z. R. (1991). Conjugates of ursodeoxycholate protect against cholestasis and hepatocellular necrosis caused by more hydrophobic bile salts. In vivo studies in the rat. Gastroenterology *100*, 203-211.

Hoenderop, J. G., van der Kemp, A. W., Hartog, A., van de Graaf, S. F., van Os, C. H., Willems, P. H., and Bindels, R. J. (1999). Molecular identification of the apical Ca2+ channel in 1, 25-dihydroxyvitamin D3-responsive epithelia. J Biol Chem *274*, 8375-8378.

Hofmann, A. F. (1999a). Bile Acids: The Good, the Bad, and the Ugly. News Physiol Sci *14*, 24-29.

Hofmann, A. F. (1999b). The continuing importance of bile acids in liver and intestinal disease. Arch Intern Med *159*, 2647-2658.

Hofmann, A. F. (2009). The enterohepatic circulation of bile acids in mammals: form and functions. Front Biosci *14*, 2584-2598.

Hofmann, A. F., Mangelsdorf, D. J., and Kliewer, S. A. (2009). Chronic diarrhea due to excessive bile acid synthesis and not defective ileal transport: a new syndrome of defective fibroblast growth factor 19 release. Clin Gastroenterol Hepatol *7*, 1151-1154.

Holt, J. A., Luo, G., Billin, A. N., Bisi, J., McNeill, Y. Y., Kozarsky, K. F., Donahee, M., Wang, D. Y., Mansfield, T. A., Kliewer, S. A., Goodwin, B., and Jones, S. A. (2003). Definition of a novel growth factor-dependent signal cascade for the suppression of bile acid biosynthesis. Genes Dev *17*, 1581-1591.

Hori, T., Matsumoto, K., Sakaitani, Y., Sato, M., and Morotomi, M. (1998). Effect of dietary deoxycholic acid and cholesterol on fecal steroid concentration and its impact on the colonic crypt cell proliferation in azoxymethane-treated rats. Cancer Lett *124*, 79-84.

Huang, W., Ma, K., Zhang, J., Qatanani, M., Cuvillier, J., Liu, J., Dong, B., Huang, X., and Moore, D. D. (2006). Nuclear receptor-dependent bile acid signaling is required for normal liver regeneration. Science *312*, 233-236.

Hylemon, P. B., Zhou, H., Pandak, W. M., Ren, S., Gil, G., and Dent, P. (2009). Bile acids as regulatory molecules. J Lipid Res *50*, 1509-1520.

Inagaki, T., Choi, M., Moschetta, A., Peng, L., Cummins, C. L., McDonald, J. G., Luo, G., Jones, S. A., Goodwin, B., Richardson, J. A., Gerard, R. D., Repa, J. J., Mangelsdorf, D. J., and Kliewer, S. A. (2005). Fibroblast growth factor 15 functions as an enterohepatic signal to regulate bile acid homeostasis. Cell Metab *2*, 217-225.

Inagaki, T., Moschetta, A., Lee, Y. K., Peng, L., Zhao, G., Downes, M., Yu, R. T., Shelton, J. M., Richardson, J. A., Repa, J. J., Mangelsdorf, D. J., and Kliewer, S. A. (2006). Regulation of antibacterial defense in the small intestine by the nuclear bile acid receptor. Proc Natl Acad Sci U S A *103*, 3920-3925.

Ishizawa, M., Matsunawa, M., Adachi, R., Uno, S., Ikeda, K., Masuno, H., Shimizu, M., Iwasaki, K., Yamada, S., and Makishima, M. (2008). Lithocholic acid derivatives act as selective vitamin D receptor modulators without inducing hypercalcemia. J Lipid Res *49*, 763-772.

Jackson, P. E., O'Connor, P. J., Cooper, D. P., Margison, G. P., and Povey, A. C. (2003). Associations between tissue-specific DNA alkylation, DNA repair and cell proliferation in the colon and colon tumour yield in mice treated with 1,2-dimethylhydrazine. Carcinogenesis *24*, 527-533.

Janssen, K. P., el-Marjou, F., Pinto, D., Sastre, X., Rouillard, D., Fouquet, C., Soussi, T., Louvard, D., and Robine, S. (2002). Targeted expression of oncogenic K-ras in intestinal epithelium causes spontaneous tumorigenesis in mice. Gastroenterology *123*, 492-504.

Jemal, A., Siegel, R., Xu, J., and Ward, E. (2010). Cancer statistics, 2010. CA Cancer J Clin *60*, 277-300.

Jez, J. M., Bennett, M. J., Schlegel, B. P., Lewis, M., and Penning, T. M. (1997). Comparative anatomy of the aldo-keto reductase superfamily. Biochem J *326 (Pt 3)*, 625-636.

Jones, G., Strugnell, S. A., and DeLuca, H. F. (1998). Current understanding of the molecular actions of vitamin D. Physiol Rev *78*, 1193-1231.

Jurutka, P. W., Thompson, P. D., Whitfield, G. K., Eichhorst, K. R., Hall, N., Dominguez, C. E., Hsieh, J. C., Haussler, C. A., and Haussler, M. R. (2005). Molecular and functional comparison of 1,25-dihydroxyvitamin D(3) and the novel vitamin D receptor ligand, lithocholic acid, in activating transcription of cytochrome P450 3A4. J Cell Biochem *94*, 917-943.

Kallay, E., Pietschmann, P., Toyokuni, S., Bajna, E., Hahn, P., Mazzucco, K., Bieglmayer, C., Kato, S., and Cross, H. S. (2001). Characterization of a vitamin D receptor knockout mouse as a model of colorectal hyperproliferation and DNA damage. Carcinogenesis *22*, 1429-1435.

Kang, D. J., Ridlon, J. M., Moore, D. R., 2nd, Barnes, S., and Hylemon, P. B. (2008). Clostridium scindens baiCD and baiH genes encode stereo-specific 7alpha/7beta-hydroxy-3-oxo-delta4-cholenoic acid oxidoreductases. Biochim Biophys Acta *1781*, 16-25.

Karnoub, A. E., and Weinberg, R. A. (2008). Ras oncogenes: split personalities. Nat Rev Mol Cell Biol *9*, 517-531.

Kim, I., Ahn, S. H., Inagaki, T., Choi, M., Ito, S., Guo, G. L., Kliewer, S. A., and Gonzalez, F. J. (2007a). Differential regulation of bile acid homeostasis by the farnesoid X receptor in liver and intestine. J Lipid Res *48*, 2664-2672.

Kim, I., Morimura, K., Shah, Y., Yang, Q., Ward, J. M., and Gonzalez, F. J. (2007b). Spontaneous hepatocarcinogenesis in farnesoid X receptor-null mice. Carcinogenesis *28*, 940-946.

Kinzler, K. W., and Vogelstein, B. (1996). Lessons from hereditary colorectal cancer. Cell *87*, 159-170.

Kliewer, S. A., Goodwin, B., and Willson, T. M. (2002). The nuclear pregnane X receptor: a key regulator of xenobiotic metabolism. Endocr Rev *23*, 687-702.

Kok, T., Hulzebos, C. V., Wolters, H., Havinga, R., Agellon, L. B., Stellaard, F., Shan, B., Schwarz, M., and Kuipers, F. (2003). Enterohepatic circulation of bile salts in farnesoid X receptor-deficient mice: efficient intestinal bile

salt absorption in the absence of ileal bile acid-binding protein. J Biol Chem *278*, 41930-41937.

Kolek, O. I., Hines, E. R., Jones, M. D., LeSueur, L. K., Lipko, M. A., Kiela, P. R., Collins, J. F., Haussler, M. R., and Ghishan, F. K. (2005). 1alpha,25-Dihydroxyvitamin D3 upregulates FGF23 gene expression in bone: the final link in a renal-gastrointestinal-skeletal axis that controls phosphate transport. Am J Physiol Gastrointest Liver Physiol *289*, G1036-1042.

Kullak-Ublick, G. A., Beuers, U., and Paumgartner, G. (2000a). Hepatobiliary transport. J Hepatol *32*, 3-18.

Kullak-Ublick, G. A., Stieger, B., Hagenbuch, B., and Meier, P. J. (2000b). Hepatic transport of bile salts. Semin Liver Dis *20*, 273-292.

Kullak-Ublick, G. A., Stieger, B., and Meier, P. J. (2004). Enterohepatic bile salt transporters in normal physiology and liver disease. Gastroenterology *126*, 322-342.

Kutuzova, G. D., and DeLuca, H. F. (2007). 1,25-Dihydroxyvitamin D3 regulates genes responsible for detoxification in intestine. Toxicol Appl Pharmacol *218*, 37-44.

Lamprecht, S. A., and Lipkin, M. (2003). Chemoprevention of colon cancer by calcium, vitamin D and folate: molecular mechanisms. Nat Rev Cancer *3*, 601-614.

Landrier, J. F., Eloranta, J. J., Vavricka, S. R., and Kullak-Ublick, G. A. (2006). The nuclear receptor for bile acids, FXR, transactivates human organic solute transporter-alpha and -beta genes. Am J Physiol Gastrointest Liver Physiol *290*, G476-485.

Lau, E. T., Cao, D., Lin, C., Chung, S. K., and Chung, S. S. (1995). Tissue-specific expression of two aldose reductase-like genes in mice: abundant expression of mouse vas deferens protein and fibroblast growth factor-regulated protein in the adrenal gland. Biochem J *312 (Pt 2)*, 609-615.

Lee, Y. K., Dell, H., Dowhan, D. H., Hadzopoulou-Cladaras, M., and Moore, D. D. (2000). The orphan nuclear receptor SHP inhibits hepatocyte nuclear factor 4 and retinoid X receptor transactivation: two mechanisms for repression. Mol Cell Biol *20*, 187-195.

Lee, Y. K., Schmidt, D. R., Cummins, C. L., Choi, M., Peng, L., Zhang, Y., Goodwin, B., Hammer, R. E., Mangelsdorf, D. J., and Kliewer, S. A. (2008). Liver receptor homolog-1 regulates bile acid homeostasis but is not essential for feedback regulation of bile acid synthesis. Mol Endocrinol *22*, 1345-1356.

Lefrancois-Martinez, A. M., Tournaire, C., Martinez, A., Berger, M., Daoudal, S., Tritsch, D., Veyssiere, G., and Jean, C. (1999). Product of side-chain cleavage of cholesterol, isocaproaldehyde, is an endogenous specific

substrate of mouse vas deferens protein, an aldose reductase-like protein in adrenocortical cells. J Biol Chem *274*, 32875-32880.

Li, T., Jahan, A., and Chiang, J. Y. (2006). Bile acids and cytokines inhibit the human cholesterol 7 alpha-hydroxylase gene via the JNK/c-jun pathway in human liver cells. Hepatology *43*, 1202-1210.

Lipkin, M., Reddy, B., Newmark, H., and Lamprecht, S. A. (1999). Dietary factors in human colorectal cancer. Annu Rev Nutr *19*, 545-586.

Liu, M. J., Takahashi, Y., Wada, T., He, J., Gao, J., Tian, Y., Li, S., and Xie, W. (2009). The aldo-keto reductase Akr1b7 gene is a common transcriptional target of xenobiotic receptors pregnane X receptor and constitutive androstane receptor. Mol Pharmacol *76*, 604-611.

Liu, M. M., Albanese, C., Anderson, C. M., Hilty, K., Webb, P., Uht, R. M., Price, R. H., Jr., Pestell, R. G., and Kushner, P. J. (2002). Opposing action of estrogen receptors alpha and beta on cyclin D1 gene expression. J Biol Chem *277*, 24353-24360.

Liu, P. T., Stenger, S., Li, H., Wenzel, L., Tan, B. H., Krutzik, S. R., Ochoa, M. T., Schauber, J., Wu, K., Meinken, C., Kamen, D. L., Wagner, M., Bals, R., Steinmeyer, A., Zugel, U., *et al.* (2006). Toll-like receptor triggering of a vitamin D-mediated human antimicrobial response. Science *311*, 1770-1773.

Liu, S., and Quarles, L. D. (2007). How fibroblast growth factor 23 works. J Am Soc Nephrol *18*, 1637-1647.

Lu, T. T., Makishima, M., Repa, J. J., Schoonjans, K., Kerr, T. A., Auwerx, J., and Mangelsdorf, D. J. (2000). Molecular basis for feedback regulation of bile acid synthesis by nuclear receptors. Mol Cell *6*, 507-515.

Lu, T. T., Repa, J. J., and Mangelsdorf, D. J. (2001). Orphan nuclear receptors as eLiXiRs and FiXeRs of sterol metabolism. J Biol Chem *276*, 37735-37738.

Lundasen, T., Galman, C., Angelin, B., and Rudling, M. (2006). Circulating intestinal fibroblast growth factor 19 has a pronounced diurnal variation and modulates hepatic bile acid synthesis in man. Journal of internal medicine *260*, 530-536.

Ma, X., Shah, Y. M., Guo, G. L., Wang, T., Krausz, K. W., Idle, J. R., and Gonzalez, F. J. (2007). Rifaximin is a gut-specific human pregnane X receptor activator. J Pharmacol Exp Ther *322*, 391-398.

Maggio-Price, L., Treuting, P., Zeng, W., Tsang, M., Bielefeldt-Ohmann, H., and Iritani, B. M. (2006). Helicobacter infection is required for inflammation and colon cancer in SMAD3-deficient mice. Cancer Res *66*, 828-838.

Maglich, J. M., Stoltz, C. M., Goodwin, B., Hawkins-Brown, D., Moore, J. T., and Kliewer, S. A. (2002). Nuclear pregnane x receptor and constitutive

androstane receptor regulate overlapping but distinct sets of genes involved in xenobiotic detoxification. Mol Pharmacol *62*, 638-646.

Makishima, M., Lu, T. T., Xie, W., Whitfield, G. K., Domoto, H., Evans, R. M., Haussler, M. R., and Mangelsdorf, D. J. (2002). Vitamin D receptor as an intestinal bile acid sensor. Science *296*, 1313-1316.

Makishima, M., Okamoto, A. Y., Repa, J. J., Tu, H., Learned, R. M., Luk, A., Hull, M. V., Lustig, K. D., Mangelsdorf, D. J., and Shan, B. (1999). Identification of a nuclear receptor for bile acids. Science *284*, 1362-1365.

Mangelsdorf, D. J., and Motola, D. L. (2005). Vitamin D Receptor as a Sensor for Toxic Bile Acids. In Vitamin D, D. Feldman, ed., p. 863.

Mangelsdorf, D. J., Thummel, C., Beato, M., Herrlich, P., Schutz, G., Umesono, K., Blumberg, B., Kastner, P., Mark, M., Chambon, P., and Evans, R. M. (1995). The nuclear receptor superfamily: the second decade. Cell *83*, 835-839.

Maran, R. R., Thomas, A., Roth, M., Sheng, Z., Esterly, N., Pinson, D., Gao, X., Zhang, Y., Ganapathy, V., Gonzalez, F. J., and Guo, G. L. (2009). Farnesoid X receptor deficiency in mice leads to increased intestinal epithelial cell proliferation and tumor development. J Pharmacol Exp Ther *328*, 469-477.

Mark, M., Ghyselinck, N. B., and Chambon, P. (2009). Function of retinoic acid receptors during embryonic development. Nucl Recept Signal *7*, e002.

Martinez, A., Aigueperse, C., Val, P., Dussault, M., Tournaire, C., Berger, M., Veyssiere, G., Jean, C., and Lefrancois Martinez, A. (2001). Physiological functions and hormonal regulation of mouse vas deferens protein (AKR1B7) in steroidogenic tissues. Chem Biol Interact *130-132*, 903-917.

Martinez, A., Lefrancois-Martinez, A. M., Manin, M., Guyot, S., Jean-Faucher, C., Veyssiere, G., Kahn, A., and Jean, C. (1999). 5'-flanking and intragenic sequences confer androgenic and developmental regulation of mouse aldose reductase-like gene in vas deferens and adrenal in transgenic mice. Endocrinology *140*, 1338-1348.

Massague, J. (1998). TGF-beta signal transduction. Annu Rev Biochem *67*, 753-791.

Matsubara, T., Yoshinari, K., Aoyama, K., Sugawara, M., Sekiya, Y., Nagata, K., and Yamazoe, Y. (2008). Role of vitamin D receptor in the lithocholic acid-mediated CYP3A induction in vitro and in vivo. Drug Metab Dispos *36*, 2058-2063.

McCarthy, T. C., Li, X., and Sinal, C. J. (2005). Vitamin D receptor-dependent regulation of colon multidrug resistance-associated protein 3 gene expression by bile acids. J Biol Chem *280*, 23232-23242.

Milovic, V., Teller, I. C., Faust, D., Caspary, W. F., and Stein, J. (2002). Effects of deoxycholate on human colon cancer cells: apoptosis or proliferation. Eur J Clin Invest *32*, 29-34.

Miyake, J. H., Wang, S. L., and Davis, R. A. (2000). Bile acid induction of cytokine expression by macrophages correlates with repression of hepatic cholesterol 7alpha-hydroxylase. J Biol Chem *275*, 21805-21808.

Modica, S., Murzilli, S., Salvatore, L., Schmidt, D. R., and Moschetta, A. (2008). Nuclear bile acid receptor FXR protects against intestinal tumorigenesis. Cancer Res *68*, 9589-9594.

Moore, D. D., Kato, S., Xie, W., Mangelsdorf, D. J., Schmidt, D. R., Xiao, R., and Kliewer, S. A. (2006). International Union of Pharmacology. LXII. The NR1H and NR1I receptors: constitutive androstane receptor, pregnene X receptor, farnesoid X receptor alpha, farnesoid X receptor beta, liver X receptor alpha, liver X receptor beta, and vitamin D receptor. Pharmacol Rev *58*, 742-759.

Moro, J. R., Iwata, M., and von Andriano, U. H. (2008). Vitamin effects on the immune system: vitamins A and D take centre stage. Nat Rev Immunol *8*, 685-698.

Nagengast, F. M., Grubben, M. J., and van Munster, I. P. (1995). Role of bile acids in colorectal carcinogenesis. Eur J Cancer *31A*, 1067-1070.

Narisawa, T., Fukaura, Y., Terada, K., and Sekiguchi, H. (1999). Inhibitory effects of ursodeoxycholic acid on N-methylnitrosourea-induced colon carcinogenesis and colonic mucosal telomerase activity in F344 rats. J Exp Clin Cancer Res *18*, 259-266.

Narisawa, T., Magadia, N. E., Weisburger, J. H., and Wynder, E. L. (1974). Promoting effect of bile acids on colon carcinogenesis after intrarectal instillation of N-methyl-N'-nitro-N-nitrosoguanidine in rats. J Natl Cancer Inst *53*, 1093-1097.

Nehring, J. A., Zierold, C., and DeLuca, H. F. (2007). Lithocholic acid can carry out in vivo functions of vitamin D. Proc Natl Acad Sci U S A *104*, 10006-10009.

Nitta, M., Ku, S., Brown, C., Okamoto, A. Y., and Shan, B. (1999). CPF: an orphan nuclear receptor that regulates liver-specific expression of the human cholesterol 7alpha-hydroxylase gene. Proc Natl Acad Sci U S A *96*, 6660-6665.

Northfield, T. C., and McColl, I. (1973). Postprandial concentrations of free and conjugated bile acids down the length of the normal human small intestine. Gut *14*, 513-518.

Ochsenkuhn, T., Bayerdorffer, E., Meining, A., Schinkel, M., Thiede, C., Nussler, V., Sackmann, M., Hatz, R., Neubauer, A., and Paumgartner, G. (1999).

Colonic mucosal proliferation is related to serum deoxycholic acid levels. Cancer *85*, 1664-1669.

Okano, T., Tsugawa, N., Morishita, A., and Kato, S. (2004). Regulation of gene expression of epithelial calcium channels in intestine and kidney of mice by 1alpha,25-dihydroxyvitamin D3. J Steroid Biochem Mol Biol *89-90*, 335-338.

Pannabecker, T. L., Chandler, J. S., and Wasserman, R. H. (1995). Vitamin-D-dependent transcriptional regulation of the intestinal plasma membrane calcium pump. Biochem Biophys Res Commun *213*, 499-505.

Papanikolaou, A., Wang, Q. S., Delker, D. A., and Rosenberg, D. W. (1998). Azoxymethane-induced colon tumors and aberrant crypt foci in mice of different genetic susceptibility. Cancer Lett *130*, 29-34.

Peiffer, L. P., Peters, D. J., and McGarrity, T. J. (1997). Differential effects of deoxycholic acid on proliferation of neoplastic and differentiated colonocytes in vitro. Dig Dis Sci *42*, 2234-2240.

Penagini, R., Spiller, R. C., Misiewicz, J. J., and Frost, P. G. (1989). Effect of ileal infusion of glycochenodeoxycholic acid on segmental transit, motility, and flow in the human jejunum and ileum. Gut *30*, 609-617.

Penning, T. M. (1997). Molecular endocrinology of hydroxysteroid dehydrogenases. Endocr Rev *18*, 281-305.

Perez, M. J., and Briz, O. (2009). Bile-acid-induced cell injury and protection. World J Gastroenterol *15*, 1677-1689.

Piemonti, L., Monti, P., Sironi, M., Fraticelli, P., Leone, B. E., Dal Cin, E., Allavena, P., and Di Carlo, V. (2000). Vitamin D3 affects differentiation, maturation, and function of human monocyte-derived dendritic cells. J Immunol *164*, 4443-4451.

Pino-Lagos, K., Benson, M. J., and Noelle, R. J. (2008). Retinoic acid in the immune system. Ann N Y Acad Sci *1143*, 170-187.

Polednak, A. P. (2008). Estimating the number of U.S. incident cancers attributable to obesity and the impact on temporal trends in incidence rates for obesity-related cancers. Cancer Detect Prev *32*, 190-199.

Prosser, D. E., and Jones, G. (2004). Enzymes involved in the activation and inactivation of vitamin D. Trends Biochem Sci *29*, 664-673.

Qiao, D., Chen, W., Stratagoules, E. D., and Martinez, J. D. (2000). Bile acid-induced activation of activator protein-1 requires both extracellular signal-regulated kinase and protein kinase C signaling. J Biol Chem *275*, 15090-15098.

Rafter, J. J., Child, P., Anderson, A. M., Alder, R., Eng, V., and Bruce, W. R. (1987). Cellular toxicity of fecal water depends on diet. Am J Clin Nutr *45*, 559-563.

Reddy, B. S. (1981). Diet and excretion of bile acids. Cancer Res *41*, 3766-3768.

Reddy, B. S., and Watanabe, K. (1979). Effect of cholesterol metabolites and promoting effect of lithocholic acid in colon carcinogenesis in germ-free and conventional F344 rats. Cancer Res *39*, 1521-1524.

Reddy, B. S., Watanabe, K., Weisburger, J. H., and Wynder, E. L. (1977a). Promoting effect of bile acids in colon carcinogenesis in germ-free and conventional F344 rats. Cancer Res *37*, 3238-3242.

Reddy, B. S., and Wynder, E. L. (1977b). Metabolic epidemiology of colon cancer. Fecal bile acids and neutral sterols in colon cancer patients and patients with adenomatous polyps. Cancer *39*, 2533-2539.

Ridlon, J. M., Kang, D. J., and Hylemon, P. B. (2006). Bile salt biotransformations by human intestinal bacteria. J Lipid Res *47*, 241-259.

Ross, A. C. (1993). Overview of retinoid metabolism. J Nutr *123*, 346-350.

Russell, D. W. (2003). The enzymes, regulation, and genetics of bile acid synthesis. Annu Rev Biochem *72*, 137-174.

Saaf, A. M., Halbleib, J. M., Chen, X., Yuen, S. T., Leung, S. Y., Nelson, W. J., and Brown, P. O. (2007). Parallels between global transcriptional programs of polarizing Caco-2 intestinal epithelial cells in vitro and gene expression programs in normal colon and colon cancer. Mol Biol Cell *18*, 4245-4260.

Sabbah, M., Courilleau, D., Mester, J., and Redeuilh, G. (1999). Estrogen induction of the cyclin D1 promoter: involvement of a cAMP response-like element. Proc Natl Acad Sci U S A *96*, 11217-11222.

Saito, H., Maeda, A., Ohtomo, S., Hirata, M., Kusano, K., Kato, S., Ogata, E., Segawa, H., Miyamoto, K., and Fukushima, N. (2005). Circulating FGF-23 is regulated by 1alpha,25-dihydroxyvitamin D3 and phosphorus in vivo. J Biol Chem *280*, 2543-2549.

Sancho, E., Batlle, E., and Clevers, H. (2004). Signaling pathways in intestinal development and cancer. Annu Rev Cell Dev Biol *20*, 695-723.

Schiff, E. R., Small, N. C., and Dietschy, J. M. (1972). Characterization of the kinetics of the passive and active transport mechanisms for bile acid absorption in the small intestine and colon of the rat. J Clin Invest *51*, 1351-1362.

Schmidt, D. R., Holmstrom, S. R., Fon Tacer, K., Bookout, A. L., Kliewer, S. A., and Mangelsdorf, D. J. (2010). Regulation of bile acid synthesis by fat-soluble vitamins A and D. J Biol Chem *285*, 14486-14494.

Schmidt, D. R., and Mangelsdorf, D. J. (2008). Nuclear receptors of the enteric tract: guarding the frontier. Nutr Rev *66*, S88-97.

Schmiedlin-Ren, P., Thummel, K. E., Fisher, J. M., Paine, M. F., Lown, K. S., and Watkins, P. B. (1997). Expression of enzymatically active CYP3A4 by Caco-2 cells grown on extracellular matrix-coated permeable supports

in the presence of 1alpha,25-dihydroxyvitamin D3. Mol Pharmacol *51*, 741-754.

Schwarz, M., Lund, E. G., Setchell, K. D., Kayden, H. J., Zerwekh, J. E., Bjorkhem, I., Herz, J., and Russell, D. W. (1996). Disruption of cholesterol 7alpha-hydroxylase gene in mice. II. Bile acid deficiency is overcome by induction of oxysterol 7alpha-hydroxylase. J Biol Chem *271*, 18024-18031.

Shea, H. C., Head, D. D., Setchell, K. D., and Russell, D. W. (2007). Analysis of HSD3B7 knockout mice reveals that a 3alpha-hydroxyl stereochemistry is required for bile acid function. Proc Natl Acad Sci U S A *104*, 11526-11533.

Shimada, T., Hasegawa, H., Yamazaki, Y., Muto, T., Hino, R., Takeuchi, Y., Fujita, T., Nakahara, K., Fukumoto, S., and Yamashita, T. (2004). FGF-23 is a potent regulator of vitamin D metabolism and phosphate homeostasis. J Bone Miner Res *19*, 429-435.

Shulman, A. I., Larson, C., Mangelsdorf, D. J., and Ranganathan, R. (2004). Structural determinants of allosteric ligand activation in RXR heterodimers. Cell *116*, 417-429.

Sinal, C. J., Tohkin, M., Miyata, M., Ward, J. M., Lambert, G., and Gonzalez, F. J. (2000). Targeted disruption of the nuclear receptor FXR/BAR impairs bile acid and lipid homeostasis. Cell *102*, 731-744.

Song, C. S., Echchgadda, I., Baek, B. S., Ahn, S. C., Oh, T., Roy, A. K., and Chatterjee, B. (2001). Dehydroepiandrosterone sulfotransferase gene induction by bile acid activated farnesoid X receptor. J Biol Chem *276*, 42549-42556.

Song, K. H., Ellis, E., Strom, S., and Chiang, J. Y. (2007). Hepatocyte growth factor signaling pathway inhibits cholesterol 7alpha-hydroxylase and bile acid synthesis in human hepatocytes. Hepatology *46*, 1993-2002.

Sonoda, J., Xie, W., Rosenfeld, J. M., Barwick, J. L., Guzelian, P. S., and Evans, R. M. (2002). Regulation of a xenobiotic sulfonation cascade by nuclear pregnane X receptor (PXR). Proc Natl Acad Sci U S A *99*, 13801-13806.

St-Pierre, M. V., Kullak-Ublick, G. A., Hagenbuch, B., and Meier, P. J. (2001). Transport of bile acids in hepatic and non-hepatic tissues. J Exp Biol *204*, 1673-1686.

Stadler, J., Stern, H. S., Yeung, K. S., McGuire, V., Furrer, R., Marcon, N., and Bruce, W. R. (1988). Effect of high fat consumption on cell proliferation activity of colorectal mucosa and on soluble faecal bile acids. Gut *29*, 1326-1331.

Staudinger, J. L., Goodwin, B., Jones, S. A., Hawkins-Brown, D., MacKenzie, K. I., LaTour, A., Liu, Y., Klaassen, C. D., Brown, K. K., Reinhard, J., Willson, T. M., Koller, B. H., and Kliewer, S. A. (2001). The nuclear

receptor PXR is a lithocholic acid sensor that protects against liver toxicity. Proc Natl Acad Sci U S A *98*, 3369-3374.

Sueyoshi, T., Kawamoto, T., Zelko, I., Honkakoski, P., and Negishi, M. (1999). The repressed nuclear receptor CAR responds to phenobarbital in activating the human CYP2B6 gene. J Biol Chem *274*, 6043-6046.

Thummel, K. E., Brimer, C., Yasuda, K., Thottassery, J., Senn, T., Lin, Y., Ishizuka, H., Kharasch, E., Schuetz, J., and Schuetz, E. (2001). Transcriptional control of intestinal cytochrome P-4503A by 1alpha,25-dihydroxy vitamin D3. Mol Pharmacol *60*, 1399-1406.

Tirona, R. G., Lee, W., Leake, B. F., Lan, L. B., Cline, C. B., Lamba, V., Parviz, F., Duncan, S. A., Inoue, Y., Gonzalez, F. J., Schuetz, E. G., and Kim, R. B. (2003). The orphan nuclear receptor HNF4alpha determines PXR- and CAR-mediated xenobiotic induction of CYP3A4. Nat Med *9*, 220-224.

Turley, S. D., and Dietschy, J. M. (1978). Re-evaluation of the 3 alpha-hydroxysteroid dehydrogenase assay for total bile acids in bile. J Lipid Res *19*, 924-928.

Tuveson, D. A., Shaw, A. T., Willis, N. A., Silver, D. P., Jackson, E. L., Chang, S., Mercer, K. L., Grochow, R., Hock, H., Crowley, D., Hingorani, S. R., Zaks, T., King, C., Jacobetz, M. A., Wang, L., *et al.* (2004). Endogenous oncogenic K-ras(G12D) stimulates proliferation and widespread neoplastic and developmental defects. Cancer Cell *5*, 375-387.

Val, P., Martinez, A., Sahut-Barnola, I., Jean, C., Veyssiere, G., and Lefrancois-Martinez, A. M. (2002). A 77-base pair LINE-like sequence elicits androgen-dependent mvdp/akr1-b7 expression in mouse vas deferens, but is dispensable for adrenal expression in rats. Endocrinology *143*, 3435-3448.

Van Cromphaut, S. J., Dewerchin, M., Hoenderop, J. G., Stockmans, I., Van Herck, E., Kato, S., Bindels, R. J., Collen, D., Carmeliet, P., Bouillon, R., and Carmeliet, G. (2001). Duodenal calcium absorption in vitamin D receptor-knockout mice: functional and molecular aspects. Proc Natl Acad Sci U S A *98*, 13324-13329.

van der Avoort, I. A., Shirango, H., Hoevenaars, B. M., Grefte, J. M., de Hullu, J. A., de Wilde, P. C., Bulten, J., Melchers, W. J., and Massuger, L. F. (2006). Vulvar squamous cell carcinoma is a multifactorial disease following two separate and independent pathways. Int J Gynecol Pathol *25*, 22-29.

Volle, D. H., Repa, J. J., Mazur, A., Cummins, C. L., Val, P., Henry-Berger, J., Caira, F., Veyssiere, G., Mangelsdorf, D. J., and Lobaccaro, J. M. (2004). Regulation of the aldo-keto reductase gene akr1b7 by the nuclear oxysterol receptor LXRalpha (liver X receptor-alpha) in the mouse

intestine: putative role of LXRs in lipid detoxification processes. Mol Endocrinol *18*, 888-898.

Wagner, M., Halilbasic, E., Marschall, H. U., Zollner, G., Fickert, P., Langner, C., Zatloukal, K., Denk, H., and Trauner, M. (2005). CAR and PXR agonists stimulate hepatic bile acid and bilirubin detoxification and elimination pathways in mice. Hepatology *42*, 420-430.

Walters, J. R., Tasleem, A. M., Omer, O. S., Brydon, W. G., Dew, T., and le Roux, C. W. (2009). A new mechanism for bile acid diarrhea: defective feedback inhibition of bile acid biosynthesis. Clin Gastroenterol Hepatol *7*, 1189-1194.

Wilpart, M., Mainguet, P., Maskens, A., and Roberfroid, M. (1983). Mutagenicity of 1,2-dimethylhydrazine towards Salmonella typhimurium, co-mutagenic effect of secondary biliary acids. Carcinogenesis *4*, 45-48.

Wolin, K. Y., Carson, K., and Colditz, G. A. (2010). Obesity and cancer. Oncologist *15*, 556-565.

Xie, W., Radominska-Pandya, A., Shi, Y., Simon, C. M., Nelson, M. C., Ong, E. S., Waxman, D. J., and Evans, R. M. (2001). An essential role for nuclear receptors SXR/PXR in detoxification of cholestatic bile acids. Proc Natl Acad Sci U S A *98*, 3375-3380.

Yang, F., Huang, X., Yi, T., Yen, Y., Moore, D. D., and Huang, W. (2007). Spontaneous development of liver tumors in the absence of the bile acid receptor farnesoid X receptor. Cancer Res *67*, 863-867.

Yin, L., Grandi, N., Raum, E., Haug, U., Arndt, V., and Brenner, H. (2009). Meta-analysis: longitudinal studies of serum vitamin D and colorectal cancer risk. Aliment Pharmacol Ther *30*, 113-125.

Zhong, H., Chiles, K., Feldser, D., Laughner, E., Hanrahan, C., Georgescu, M. M., Simons, J. W., and Semenza, G. L. (2000). Modulation of hypoxia-inducible factor 1alpha expression by the epidermal growth factor/phosphatidylinositol 3-kinase/PTEN/AKT/FRAP pathway in human prostate cancer cells: implications for tumor angiogenesis and therapeutics. Cancer Res *60*, 1541-1545.

Zhu, Y., Richardson, J. A., Parada, L. F., and Graff, J. M. (1998). Smad3 mutant mice develop metastatic colorectal cancer. Cell *94*, 703-714.

Zile, M. H. (1998). Vitamin A and embryonic development: an overview. J Nutr *128*, 455S-458S.